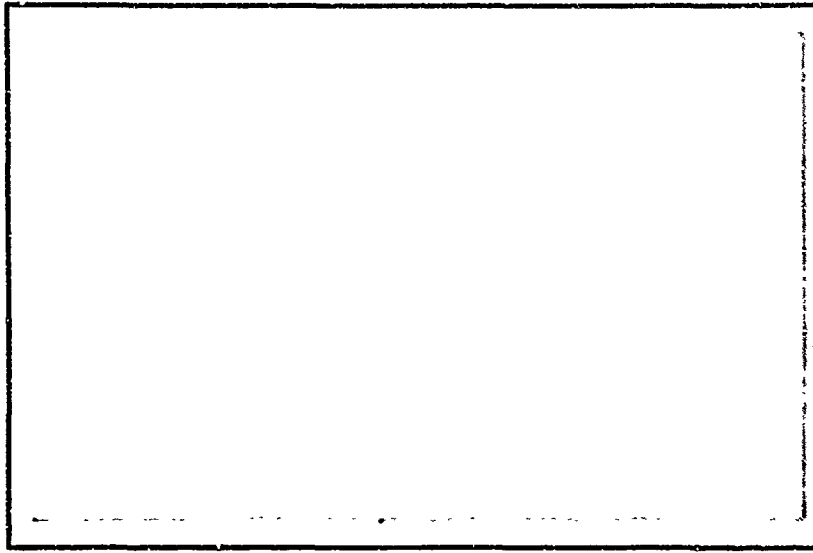
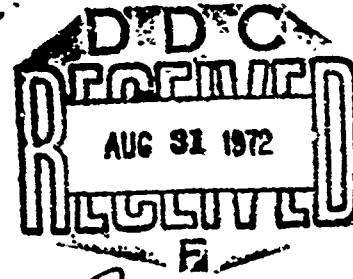


AD 747281

2



Reproduced by  
NATIONAL TECHNICAL  
INFORMATION SERVICE  
U S Department of Commerce  
Springfield VA 22151



Department of Mechanical Engineering

THE UNIVERSITY OF IOWA

Iowa City, Iowa

This document has been approved  
for public release and sale; its  
distribution is unlimited. 190

Unclassified  
Security Classification

DOCUMENT CONTROL DATA - R & D .

(Security classification of title, body of abstract and indexing annotation must be entered when the overall report is classified)

1. ORIGINATING ACTIVITY (Corporate author) The University of Iowa College of Engineering Iowa City, Iowa 52240		2a. REPORT SECURITY CLASSIFICATION Unclassified	
3. REPORT TITLE An experimental and Theoretical Study on Ablative and Evaporative Cooling in the Interior Ballistics		2b. GROUP	
4. DESCRIPTIVE NOTES (Type of report and Inclusive Dates) Scientific Report Final (August 1971)			
5. AUTHOR(S) (First name, middle initial, last name) Chen, Ching-J and Chang, Lang-M.			
6. REPORT DATE August 1971		7a. TOTAL NO. OF PAGES 187	7b. NO. OF REFS 13
8a. CONTRACT OR GRANT NO. DAAF 01-70-C-0380		9a. ORIGINATOR'S REPORT NUMBER(S)	
b. PROJECT NO. 11-9			
c. 50920-01		9b. OTHER REPORT NO(S) (Any other numbers that may be assigned this report)	
d. M1-M5			
10. DISTRIBUTION STATEMENT No Restrictions			
11. SUPPLEMENTARY NOTES		12. SPONSORING MILITARY ACTIVITY Weapons Laboratory at Rock Island SWERR-R, Rock Island Arsenal Rock Island, Illinois 61201	
13. ABSTRACT The report explores a better prediction of film cooling convective coefficient for a simplified model of the interior ballistics problem. The experiment includes design and modification of cooling projectile, conversion and interpretation of experimental data. The theoretical study deals with the solution of gas dynamic and heat transfer in a unsteady compressible, two phase flow with non-isothermal wall.			

DD FORM 1473

REPLACES DD FORM 1473, 1 JAN 64, WHICH IS OBSOLETE FOR ARMY USE.

Unclassified

Security Classification

Unclassified

Security Classification

14. KEY WORDS	LINK A		LINK B		LINK C	
	ROLE	WT	ROLE	WT	ROLE	WT
Boundary layer Profiles, velocity and temperature Liquid film Heat transfer Interior Ballistics						

ib

Unclassified

Security Classification

FINAL REPORT

Army Weapons Command  
Contract DAAF 01-70-C-0380

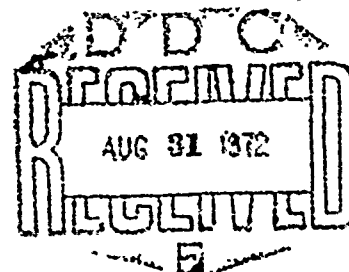
AN EXPERIMENTAL AND THEORETICAL STUDY  
ON ABLATIVE AND EVAPORATIVE COOLING  
IN THE INTERIOR BALLISTICS

Submitted by

C. J. Chen and L. M. Chang  
Department of Mechanical Engineering  
The University of Iowa  
Iowa City, Iowa

to

COMMANDING GENERAL  
U.S. ARMY WEAPONS COMMAND  
ROCK ISLAND ARSENAL  
ROCK ISLAND, ILLINOIS 61201



CONTRACTING OFFICER'S REPRESENTATIVE:

Mr. Darrel M. Thomsen  
Science and Technology Laboratory  
AMSWER - RET

This document has been approved  
for public release and sale; its  
distribution is unlimited.



## FORWORD

Although the problem of ablative and evaporative cooling in the interior ballistics had been considered before, the mechanism of the cooling is not clearly understood. In order to optimize the cooling effectiveness a thorough theoretical and experimental study must be made.

This report summarizes the effort in the period from January 1970 to April 1971 to study the cooling mechanism in the interior ballistics. The basic aim is to explore a better prediction of film cooling, convective coefficient for a simplified model which however retains the basic characteristics of the interior ballistics problem.

The experimental study was carried out at Rock Island Arsenal by personnel from Science and Technology Laboratory of the Rock Island Arsenal. This part includes design and modification of cooling projectile, conversion and interpretation of experimental data. The theoretical study deals with the solution of gas dynamics and heat transfer in a unsteady incompressible, two-phase flow with non-isothermal wall. Heat transfer convective coefficients are predicted or correlated with the experimental results.

The work reported herein was done under contract number DAAF-01-C-0380 with Rock Island Arsenal, U.S. Army Weapons Command.

## TABLE OF CONTENTS

FOREWORD	ii
TABLE OF CONTENTS	iii
NOMENCLATURE	v
LIST OF FIGURES	ix
LIST OF TABLES	x
I. INTRODUCTION	1
II. CONCLUSIONS	2
III. EXPERIMENTAL STUDIES	9
III-1 Projectile Modification	9
III-2 Instrumentation	10
III-3 Results and Discussion	11
III-31 Recommended Model	11
III-32 Temperature Response	12
III-33 Pressure Response	13
IV. FORMULATION OF THEORETICAL ANALYSIS	14
IV-1 General Considerations	14
IV-2 Assumption	15
IV-3 Governing Equations	16
IV-4 Boundary and Matching Conditions	24
IV-5 Nondimensionalization	25
V. ANALYSIS OF CORE SOLUTION	30
V-1 Core Problem	30
V-2 Method of Solution	31
V-3 Result and Discussion	34

VI. BOUNDARY LAYER SOLUTION WITHOUT COOLING	40
VI-1 Governing Equations and Similarity Transform	40
VI-2 Initial and Boundary Conditions	44
VI-3 Method of Solution	45
VI-4 Heat Transfer	46
VI-5 Discussion	48
VII. THEORETICAL ANALYSIS OF TWO PHASE FLOW	51
VII-1 Determination of Liquid Film Thickness	51
VII-2 Two-Phase Gas and Liquid Layer Flow	54
VII-21 Gas Boundary Layers with Liquid Cooling	54
VII-22 Liquid Velocity Field	56
VII-23 Liquid Temperature Field	58
VII-3 Discussion	60
VIII. RECOMMENDATION	67
REFERENCES	69
APPENDIX II A DETERMINATION OF MODIFIED PROJECTILE	70
APPENDIX II B CORE SOLUTION OF THE STANDARD ROUND PROJECTILE	71
APPENDIX III A EXPERIMENTAL DATA (June 3, 1970)	85
APPENDIX III B EXPERIMENTAL DATA (June 19, 1970)	115
APPENDIX III C EXPERIMENTAL DATA (August 17, 18, 1970)	143
APPENDIX V A DETERMINATION OF CONSTANTS FOR EQS. (5-6) AND (5-11)	156
APPENDIX VI A DERIVATION OF EQS. (6-13) AND (6-15) BY SIMILARITY TRANSFORMATION	157
APPENDIX VI B DETERMINATION OF $F_1(\eta)$ AT $\eta = 0$ FOR EQ. (6-16)	160
APPENDIX VI C BOUNDARY LAYER SOLUTION WITHOUT COOLING	164
APPENDIX VII A A DERIVATION OF $m_q(t)$ FOR EQ.(7-2) AND $h_1(t)$ FOR EQ.(7-6)	176

## NOMENCLATURE

### Dimensional Nomenclature

$\bar{A}$	Total cross-sectional area of the small holes on the projectile
$c_p$	Constant pressure specific heat of the propellant gas
$c_{p\ell}$	Constant pressure specific heat of the liquid
$c_v$	Constant volume specific heat of the liquid
$D_o$	Internal diameter of the barrel
$k$	Thermal conductivity of the gas
$k_\ell$	Thermal conductivity of the liquid
$L$	Total length of the barrel
$M_\ell$	Total amount of the liquid
$P$	Pressure of the gas
$P_\ell$	Pressure of the liquid
$P_b$	Pressure at the breech of the barrel
$q$	Heat flux
$Q_h$	Heat generation
$R$	Coordinate in radial direction
$R_o$	Internal radius of the barrel
$\bar{R}$	Universal gas constant
$T$	Gas temperature
$T_c$	Temperature at core
$T_\ell$	Liquid temperature
$T_{\ell w}$	Wall temperature with cooling
$T_o$	Initial temperature (= room temp)
$T_r$	Reference temperature
$T_w$	Wall temperature without cooling
$\bar{T}_c$	$= T_c - T_o$

$\bar{T}_w$	$= T_w - T_o$
$\bar{t}$	Time
$\bar{t}'$	$= \bar{t} - t_p$
$t_p$	Correspondent time where the projectile is located
$t_r$	Reference time
$U$	Gas velocity in radial direction
$U_e$	Exit velocity of the projectile
$U_L$	Liquid velocity in R-direction
$U_x$	Reference vleocity ( $= U_e$ )
$V$	Velocity in $\theta$ -direction
$W$	Gas velocity in Z-direction
$W_L$	Liquid velocity in z-direction
$W_p$	Projectile velocity
$Y$	$= \sqrt{Re} (R_o - R)$ , distance from the wall
$Y_i$	Position of gas-liquid interface
$Y_s$	$= -Y$ , pointing to the solid wall
$Z$	corrdiante along the barrel
$Z_p$	Position of the projectile
$\bar{\rho}$	Gas density
$\bar{\rho}_L$	Liquid density
$\rho_r$	Reference desnity
$\mu$	Gas viscosity
$\mu_L$	Liquid viscosity
$\phi$	Coordinate around the center of the barrel

# Non Dimensional Nomenclature.

$A$	$= \frac{n-1}{2}$ , a constant
$a$	Total cross-sectional area of the small holes in the projectile
$C$	$= 0.5928$ , a constant
$C_c$	$= 0.726$ , a constant
$d_o$	Internal diameter of the barrel
$E$	Eckert number of the gas
$E_l$	Eckert number of the liquid
$f_1$	Functions of $\eta$
$f_2$	Functions of $\eta$
$f_3$	Functions of $\eta$
$f_4$	$= f_1 f_2$
$H$	A function of $(t, y)$
$h$	Heat transfer coefficient
$h_1$	Thickness of the liquid at $z = z_p$
$m$	$= 1.82$ , a constant
$m_l$	Total amount of the liquid
$n$	$= -3.65$ , a constant
$Nu$	Nusselt number
$p$	Pressure of the gas
$p_b$	Pressure at the breech
$p_l$	Pressure of the liquid
$Pr$	Prandtl number
$q_{B.L}$	Heat generation in the boundary layer
$q_{core}$	Heat generation in the core solution

$r$	Coordinate in radial direction
$r_0$	Internal radius of the barrel
$Re$	Reynolds number
$t$	Time
$u$	Gas velocity in $r$ -direction
$u_l$	Liquid velocity in $r$ -direction
$\bar{u}$	$= - \sqrt{Re} \ u$
$w$	Gas velocity in $z$ -direction
$w_l$	Liquid velocity in $z$ -direction
$w_p$	Velocity of the projectile
$y$	$= \sqrt{Re} \ (\gamma_0 - \gamma)$
$y_f$	Thickness of the liquid film
$z$	coordinate along the barrel
$z_p$	Position of the projectile
$\rho$	Gas density
$\xi$	Similarity transformation invariant variables
$\eta$	
$\gamma$	$= \frac{c_p}{c_v}$
$\theta$	Gas temperature
$\theta_c$	Gas temperature in the core
$\theta_l$	Liquid temperature
$\theta_{lw}$	Wall temperature with cooling
$\theta_w$	Wall temperature without cooling
$\alpha$	Thermal diffusivity

## LIST OF FIGURES

Figure	
II-1	General Modification of the Projectile
II-2	Comparison of Internal Wall Temperatures With and Without Cooling
II-3	Pressure and Time Correlation
III-1	Arrangement of Probes
III-2	Arrangement of Temperature Probes for the Test on Jan. 12, 1971
III-3	Internal Wall Temperature $T_1$ (2.37" from Muzzle) v.s. Time for Continuous Firing
III-4	External Wall Temperature v.s. Time for Continuous Firing of Modified Projectile
III-5	External Wall Temperature v.s. Time for Continuous Firing of Standard Projectile
IV-1	Schematic Drawing of Flow Fields
V-1	Projectile Velocity and Acceleration v.s. Time
V-2	Gas Velocity in Core, $W$ , and Projectile Velocity $W_p$ , v.s. Time
V-3	Core Propellant Gas and Wall Temperatures at Various Positions
V-4	Heat Generation v.s. Time in Core
VI-1	Comparison of Experimental and Approximated Values for Boundary Layer Analysis
VII-1	Internal Wall Temperature, $\bar{T}_w$ , With and Without Cooling v.s. Time, $\bar{t}'$ .



LIST OF TABLES

TABLE IV A      Viscosity of Equilibrium Air

## I INTRODUCTION

It is well known that the present firing arms are limited for their continuous firing capability due to the thermal expansion or cook-off from the excessive heating in firing. For example, Cohn [1]\* and Corner [2] show that a heat input of  $1,000 \text{ Btu/ft}^2 \text{ sec.}$  is possible. Many approaches have been attempted to remove this large amount of heat transfer such as the change of configuration, different propellant, change in firing frequency, and liquid cooling. Without changing the existing design, one of the most promising methods of cooling is to coat an ablative and evaporative material on the interior wall by the projectile as it passes through. The thermal resistance of the so generated vapor may seal off the heat transfer from the combusted gas to the wall. It was shown by Cohn [1] and Adams and et al [3] that even smearing with silicone oil or coating with teflon or beeswax on a projectile does have some cooling effect. However the exact mechanism of the insulation is not clearly understood. The present theoretical and experimental research is motivated to study the cooling mechanism and to optimize the effectiveness of such cooling devices.

The experimental study used an XM140 Aircraft Automatic Gun as the model to analyze the cooling effectiveness of the cooling projectile which contains water as coolant and to obtain the boundary conditions that are needed in the theoretical analysis. The theoretical study analyzes the gas dynamics of the propellant gas to the barrel occurring behind the projectile.

Convective heat transfer coefficient which is important in heat transfer calculation was derived for unsteady compressible flow with and without liquid cooling in a barrel.

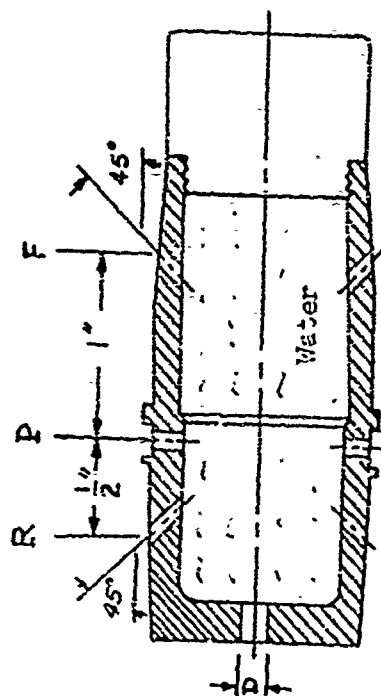
---

\* The number in the bracket denotes the reference number listed in REFERENCES

## II CONCLUSIONS

Before details of experimentation and theoretical analysis are reported, important conclusions are first presented in this section for readers who are interested in the present results and the application of the solutions obtained. It is concluded that:

1. Solid material coated on the projectile is not an effective coolant because of the low melting rate in a time interval of two to three milliseconds. Therefore, liquid is adapted as the coolant.
2. Water as a coolant is proved to be excellent, since it is inert, nontoxic in both liquid and vapor phase, more transparent than silicone oil in vapor phase. Antifreezer may be added to water to lower the freezing point in use.
3. Proper geometry of the modified projectile that contains coolant is essential for an effective and uniform cooling. Of the eight modified configurations (see Fig II-1) tested, the No. 2 type gave a distinctively effective and uniform cooling. These modifications are based on the analysis given in Appendix IIA. We conclude that injection of coolant through side copper band and the front portion of a projectile gives a better, even distribution of coolant than other combinations.
4. Experimenting with water as the coolant in the No. 2 type modified projectile the peak temperature on the interior wall is reduced by as much as 40% in comparison with the standard round based on the single shot experiment as shown in Fig II-2. Cooling is particularly effective near the muzzle end.
5. The analysis of the gas dynamics of the propellant gas behind the projectile and the heat transfer through the propellant and the coolant to the wall may be divided into three regions - core flow, gas boundary layer flow and liquid layer flow.



DIMENSION IN INCHES

PROJECTILE NUMBER	D	P		R		F	
		DIA. OF HOLES	# OF HOLES	DIA. OF HOLES	# OF HOLES	DIA. OF HOLES	# OF HOLES
1	1/8	3/32	4	3/32	4	*	*
2	1/8	3/32	4	*	*	3/32	4
3	1/8	3/32	4	3/32	4	3/32	4
4	1/4	3/32	4	3/32	4	*	*
5	1/4	3/32	4	*	*	3/32	4
6	1/4	3/32	4	3/32	4	3/32	4
7	1/4	1/8	4	1/8	4	*	*
8	3/8	*	*	*	*	*	*

Note:

- (1) Water contained: 0.039 lbm.
- (2) All holes are drilled in evenly spacing around the projectile.
- (3) Vertical and inclined holes differ by 45° in the azimuthal direction.
- (4) '\*' denotes no holes to be drilled.

Fig. II-1. General Modification of the Projectile

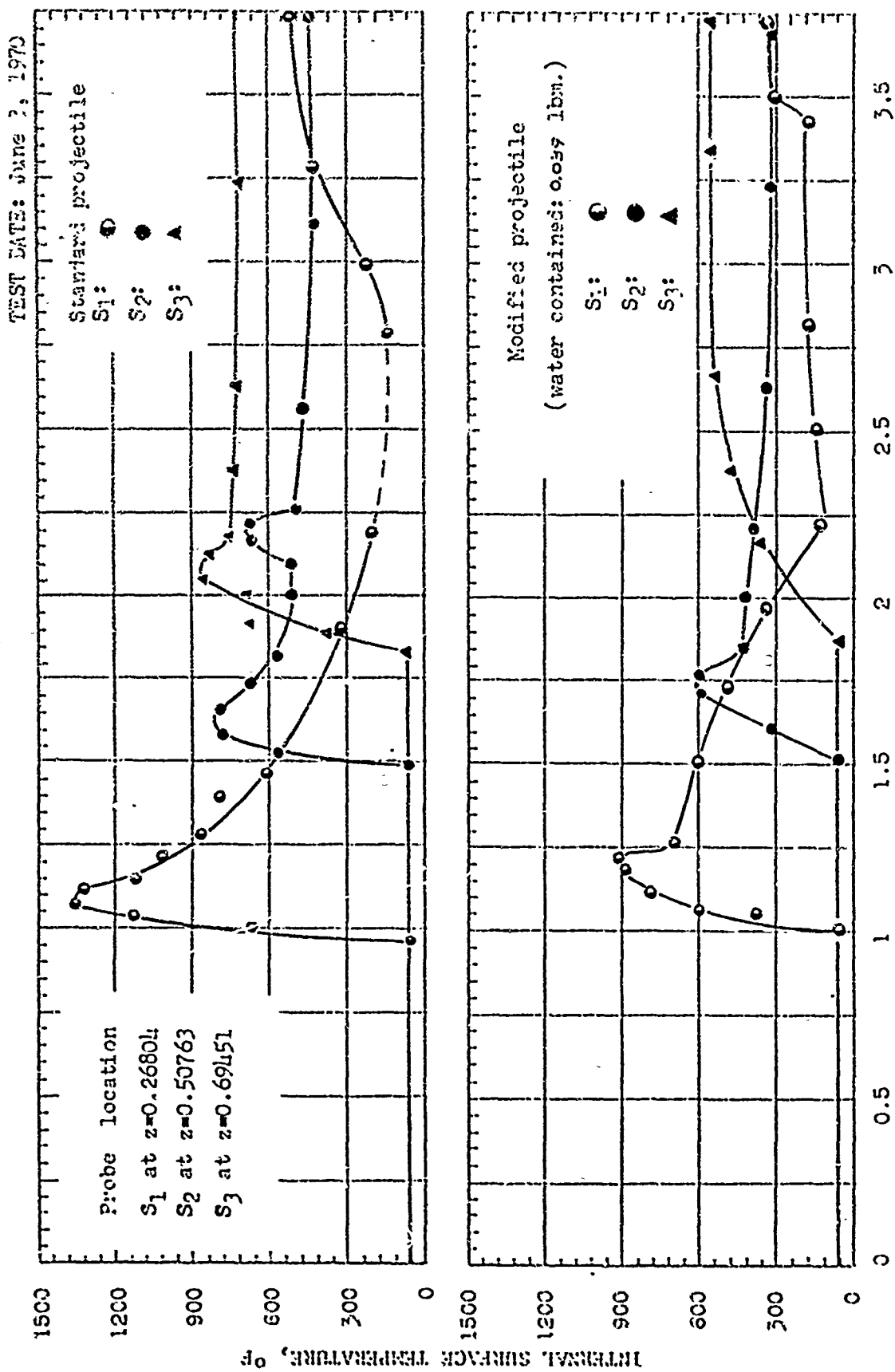


Fig. II-2. Comparison of Internal Wall Temperatures With and Without Cooling

6. Gas and liquid boundary layers are found to be small compared with the diameter of the barrel. The thickness of the layer is about one hundredth of the diameter.
7. The gas core solution is solved provided that the pressure response at the breech and the projectile position as a function of time are known. The result gives the following dependent variables in dimensionless form (deviation given in Chapter V).

Pressure:

$$p(z, t) = p_b(t) - 0.5928 \ddot{z}_p (z^2 - z_p^2(0)) / (2 z_p^3(t)) \quad (2-1)$$

Density:

$$\rho(t) = 0.5928 / z_p(t) \quad (2-2)$$

Temperature:

$$\theta(z, t) = [p_b(t) \dot{z}_p / 0.5928] - [\ddot{z}_p (z^2 - z_p^2(0)) / (2 z_p^3(t))] \quad (2-3)$$

Gas velocity:

$$w(z, t) = \dot{z}_p z / z_p(t) \quad (2-4)$$

Heat generation;

$$\begin{aligned} q_{ure} = & [(p_b \dot{z}_p / z_p) + \dot{p}_b / t] - [\dot{z}_p \ddot{z}_p z_p^2(0) / z_p^3(t) \gamma] \\ & - \frac{0.5928 (z^2 - z_p^2(0))}{2 z_p^2} [\ddot{z}_p / t + \dot{z}_p \ddot{z}_p / z_p] \end{aligned} \quad (2-5)$$

The analysis shows that the pressure distribution can be predicted to a

15% accuracy at any location behind the projectile. Fig II-3 shows the comparison between theory and experiment. The above solutions are also programmed in Appendix IIB for general input of projectile position versus time and breech pressure functions. The above analysis should be used 0.15 milliseconds after the firing, since the solution is inaccurate during the strong propellant reaction.

8. The gas boundary layer flow without liquid cooling is first solved to understand the heat transfer mechanism. The solution is obtained through similarity transform. The analysis deals with an unsteady compressible laminar flow with heat generation and non-isothermal wall. For the wall temperature of the type (see Chapter V, Eq (5-13))

$$\theta_w = \frac{t^{1.65}}{f_1(t)} \left[ p_b - 0.54 t^{-3.25} (z^2 - z_p^2(t)) \right] \quad (2-6)$$

the local Nusselt number which is function of time and position is

$$Nu = \frac{h(z,t)L}{K} = Re^{0.5} \left( \frac{-f_1'(t)}{f_1^2(t)} \right) t^{0.325} \left[ p_b(t) - 0.54 t^{-3.25} (z^2 - z_p^2(t)) \right] \quad (2-7)$$

For the XM140 Model or the like  $f_1(0) = 3.2, f_1'(0) = -0.12$ . It should be noted that Newton's cooling law is defined here as

$$\dot{q} = h T_r \left[ \frac{\beta t u}{h r f t^2} \right] \quad (2-8)$$

$$\text{where } T_r = \frac{u^2}{R}$$

and that the time and location in Eqs (2-6) and (2-7) must be behind the projectile or  $z < z_p(t)$ . For other type of interior ballistics  $-f_1'(t)/f_1^2(t)$

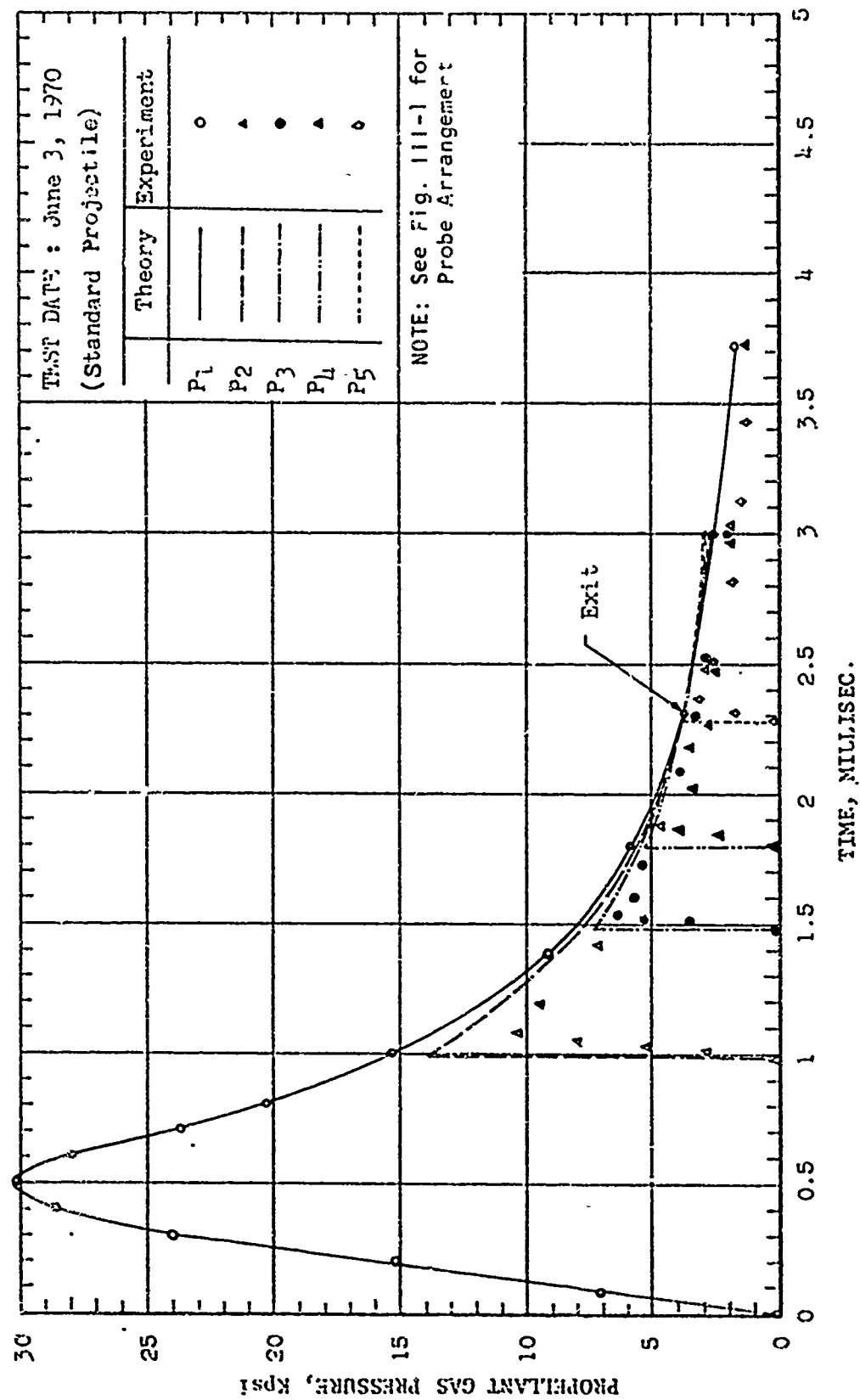


Fig. II-3. Pressure and Time Correlation



in the equation (2-7) may be taken as a constant to be determined from experimental data. The limitation of the formula (2-7) is that the non-isothermal wall temperature must be given by Eq. (2-6) which may only approximately represent the actual response in experiment. Nevertheless it is recommended over the use of steady incompressible laminar formula. Examples of using Eq. (2-7) can be found in Chapter VI.

9. The heat transfer from the propellant to the wall through a liquid layer is solved approximately in Chapter VII. The Nusselt number which is also function of time and distance along the axial direction is given as

$$Nu = \frac{h(z,t)L}{k_l} = Re^{0.5} \frac{1}{y_l} \left[ \theta_{j_i} - \theta_{l_w} - \frac{\partial \theta_{l_w}}{\partial t} \frac{Q}{z} z^2 y_l^2 \right] \quad (2-9)$$

where  $y_l$  is the liquid film thickness. A method of calculating  $y_l$  is given in Chapter VII section 1. Because there is not enough information about the existence of a liquid film behind the projectile and about the percentage of liquid in the modified projectile that may get behind the projectile the solution thus obtained from Eq. (2-9) can only be taken as preliminary one. Further study is needed to verify many assumptions which are not theoretical, but are experimental and yet to be established. An alternative heat transfer formula is also derived in Chapter VII section 3 based on the response of the solid wall of the barrel.

10. In general with cooling liquid there is about 30% of reduction in heat flux from the propellant gas to the wall for the modified projectile of No. 2 (see Fig II-1). The mechanism of cooling effect mainly comes from the absorption of heat by the liquid and therefore the reduction of temperature gradient near the wall.

### III EXPERIMENTAL STUDIES

#### III-1 Projectile Modification

In the design of the modified projectiles for experiment, considerations were made to provide an even distribution of coolant on the interior wall and a good lubrication effect for the motion of projectile. Then several single shot experiments were conducted to determine the best coolant exit locations and hole diameters among the proposed modified models. The hole diameters are calculated from a theoretical analysis under the criterion that the coolant is completely squeezed out by the time when the projectile leaves the muzzle end. In the analysis the effective pressure to squeeze the coolant out of the projectile is assumed to be one half of the bore pressure at that given instant. (See Appendix II A)

A capsule containing water is inserted into the hollow space of the projectile as shown in Fig. II-1 for an initial test. One hole at the bottom and four to eight holes evenly spaced around the projectile are drilled. As the projectile is fired the pressure on the base of the projectile will squeeze the water out of the projectile through the holes around the projectile. The water then is coated to the inner wall of the barrel. The precise dimensions for machining are shown in Fig. II-1.

Approximately 17 grams of water were sealed in the projectile by a polyethylene capsule, a rubber bag, and a polyethylene tape respectively. The experimental results show that the modified projectiles NO. 2, gave the best result with uniform cooling and lower wall temperature (40% reduction in the maximum wall temperature from that of the standard round. See Comparison of Figs. II-2) It was established that the front holes and peripheral holes located between the copper band gave the best result. Therefore No. 2 is adapted for experiments of continuous firing. The

data obtained for single shot experiment are the measurements of the interior and exterior wall temperature, and the pressure response in five locations of the gun barrel. All experiments were performed at the Rock Island Arsenal by personnel of the Science and Technology Laboratory. The data are included in Appendixes III A, B, and C.

### III-2 Instrumentation

The Instrumentation of the experiment was also set up by personnel of Science and Technology Laboratory at Rock Island Arsenal. The model used for the experiment was XM140 barrel. Five pressure probes, four interior wall temperature probes and six external thermocouples were used to record data. Kistler pizo-electric high pressure transducers were used for pressure measurements. The platinum-platinum 10% rhodium Mo-Re surface temperature probes were used to measure internal wall temperature. Both probes have a response time of microseconds which is sufficiently accurate for a test interval of 2 to 3 milliseconds. The external temperatures were measured by chromel-Alumel thermocouples welded on the outer barrel surface. The arrangement of probe locations is shown in Fig. III-1.

### III-3 Results and Discussion

#### III-31 Recommended Model

Eight proposed modifications of the projectile shown in Fig. II-1 were tested on a single shot basis in the first two experiments and compared with the standard round. Each modified projectile contains 0.039 lbm (17.6 grams) of water. All eight modified projectiles exhibited substantial cooling effect in the first experiment. In particular, the peak internal surface temperature can be reduced as much as 40% from the standard projectile. This can be seen from figures in Appendix III, where internal surface temperatures are designated by  $S_1$ ,  $S_2$ , and  $S_3$ . Among the

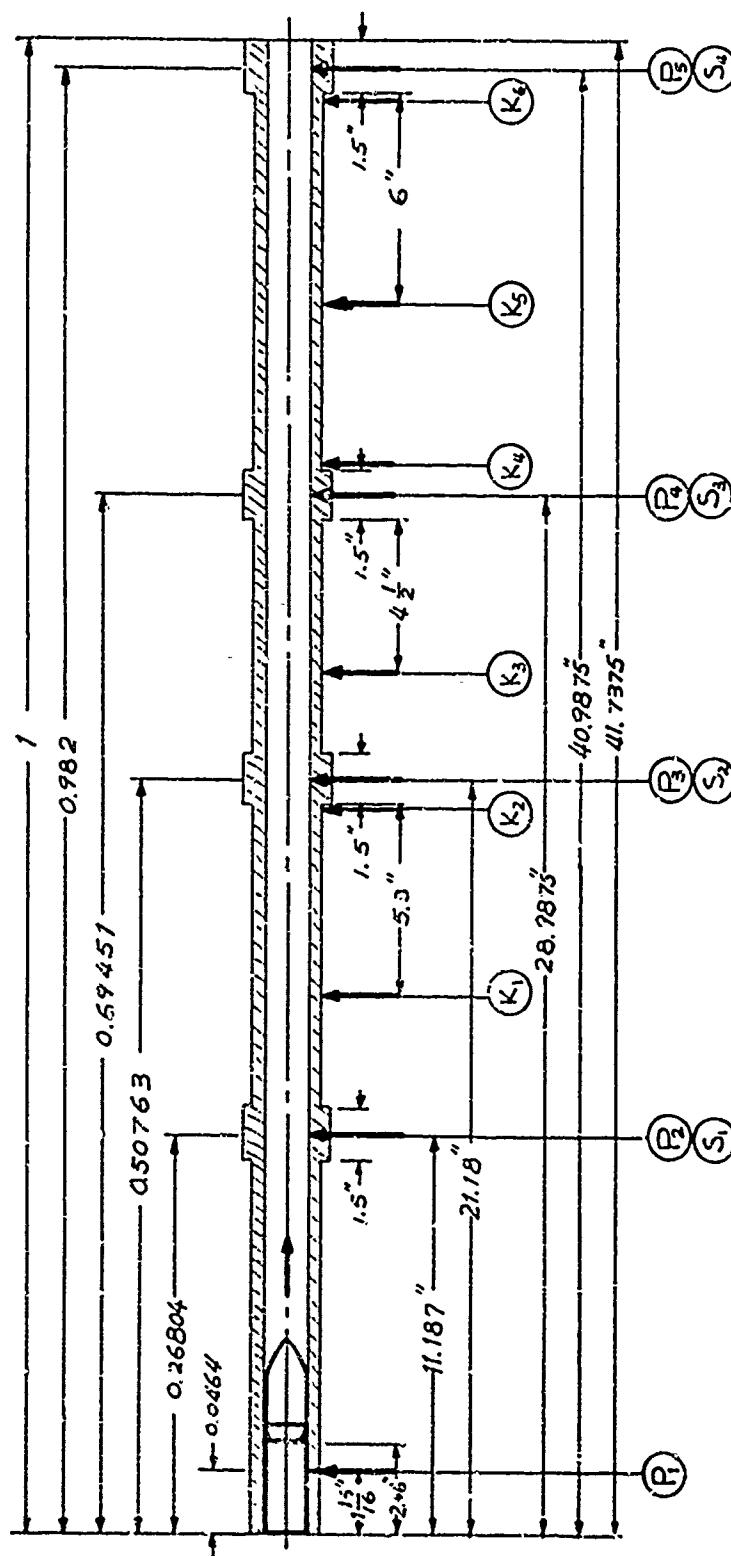


Fig. JII-1. Arrangement of Probes

- (1)  $P_1, P_2, P_3, P_4, P_5$ , and  $P_6$  are pressure probes;  
 $S_1, S_2, S_3$ , and  $S_4$  are internal wall temp. probes;  
 $K_1, K_2, K_3, K_4, K_5$ , and  $K_6$  are external wall temp. probes.
- (2) The arrows indicate the locations of the probes.
- (3) The values on the upper side of the barrel are dimensionless.

eight experiments of modified projectiles the first three rounds #1, #2, and #3 (specified in Fig. II-1) are judged to provide satisfactory results. For test projectiles #4 through #8 data obtained in a short time after the firing are satisfactory. However, because of the separation of the aluminum cap from the projectile at approximately 1 millisecond after firing, data thus obtained are insufficient to indicate the effectiveness of the modification. Nevertheless, these data provide a relative comparison among the projectiles #4 through #8. Based on the results of projectiles #1, #2, and #3 projectile #2 gives the best cooling effect through out the barrel. This modification shows that a better, uniform coating of liquid on the surface of the barrel can be achieved by squeezing liquid out from the front portion and between the copper rings of the projectile as shown in the Fig II-1 by P and F. Since the cap of projectile separated from the projectile for #5 (which has the same configuration as #2 except a larger diameter at the bottom of the projectile denoted D in Fig. II-1) this series of the test did not allow us to compare the effectiveness of projectiles #2 and #5. Therefore, the type #2 is recommended

### III-32 Temperature Response

From Fig. II-2 we see that with liquid cooling the peak internal wall temperatures are greatly reduced. This may attribute to the liquid sealing effect that prevents the hot, propellant gas from contacting the wall. It should be noted that with a pressure higher than the critical pressure of water in the barrel the evaporation effect of liquid is almost negligible. Only when the projectile has left the muzzle can evaporation be a cooling effect. Note also that at a given instant, say 2.3 millisecond, Fig. II-2 gives a high temperature for a larger distance from the breech. This can be explained from the fact that a larger projectile velocity near the

muzzle end contributes to a larger friction heating and hence a larger temperature response.

Referring to Appendix IIIA, on external wall temperature we observed that temperature response at  $K_5$  appears to be the highest one. This is because the barrel thickness at  $K_5$  position is the thinnest over the entire length of the barrel. We note also that temperature response at  $K_1$  is high although the thickness of  $K_1$  is thick. However this may be explained by the fact the core temperature inside the  $K_1$  position is hottest of the core temperatures.

### III-33 Pressure Response:

In the case of liquid cooling the peak pressure of  $P_1$ , at the breech, was cut down about 5 kpsi, compared with a standard round, while the response at other positions remain the same. This can be seen from the pressure curves of PROOF ROUND NO. 3 and PROJECTILE NO. 2 tested on June 3, 1970, Appendix III A. This is due to a pressure release to fill up the hollow space inside the modified projectile at the early stage. However, this does not seem to slow down the exit velocity. It can be seen from the following fact:

For standard projectile (without cooling PROOF ROUND NO.3) the projectile velocity at the exit,  $W_p$ , is, based on the core solution

$$W_p = 2130.8 \text{ ft/sec}$$

and for modified projectile (modified Projectile No. 2) its velocity in ft/millisecc. is, based on experimental data,

$$\bar{W}_p = \frac{dZ_p}{dt} = 1.87696 \bar{t} - 0.55665 \bar{t}^2 + 0.05672 \bar{t}^3$$

at the exit of the barrel  $\bar{t} = 2.38$  millisecc.

$$W_p = 2079 \text{ ft/sec.}$$

The above evidence indicates that the exit velocity of the modified projectile can reach the velocity attained by the standard projectile even though

there is a drop in peak pressure. This indicates that the liquid squeezed from the lateral and front sides of the projectile on the wall of the barrel does serve as a lubricant and reduces the friction force between the wall and the projectile. This reduction in drag force provides a higher acceleration near the muzzle end for the modified projectile.

#### III-34 Continuous Firing

Twenty rounds of the modified projectile number 2 were tested in an experiment of continuous firing. However only ten rounds were fired when a malfunction of test gun occurred. The result of the experiment was given in Fig. III-2 III-3, III-4, and III-5. Where Fig. III-2 gives the location of temperature probes and Fig. III-3 gives the internal wall temperature measurement at 2.37" from the muzzle end without cooling. Figs. III-4 and III-5 are external wall temperature measurements with and without cooling respectively. It should be noted that there were twenty rounds of standard projectile fired during the experiment which does not allow a direct comparison with the data of modified projectiles where only ten rounds were fired. Nevertheless, we observed that with and without cooling the external temperature increases linearly with time after the first five rounds. Although based on the single shot experiment the heat transfer behind the projectile can be reduced by liquid cooling, the combined total cooling effect under continuous firing needs further investigation before conclusions can be reached.

Note: (1)  $T_1$  and  $T_2$  are internal wall temperature probes  
 (2)  $T_3$ ,  $T_4$ ,  $T_5$ ,  $T_6$ , and  $T_7$  are external wall temperature probes

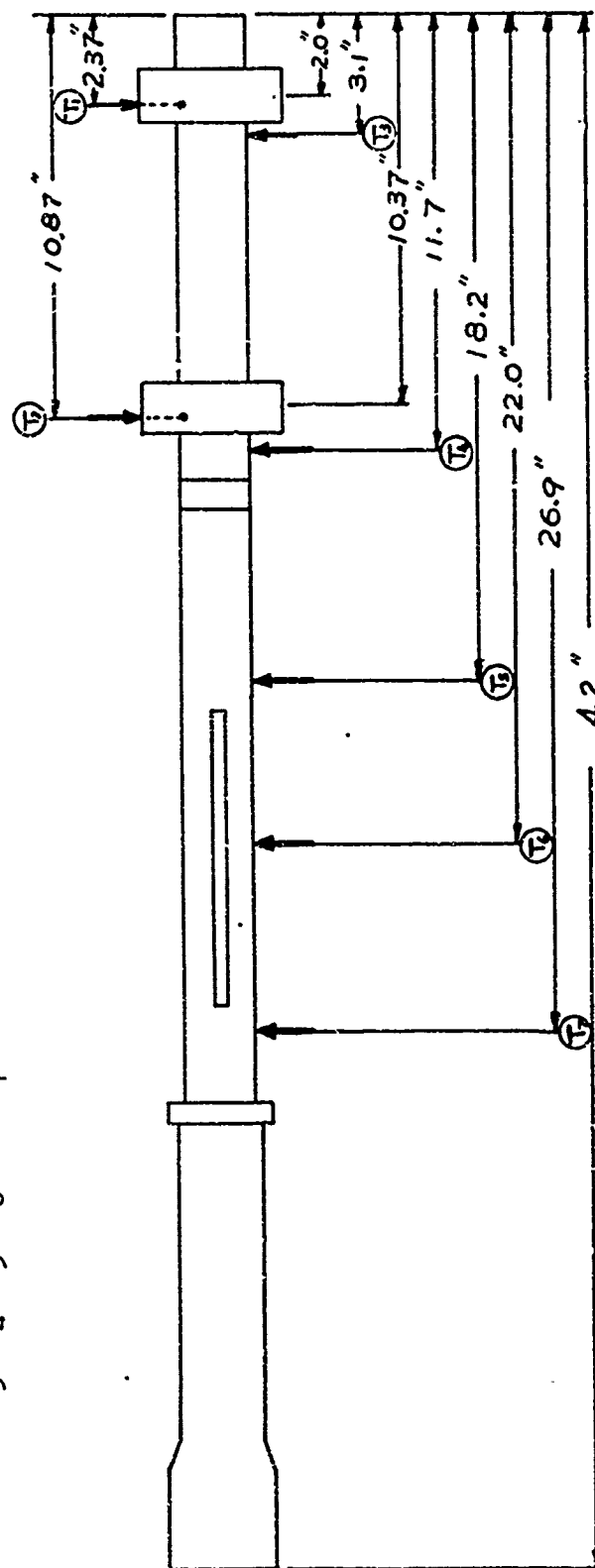


Fig. III-2 Arrangement of temperature probes for the Test of Jan. 12, 1971



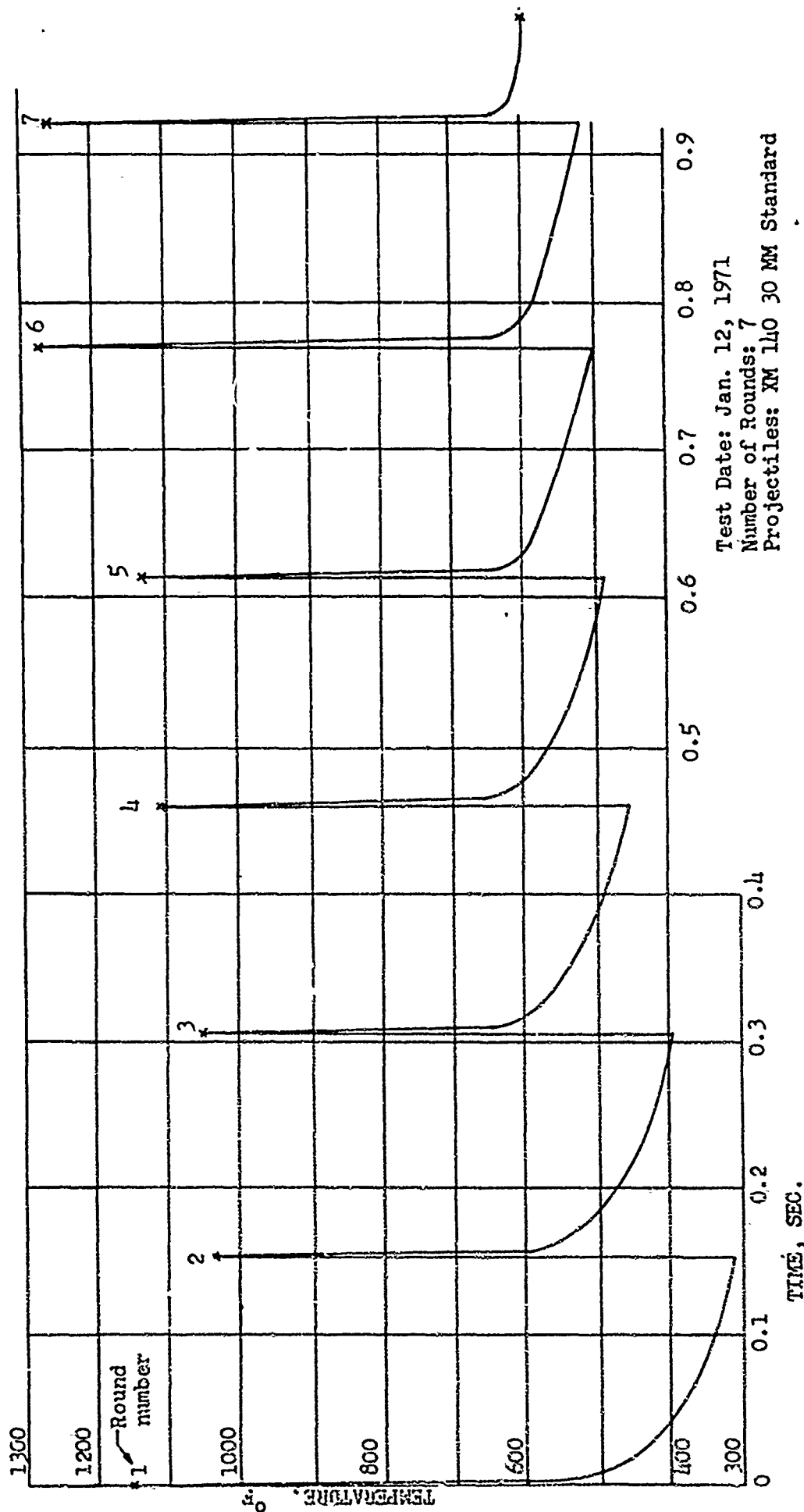
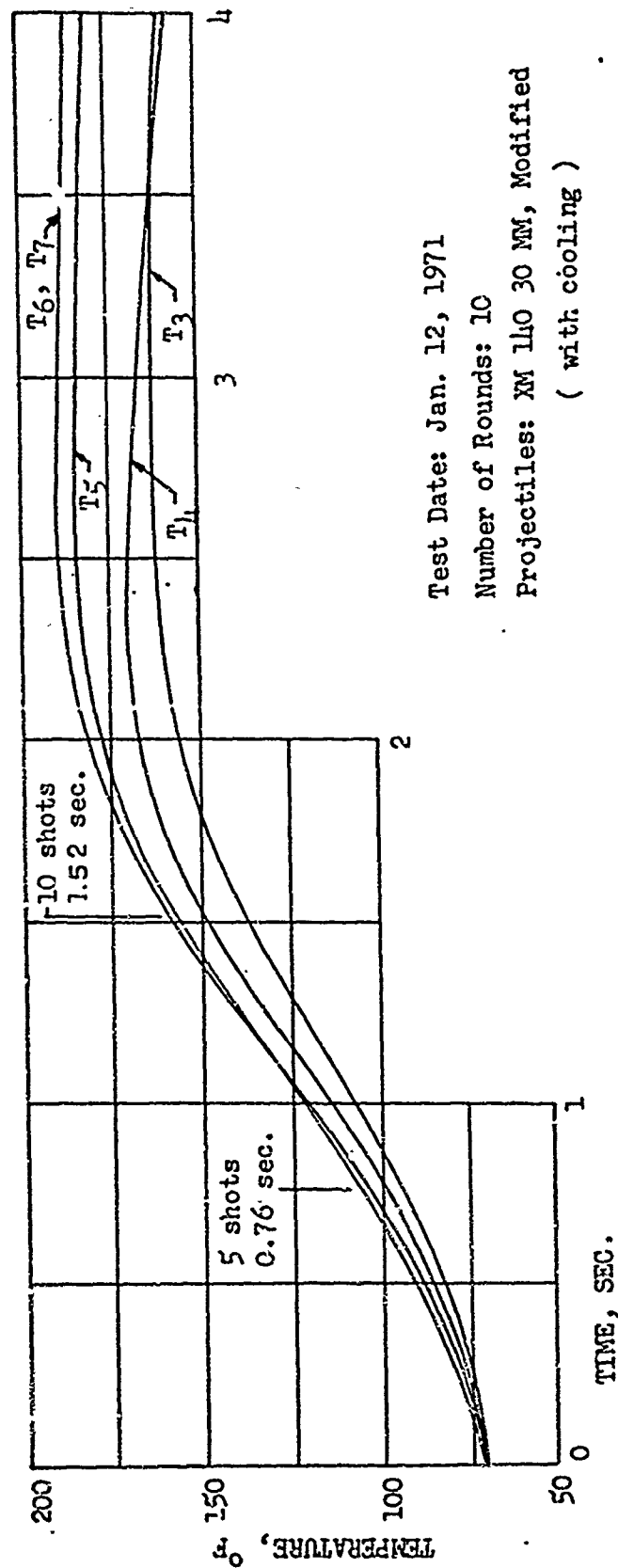


Fig. III-3 Internal Wall Temperature  $T_1$  ( 2.37" from muzzle) v.s. Time for Continuous Firing

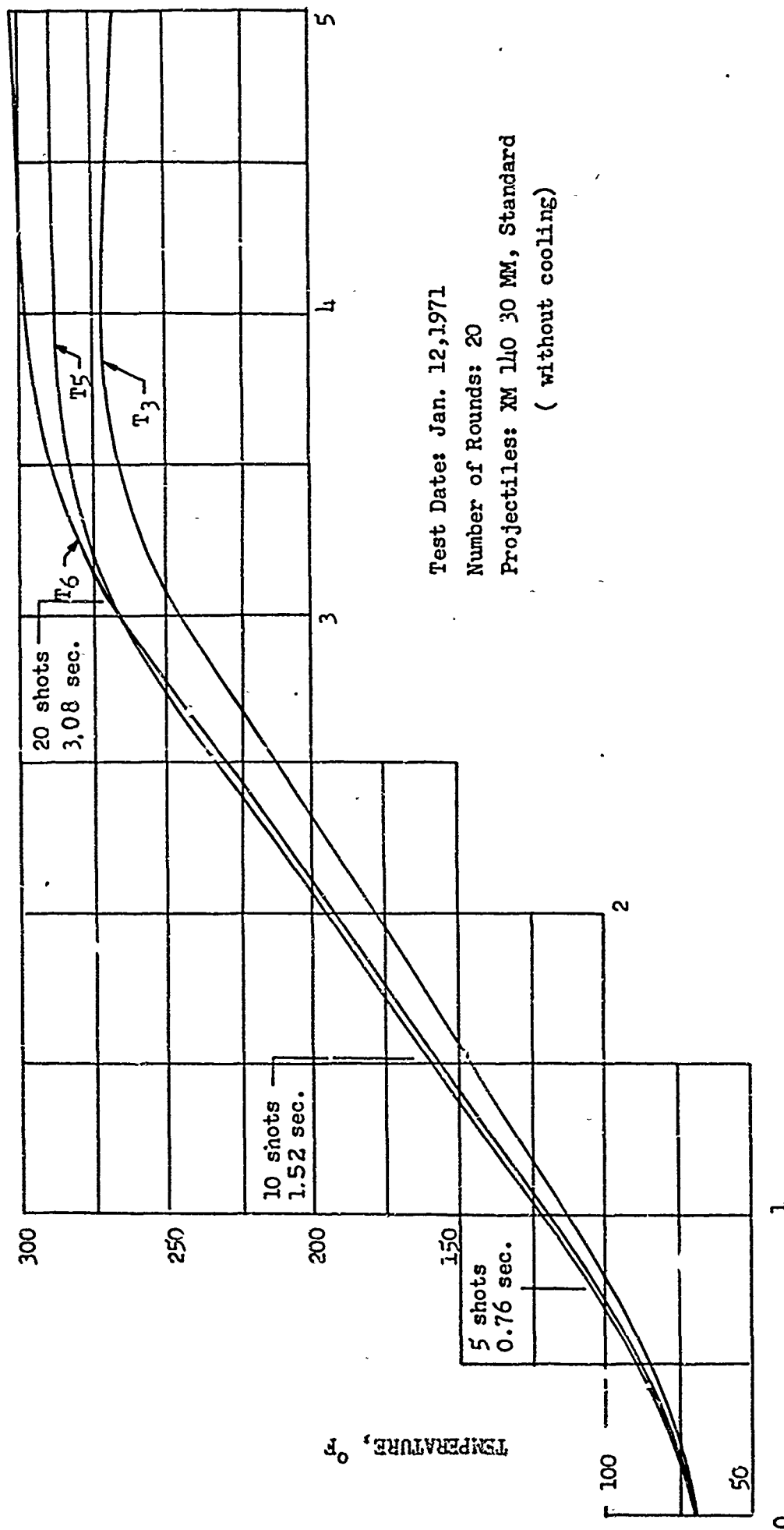


Test Date: Jan. 12, 1971

Number of Rounds: 10

Projectiles: XM 140 30 MM, Modified  
( with cooling )

Fig. III-4 External Wall Temperatures v.s. Time for Continuous Firing of Modified Projectiles



Test Date: Jan. 12, 1971

Number of Rounds: 20

Projectiles: XM 140 30 MM, Standard  
( without cooling)

TIME, SEC.:

Fig. III-5 External Wall Temperatures v.s. Time for Continuous Firing of Standard Projectiles

## IV FORMULATION OF THEORETICAL ANALYSIS

### IV-1 General Consideration

Consider that projectiles are continuously fired with a certain frequency. The analysis of the gas dynamics behind the projectile is then basically a viscous, compressible periodic flow with heat transfer. Although the analysis of gas flow without liquid cooling is not contained in the original proposal it is included here because with some modification the solution can be extended to the flow with liquid cooling.

The mathematical analysis consists of two essential parts. They are the gas core flow where the viscosity and conductivity are not important and the boundary layer flow where the viscosity and conductivity plays the major role. This division is based on the order of magnitude analysis of an unsteady viscous flow in the following. From the characteristic of the viscous diffusion of an unsteady flow it is known (for example see Chapter V of Reference (4)) that thickness of the velocity boundary layer,  $\frac{r_0}{\sqrt{2}}$ , at a given time under an accelerated flow is  $\sqrt{\frac{\nu t}{l}}$ . Where  $l$  is the characteristic length,  $t$ , the characteristic time, and  $\nu$ , the kinematic viscosity of the propellant gas. Also it is known (for example see Chapter XII, p. 270 Effect of Prandtl Number of Ref. (4)) that the temperature boundary layer is of same order as the velocity layer if the Prandtl number of the fluid is of the order of magnitude one. Consider that for the present problem  $l$  is the radius of the barrel, 0.6 inches, and  $t$ , the duration of the projectile in the barrel, 2 milliseconds. Then the maximum boundary layer thickness is only one hundredth of the radius. Therefore 99% of the gas flow near the center of the barrel is not affected by the viscosity and the conductivity of the fluid. Hence a core analysis may be performed independently of barrel wall conditions. When the core solution is obtained the boundary

layer solution can be solved. Also when the cooling liquid film is included, the analysis in the boundary layer becomes a rather complicated two-phase flow. Fig. IV-1 illustrates the division of the analysis in the following sections.

#### IV-2 Assumptions

According to the general physical understanding, the following assumptions are made.

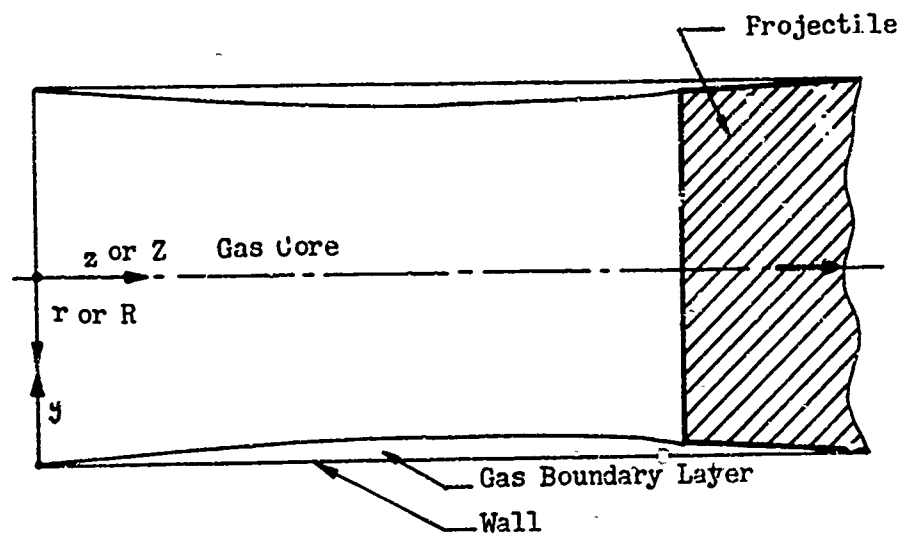
- (1) The flow is not too far away from the laminar flow and the Navier-Stokes Equations can be used for the present analysis.
- (2) The gravitational force is negligible.
- (3) The flow is axially symmetric (i.e.,  $\frac{\partial}{\partial \phi} = 0$ ) and there is no circumferential velocity component (i.e.,  $V = 0$ ).
- (4) The liquid layer is incompressible, and the gas is compressible.
- (5) The flow is periodic in time.
- (6) The wall is smooth but non-isothermal.
- (7) Transport properties are constant.

#### IV-3 Governing Equations

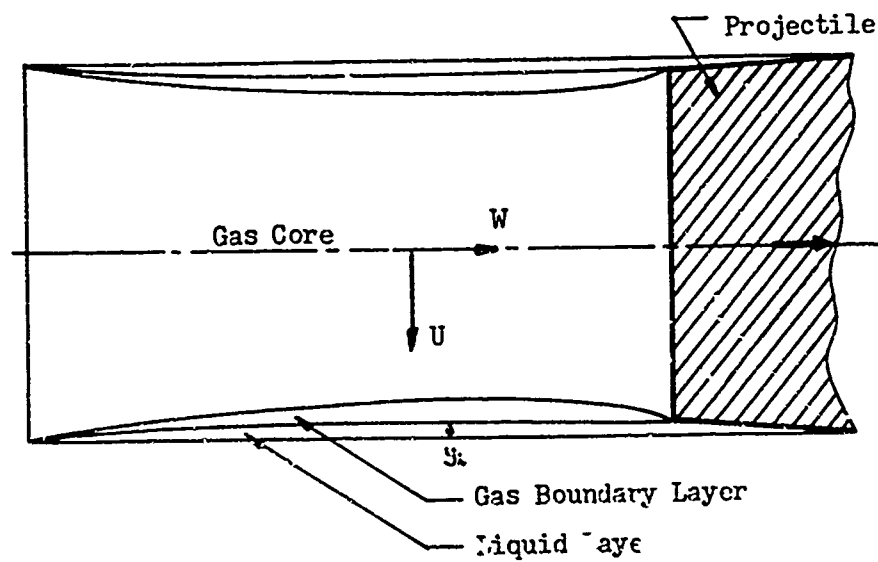
It will be convenient to take the cylindrical coordinate system with axis being the center line of the barrel. Let  $(U, V, W)$  be the velocity components in the direction of  $(R, \phi, Z)$  respectively. Then  $U, W, T, P$  are functions of  $(\bar{t}, R, Z)$  (see Fig. IV-1). For the gas stream (without subscript):

##### (A) Continuity equation

$$\frac{\partial \bar{P}}{\partial \bar{t}} + \frac{1}{R} \frac{\partial}{\partial R} (\bar{P} R U) + \frac{\partial}{\partial Z} (\bar{P} W) = 0 \quad (4-1)$$



(a) Flow without cooling



(b) Flow with cooling

Fig. IV-1. Schematic Drawing of Flow Fields

## (B) Momentum equations

R-direction,

$$\bar{p} \left( \frac{\partial U}{\partial t} + U \frac{\partial U}{\partial R} + W \frac{\partial U}{\partial Z} \right) = -\frac{\partial p}{\partial R} + \mu \left[ \bar{\nabla}^2 U + \frac{1}{3} \frac{\partial}{\partial R} (\bar{\nabla} \cdot \underline{\underline{f}}) - \frac{U}{R^2} \right] \quad (4-2)$$

where  $\mu$  is the viscosity of the gas, and

$$\underline{\underline{f}} = U \hat{i} + W \hat{j} \quad \text{where } \hat{i} \text{ and } \hat{j} \text{ are unit vectors}$$

$$\bar{\nabla} \cdot \underline{\underline{f}} = \frac{1}{R} \frac{\partial}{\partial R} (RU) + \frac{\partial W}{\partial Z}$$

$$\bar{\nabla}^2 = \frac{1}{R} \frac{\partial}{\partial R} \left( R \frac{\partial}{\partial R} \right) + \frac{\partial^2}{\partial Z^2}$$

Z-direction,

$$\bar{p} \left( \frac{\partial W}{\partial t} + U \frac{\partial W}{\partial R} + W \frac{\partial W}{\partial Z} \right) = -\frac{\partial p}{\partial Z} + \mu \left[ \bar{\nabla}^2 W + \frac{1}{3} \frac{\partial}{\partial Z} (\bar{\nabla} \cdot \underline{\underline{f}}) \right] \quad (4-3)$$

## (C) Energy equation

$$\begin{aligned} \bar{p} c_p \left( \frac{\partial T}{\partial t} + U \frac{\partial T}{\partial R} + W \frac{\partial T}{\partial Z} \right) &= \frac{k}{R} \frac{\partial}{\partial R} R \frac{\partial T}{\partial R} + k \frac{\partial^2 T}{\partial Z^2} + \frac{\partial p}{\partial t} + U \frac{\partial p}{\partial R} \\ &+ W \frac{\partial p}{\partial Z} + \mu \bar{\Phi} + Q_h \end{aligned} \quad (4-4)$$

where

$$\bar{\Phi} = 2 \left[ \left( \frac{\partial U}{\partial R} \right)^2 + \left( \frac{U}{R} \right)^2 + \left( \frac{\partial W}{\partial Z} \right)^2 \right] + \left( \frac{\partial U}{\partial Z} + \frac{\partial W}{\partial R} \right)^2 - \frac{2}{3} \left[ \frac{1}{R} \frac{\partial}{\partial R} (RU) + \frac{\partial W}{\partial Z} \right]^2 \quad (4-5)$$

$k$  is the thermal conductivity of the gas,  $Q_h$  is the heat generation due to combustion.

(D) Equation of state

$$P = \bar{P} \bar{R} T C_c \quad (4-6)$$

where  $C_c$  is a correction factor depending on the range of pressure under consideration. For a pressure below 37 kpsi  $C_c$  is 0.726 approximately.

For the liquid layer (with subscript  $l$ ):

(A) Continuity equation

$$\frac{1}{R} \frac{\partial}{\partial R} (R U_l) + \frac{\partial}{\partial z} W_l = 0 \quad (4-7)$$

(B) Momentum equations

R-direction,

$$\bar{\rho}_l \left( \frac{\partial U_l}{\partial t} + U_l \frac{\partial U_l}{\partial R} + W_l \frac{\partial U_l}{\partial z} \right) = - \frac{\partial P_l}{\partial R} + \mu_l \left[ \frac{1}{R} \frac{\partial}{\partial R} \left( R \frac{\partial U_l}{\partial R} \right) + \frac{\partial^2 U_l}{\partial z^2} - 2 \frac{U_l}{R^2} \right] \quad (4-8)$$

where  $\bar{\rho}_l$  and  $\mu_l$  are density and viscosity of the liquid layer respectively.

Z-direction,

$$\bar{\rho}_l \left( \frac{\partial W_l}{\partial t} + U_l \frac{\partial W_l}{\partial R} + W_l \frac{\partial W_l}{\partial z} \right) = - \frac{\partial P_l}{\partial z} + \mu_l \left[ \frac{1}{R} \frac{\partial}{\partial R} \left( R \frac{\partial W_l}{\partial R} \right) + \frac{\partial^2 W_l}{\partial z^2} \right] \quad (4-9)$$

(C) Energy equation

$$\bar{\rho}_l C_p \left( \frac{\partial T_l}{\partial t} + U_l \frac{\partial T_l}{\partial R} + W_l \frac{\partial T_l}{\partial z} \right) = k_l \left[ \frac{1}{R} \frac{\partial}{\partial R} \left( R \frac{\partial T_l}{\partial R} \right) + \frac{\partial^2 T_l}{\partial z^2} \right] \quad (4-10)$$

$T_l$  and  $k_l$  are temperature and thermal conductivity respectively.

Here we have nine unknowns (i.e., liquid  $U_l$ ,  $W_l$ ,  $P_l$ ,  $T_l$ , and gas  $U$ ,  $W$ ,  $P$ ,  $T$ ,  $\bar{\rho}$ ) with nine equations.



## IV-4 Boundary and matching conditions

## (1) Boundary Conditions

At wall ( $R = R_0$ )

$$\bar{u}_z(\bar{t}, R_0, z) = 0 \quad (4-11)$$

$$\bar{T}_l = \bar{T}_{l,w}(\bar{t}, \bar{t}) \quad (4-12)$$

At breach  $z = z_p(0)$ 

$$P = P_b(\bar{t}, R, z_p(0))$$

$$W = W_b(\bar{t}, R, z_p(0))$$

$$\bar{u} = 0 \quad (4-13)$$

$$T = T(\bar{t}, R, z_p(0))$$

At the projectile at any instance  $z = z_p(t)$ 

$$P = P_p(\bar{t}, R, z_p(t))$$

$$W = W_p(\bar{t}, R, z_p(t)) \quad (4-14)$$

$$\bar{u} = 0$$

$$T = T(\bar{t}, R, z_p(t))$$

## (2) Matching conditions (the subscript 1 denoting the gas-liquid interface)

## (A) Kinematic condition

The continuity of velocity components

$$\bar{u}_{1,1} = \bar{u}_1, \quad \bar{w}_{1,1} = \bar{w}_1 \quad (4-15)$$

## (B) Dynamic condition

The continuity of normal stress

$$P_{1,1} + 2\mu_1 \left( \frac{\partial \bar{u}_1}{\partial R} \right)_1 = P_1 + 2\mu \left( \frac{\partial \bar{u}}{\partial R} \right)_1 \quad (4-16)$$

The continuity of tangential stress

$$\mu_1 \left( \frac{\partial \bar{w}_1}{\partial R} + \frac{\partial \bar{u}_1}{\partial z} \right)_1 = \mu \left( \frac{\partial W}{\partial R} + \frac{\partial \bar{u}}{\partial z} \right)_1 \quad (4-17)$$

## (C) Thermodynamic conditions

The conservation of energy

$$\Delta h + k_L \left( \frac{\partial T_L}{\partial R} \right)_A = K \left( \frac{\partial T}{\partial R} \right)_A \quad (4-18)$$

The continuity of temperature

$$T_{L_A} = T_A \quad (4-19)$$

where  $\Delta h$  is the heat of evaporation. However  $\Delta h$  is negligible for the operating pressure near or above the critical pressure of the fluid. For water the critical pressure is 3.21 kpsi.

## IV-5 Nondimensionalization

We make the above variables dimensionless by letting

$$\begin{aligned} u_R &= \frac{U_R}{U_r} & w_L &= \frac{W_L}{U_r} & p_L &= \frac{P_L}{\rho_r U_r^2} & \theta_L &= \frac{T_L}{T_r} & \gamma &= \frac{Q_h L}{\rho_r C_p T_r U_r} \\ u &= \frac{U}{U_r} & w &= \frac{W}{U_r} & p &= \frac{P}{\rho_r U_r^2} & \theta &= \frac{T}{T_r} & \phi &= \frac{\Phi L^2}{U_r^2} \\ r &= \frac{R}{L} & z &= \frac{Z}{L} & t &= \frac{t}{t_r} & p &= \frac{P}{P_r} \end{aligned} \quad (4-20)$$

where  $\bar{U}_r$ ,  $\rho_r$ ,  $L$ ,  $t_r$ ,  $T_r$ , are dimensional characteristic quantities defined as follows with typical values in the parentheses.

$L$  = characteristic length of the barrel (3.478 ft)

$U_r$  = projectile velocity at exit. (2130.8 ft/sec)

$t_r$  = characteristic time  $\frac{L}{U_r}$  (1.6322 millisec.)

$\rho_r$  = density of the propellant gas right behind the projectile at the exit (5.504 lb<sub>m</sub>/ft<sup>3</sup>)

$T_r$  = characteristic temperature  $\frac{U_r^2}{R}$  (2173.9 °R)

$D$  = diameter of the barrel (1.2 inch)

$P$  = characteristic pressure  $\rho_r U_r^2$  (5.388 kpsi)

$M_o$  = molecular weight of the propellant gas (23.805)

$\bar{R}$  = Gas constant  $\left( \frac{1545.33}{M_o} = 64.9142 \frac{\text{ft} \cdot \text{lb}_f}{\text{lb}_m \cdot ^\circ \text{R}} \right)$

$\Delta h$  = latent heat

with known transport properties

$$\mu = 2.8 \times 10^{-5} \frac{\text{lb}_m}{\text{ftsec}} \quad (\text{see TABLE IVA})$$

$$\gamma = 1.243 \quad \frac{\text{lb}_m}{\text{ftsec}}$$

$$\mu_g = 0.071 \times 10^{-3} \frac{\text{lb}_m}{\text{ftsec}}$$

$$K = 0.04 \text{ Btu/hr.ft } ^\circ\text{R} \quad (1500 ^\circ\text{F}) \quad (\text{gas})$$

$$K_g = 0.35 \text{ Btu/hr.ft } ^\circ\text{R} \quad (500 ^\circ\text{F})$$

$$c_p = 0.435 \text{ Btu/lb } ^\circ\text{R} \quad (\text{gas})$$

$$c_{p_g} = 0.35 \text{ Btu/lb } ^\circ\text{R} \quad (\text{gas})$$

Define the dimensionless parameter:

$$\text{Reynolds number } R_e = \frac{U_r \rho_r L}{\mu}$$

$$\text{Prandtl number } P_r = \frac{c_p \mu}{K}, \quad P_{r_g} = \frac{c_{p_g} \mu_g}{K_g}$$

$$\text{Eckert number } E = \frac{U_r^2}{c_p T_r} = \frac{\gamma - 1}{\gamma}, \quad E_g = \frac{U_r^2}{c_{p_g} T_r}$$

We have then the governing equations, in dimensionless form as

(1) For the gas stream

(A) Continuity equation

$$\frac{\partial \rho}{\partial t} + \frac{1}{r} \frac{\partial}{\partial r} (\rho r u) + \frac{\partial}{\partial z} (\rho w) = 0 \quad (4-21)$$

(B) Momentum equations

$$\rho \left[ \frac{\partial u}{\partial t} + u \frac{\partial u}{\partial r} + w \frac{\partial u}{\partial z} \right] = -\frac{\partial p}{\partial r} + \frac{1}{R_e} \left[ \nabla^2 u - \frac{u}{r^2} + \frac{1}{3} \frac{\partial}{\partial r} (\nabla \cdot \underline{\underline{g}}) \right] \quad (4-22)$$

$$\rho \left[ \frac{\partial w}{\partial t} + u \frac{\partial w}{\partial r} + w \frac{\partial w}{\partial z} \right] = -\frac{\partial p}{\partial z} + \frac{1}{R_e} \left[ \nabla^2 w + \frac{1}{3} \frac{\partial}{\partial z} (\nabla \cdot \underline{\underline{g}}) \right] \quad (4-23)$$

where

$$\nabla \cdot \underline{\underline{g}} = \frac{1}{r} \frac{\partial}{\partial r} (r u) + \frac{\partial w}{\partial z}$$

$$\nabla^2 = \frac{1}{r} \frac{\partial}{\partial r} \left( r \frac{\partial}{\partial r} \right) + \frac{\partial^2}{\partial z^2}$$

TABLE IVA    Viscosity of equilibrium air  
( from ARS Journal, Aug. 1961, p.1152 )

T (*K)	$\mu$ (millipoise)				
	0.1 atm	1 atm	10 atm	100 atm	1000 atm
3000	0.87	0.86	0.85	0.85	0.85
4000	1.13	1.12	1.09	1.08	1.07
5000	1.37	1.36	1.34	1.32	1.29
6000	1.67	1.61	1.58	1.54	1.51
7000	1.97	1.91	1.82	1.78	1.74
8000	2.20	2.17	2.11	2.03	1.97

(C) Energy equation

$$\rho \left[ \frac{\partial \theta}{\partial t} + u \frac{\partial \theta}{\partial r} + w \frac{\partial \theta}{\partial z} \right] = \frac{1}{Pr Re} \nabla^2 T + E \left[ \frac{\partial p}{\partial t} + u \frac{\partial p}{\partial r} + w \frac{\partial p}{\partial z} \right] \quad (4-24)$$

$$+ \frac{E}{Re} \phi + q$$

(D) Equation of state

$$p = \rho \theta C_c \quad (4-25)$$

(2) For the liquid layer

(A) Continuity equation

$$\frac{1}{r} \frac{\partial}{\partial r} (r u_r) + \frac{\partial w_r}{\partial z} = 0 \quad (4-26)$$

(B) Momentum equations

R-direction

$$\frac{\rho_l}{r} \left( \frac{\partial u_r}{\partial t} + u_r \frac{\partial u_r}{\partial r} + w_r \frac{\partial u_r}{\partial z} \right) = - \frac{\partial p_r}{\partial r} + \frac{1}{Re} \frac{\mu_l}{\mu} \left[ \nabla^2 u_r - \frac{u_r}{r^2} \right] \quad (4-27)$$

Z-direction

$$\frac{\rho_l}{r} \left( \frac{\partial w_r}{\partial t} + u_r \frac{\partial w_r}{\partial r} + w_r \frac{\partial w_r}{\partial z} \right) = - \frac{\partial p_r}{\partial z} + \frac{1}{Re} \frac{\mu_l}{\mu} \left[ \nabla^2 w_r \right] \quad (4-28)$$

(C) Energy Equation

$$\left( \frac{\partial \theta_r}{\partial t} + u_r \frac{\partial \theta_r}{\partial r} + w_r \frac{\partial \theta_r}{\partial z} \right) = \frac{1}{Pr_l Re} \frac{\rho_l \mu_l}{\rho_l \mu} \left[ \nabla^2 \theta_r \right] \quad (4-29)$$

(3) Boundary and matching conditions

At wall ( $r = r_0$ )

$$u_r = w_r = 0 \quad (4-30)$$

$$\theta_r = \theta_{rw}(t, z)$$

At breech ( $z = 0$ )

$$p = p_b(t, r, 0)$$

$$w = 0$$

$$u = 0$$

$$\theta = \theta(t, r, 0)$$

$$(4-31)$$

At projectile ( $z = z_p$ )

$$p = p_p(t, r, z_p)$$

$$w = w_p(t, r, z_p)$$

$$u = 0$$

(4-32)

$$\theta = \theta_p$$

At interface

$$u_{21} = u_1, w_{21} = w_1$$

(4-33)

$$\left( p + \frac{\mu_2}{\mu_1} \frac{z}{R_e} \frac{\partial u_1}{\partial r} \right)_i = \left( p + \frac{z}{R_e} \frac{\partial u}{\partial r} \right)_i$$

(4-34)

$$\frac{\mu_2}{\mu_1} \left( \frac{\partial w_1}{\partial r} + \frac{\partial u_1}{\partial z} \right)_i = \left( \frac{\partial w}{\partial r} + \frac{\partial u}{\partial z} \right)_i$$

$$\frac{k_2}{k} \left( \frac{\partial \theta_1}{\partial r} \right)_i = \left( \frac{\partial \theta}{\partial r} \right)_i$$

(4-35)

Obviously the above problem is difficult to solve. However with the division of flow region given in IV-1 we may proceed to solve the problem in the following sections.

## V ANALYSIS OF CORE SOLUTION

## V-1 Core Problem

From the general consideration in Section IV-1 we found that the boundary layer thickness is very small compared with the diameter of the barrel. The propellant gas flow near the center of the barrel can be solved by neglecting the boundary layer. Accordingly, the analysis becomes that of one-dimensional unsteady compressible flow with the governing equations as follows:

$$\frac{\partial \rho}{\partial t} + \frac{\partial}{\partial z}(\rho w) = 0 \quad (5-1)$$

$$\rho \left( \frac{\partial w}{\partial t} + w \frac{\partial w}{\partial z} \right) = - \frac{\partial p}{\partial z} \quad (5-2)$$

$$\rho \left( \frac{\partial \theta}{\partial t} + w \frac{\partial \theta}{\partial z} \right) = E \left( \frac{\partial p}{\partial t} + w \frac{\partial p}{\partial z} \right) + q_{core} \quad (5-3)$$

$$p = c_p \rho \theta = 0.726 \rho \theta \quad (5-4)$$

where  $\rho, w, p$  and  $\theta$  are unknown core density, velocity, pressure, and temperature.  $q_{core}$  is the heat generation of the propellant gas.

The above governing equations are solved with the following boundary and initial conditions

$$\text{at } z = z_p(0) \quad w = 0 \quad p = p_b(t) \text{ (breach pressure)} \quad (5-5)$$

$$\text{at } z = z_p(t) \quad w = w_p = \frac{dz_p}{dt}$$

where  $z_p(t)$  is the projectile position at the given instant. For the present case  $z_p(0) = 0.04642$ .

$$\text{At } z_p = 0.268 \text{ (where data is available) } \rho = 2.21 \quad (5-6)$$

where  $\rho$  is determined in Appendix VA.

$$\text{at } t = 0 \quad w = 0 \quad (5-7)$$

The projectile position as function of time is obtained from the experiment through the method of least squares as (standard round)

$$z_p = 0.04642 + 0.92578 t^2 - 0.11475 t^3 - 0.00919 t^4 \quad (5-8)$$

Thus we have the projectile velocity

$$w_p = \frac{dz_p}{dt} = 1.85156 - 0.34425 t^2 - 0.03676 t^3 \quad (5-9)$$

Equations (5-8) (5-9) are plotted in Fig. V-1 and Fig V-2.

#### V-2 Method of Solution

We assume that the density is a function of time only. This assumption leads to a sufficient condition of Lagrange's assumption which has been shown by Heiney (5) to be an adequate one for the interior ballistic problem. Under this assumption the pressure and temperature are still functions of the position,  $z$ , and time,  $t$ . From Eq. (5-1) we have

$$\frac{\partial w}{\partial z} = -\frac{1}{\rho} \frac{\partial \rho}{\partial t}, \quad \rho = \rho(t)$$

Integrating with respect to  $z$

$$w = -\frac{1}{\rho} \frac{d\rho}{dt} z + f_n(t)$$

Noting that at  $z = 0$ ,  $w = 0$ , so that  $f_n(t) = 0$ , and that at  $z = z_p$ ,  $w = w_p$ , we have

$$w = \frac{w_p}{z_p} z \quad (5-10)$$

$$\frac{\frac{dz_p}{dt}}{z_p} = -\frac{1}{\rho} \frac{d\rho}{dt} \quad (5-10a)$$

Integrating Eq (5-10a) with respect to  $t$

$$\rho(t) = \frac{C'}{z_p}$$

where  $C'$  is integration constant and is determined as  $C' = 0.5928$  by using the condition in Eq (5-6).



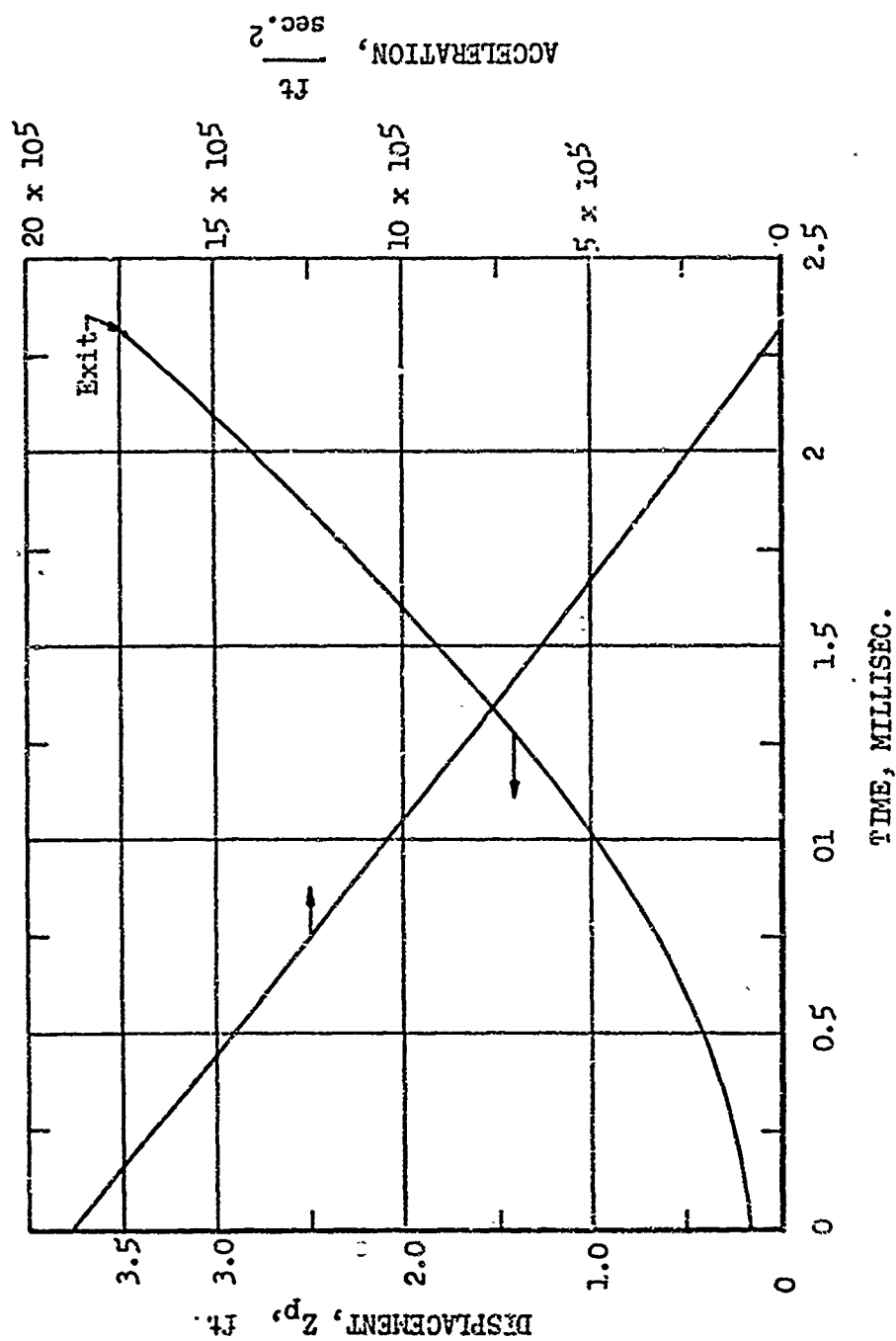


Fig. V-1 Projectile Displacement and Acceleration v.s. Time

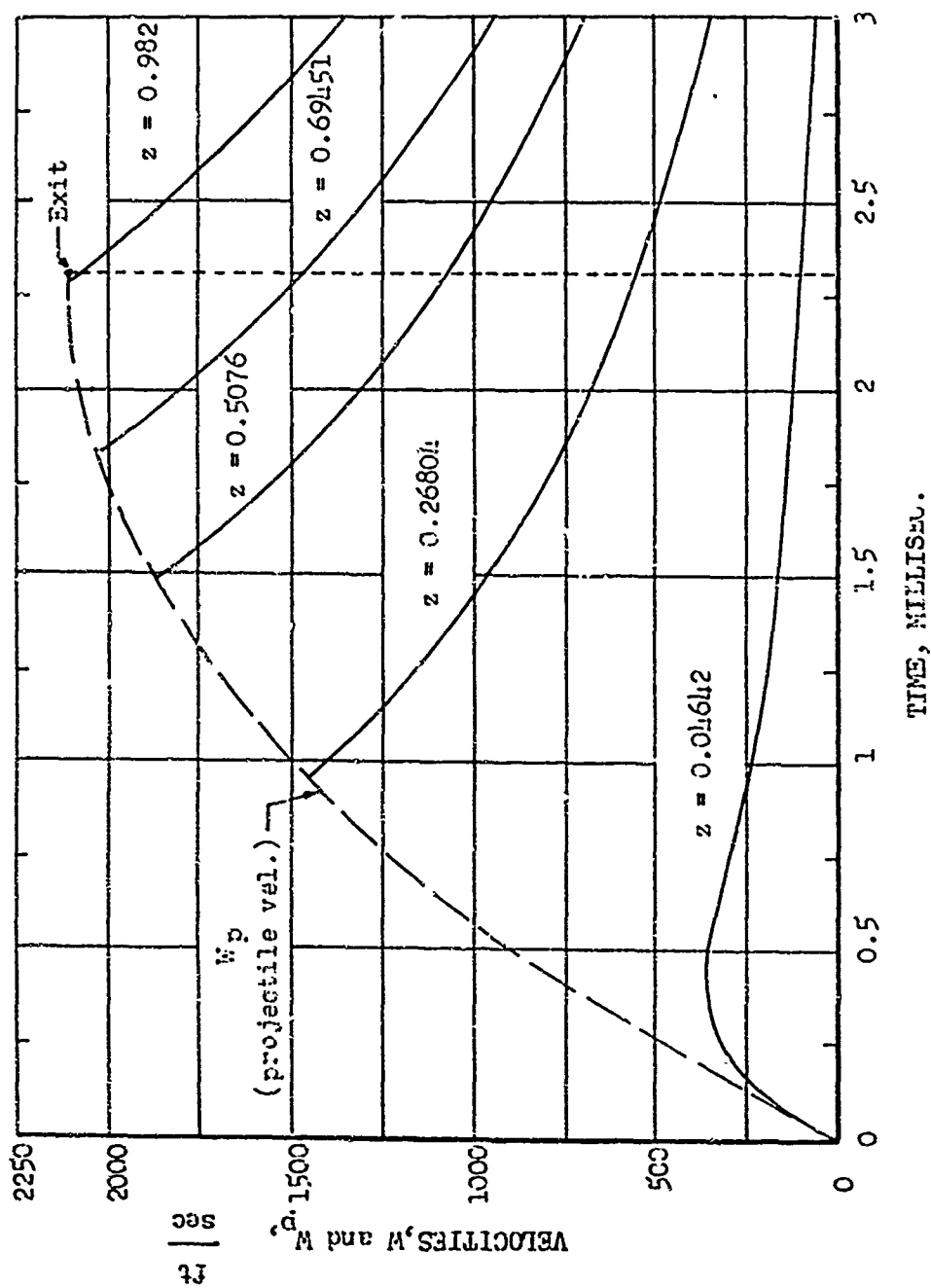


Fig. V-2 Gas velocity in Core,  $W$ , and Projectile Velocity,  $W_p$ , v.s. Time  
 (  $z = \frac{Z}{L}$ ,  $L = 3.478$  ft )

Then

$$\rho(t) = \frac{0.5928}{z_p(t)} \quad (5-11)$$

To find the pressure distribution we substitute Eqs. (5-10a) and (5-11) into (5-2) and integrate to obtain

$$P(z,t) = p_b(t) - \frac{C' \ddot{z}_p (z^2 - z_p^2(o))}{z_p^2} \quad (5-12)$$

after satisfying the boundary condition (5-5). The temperature profile follows readily by substituting (5-10a), (5-11), and (5-12) into Eq. (5-4).

That is

$$\theta = \left[ \frac{p_b z_p}{0.5928} - \frac{\ddot{z}_p (z^2 - z_p^2(o))}{2 z_p} \right] \frac{1}{0.726} \quad (5-13)$$

From energy equation (5-3) we obtained the heat generation of the propellant

as

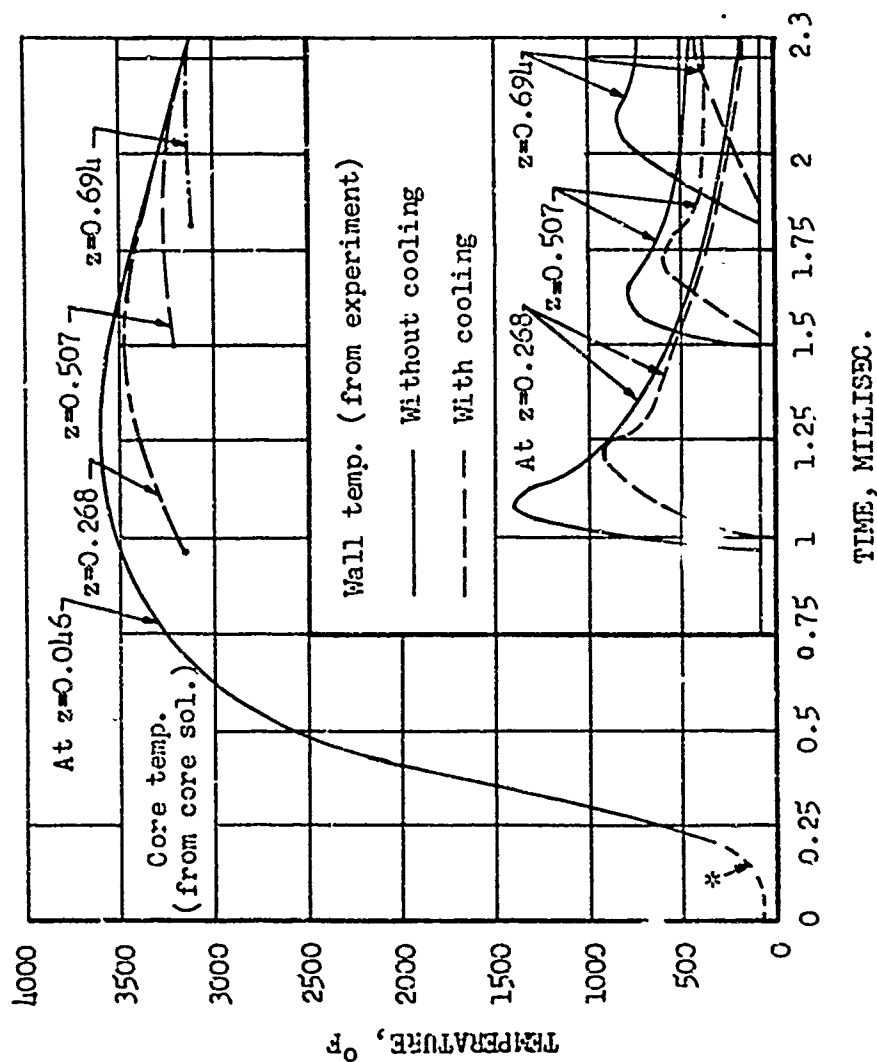
$$q_{core} = - \frac{C' (z^2 - z_p^2(o))}{2 z_p^2} \left\{ \frac{\ddot{z}_p}{\gamma} + \frac{\dot{z}_p \dot{z}_p}{z_p} \right\} + \left[ \frac{p_b \dot{z}_p}{z_p} + \frac{\dot{p}_b}{\gamma} \right] - \frac{\dot{z}_p \dot{z}_p}{z_p^3 \gamma} z_p^2(o) C' \quad (5-14)$$

where the dot denotes the differentiation with respect to time (i.e.,

$\frac{d(\quad)}{dt} = (\dot{\quad})$ ). Therefore we have solved the core solution of the interior ballistic problem in terms of the projectile motion,  $z_p(t)$ , breech pressure,  $p_b(t)$ , for IMR propellant. The solution is computerized in Appendix B. The propellant gas velocity,  $w$ , behind the projectile, the temperature,  $T = QT_r$ , the density,  $\rho$ , pressure,  $p$ , and heat generation  $q_{core}$  are all plotted in figures V-2 V-3, V-4, II-3, and V-5.

### V-3 Result and Discussion

Although many works on core solution of the interior ballistics are available such as Spurk [6], Heiney [5] Love and Pidduck [7], Vottis [8], and Carriere [9] the present solution has an advantage that the burning rate of



Note: Dashed line in '\*' indicates uncertainty

Fig. V-3 Core Propellant Gas and Wall Temperatures at Various Positions

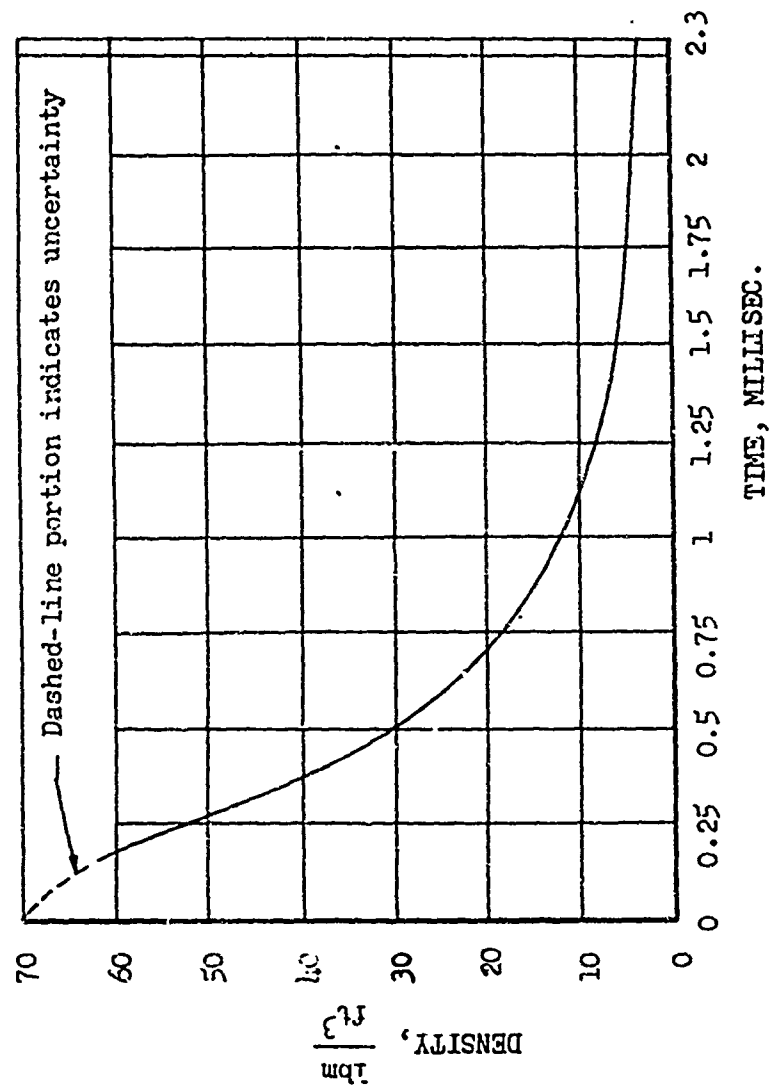


Fig. 7-4 Density v.s. Time in Core

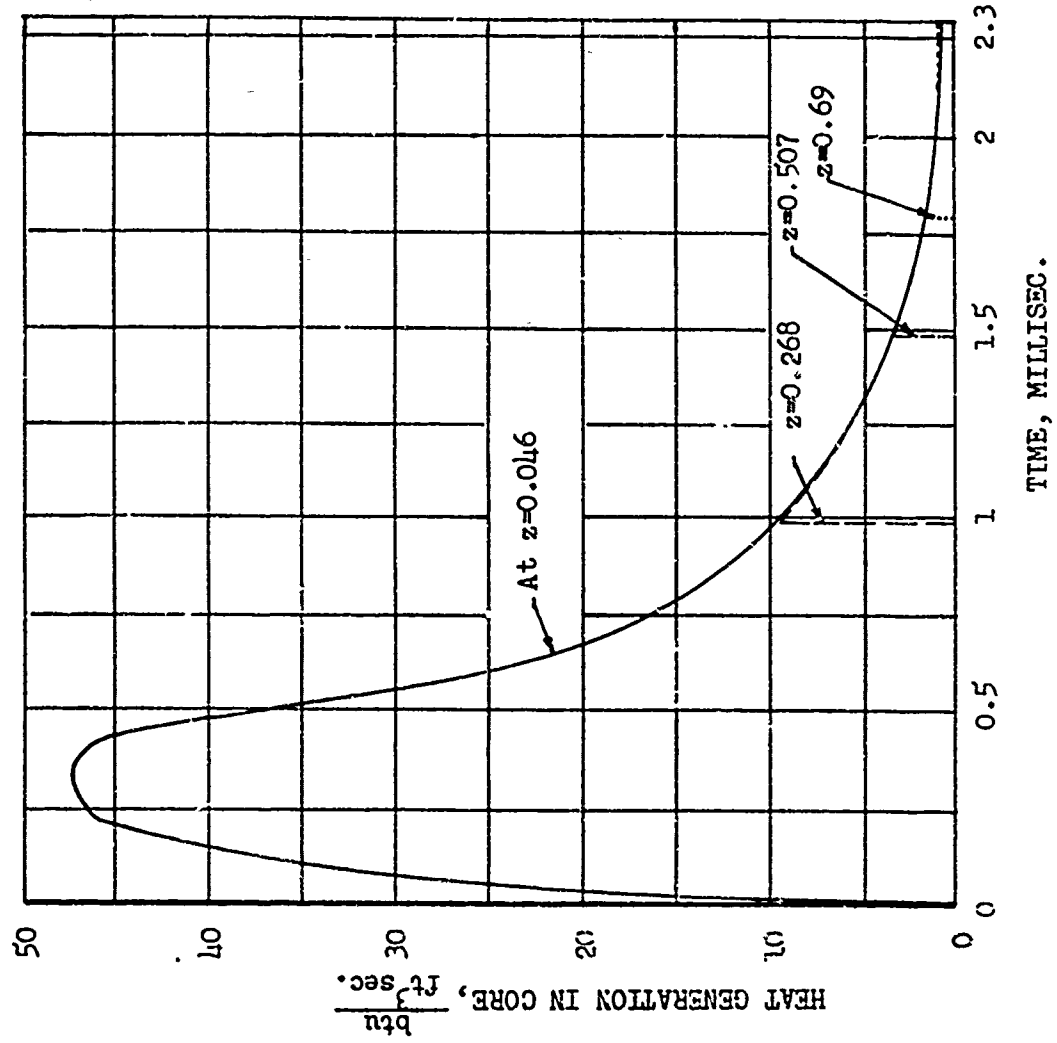


Fig. V-5 Heat Generation v.s. Time in Core  
(  $z = \frac{Z}{L}$ ,  $L = 3.478$  ft )

the propellant and the friction between the projectile and the barrel are not assumed, instead, they are all absorbed in the specified boundary conditions of projectile motion and the breech pressure. Both boundary conditions come directly from experimental measurements. Hence the error due to assumptions of burning rate and friction effects are eliminated. Also the present solution has an advantage of simplicity in analytical form over the solution obtained from theory of characteristics.

In the theory of characteristics the solution must be obtained from series of numerical evaluation of characteristics. Furthermore when heat generation is included in the gas flow the characteristic solution can become very complicated. Therefore the present solution although less versatile is more desirable for prediction of convective heat transfer through the gas boundary layer.

In Fig. V-2 we plot both projectile velocity and fluid velocity behind the projectile. The dashed line is the experimental data obtained in Fig. V-1 while the solid lines show the theoretical gas velocity. It is interesting to note that the gas velocity near the breech end first increases and then decreases, but at a larger distance the gas velocity decreases monotonically with time.

Fig. V-3 shows the predicted core temperature and measured wall temperature with and without cooling. The difference in the core temperature and wall temperature at a given time drives the heat flux from the core to the barrel. We note that at any given time the core temperature behind the projectile always decreases from the breech to the muzzle end. However the wall temperature at a given time with and without cooling increases from the breech to the muzzle end. More will be discussed in Chapter VI when boundary

layer analysis is given. Fig. V-4 gives the density variation with respect to time. The dashed at the small time was computed from the core solution. However in this period because propellant combustion is strong it is felt that the core solution should not be taken too seriously for its validity. Fig. V-5 is the plot of heat generation in the core. It is obvious that generation is the largest near the breech end. About 80 percent of total heat generation is confined in the ten percent of the barrel length near the breech.

With the core solution obtained the heat transfer and gas dynamics of boundary layer flow behind the projectile may be analyzed.



## VI BOUNDARY LAYER SOLUTION WITHOUT COOLING

### VI-1 Governing Equation and Similarity Transform

As already discussed in Chapter IV there are two flow regions in the barrel. One is the core stream in the central portion of the barrel and the other is the boundary layer near the wall. This boundary layer flow will be analyzed here. According to the boundary layer theory (see Ref. (4)) the pressure in the boundary layer is still that of core solution. The other dependent variables such as density, temperature, velocity, and heat generation must now be a function of an additional variable  $r$  which does not appear in the core analysis. The core solution now becomes the outer boundary condition of the boundary layer, while the wall condition is the other condition of the flow. Only when this flow is solved can the heat transfer between the propellant gas and the barrel be predicted. This problem is much more complicated to analyze in comparison with steady boundary layer flow because there are three independent variables  $r, t, z$  and both outer and wall condition are non isothermal and unsteady.

In dealing with this complicated problem, we note that Reynolds number in the flow is  $Re = \frac{\rho_r U_r L}{\mu} = 1.45 \times 10^9$  (or, in the conventional definitions  $Re = \frac{\rho_r U_r R_0}{\mu} = 2.9 \times 10^7$ ) which is very large. Consequently, the boundary layer thickness, in order of  $\frac{1}{\sqrt{Re}}$ , is very small. Therefore, for the boundary layer flow we shall define the new variables

$$y = \sqrt{Re} (r_0 - r), \text{ distance from the internal wall of the barrel, and}$$

$$u = \sqrt{Re} u, \text{ velocity in } y\text{-direction} \quad (6-1)$$

to stretch the small quantities  $(r_0 - r)$  and  $u$  so that each term in the governing equations in these new variables is of order of unity. Upon neglecting the terms of small order we reduced the Eqs. (4-21) through (4-24) in terms of new variables,  $y$  and  $u$ , of gas boundary layer as

## Continuity Equation

$$\frac{\partial \rho}{\partial t} + \frac{\partial}{\partial y} u \rho + \frac{\partial}{\partial z} w \rho = 0 \quad (6-2)$$

## Momentum Equations

In y - direction

$$-\frac{\partial p}{\partial y} = 0 \quad (6-3)$$

In z - direction

$$\rho \left( \frac{\partial w}{\partial t} + u \frac{\partial w}{\partial y} + w \frac{\partial w}{\partial z} \right) = -\frac{\partial p}{\partial z} + \frac{\partial^2 w}{\partial y^2} \quad (6-4)$$

## Energy Equation.

$$\rho \left( \frac{\partial \theta}{\partial t} + u \frac{\partial \theta}{\partial y} + w \frac{\partial \theta}{\partial z} \right) = \frac{1}{Pr_g} \frac{\partial^2 \theta}{\partial y^2} + E \left( \frac{\partial p}{\partial t} + u \frac{\partial p}{\partial y} + w \frac{\partial p}{\partial z} \right) + E \left( \frac{\partial w}{\partial y} \right)^2 + q_{B.L.} \quad (6-5)$$

## Equation of State

$$p = \rho \theta 0.726 \quad (\text{see Eq. (5-12) for } p) \quad (6-6)$$

Considering the solution form obtained in the core solution we see that the independent variable  $z$  can be separated out in the boundary layer flow by setting

$$w(t, y, z) = H(t, y) z \quad \rho = \rho(t, y) \quad (6-7)$$

Furthermore, the heat generation  $q_{B.L.}$  in Eq. (6-5) is assumed to possess the similar form of  $q_{core}$  in Eq. (5-3), that is

$$q_{B.L.} = \rho \left( \frac{\partial \theta}{\partial t} + w \frac{\partial \theta}{\partial z} \right) - E \left( \frac{\partial p}{\partial t} + w \frac{\partial p}{\partial z} \right) \quad (6-8)$$

And it is noted that the Eckert number

$$E = \frac{U_r^2}{c_p T_r} = \frac{\gamma - 1}{\gamma} \approx 0.195$$

in the present case. The term  $E \left( \frac{\partial w}{\partial y} \right)^2$  is thus negligible compared with other terms in Eq. (6-5) which are of order of unity.

Substituting Eqs. (6-6), (6-7), and (6-8) into Eqs. (6-2) to (6-5) we have the resulting governing equations

$$\frac{\partial \rho}{\partial t} + \frac{\partial}{\partial y} u \rho + \rho H = 0 \quad (6-9)$$

$$\rho \left( \frac{\partial H}{\partial t} + u \frac{\partial H}{\partial y} + H^2 \right) = c' \frac{z_p}{z_p^2} + \frac{\partial^2 H}{\partial y^2} \quad (6-10)$$

$$-P_{r_g} u \frac{\partial \rho}{\partial y} = \frac{2}{\rho} \left( \frac{\partial \rho}{\partial y} \right)^2 - \frac{1}{\rho} \frac{\partial^2 \rho}{\partial y^2} \quad (6-11)$$

These unsteady compressible boundary layer equations are solved with initial and boundary conditions to be described in VI-2. The method of similarity transformation will be used to solve the above problems. The method of similarity transformation can be divided into two kinds, i.e., via separation of variables and one-parameter group theory. The excellent references for the latter method can be found in the books by Hansen [10] and Ames [11] and the paper by Morgan [12].

From the present experimental result we found that  $\frac{z_p}{z_p^2}$  in equation (6-10) could be approximated by a form of  $\frac{z_p}{z_p^2} = m t^n$  as shown in Fig. VI-1, where both  $m$  and  $n$  are constants. This makes it possible to apply one-parameter group theory of similarity transform to reduce our partial differential equations into a set of ordinary differential equations which can be solved numerically. In order to satisfy the invariant requirement of the method we have to choose the similarity variables as follows

$$\begin{aligned} \xi &= t & \eta &= t^{-A} y \\ \rho &= \xi^{1-2A} f_1(\eta) & u &= \xi^{A-1} f_2(\eta) \\ H &= \xi^{-1} f_3(\eta) \end{aligned} \quad (6-12)$$

where

$\xi$  and  $\eta$  are new variables in another group

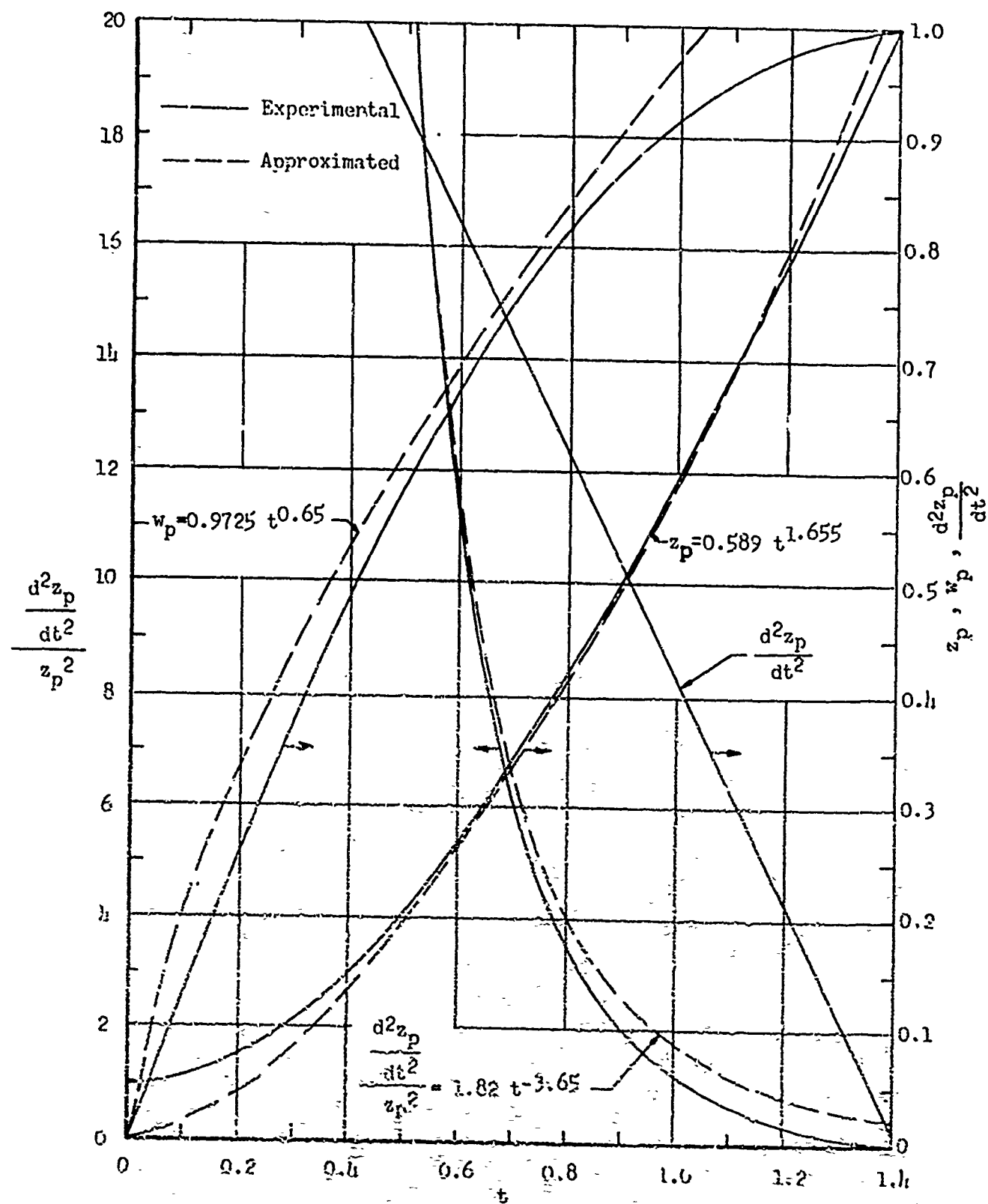


Fig. 9I-1 Comparison of Experimental and Approximated Values for Boundary Layer Analysis

$$A = -\frac{n+1}{2}, \quad n \text{ is the index of } mt^n$$

$f_1$ ,  $f_2$ , and  $f_3$  are arbitrary functions of  $\eta$ .

Substituting Eq. (6-12) into Eqs (6-9), (6-10), and (6-11) we have a set of ordinary differential equations

$$(f_2 + \frac{n+1}{2} \eta) f_1' + f_1 f_2' + (f_3 + n+2) f_1 = 0 \quad (6-13)$$

$$(f_1 f_2 + \frac{n+1}{2} \eta f_1) f_3' + (f_3 - 1) f_1 f_3 - f_3'' = m \eta' \quad (6-14)$$

$$2 f_1^{-2} f_1'^2 + P_g f_2 f_1' - f_1^{-1} f_1'' = 0 \quad (6-15)$$

where the primes denote the differentiation with respect to  $\eta$ . The detailed derivation is presented in Appendix VIIA. From Fig VI-1 we see that

$$\frac{d^2 z_p}{dt^2} / z_p^2 = m t^n \text{ can be approximated by } 1.82 t^{-3.65}, \text{ i.e., } m = 1.82, n = -3.65.$$

These values give  $A = 1.325$ . The above differential equations then can be rewritten for XM140 model as

$$(f_2 - 1.325 \eta) f_1' + f_1 f_2' + (f_3 - 1.65) f_1 = 0 \quad (6-13a)$$

$$(f_1 f_2 - 1.325 \eta f_1) f_3' + (f_3 - 1) f_1 f_3 - f_3'' = 1.08 \quad (6-14a)$$

$$2 f_1^{-2} f_1'^2 + P_g f_2 f_1' - f_1^{-1} f_1'' = 0 \quad (6-15a)$$

## VI-2 Initial and Boundary Conditions

It is seen that five conditions that combined initial and boundary conditions are needed to solve the problem.

At the wall,  $y = 0$ , or  $\eta = 0$ , the density related function can be approximated from the experimental data (see Appendix VI B) as

$$f_1(\eta) = 3.2$$

and the no-slip and impermeable condition give

$$f_2(0) = 0 \quad \text{for } u = 0 \quad (6-16)$$

$$f_3(0) = 0 \quad \text{for } w = 0$$

From the core stream,  $y \rightarrow \infty$ ,  $\eta \rightarrow \infty$ , no gradients in  $y$  direction can exist, thus

$$\begin{aligned} f_1'(\infty) &= 0 & \text{for } \frac{\partial \rho}{\partial y} &= 0 \\ f_3'(\infty) &= 0 & \text{for } \frac{\partial w}{\partial y} &= 0 \end{aligned} \quad (6-17)$$

### VI-3 Method of Solutions

The IBM 360 CSMP (Continuing System Modeling Program) computer language was employed to provide the numerical solutions. As CSMP program handles initial value problem, only condition (6-16) at  $\eta = 0$  can be used. Therefore, we must guess the values of  $f_1'(0)$  and  $f_3'(0)$  such that  $f_1'(\infty) = 0$  and  $f_3'(\infty) = 0$  at  $\eta \rightarrow \infty$ . After several attempts were made we found that  $f_1'(0) = -0.12$  and  $f_3'(0) = 2.024$  provided us satisfactory results. The computerized print-plots are presented in table and figures in Appendix VIC.

We examine the convergence of solutions in the following manner. From Eq (6-7) we have  $\rho = t^{1-2A} f_1(\eta) = t^{-1.65} f_1(\eta)$ . Now as  $\eta \rightarrow \infty$  the density in the boundary layer,  $\rho$ , should approach  $\rho_{\text{core}} = \frac{C'}{z_p}$ , where  $C' = 0.5928$  and  $z_p = 0.589 t^{1.65}$  approximated from Fig. IV-1. Thus

$$\rho(t, \infty) = t^{-1.65} f_1(\infty) = \frac{0.5928}{0.589} t^{-1.65} = t^{-1.65}.$$

that is,  $f_1(\infty) = 1$  at  $\eta \rightarrow \infty$ . This condition is satisfied by the numerical solution as shown in the first figure in Appendix VIC.

From Eq. (6-13a), as  $\eta \rightarrow \infty$ ,  $f_1' \rightarrow 0$ ,  $f_2' \rightarrow 0$ , then  $f_3 = 1.65$ . From the computerized print-plots it is seen that  $f_2$  converges to  $-2.426$  where  $f_2' \rightarrow 0$  satisfying  $\frac{\partial \rho}{\partial y} = 0$ , and  $f_3$  converges to  $1.65$ , as  $\eta$  goes larger.

Finally, Eqs. (6-12) and (6-7) can be rewritten as

$$\eta = t^{-1.325} y \quad (6-18)$$

$$\rho = t^{-1.65} f_1(\eta) \quad (6-19)$$

$$u = t^{0.325} f_2(\eta) \quad (6-20)$$

$$w = Hz = t^{-1} f_3(\eta) z \quad (6-21)$$

With these expressions and the table in Appendix VIC we are able to evaluate the values of  $\rho$ ,  $u$ , and  $w$  for any given value of  $\eta$ .

Now we examine the validity of our prior boundary layer approximation, in which we assume the boundary layer is thin compared with barrel diameter.

To evaluate the maximum boundary layer thickness that occurs at the maximum time  $t = 1.409$ , dimensionless, (the time the projectile exits) we observe from  $F_3$  plot in Appendix VIC that the velocity approaches the core solution  $f_3 \rightarrow 1.65$  at  $\eta \rightarrow 4$ . That is in  $y$  dimensionless coordinate

$$y = t^{1.325} \eta = (1.409)^{1.325} 4 = 6.3$$

The boundary layer thickness is estimated to be

$$(r_o - r) = \frac{y}{\sqrt{Re}} = \frac{6.3}{\sqrt{1.45 \times 10^9}} = 1.66 \times 10^{-4}$$

$$r_o = \frac{R_o}{L} = \frac{0.6}{42} = 1.43 \times 10^{-2}$$

thus

$$\frac{(r_o - r)}{r_o} = \frac{1.66 \times 10^{-4}}{1.43 \times 10^{-2}} = \frac{1}{86}$$

It is readily seen that the ratio of boundary layer thickness to the barrel radius is  $\frac{1}{86}$  which is about one percent of the barrel radius. Therefore, we conclude that our prior boundary layer approximation is valid.

#### VI-4 Heat Transfer

Now we should consider heat flux from the gas to the cold wall and the heat transfer coefficient in the temperature field.

From the equation of state and the expressions for  $p$  and  $\rho$  in Eqs(5-12) and (6-19), respectively, we obtain

$$\theta = \frac{p}{0.726\rho} = t^{1.65} \frac{f_1^{-1}}{0.726} \left\{ p_h - 1.08t^{-3.65} \frac{z^2 - z_p^2(0)}{2} \right\} \quad (6-22)$$

Here we should remark that the boundary condition  $f_1(0) = 3.2$  in Eq(6-16) was approximated one. For the detailed evaluation is referred to Appendix VIB. In this approximation we did not take into account of the short time interval in which the temperature changed from room temperature to the approximated mean value,  $750^\circ\text{F}$ . Therefore, the temperature profile obtained from Eq. (6-22) and heat transfer formulas must exclude that short time interval.

Under the above restriction the local heat transfer is given by Fourier's law

$$q = -k \frac{\partial T}{\partial R} \Big|_{R=R_0} \quad (6-23)$$

Recall that

$$y = \sqrt{Re} \left( \frac{R_0}{L} - \frac{R}{L} \right) = \sqrt{Re} (r_0 - r)$$

Defining  $Nu = \frac{qL}{k Tr} = \frac{hL}{k}$ , Nusselt number, from the modified Newton's cooling law  $q = hTr$  we obtain the dimensionless form of Eq(6-23) as,

$$Nu = \sqrt{Re} \frac{\partial \theta}{\partial y} \Big|_{y=0} \quad (6-24)$$

The expression for  $\frac{\partial \theta}{\partial y} \Big|_{y=0}$  can be derived from Eq. (6-22). Upon substituting we obtain

$$Nu = -\sqrt{Re} \frac{f_1'(t)}{f_1(t)} \frac{t^{0.325}}{0.726} \left[ p_h(t) - 1.08 t^{-3.65} \frac{(z^2 - z_p^2(t))}{2} \right] \quad (6-25)$$



where  $f_1'(0) = -0.12$ ,  $f_1(0) = 3.2$  are obtained previously from similarity solution. Thus we have for laminar unsteady compressible flow in a pipe with a standard projectile the local heat transfer coefficient as

$$Nu = \frac{hL}{k} = 0.01614 \sqrt{Re} t^{0.325} \left[ P_b(t) - 1.08 t^{-3.65} \frac{(3^2 - 3_{p(0)}^2)}{2} \right] \quad (6-26)$$

Since the last term in the equation (6-26) usually is small compared with  $P_b$  term for approximate evaluation the Nusselt number may be taken as

$$Nu = 0.01614 \sqrt{Re} t^{0.325} P_b(t) \quad (6-27)$$

where

$$P_b = \text{dimensionless breech pressure} = \frac{P_b}{\rho_r U_r^2}$$

$U_r$  = the exit velocity

$\rho_r$  = the reference density right behind the projectile at the exit.

$$Re = \frac{U_r L}{\nu}$$

#### VI-5 Discussion

From the  $f_2$  print-plot in Appendix VIC we note that  $f_2$  ( $F_2$  in computer program notation) keeps increasing till a value of  $\eta = 1.4$  is reached. Then it starts decreasing and finally converges to a value of  $f_2 = -2.426$ . As the vertical component of gas velocity  $u$  relates to  $f_2$  by Eq(6-20) this means that there are two flows coming together from the wall and the core, respectively, and then joining at a region where  $\eta = 1.4$ . We note that the true value of the velocity  $u$  is very small since  $\eta$  relates to  $u$  by  $u = -u\sqrt{Re}$  in which  $Re$  generally is very large. Therefore, the radial velocity  $u$  does not affect significantly the one dimensional core flow outside the boundary layer.

In the following an example and a comparison of the present result with incompressible steady state flat plate boundary layer solution may illustrate the procedure for calculation. Consider the heat transfer calculation with present formula at the time  $t = 1.2$  (i.e.  $\bar{t} = 1.9586$  milliseconds) and the position  $z = 0.5076$  (i.e.  $Z = 1.7655$  ft from breech) we have for the standard projectile in XM 140 model

$$\rho_r = 5.504 \frac{\text{lb}_m}{\text{ft}^3}$$

$$U_r = 2130.8 \frac{\text{ft}}{\text{sec.}}$$

$$L = 3.478 \text{ ft}$$

$$\mu = 2.8 \times 10^{-5} \frac{\text{lb}_m}{\text{ft sec.}}$$

$$P_r = 0.962 \text{ (at } t = 1.2)$$

$$P_r = 5.04 \text{ Kpsi}$$

$$T_r = 2174 \text{ }^\circ\text{R}$$

$$\beta_{p(0)} = 0.0464$$

$$Re = \frac{\rho_r U_r L}{\mu} = 1.4567 \times 10^9 \quad K = 0.04 \frac{\text{Btu}}{\text{hr ft } ^\circ\text{R}}$$

Thus from Eq. (6-26) we have

$$Nu = \frac{hL}{k} = 5.82 \times 10^3$$

the heat flux is then

$$q = hTr = 403 \text{ Btu/ft}^2\text{sec.}$$

Although there is no similarity for the physical phenomenon between the present solution and steady laminar flow. If however the laminar solution is applied instantaneously at a local position some comparison may be made. We thus now assume that at the time  $t = 1.2$  and position  $z = 0.5076$  the steady incompressible flow solution (see p. 285 of Ref. 4) applies the above example.

That is

$$Nu_z = \frac{h_z}{k} = 0.332 \cdot \left( \frac{U z \rho_r}{\mu} \right)^{0.5} (N_{Pr})^{0.133} \quad (6-28)$$

where

$$U = 1375 \text{ ft/sec (from core solution)}$$

$$Z = 0.5076 \times L$$

$$N_{Pr} = \text{Prandtl number} = 0.75$$

Thus

$$Nu_z = \frac{h_z}{k} = 0.7237 \times 10^4$$

heat transfer is

$$q = h(T_{\text{core}} - T_{\text{wall}}) =$$

$$= \frac{0.7237 \times 10^4 \times k}{0.5076 \text{ L}} (3250 - 520) = 1340 \frac{\text{Btu}}{\text{ft}^2 \text{sec.}}$$

The above comparison shows the steady state heat transfer over estimates heat transfer at  $t = 1.2$  and  $z = 0.507$ . Therefore the steady flow formula is not applicable to the present problem.

## VII THEORETICAL ANALYSIS OF TWO PHASE FLOW

In the analysis of liquid cooling effect many difficulties and uncertainties appear. For example, it is not known in what manner the cooling liquid is squeezed out from the modified projectile; how much of the liquid will get behind the projectile; and that whether or not the liquid will stay in a film layer. Also the extent of the influence of grooves on the cooling effect is not known. However an attempt is made to obtain some solutions even they are solved under crude assumptions. Therefore, the analysis herein should be viewed as preliminary result and further improvement certainly is necessary.

## VII-1 Determination of Liquid Film Thickness

In the following analysis we shall assume for lack of experimental evidence that the liquid squeezed out from the projectile will form a film behind the projectile. Then the total amount of the liquid behind the projectile,  $M_L(\bar{t})$ , from the breech to the projectile at any given time  $\bar{t}$  is

$$M_L(\bar{t}) = \bar{\rho}_L \pi D_o \int_0^{z_p} (R_o - R_i) dz \quad (7-1)$$

where  $z$  = axial length

$\bar{\rho}_L$  = liquid density = const.

$D_o$  = inside diameter of the barrel

$R_o - R_i$  = thickness of liquid film on the wall

$R_i$  = radius of interface

Eq. (7-1) can be written in dimensionless form as

$$m_L(t) = \frac{M_L(\bar{t})}{\rho_r L^3} = \rho_L \pi d_o \int_0^{z_p} (r_o - r_i) dz \quad (7-2)$$

where

$$\rho_2 = \frac{\rho_0}{\rho_1}$$

$$r_0 = \frac{R_0}{L}$$

$$r_1 = \frac{R_1}{L}$$

$$d_0 = \frac{D_0}{L}$$

$$z = \frac{Z}{L}$$

$$z_p = \frac{Z_p}{L}$$

$$a = \frac{\bar{A}}{L^2}$$

Although the exact amount of liquid,  $m_2(t)$ , at a given time is not known a crude estimate of  $m_2(t)$  is given in Appendix VIIA from which we have

$$m_2(t) = \rho_2 a \int_0^t \sqrt{\frac{p(t')}{\rho_2}} dt' \quad t \leq 1.409 \quad (7-2a)$$

where  $p(t')$  is the pressure at the base of the projectile.

The liquid layer thickness ( $r_0 - r_1$ ) may be approximated by a polynomial form.

$$r_0 - r_1 = f_a(t) [a_0 + a_1 z + a_2 z^2] \quad (7-3)$$

where  $f_a(t)$  = function of  $t$ , and

$a_0, a_1$ , and  $a_2$  are constants to be determined as follows.

At the breech,  $z = 0$ , ( $r_0 - r_1$ ) = 0, so that  $a_0 = 0$ . Eq. (7-3) becomes

$$r_0 - r_1 = f_a(t) [a_1 z + a_2 z^2] \quad (7-4)$$

Substituting Eq (7-4) into Eq (7-2) and integrating we obtain

$$m_2(t) = \rho_2 \pi d_0 f_a \left[ \frac{a_1}{2} z_p^2 + \frac{a_2}{3} z_p^3 \right] \quad (7-5)$$

At the position immediately behind the projectile,  $z = z_p$ ,  $r_0 - r_1 = h_1(t)$ . Where  $h_1(t)$  is the liquid thickness at the base of the projectile and is derived in Appendix VIIA. From Eq. (7-4) we have

$$h_1(t) = f_a [a_1 z_p + a_2 z_p^2] \quad (7-6)$$

Then  $a_1$  and  $a_2$  are determined from Eqs (7-5) and (7-6) as

$$a_1 = \frac{h_a'}{f_a z_p} - z_p \left[ \frac{3 h_a'}{f_a z_p^2} - \frac{6 m_e(t)}{\rho_e \pi d_o f_a z_p^3} \right] \quad (7-7)$$

$$a_2 = \frac{3 h_a'}{f_a z_p^2} - \frac{6 m_e(t)}{\rho_e \pi d_o f_a z_p^3}$$

Substituting Eq. (7-7) into Eq (7-4) and noting that  $y_1 = \sqrt{Re} (r_0 - r_1)$  we have

$$y_1 = \sqrt{Re} (r_0 - r_1) = \sqrt{Re} \left[ \left( 6 m_e - 2 h_a' z_p \rho_e \pi d_o \right) \frac{z}{z_p} + \frac{(3 h_a' z_p \rho_e \pi d_o - 6 m_e) z^2}{z_p^2} \right] \frac{1}{\rho_e \pi d_o z_p} \quad (7-8)$$

Once  $m_e$  (Eq. 7-2a),  $h_1$  (Eq. 7-6), and  $z_p$  (Eq. 5-8) are calculated the liquid film thickness,  $y_1$ , at a given time and a given position along z-axis can be evaluated from Eq. (7-8).

A alternative simple estimation of liquid film thickness is also presented as follows:

water filled in the projectile,  $M_0 = 0.039 \text{ lb}_m$ .

water density,  $\rho_e = 62.4 \text{ lbm/ft}^3$

diameter of the barrel,  $D_0 = 1.2 \text{ inches}$

length of the barrel,  $L = 3.478 \text{ ft}$

Consider that all water is completely squeezed out and uniformly coated on the wall of the barrel during the time interval,  $t = 0 \sim 2.3 \text{ m.s.}$  Then the liquid film thickness,  $R_0 - R_1$ , is

$$R_o - R_i = \frac{M}{\rho \pi D_o L} = \frac{0.039}{62.4 \cdot \pi \cdot \frac{1.2}{12} \cdot 3.478} = 5.725 \times 10^{-4} \text{ ft}$$

The ratio of  $R_o - R_i$  to barrel radius  $R_o$  is

$$\frac{R_o - R_i}{R_o} = 0.01145$$

which is one percent of the barrel radius.

## VII-2 Two-Phase Gas and Liquid Layer Flow

There are three zones in the flow, free stream (core solution) around the barrel center, liquid layer near the wall, and gas boundary layer in between. Among these regions the core solution is already obtained previously.

### VII-21 Gas Boundary Layers with Liquid Cooling

The liquid layer from the above estimation is very thin and the flow velocity in it is small compared with that in gas layer. Therefore, the existence of the liquid layer does not affect the gas velocity boundary layer presented in Chapter VI. For the gas temperature layer, since the cooler liquid film presents near the wall, it needs some modification. We thus assume that the mass flux  $\rho u$  in the  $y$  direction remains that of the gas boundary layer without cooling.

Substituting  $\theta = \frac{p}{\rho}$  into Eq. (6-11) we have the energy equation

$$\rho u \frac{\partial \theta}{\partial y} = \frac{1}{Pr_g} \frac{\partial^2 \theta}{\partial y^2} \quad (7-9)$$

Making the substitution for  $\rho$  and  $u$  from Eq. (6-12) and setting

$f_4 = f_1 f_2$ . Here  $f_4$  can be approximated by the following

$$f_4 = 7\eta - 5.225\eta^2 + 1.1923\eta^3 - 0.0874\eta^4 \quad \left(\eta = \frac{y}{\delta}\right) \quad (7-10)$$

we have  $t^{-A} f_4 \frac{\partial \theta}{\partial y} = \frac{1}{Pr_g} \frac{\partial^2 \theta}{\partial y^2}$ ,  $A = 1.325$

Dividing by  $\frac{\partial \theta}{\partial y}$ , it becomes

$$t^{-A} f_4 = \frac{1}{Pr_g} \frac{\frac{\partial^2 \theta}{\partial y^2}}{\frac{\partial \theta}{\partial y}} = \frac{1}{Pr_g} \frac{\partial}{\partial y} \ln \left( \frac{\partial \theta}{\partial y} \right)$$

Integrating once

$$\ln \frac{\partial \theta}{\partial y} = Pr_g t^{-A} \int_{y_a}^y f_4 dy + \bar{f}(t, z)$$

or

$$\frac{\partial \theta}{\partial y} = e^{Pr_g t^{-A} \int_{y_a}^y f_4 dy + \bar{f}(t, z)} \quad (7-11)$$

where  $\bar{f}(t, z)$  is a function of  $t$  and  $z$ .

Integrating Eq (7.11) once more

$$\theta = \int_{\infty}^y e^{Pr_g t^{-A} \int_{y_a}^y f_4 dy + \bar{f}(t, z)} dy + \bar{f}(t, z)$$

As  $y \rightarrow \infty$ ,  $\theta = \theta_{core} = \bar{f}$ , where  $\theta_{core}$  is given in Eq. (5-13)

Then the temperature distribution across the gas thermal boundary layer is

$$\theta = \theta_{core} - e^{\bar{f}(t, z)} \int_y^{\infty} e^{Pr_g t^{-A} \int_{y_a}^y f_4 dy} dy \quad (7-12)$$



with  $\theta = \theta_{gi}$  at  $y = y_1$  we have

$$e^{\tilde{f}(t,z)} = \frac{\theta_{gi} - \theta_{gi}}{\int_{y_1}^{\infty} e^{\rho_{12} t^{-A}} \int_{y_1}^y f_{12} dy dy} \quad (7-13)$$

The interface temperature will be determined by Eq (7-37) later. Here

$y_1(t,z)$  is the position of the interface, given in Eq. (7-8).

#### VII-22 Liquid Velocity Field

Since the velocities  $U_L$  and  $W_L$  in liquid layer are small, we consider viscosity and pressure terms only. The governing equation is, therefore, from Eq. (4-27) in  $y$  coordinate variable

$$\frac{\partial p}{\partial y} = \frac{\mu_L}{\mu} \frac{\partial^2 w_L}{\partial y^2} \quad (7-14)$$

Integrating with respect to  $y$

$$\frac{\partial w_L}{\partial y} = \frac{\mu}{\mu_L} \frac{\partial p}{\partial z} y + g_1(z) \quad (7-15)$$

At the gas-liquid interface the shear force should be matched, i.e.

$$\left. \frac{\partial w_L}{\partial y} \right|_{y_1} = \frac{\mu}{\mu_g} \left. \frac{\partial w}{\partial y} \right|_{y_1} \quad (7-16)$$

Then  $g_1(z)$  is determined as

$$g_1(z) = \frac{\mu}{\mu_L} \left( \left. \frac{\partial w}{\partial y} \right|_{y_1} - \frac{\partial p}{\partial z} y_1 \right)$$

Integrating Eq (7-15) once more

$$w_k = \frac{\mu_1}{\mu_2} \left[ \frac{\partial p}{\partial z} \frac{y^2}{2} + \frac{\partial w}{\partial y} \right]_k - \frac{\partial p}{\partial z} \frac{y_k^2}{2} + f_2(z) \quad (7-17)$$

It is readily seen that  $g_2(z) = 0$  for  $y = 0$ ,  $w_k = 0$ .

As the liquid layer is very thin we may approximate

$$\left. \frac{\partial w}{\partial y} \right|_k \approx \left. \frac{\partial w}{\partial y} \right|_{y=0} \quad (7-18)$$

which is obtained Chapter VI.

Since Eq. (6-7) gives  $w = z H(t, y)$ , we have

$$\left. \frac{\partial w}{\partial y} \right|_k = z \left. \frac{\partial H}{\partial y} \right|_k = z t^{-A-1} f_3'(0) = 2.024 z t^{-2.325} \quad (7-19)$$

where we have substituted  $H = t^{-1} f_3$  and  $f_3'(0) = 2.024$ .

Upon substituting Eq. (7-19) back to Eq. (7-17) and noting that

$$\frac{\partial p}{\partial z} = -1.08 t^{-3.65} z \quad (7-20)$$

from the core solution we obtain a final form for  $w_k$  in liquid layer

$$w_k = \frac{\mu_1}{\mu_2} \left[ -1.08 t^{-3.65} z \frac{y^2}{2} + 1.08 t^{-1.65} z y + 2.024 z t^{-2.325} y \right] \quad (7-21)$$

With the velocity profile known we may approximately solve the liquid energy equation by assuming that the dissipation is negligible.

We have the energy equation as

$$\frac{\partial \theta_l}{\partial t} + u_z \frac{\partial \theta_l}{\partial y} = \frac{1}{Q} \frac{\partial^2 \theta_l}{\partial y^2} \quad (7-22)$$

$$\text{where } \frac{1}{Q} = \frac{\rho_r \mu_l}{\rho_l \mu_r \rho_{rl}} \quad (7-23)$$

Since the equation is still complicated we solve it by an approximation method in which the temperature profile is assumed in view of Eq. (5-13) as

$$\theta_l = C_0(t, y) + C_1(t, y) z^2 \quad (7-24)$$

where  $C_0$  and  $C_1$  are to be determined with known conditions.

We know that at  $z = 0$ ,  $\theta_l = \theta_{l,c}(z=0)$  because there will be no liquid cooling or gas boundary layer. Thus we have  $C_0(t, y) = \theta_{l,c}(z=0)$ .

Eq. (7-24) becomes

$$\theta_l = \theta_{l,c}(z=0, t) + C_1(t, y) z^2 \quad (7-25)$$

If  $C_1(t, y)$  is further approximated by

$$C_1(t, y) = a_0(t) + a_1(t) y + a_2(t) y^2 \quad (7-26)$$

Now at  $y = 0$ ,  $\theta_l = \theta_{l,w}$  we have

$$\theta_{l,w} = \theta_{l,c}(z=0, t) + a_0(t) z^2 \quad (7-27)$$

$$a_0 = \frac{1}{z^2} [\theta_{l,w} - \theta_{l,c}(z=0, t)]$$

at  $y = y_1$ ,  $\theta_l = \theta_{l,g}$  we have

$$\theta_{l,g} = \theta_{l,c}(z=0, t) + [a_0(t) + a_1(t) y_1 + a_2(t) y_1^2] z^2 \quad (7-28)$$

Also from the governing equation (7-22) evaluated at  $y = 0$  we have

$$\frac{\partial \theta_{aw}}{\partial t} = \frac{1}{Q} \frac{\partial \theta_{aw}}{\partial y^2} \quad (7-29)$$

Substitute Eq. (7-26) into the right side of Eq. (7-29) we get

$$Q_z(t) = \frac{\partial \theta_{aw}}{\partial t} \frac{Q_z}{z} \quad (7-30)$$

Eq. (7-28) with Eq (7-30) gives

$$Q_z(t) = \frac{\theta_{gi} - \theta_{aw}}{y_i^2} - \frac{\partial \theta_{aw}}{\partial t} \frac{Q_z}{z} y_i \quad (7-31)$$

We therefore obtain the approximated temperature distribution in the liquid layer as

$$\theta_L(z, t, y) = \theta_{aw}(z=0, t) + (\theta_{gi} - \theta_{aw}) \frac{y}{y_i} + \frac{\partial \theta_{aw}}{\partial t} \frac{Q_z}{z} y^2 (y_i^2 - y_i^2) \quad (7-32)$$

If  $\theta_{gi}$ , the interface temperature, is known heat transfer can be easily calculated from Eq. (7-32) as

$$q = -k_L \frac{\partial T_L}{\partial R} \Big|_{R=R_0} = \frac{k_L T_r}{L} \sqrt{R_e} \frac{\partial \theta_L}{\partial y} \Big|_0 \quad (7-33)$$

When the heat transfer coefficient is defined as

$$q = h T_r \quad (7-34)$$

then the local Nusselt number is

$$N_u = \frac{hL}{k_L} = \sqrt{R_e} \frac{1}{y_i} \left[ \theta_{gi} - \theta_{aw} - \frac{\partial \theta_{aw}}{\partial t} y_i^2 \frac{Q_z}{z} \right] \quad (7-35)$$

where  $Q$  and  $y_i$  are given by Eq. (7-23) and (7-8) respectively. To derive the interface temperature,  $\theta_{gi}$ , theoretically we must match the liquid

temperature profile with the gas profile. To do this we use the matching condition of heat flux at interface  $y = y_i$ . That is

$$\left. \frac{\partial \theta}{\partial y} \right|_i = \frac{k_1}{K} \left. \frac{\partial \theta_1}{\partial y} \right|_i \quad (7-36)$$

Substitute Eqs. (7-11) and (7-13) for the left hand side of Eq. (7-36) and Eq. (7-32) evaluated at interface for the right hand side of Eq. (7-30) we have

$$\theta_{gi} = \frac{\theta_{core} + \frac{k_1}{K} \frac{1}{y_i} (\theta_{ew} - \frac{\partial \theta_{ew}}{\partial t} \frac{Q}{2} y_i^2) \int_{y_i}^{\infty} e^{-Pr t^{-1.325}} \int_{y_i}^x f_2 dy dy}{1 + \frac{k_1}{K} \frac{1}{y_i} \int_{y_i}^{\infty} e^{-Pr t^{-1.325}} \int_{y_i}^x f_2 dy dy} \quad (7-37)$$

It is suggested that this equation should be evaluated in the further study.

### VII-3 Discussion

First it should be remarked that the solution obtained is an approximated one. Further improvement and study is certainly needed. However some conclusion based on the present result may be drawn. Let us consider a calculation of heat transfer with liquid cooling by Eq. (7-35) for XM140 Model at  $t = 1.2$  and  $z = 0.507$ .

$$Nu = \frac{hL}{K_1} = \sqrt{Re} \frac{1}{y_i} \left[ \theta_{gi} - \theta_{ew} - \frac{\partial \theta_{ew}}{\partial t} \cdot \frac{Q}{2} y_i^2 \right] \quad (7-35)$$

Here  $y_i$  is the dimensionless liquid thickness. To estimate this thickness we assume that three quarters of liquid in the projectile may reach behind the projectile and is uniformly coated on the barrel surface. Thus from Eq. (7-8)

$$y_i = \sqrt{Re} \frac{(R_0 - R_i)}{4L} = \sqrt{1.456 \times 10^9} \frac{5.725 \times 10^{-4}}{4 \times 3.478} = 1.57$$

$(\theta_{gl} - \theta_{lw})$  in Eq. (7-35) is the dimensionless temperature difference between the gas liquid interface and the wall. To estimate this we assume that the gas-liquid interface temperature is approximately equal to that of the wall temperature of the standard round without cooling. From Fig II-2 we find that at  $z = 0.507$  (i.e., where  $s_2$  probe is located) at  $t = 1.2$  (i.e., 1.9586 milliseconds) the temperature difference is

$$\theta_{gl} - \theta_{lw} = \frac{T_{gi} - T_{lw}}{T_r} = \frac{500^\circ\text{F} - 420^\circ\text{F}}{2174^\circ\text{R}} = 0.0368$$

For  $\frac{\partial \theta_{lw}}{\partial t}$ , the time rate change of the wall temperature, we have from Fig II-2 at the same time and position as

$$\frac{\partial \theta_{lw}}{\partial t} = \frac{\Delta T_{lw}}{\Delta t} \frac{t_r}{T_r} = \frac{-120}{0.5} \frac{1.6322}{2174} = -0.032$$

$Q$  from Eq. (7-23) gives

$$Q = 3.489$$

Note that Reynolds number and the reference quantities are the same as given in Chapter IV. Now we may calculate the local Nusselt number from Eq. (7-35) as

$$Nu = \frac{hL}{k_e} = 4.63 \times 10^2$$

To calculate heat transfer we have from the definition of modified Newton's Law

$$\begin{aligned} q &= h \cdot T_i = \frac{Nu k_e}{L} T_r \\ &= 4.63 \times 10^2 \times \frac{0.32 \frac{\text{Btu}}{\text{hr ft } ^\circ\text{R}} \cdot 2174^\circ\text{R}}{3.478 \text{ ft}} \end{aligned}$$

or

62

$$q = 281 \frac{Rtu}{ft^2sec}$$

Recall that we had  $q = 403 \text{ Btu/ft}^2\text{sec}$  for without cooling. This means that there is approximately 30% in reduction of heat transfer to the wall at  $t = 1.2$  and  $z = 0.507$  when modified projectile was used. Although the above calculation gives approximately the right order of reduction in heat transfer it is felt that there are many assumptions involved that may not be easily verified.

An alternative short way to estimate the heat flux and its coefficient is presented as follows. From the experiment we learned that the heat flow does not reach the external wall of the barrel at  $\bar{t} = 2.3 \text{ m.s.}$  after the projectile was fired. We may, therefore, assume that within this time interval the heat transfer may be represented by the heat flow to a semi-infinite solid body exposed to a time-dependent temperature on the surface as  $\bar{t} > 0$ . See Fig VII-1. The internal barrel surface is simulated as the surface of the semi-infinite body. Then at a given position of  $z$  we have the following governing equation on solid wall side, in dimensional

$$\frac{\partial(T - T_0)}{\partial \bar{t}} = \alpha \frac{\partial^2(T - T_0)}{\partial y^2} \quad (7-38)$$

where

$T$  = temperature profile in the solid wall

$T_0$  = room temperature at  $t = 0$

$\bar{t}$  = time variable

$Y_s$  = distance from the surface pointing to the solid wall

$\alpha$  = the thermal diffusivity of the solid.

Let

$$\bar{T} = T - T_0 \quad (7-39)$$

$$\bar{t}' = \bar{t} - t_p$$

where

$t_p$  = the correspondent time where the projectile is located, in the barrel after the firing

We have Eq. (7-38)

$$\frac{\partial \bar{T}}{\partial \bar{t}'} = \alpha \frac{\partial^2 \bar{T}}{\partial Y_s^2} \quad (7-40)$$

with the initial condition

$$\text{at } t \leq t_p \text{ and } 0 \leq Y_s < \infty$$

$$\bar{t}' = 0 \text{ and } T = T_0, \bar{T} = 0 \quad (7-41)$$

and boundary conditions

$$\text{at } t > t_p \text{ or } \bar{t}' > 0$$

$$Y_s = 0 \quad T = T_w(\bar{t}', z), \bar{T} = T_w - T_0 = \bar{T}_w \quad (7-42)$$

$$Y_s \rightarrow \infty \quad \bar{T} = 0$$



The solution for  $\bar{T}$  is readily obtained from the book by Carslaw and Jaeger (13) p.62.

$$\bar{T} = \frac{Y_s}{2\sqrt{\pi d}} \int_0^{\bar{t}'} \frac{\bar{T}_w(\lambda, z) e^{-\frac{Y_s^2}{4d(\bar{t}'-\lambda)}}}{(\bar{t}'-\lambda)^{3/2}} d\lambda \quad (7-43)$$

and

$$\left. \frac{\partial \bar{T}}{\partial Y_s} \right|_0 = \frac{1}{2\sqrt{\pi d}} \int_0^{\bar{t}'} \frac{\bar{T}_w(\lambda, z)}{(\bar{t}'-\lambda)^{3/2}} d\lambda \quad (7-44)$$

where  $\lambda$  is a dummy variable. The internal surface temperature  $\bar{T}_w(\lambda, Z)$  is a function of time and position along Z-axis and can be approximated from experimental data. Once  $\bar{T}_w$  is known the integration in Eq (7.44) can be performed. However, the irregularity of the present experimental curves, Fig VII-1, did not allow us to provide an appropriate equation for  $\bar{T}_w$  at the time when this report was written. A further effort is certainly needed to investigate the Eq.(7.44).

Then the local heat flux to the solid wall is

$$q = -k_s \left. \frac{\partial \bar{T}}{\partial Y_s} \right|_0 = k \left. \frac{\partial \bar{T}}{\partial Y} \right|_0 \quad (7-45)$$

where

$-Y_s = Y$  = distance from the surface pointing to the gas flow

From Newton's cooling law we have

$$q = h(\bar{T}_{core} - \bar{T}_w) = h[(T_{core} - T_o) - (T_w - T_o)] \quad (7-46)$$

With Eq. (7-45) we have

$$h(\bar{T}_{core} - \bar{T}_w) = k_s \left. \frac{\partial \bar{T}}{\partial Y} \right|_0 \quad (7-47)$$

Then the heat coefficient is

$$h = \frac{k_s \left. \frac{\partial \bar{T}}{\partial y} \right|_0}{(\bar{T}_{core} - \bar{T}_w)} \quad (7-48)$$

Substituting for  $\left. \frac{\partial \bar{T}}{\partial y} \right|_0$  from Eq. (3-36) we obtain

$$h = \frac{k_s}{(\bar{T}_{core} - \bar{T}_w)} \frac{1}{2\sqrt{\pi d}} \int_0^{\bar{t}'} \frac{\bar{T}_w(\lambda, z)}{(\bar{t}' - \lambda)^{3/2}} d\lambda \quad (7.49)$$

Thus the local Nusselt number becomes

$$Nu = \frac{hL}{K} = \frac{k_s}{K} \frac{L}{2\sqrt{\pi d} (\bar{T}_{core} - \bar{T}_w)} \int_0^{\bar{t}'} \frac{\bar{T}_w(\lambda, z)}{(\bar{t}' - \lambda)^{3/2}} d\lambda \quad (7-50)$$

where

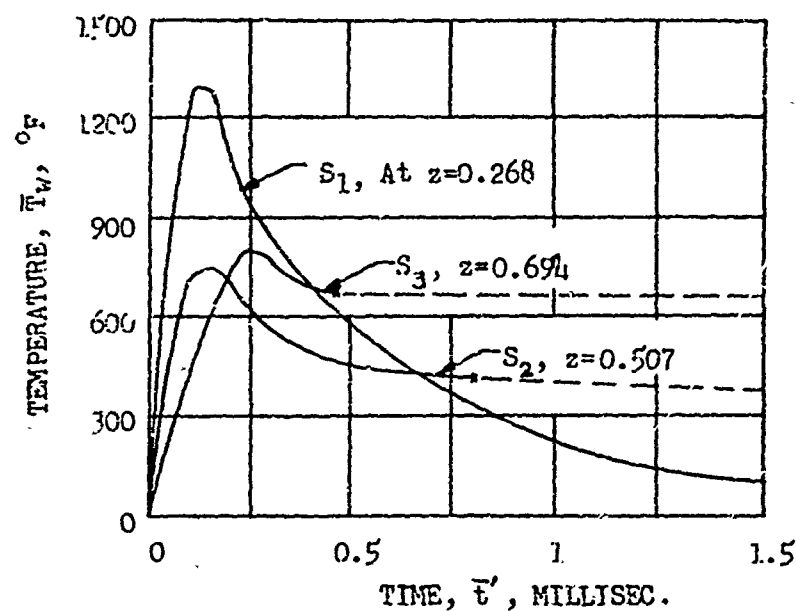
$k_s$  = Conductivity of solid wall

$k$  = Conductivity of gas boundary layer

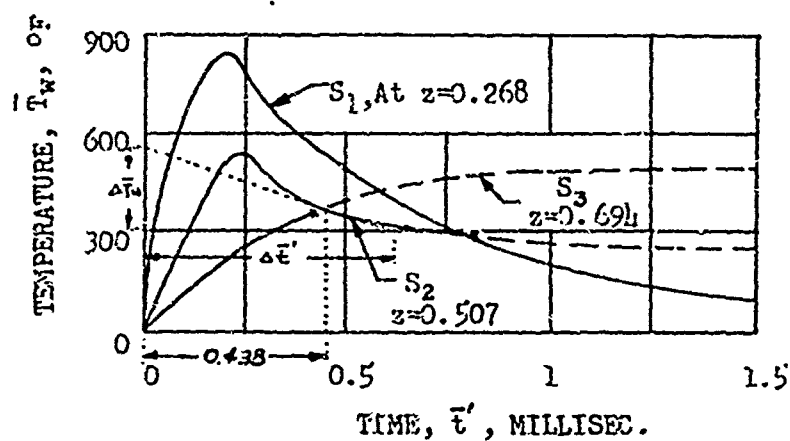
$\bar{T}_w(\bar{t}', z)$  = internal surface temperature of the barrel which is

given in Fig VII-1

Due to the irregularity of the experimental curves it is very difficult to provide an approximated curve to represent  $\bar{T}_w(\bar{t}', z)$  properly. However numerically integration of Eq(7-50) may be performed to find the local Nusslet number. It should be noted that for this Nusselt number the heat transfer calculation should follow the conventional Newton's cooling law given in Eq. (7-46).



(a) Without cooling



(b) with cooling

- Note: (1)  $\bar{T}_w = T_w - T_0$ , where  $T_w$  = absolute wall temperature,  $T_0$  = room temperature.  
 (2)  $\bar{t}' = \bar{t} - \bar{t}_p$ , where  $\bar{t}$  = any time from 0 to 2.3 millisecc.,  $\bar{t}_p$  = time interval for the projectile passes a given position after firing,  $\bar{t} \geq \bar{t}_p$ .  
 (3) Dashed lines indicate  $\bar{t} > 2.3$  millisecc., which does not apply to the present problem.

Fig. VII-1 Internal Wall temperatures,  $\bar{T}_w$ , With and Without Cooling v.s. Time,  $\bar{t}'$ .

## VIII RECOMMENDATION

The study of the last fifteen months under the contract recommends the following continuing studies:

- (A) The experimental results obtained up to now show that the modified projectile with coolant does have substantial cooling effect. However, much more data is needed in order to understand the mechanism of cooling and to calculate heat transfer. An improvement in measuring the interior surface temperature is needed. In particular, at the breech end a high temperature probe with fast response should be installed. This measurement is important since it is one of the boundary conditions needed in the heat transfer analysis. A measurement of the core temperature behind the projectile can be made by implanting a thermocouple in the projectile flush with its base. The thermocouple wire protected in plastic tube is led through the gun barrel to the muzzle end and is then connected to the recording device. To the present investigator's knowledge the measurement of core temperature following a projectile has not been done before.
- (B) Movie pictures may be used to record the spreading of the coolant when it comes out of the muzzle end.
- (C) Hot wire measurements of velocity and Schlieren pictures can be used to study the gas dynamic behavior of the mixing of the coolant and the propellant gas at the exit.
- (D) A series of continuous firing should be continued at the Rock Island Arsenal to determine the cooling effect of the modified projectile No. 2. That is to find for the modified projectile the maximum interior and exterior wall temperature, maximum heat transfer, maximum rounds of continuous firing within the limits of yield stress and cook-off.

(E) From the measured data, the friction between the modified projectile and the gun barrel, a parameter heretofore unavailable can be calculated. Hence, the efficiency of lubrication by the coolant may be determined.

(F) The mathematical analysis obtained under the present contract is preliminary in nature. Further study is certainly needed in order to achieve a better prediction. Refinement of the core solution can be achieved by considering that the density is both time and spatially dependent. The present laminar solution of unsteady, compressible flow should be extended to the turbulent region so that the effect of the mixing of the coolant and the propellant gas can be included.

(G) A suitable integral method can be developed for the turbulent, unsteady compressible gun barrel flow. This is not the conventional Kármán - Pohlhausen method since in the present case there are three independent variables namely, the axial variable,  $z$ , the radial variable,  $r$ , and the time,  $t$ . The derivation can be made specifically for the interior ballistics problem.

(H) Study of the flow in front of the projectile has little effect on heat transfer between the propellant gas and the gun barrel. However, in case of continuous firing gas dynamics in front of a projectile may appreciably affect the amount of heat transfer. These gas dynamic effects include the shock formation and the propagation of expansion waves.

(I) Eq. (7-37) should be computed to compare with the assumed experimental one.

(J) Some form of study on the mixing of the cooling liquid and the propellant gas should be initiated since it is important for the calculation of heat transfer.

(K) The effect of rifling groove must be considered in order that a better prediction of heat transfer coefficient can be achieved.

## REFERENCES

1. Cohn, G., "Cook-Off in Aircraft Guns", Report F-A2144-2, The Franklin Institute, June 1960.
2. Corner, J., "Theory of the Interior Ballistics of Guns", John Wiley and Sons, New York, 1950.
3. Adams, D.E., Brown, W.R. Miller, P.M., Sterbutzel, G.A., Vassallo, F.A., "Design Studies of the XM140 Barrel", Cornell Aeronautical Laboratory, Inc. Report No. GA-2324-W-1, Feb 1969.
4. Schlichting, H., "Boundary Layer Theory" Sixth Ed., McGraw-Hill Book Company, 1968.
5. Heiney, O.K., "Analytic and Experimental Interior Ballistics of Closed Breech Guns", AFATL-TR-69-42. Eglin Air Force Base, Florida 32542, May 1969.
6. Spurk J. H., "The Gas Flow in Gas-Operated Weapons" BRL R1475, Aberdeen Proving Ground, Maryland Feb. 1970.
7. Love E.H., and F. B. Pidduck "Lagrange's Ballistic Problem", Phil. Trans., A. Vol 222., p 167, 1921.
8. Vottis, P.M. "Digital Computer Simulation of the Interior Ballistic Process in Guns" WVT-6615, Watervliet Arsenal, New York, Oct. 1966.
9. C  rriere, P. "The Method of Characteristics Applied to the Problems of Interior Ballistics", Pro. 7th International Congress For Applied Mechanics (Paris) Vol 3, p. 139, 1948.
10. Hansen, A. G. "Similarity Analysis of Boundary Value Problem in Engineering" Prentice-Hall 1964.
11. Ames, W.F., "Non Linear Partial Differential Equations in Engineering", Academic Press 1965.
12. Morgan, A.J.A. "Similarity Transform" Quart-J Math(Oxford) 2, p. 250, 1952.
13. Carslaw, H.S. and J. C. Jaeger "Conduction of Heat in Solids" 2nd Ed. Oxford Press.

## APPENDIX IIA

## DETERMINATION OF MODIFIED PROJECTILE

Consider a total amount of water  $M_0 = 0.039$  lbm in a modified projectile to be squeezed out in a time interval of 2.3 milliseconds.

Based on Fig. II-3 we choose a mean pressure difference,  $\Delta p$ , between both ends of the small hole to be  $\Delta p = 10$  KPSi approximately.

Substituting into the formula

$$V = \sqrt{\frac{\Delta p}{\gamma} \cdot 2g}, \text{ where } V \text{ is the water velocity at the exit of the small hole.}$$

$$\text{We have } V = \sqrt{\frac{10 \times 10^3 \times 144}{62.4}} \times 2 \times 32.2 = 1220 \text{ ft/sec.}$$

Then the total area needed for the small holes is

$$A = 2.23 \times 10^{-4} \text{ ft}^2$$

If the number of the small holes is 8, then their diameter is

$$C = \sqrt{\frac{A}{\frac{\pi}{4} \times 8}} = 0.0715''$$

This leads us to use a diameter of  $\frac{3}{32}$  " ( $\approx 0.094$ " )

# APPENDIX IIB

```

*****
* CORE SOLUTION OF THE STANDARD RCOND PROJECTILE (PPCOF. NO. 3)
* TESTED ON JUNE 3, 1972
* THIS JOB IS TO FIND DPB,ZP1,ZP2,ZP3,R,PRD,P,THETA,Q,4ND W
* WITH GIVEN I,PB, AND ZP
* ALL VALUES ARE DIMENSIONLESS EXCEPT THOSE ARE SPECIFIED
* L=REF. LENGTH=LENGTH OF GUN BARREL=3.478 FT
* ZP=PROJECTILE POSITION
* ZP=0.7192 T**2-0.17357 T**3+0.0305 T**4+C.04642 BY THE
* METHOD OF LEAST SQUARES
* WHERE C.04642=INITIAL POSITION OF THE PROJECTILE AT TIME=0
* ZP1=VEL. OF THE PROJECTILE, ZP2=ACC. OF THE PROJECTILE,
* ZP3=DERIVATIVE OF ZP2 W.R.T. TIME
* R=DENSITY
* RCR=REF. DENSITY=0.1709 LB*SEC**2/FT**4, OR,=5.504 LBM/FT**3
* T=TIME HISTORY AFTER FIRING
* TFR=REF. TIME=L/UR=1.6322 M.S.
* W=VEL. OF THE FLUID BEHIND THE PROJECTILE,
* WP=VEL. OF THE PROJECTILE
* UR=REF. VEL.=PROJECTILE VEL. AT EXIT (ZP=1,T=2.315 M.S.)
* =2130.8 FT/SEC; REF. ACCELERATION= 1.305,477 ft/sec2
* P=PRESSURE,
* PR=REF. PRESSURE=R*(UR**2)=5.31 KPSI
* PU=PRESS. AT BRECH, FROM EXPERIMENTAL DATA
* PE=PRESS. AT EXIT =3 KPSI
* CPB=FIRST DERIVATIVE OF P W.R.T. TIME
* PRD=PRESS. GRADIENT=ZP2/ZP**2
* THETA=TEMPERATURE
* TR=REF. TEMP.=UR**2/(UNIVERSAL GAS CONST.)=2173.9 RANKINE DEG.
* Q=HEAT GENERATION. QR=REF. HEAT GENERATION=2,199,100 btu/ft**3-sec.
* T=0.77, 1.485, 1.8, AND 2.28 M.S. ARE THE POSITIONS WHERE
* PRESSURE PROBE P2,P3,P4, AND P5 RESPECTIVELY START TO RESPOND
* THE OUTPUT AT ZP=0.26894 SHOULD BE READ FROM T=0.513 TO T=1.409
* THE OUTPUT AT ZP=0.576 SHOULD BE READ FROM T=0.919 TO T=1.409
* THE OUTPUT AT ZP=0.69451 SHOULD BE READ FROM T=1.103 TO T=1.409
* THE OUTPUT AT ZP=0.922 SHOULD BE READ AT T=1.409
*****

```



```

1  DIMENSION A(6), PB(31), OPB(31), PR(31), PRP(31), PRED(31)
2  DIMENSION ZPP(31), ZPP1(31), ZPP2(31), ZPP3(31),
3  DIMENSION P(31), THETA(31), Q(31)
4  DIMENSION W(31)
5  DIMENSION Z(5)
6  READ(5,10.1) (A(I),I=1,6),(PB(J),J=1,31)
7  100 FORMAT (8F10.5)
8  DO 9 J=1,30
9  JJ=J+1
10  OPB(J)=(PB(JJ)-PB(J))*10,
11  5 CONTINUE
12  D=9(31)*0.2
13  READ(5,101) G
14  101 FORMAT (1F10.5)
15  READ(5,102) (Z(I),I=1,5)
16  102 FORMAT (5F10.5)
17  WRITE (6,1000)
18  1000 FORMAT (9X,'I
19  DO 1 I=1,6
20  WRITE(6,1001) I,A(I)
21  1001 FORMAT (11F,1F25.5/)
22  1 CONTINUE
23  WRITE (6,1002)
24  1002 FORMAT (///8X,'T
25  1T, '
26  Y=C
27  DO 2 J=1,31
28  WRITE (6,1010) Y, PB(J), OPB(J)
29  1010 FORMAT(1F10.3,2F25.5/)
30  C TIME INCREMENT
31  Y=Y+1/1.6322
32  WHERE 1.6322=REFERENCE TIME
33  2 CONTINUE

```

OPB(

PR(T)

```

31 DO 1012 L=1,5
32 Z=Z2(L)
33 WRITE (6,1003)
34 1003 FORMAT (//////////3X,'GAMMA FOLLOWS'//)
35 WRITE (6,1004) G
36 1004 FORMAT (1F15.5)
37 WRITE (6,1007)
38 1007 FORMAT (////5X,'Z FOLLOWS'//)
39 T=G,
40 WRITE (6,1004) Z
41 DO 3 K=1,31
C THE APPROXIMATED DISPLACEMENT OF THE PROJECTILE (FROM
C EXPERIMENTAL DATA) BY THE METHOD OF LEAST SQUARES
42 ZP=A(1)+T*A(2)+T**2+A(3)+T**3+A(4)+T**4+A(5)+T**5+A(6)
43 ZP1=A(1)+2,*A(2)+T+3,*A(3)+T**2+4,*A(4)+T**3+5,*A(5)+T**4
44 ZP2=2,*A(2)+6,*A(3)+T+12,*A(4)+T**2+20,*A(5)+T**3
45 ZP3=6,*A(3)+24,*A(4)+T+60,*A(5)+T**2
C DENSITY
46 R=C,5928/ZP
C LET
47 PRD=ZP2/ZP**2
48 ZPP(K)=ZP
49 ZPP1(K)=ZP1
50 ZPP2(K)=ZP2
51 ZPP3(K)=ZP3
52 RPP(K)=R
53 PRD(K)=PRD
C SPDM CORE SOLUTION
54 P(K)=PB(K)-(C,5928*ZP2/ZP**2)*((Z**2-C,04642**2)/Z,0)
C P(ACTUAL)=C,726*P(IDEAL)
55 THETA(K)=P(K)*ZPP(K)/(C,5928*0,726)

```

```

56 Q(K)=-0.5928*((Z**2-0.04642**2)/2.0**ZP**2)*(ZP3/G+7P1*ZP2/ZP)
57 1+(PB(K)*ZP1/ZP+DPB(K)/G)-0.5928*ZP1*ZP2*0.04642**2/(ZP**3*G)
58 W(K)=ZP1/ZP*Z
59 TIME INCREMENT
59 T=T+1/1.5322
59 3 CONTINUE
60 WRITE(6,1005)
61 1005 FORMAT (//,
62 , ZP3
63 , Y=0.
64 DO 4 K=1,31
64 WRITE(6,1006) Y,ZPP(K),ZPP1(K),ZPP2(K),ZPP3(K),RPP(K),PQED(K)
65 1006 FORMAT (1F10.3,6F15.5/)
65 Y=Y+1/1.5322
66 4 CONTINUE
67 WRITE(6,1011)
68 1011 FORMAT (//,
69 , T W P
70 , Y=C.
71 DO 7 K=1,31
72 WRITE (6,1008)Y,P(K),THETA(K),Q(K),W(K)
73 1008 FORMAT (1F10.3,4F18.5/)
74 Y=Y+1/1.6022
75 7 CONTINUE
76 1012 CONTINUE
77 CALL EXIT
78 END

```

At  $z = 0.04642$

T	P <sub>g</sub> (T)	np <sub>g</sub> (T)
0.000	0.00300	13.14700
0.061	1.31770	14.56200
0.123	2.78390	16.70000
0.184	4.45400	7.98400
0.245	5.25240	3.34000
0.306	5.58640	-3.90700
0.368	5.19670	-7.79500
0.429	4.41720	-6.12500
0.490	3.90470	-5.39190
0.551	3.26650	-4.64000
0.613	2.80250	-3.34400
0.674	2.46900	-2.78000
0.735	2.19000	-2.41300
0.796	1.94870	-2.22700
0.858	1.72600	-1.95600
0.919	1.54040	-1.67000

Reproduced from  
best available copy.

Reproduced from  
best available copy.

At z = 0.01612

T	PB(T)	DPB(T)
C, 980	1, 37340	-1, 48499
1, 042	1, 22490	-1, 11999
1, 103	1, 11300	-1, 01500
1, 164	1, 01150	-0, 98400
1, 225	0, 91310	-0, 78999
1, 287	0, 83510	-0, 64900
1, 348	0, 77020	-0, 55550
1, 409	0, 71455	-0, 46490
1, 470	0, 66815	-0, 33450

At. z = 0.04642

Reproduced from  
best available copy.

$\gamma$	ZP	ZP1	ZP2	ZP3	$\xi(T)$	PRP
0.000	0.04642	0.00000	1.43340	-1.04022	12.77035	667.52730
0.061	0.04908	0.08617	1.37469	-1.03948	12.07817	570.69960
0.123	0.05690	0.16845	1.31103	-1.03875	10.41835	404.94160
0.184	0.06464	0.24682	1.24741	-1.03801	8.51227	257.20700
0.245	0.08776	0.32130	1.18393	-1.03729	6.80877	156.17500
0.306	0.10893	0.39189	1.12031	-1.03654	5.44133	96.61353
0.368	0.13500	0.45857	1.0562	-1.03581	4.39171	57.09677
0.429	0.16504	0.52138	0.99339	-1.03507	3.59137	36.46921
0.490	0.19891	0.58030	0.92909	-1.03434	2.98173	23.52991
0.551	0.23607	0.65534	0.86667	-1.03360	2.51112	15.55100
0.613	0.27658	0.68469	0.80334	-1.03297	2.14331	10.50155
0.674	0.32011	0.73377	0.74008	-1.03213	1.85197	7.22245
0.735	0.36641	0.77719	0.67687	-1.03140	1.61794	5.04150
0.796	0.41526	0.81671	0.61370	-1.03065	1.42754	3.55899
0.858	0.46641	0.85239	0.55058	-1.02993	1.27093	2.52096

Reproduced from  
best available copy.

At  $z = 0.01642$

T	ZP	CP1	ZP2	ZP3	R(T)	PRD
0.919	0.51963	0.88418	0.48750	-1.02919	1.14092	1.37547
0.980	0.57467	0.91211	0.42447	-1.02846	1.03154	1.28529
1.042	0.63131	0.93619	0.36148	-1.02772	0.93897	1.09697
1.103	0.68931	0.95641	0.29854	-1.02597	0.85999	0.62830
1.164	0.74843	0.97277	0.23564	-1.02625	0.79206	0.42068
1.225	0.80843	0.98528	0.17279	-1.02551	0.73327	0.26438
1.287	0.86908	0.99395	0.10998	-1.02478	0.68217	0.14541
1.348	0.93014	0.99876	0.04722	-1.02404	0.63732	0.05459
1.409	0.99138	0.99973	-0.01550	-1.02331	0.59795	-0.01577

At z = 0.04542

Reproduced from  
best available copy.

T	D	THETA	$\theta$	$\theta'$
0.000	0.00300	0.00032	10.41751	0.00000
0.061	1.31770	0.15023	12.91738	0.09150
0.123	2.078300	0.36795	20.26176	0.13742
0.184	4.45400	0.72053	21.18959	0.14452
0.245	5.25240	1.06227	21.44646	0.17131
0.306	5.58640	1.41358	16.66547	0.15700
0.368	5.19670	1.67970	11.27596	0.15768
0.429	4.41720	1.69348	8.98422	0.14644
0.490	3.80470	1.75710	6.77122	0.13549
0.551	3.26550	1.79126	5.07211	0.12403
0.613	2.80250	1.90055	4.27907	0.11522
0.674	2.46800	1.83514	3.43770	0.10641
0.735	2.19000	1.86403	2.72222	0.09846
0.796	1.94870	1.97976	2.06097	0.09130
0.858	1.72600	1.87007	1.67996	0.08483
0.919	1.54040	1.95935	1.24459	0.07899



At  $z = 0.01642$

T	P	THETA	Q	W
0,980	1,37340	1,43339	1,00108	0,07363
1,042	1,22490	1,79632	0,92939	0,06994
1,103	1,11300	1,78216	0,7391	0,05441
1,164	1,01150	1,75854	0,53444	0,05033
1,225	0,91310	1,71474	0,40446	0,05657
1,287	0,83510	1,68591	0,44766	0,05309
1,348	0,77020	1,56414	0,38600	0,04934
1,409	0,71455	1,64555	0,35292	0,04681

Reproduced from  
best available copy.

At  $z = 0.26804$

T	P	THETA	O	W
0.613	2.58558	1.66118	4.27721	0.66529
0.674	2.31391	1.72425	3.43584	0.61442
0.735	2.08586	1.77539	2.72050	0.56852
0.796	1.87519	1.80985	2.05947	0.52717
0.858	1.67372	1.91338	1.67810	0.43985
0.919	1.50311	1.91434	1.20461	0.45609
0.980	1.34685	1.79795	1.00205	0.42543
1.042	1.20617	1.76884	0.93068	0.39748
1.103	1.10002	1.76138	0.74324	0.37190
1.164	1.00281	1.74363	0.54030	0.34839
1.225	0.90764	1.74448	0.50259	0.32668
1.287	0.83209	1.67984	0.45136	0.30655
1.348	0.76907	1.66170	0.39959	0.29781
1.409	0.71488	1.64630	0.36970	0.27030

At z = 0.50763

T	P	T4ETA	C	W
0.919	1.40365	1.69429	1.29440	0.36376
0.980	1.27525	1.70344	1.00462	0.90570
1.042	1.15621	1.69557	0.93679	0.75273
1.103	1.06541	1.70596	0.75350	0.70433
1.164	0.97964	1.70315	0.55594	0.55980
1.225	0.89308	1.67713	0.52427	0.61969
1.287	0.82407	1.66365	0.47991	0.53056
1.348	0.76507	1.65521	0.43585	0.54508
1.409	0.71574	1.64830	0.41444	0.51191

At  $\lambda = 0.69451$

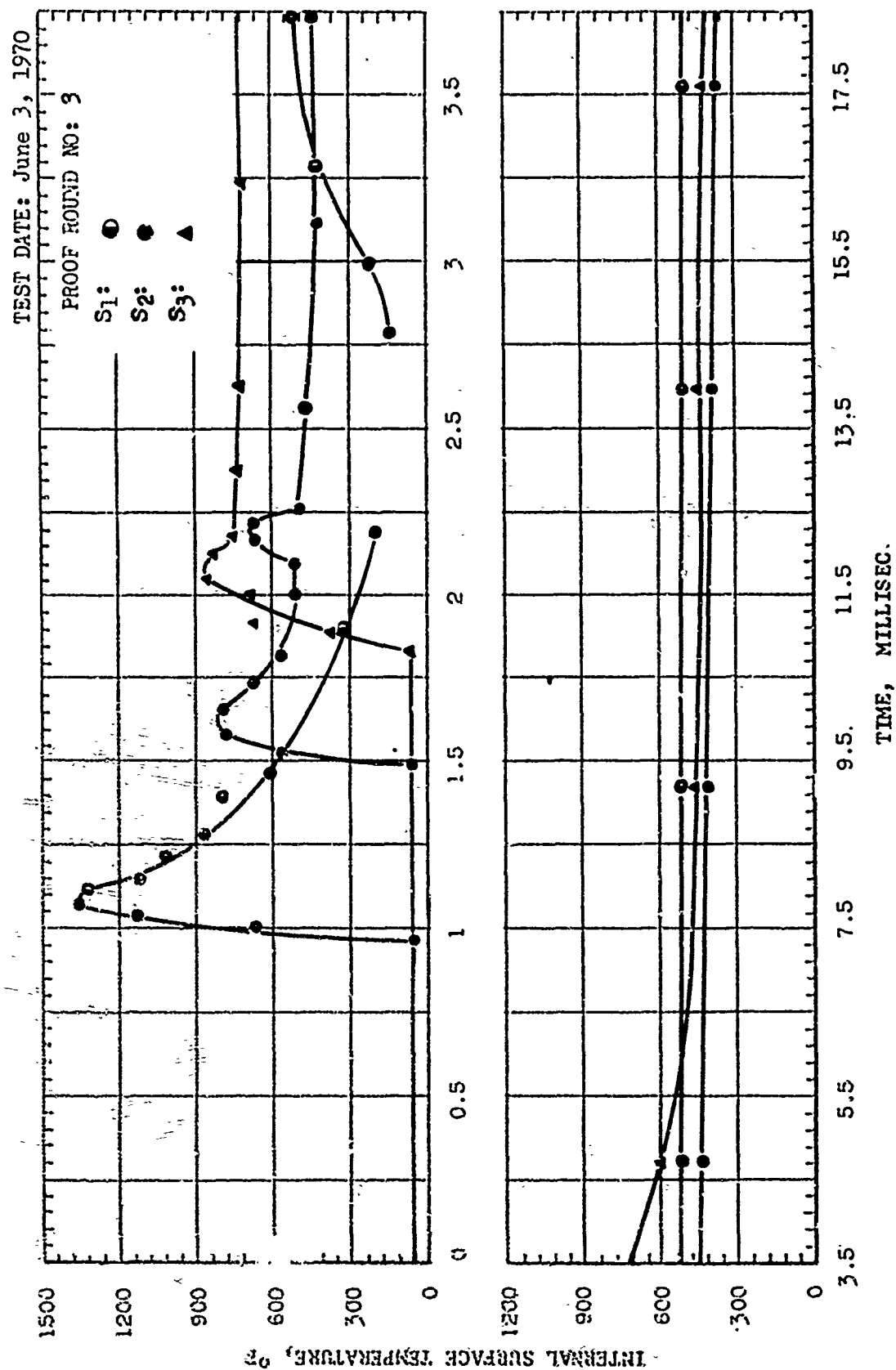
T	P	THETA	Q	W
1.103	1.02357	1.63897	0.76614	0.96362
1.164	0.95163	1.65445	0.57485	0.97269
1.225	0.87547	1.66407	0.55746	0.94644
1.287	0.81438	1.66407	0.51443	0.79429
1.348	0.76243	1.66473	0.47967	0.74575
1.409	0.71679	1.65072	0.46853	0.70036

At  $z = 0.982$

T	P	THETA	Q	Y
1.348	0.75464	1.53051	0.57370	1.05445
1.409	0.71905	1.55591	0.58458	0.92027

## APPENDIX IIIA EXPERIMENTAL DATA (June 3, 1970)

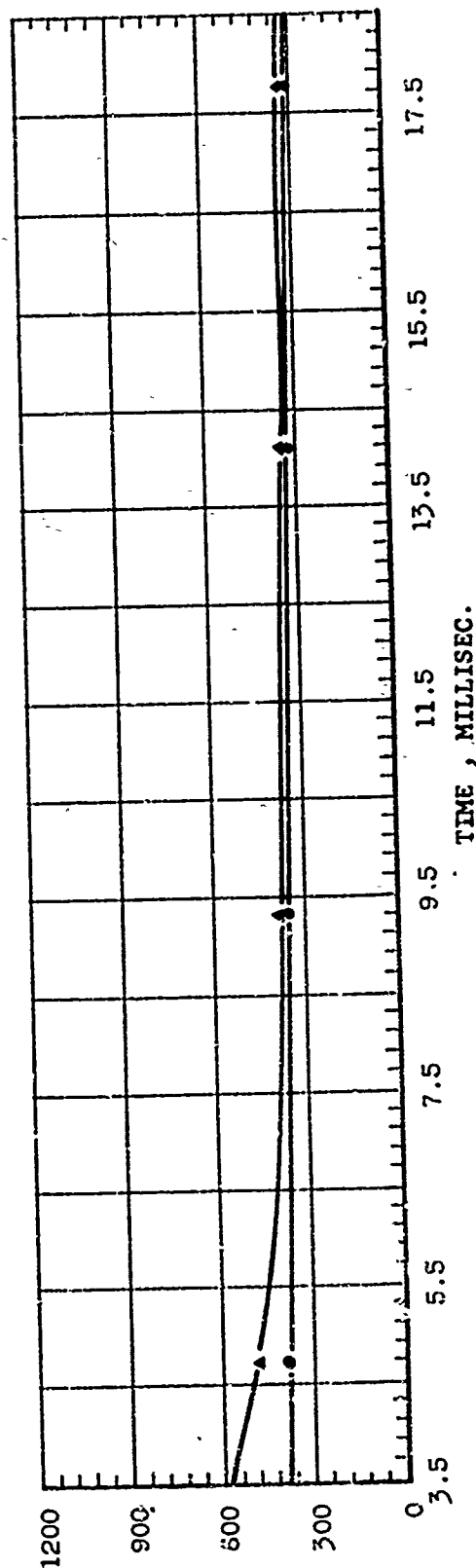
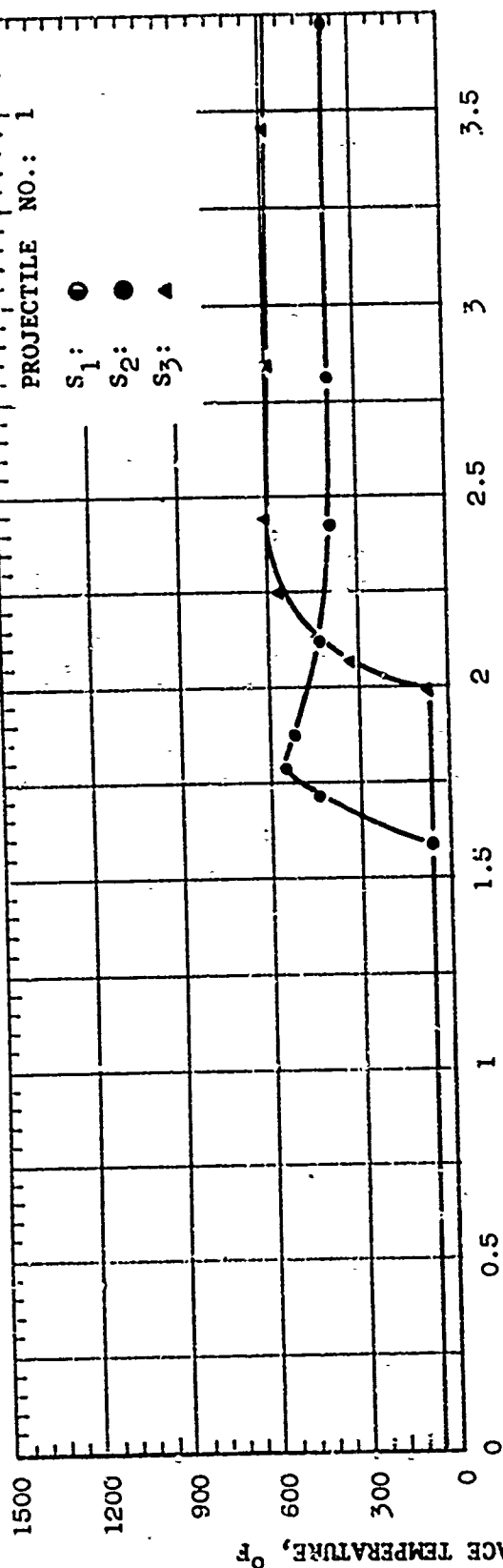
NOTE: See Fig. III-1 for Arrangement of Probes



TEST DATE: June 3, 1970

PROJECTILE NO.: 1

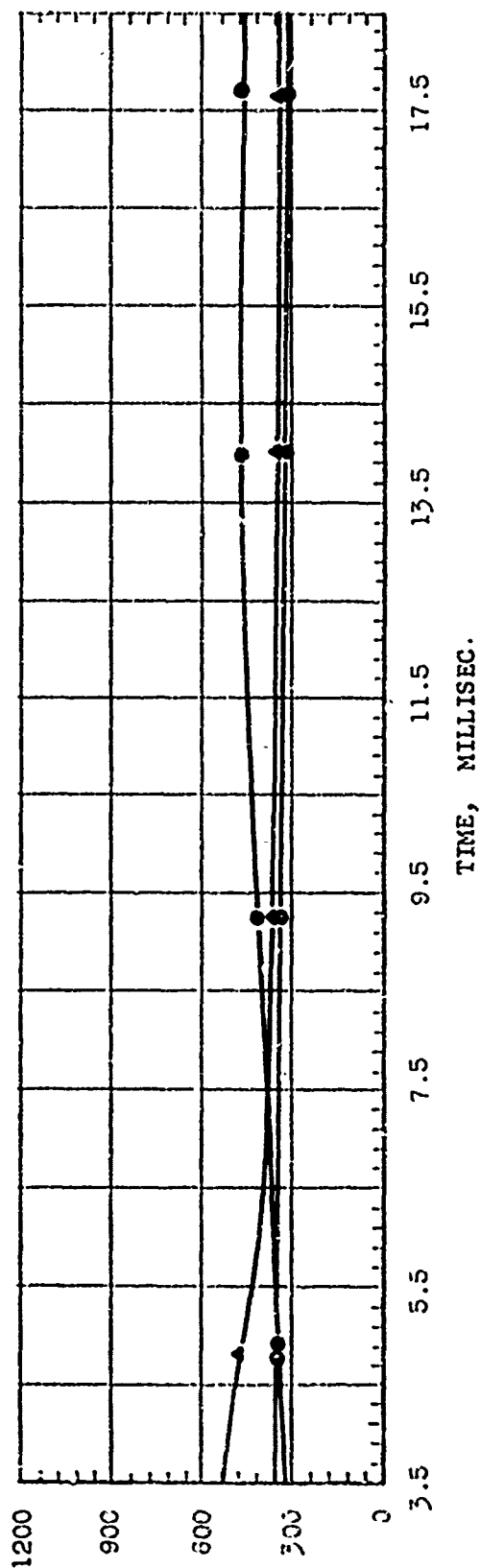
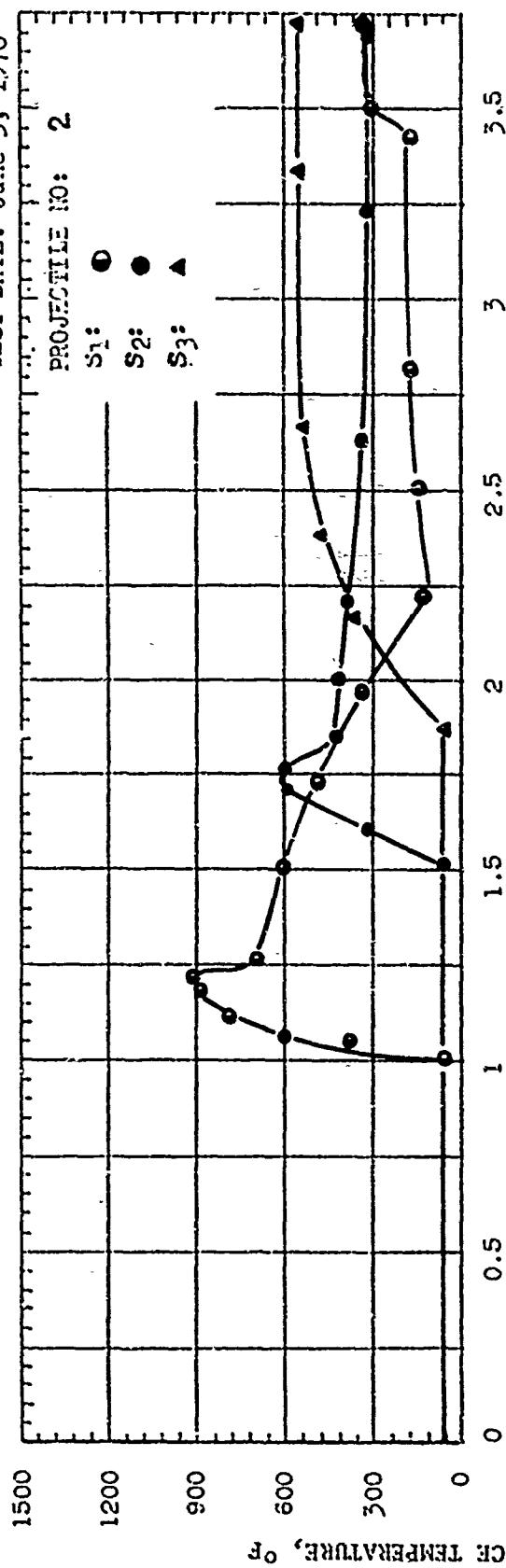
S<sub>1</sub>: ○  
S<sub>2</sub>: ●  
S<sub>3</sub>: ▲

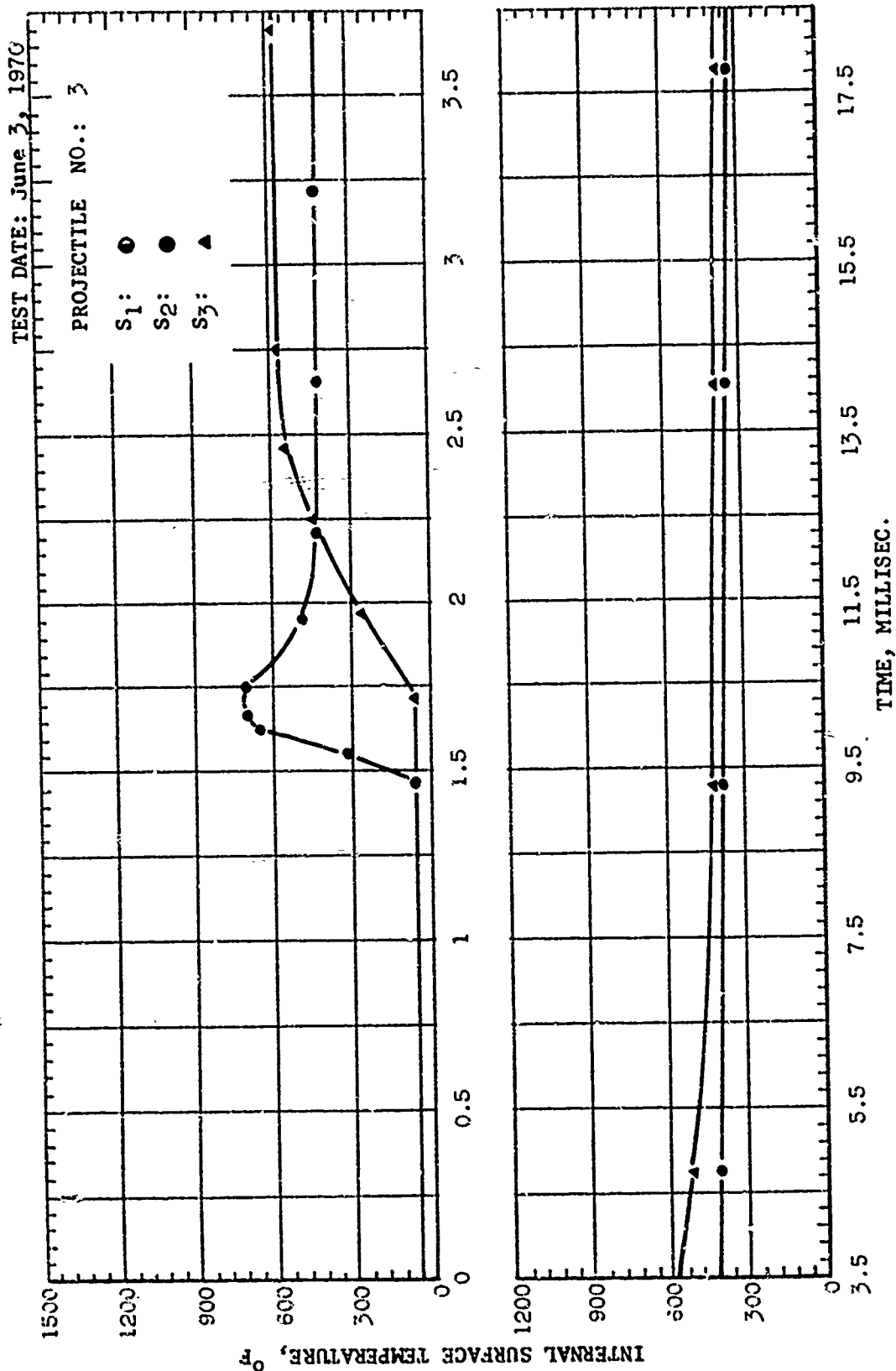


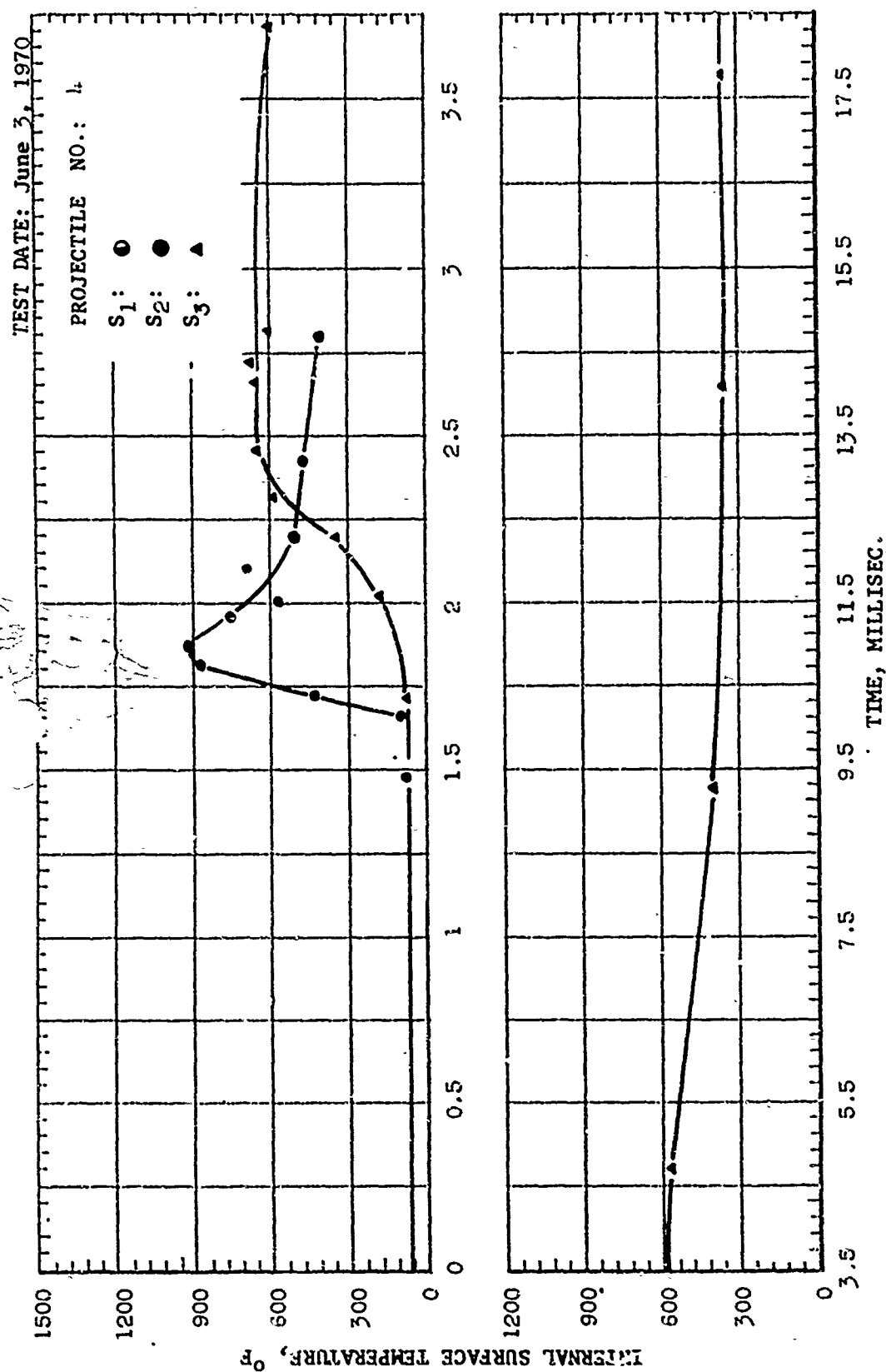


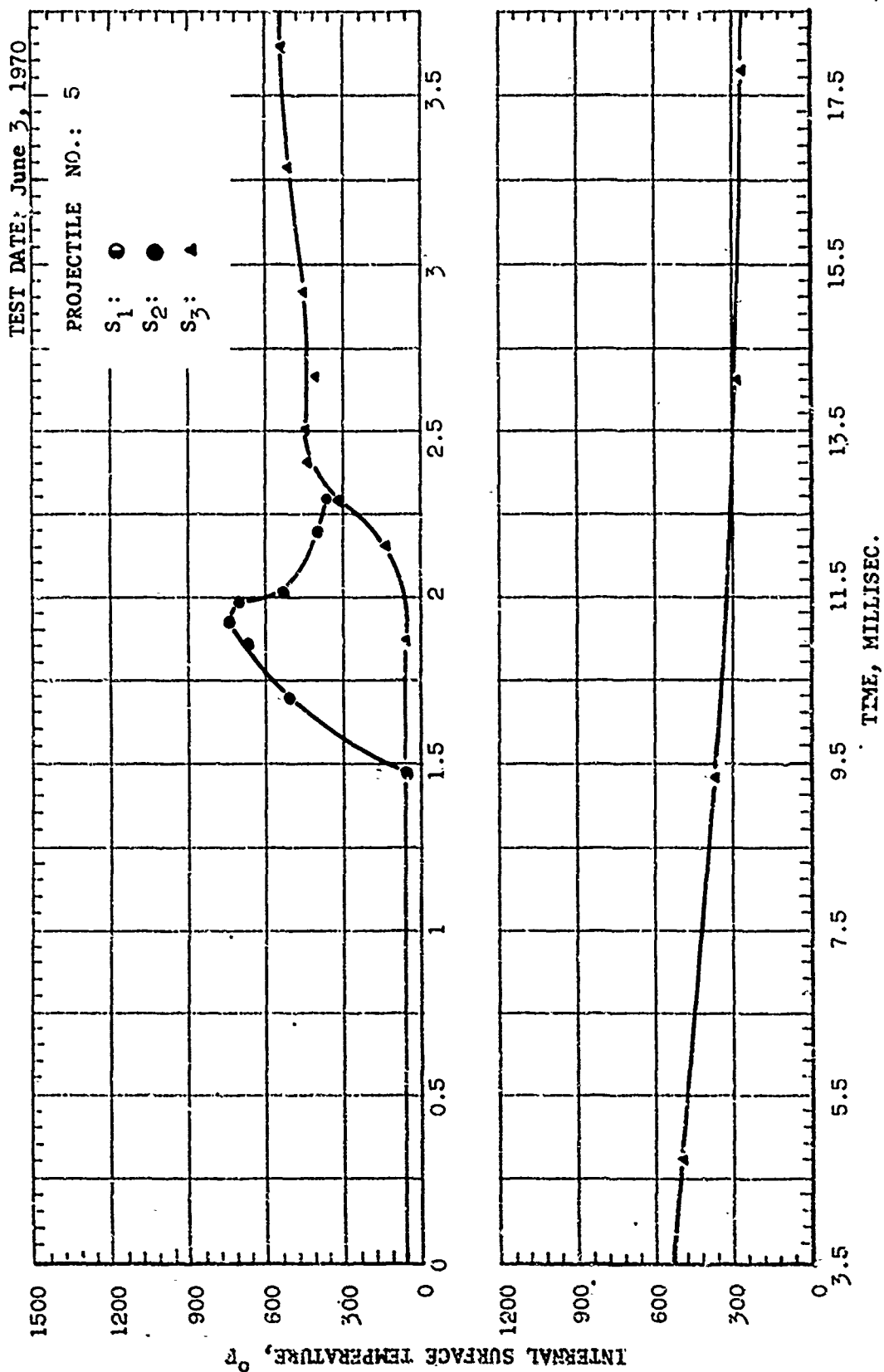
TEST DATE: June 3, 1970

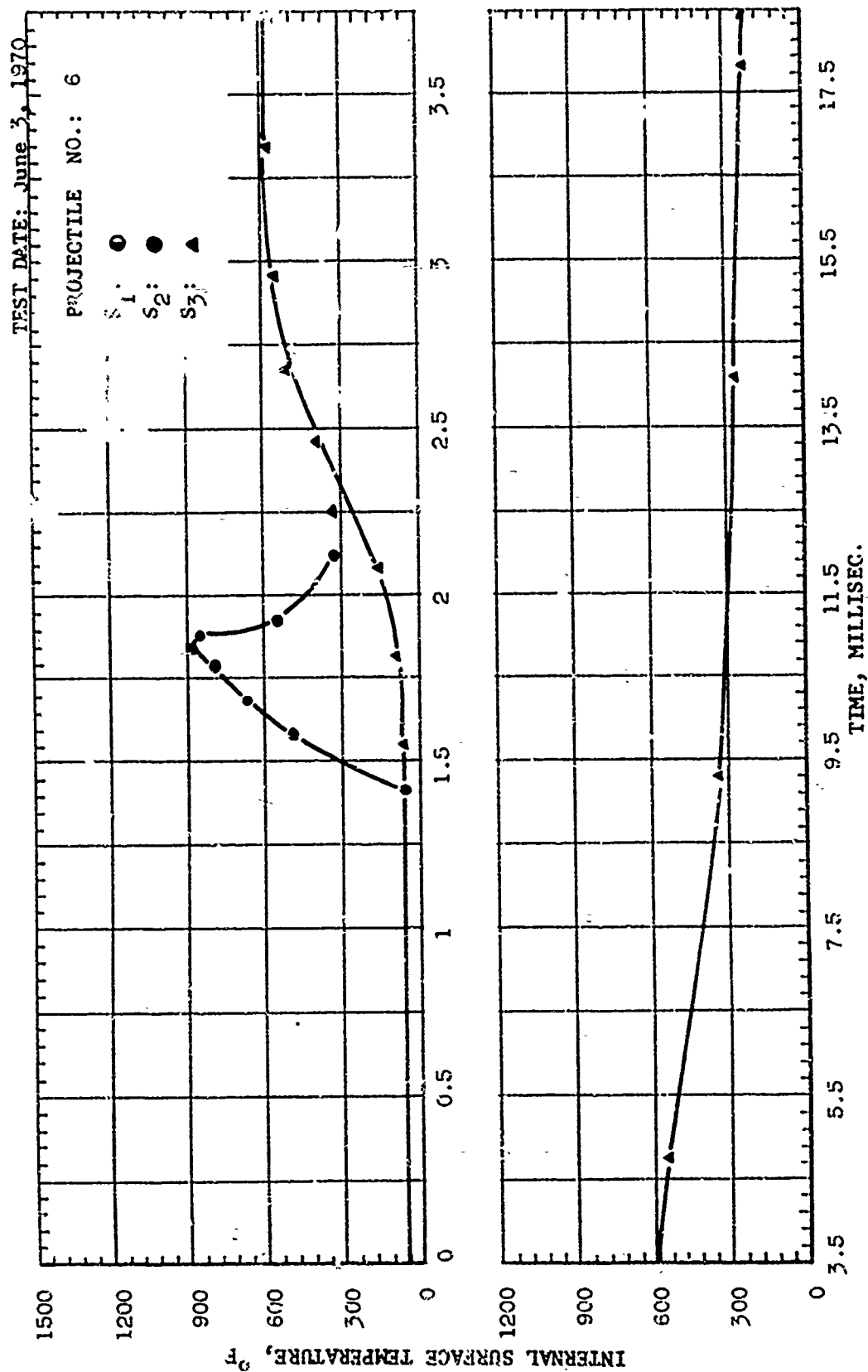
PROJECTILE NO: 2

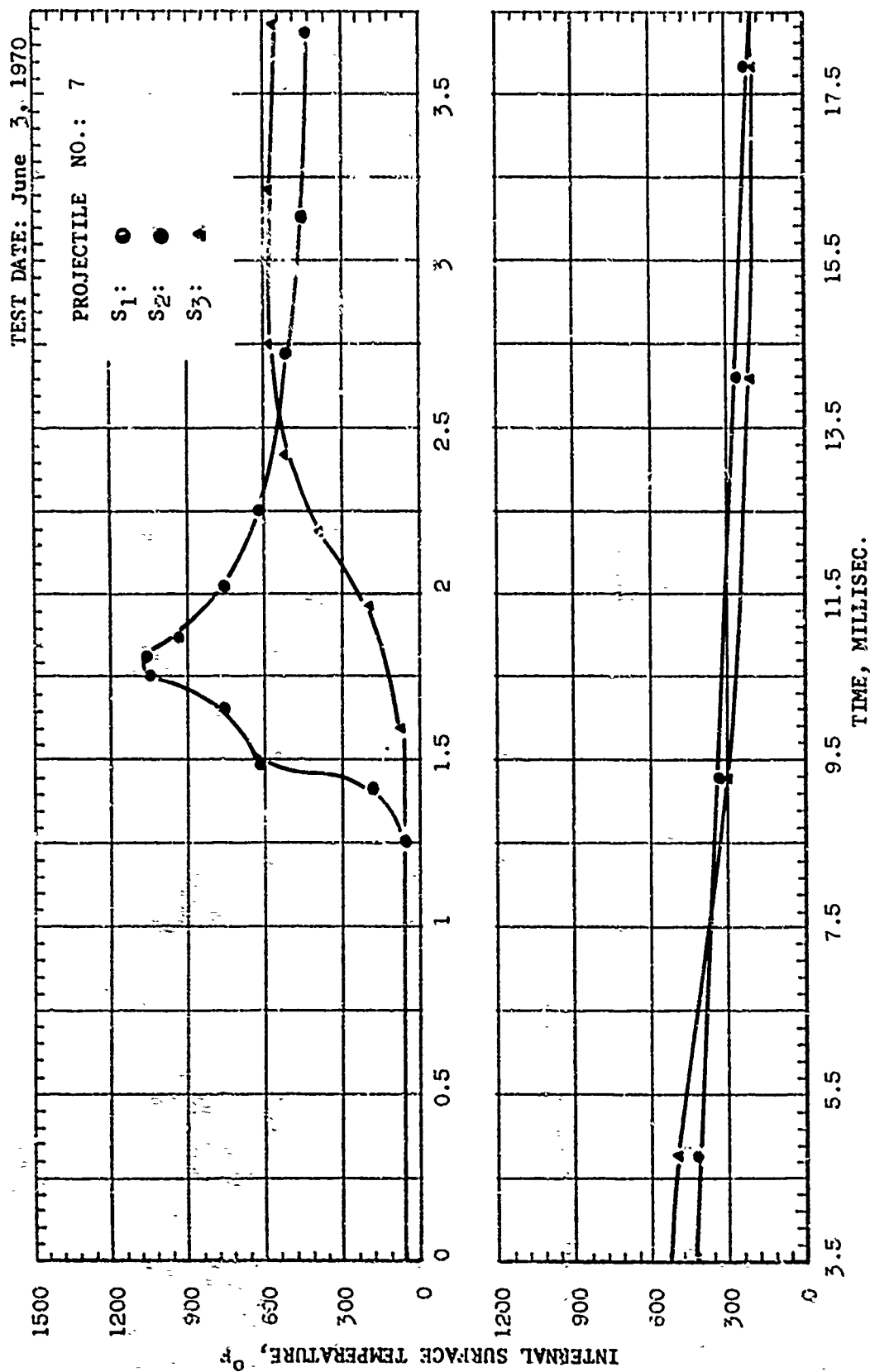
S<sub>1</sub>: ●S<sub>2</sub>: ●S<sub>3</sub>: ▲

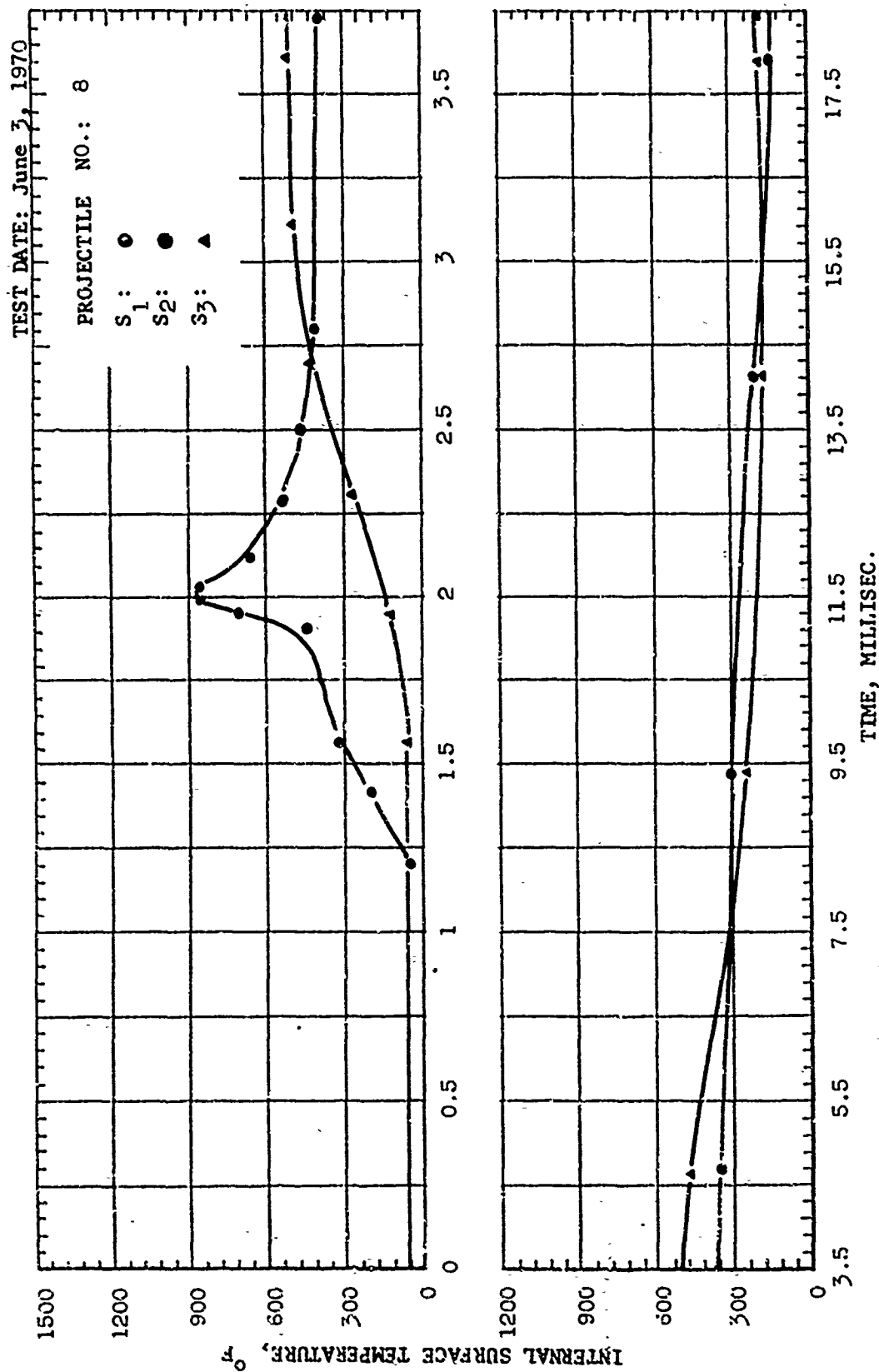


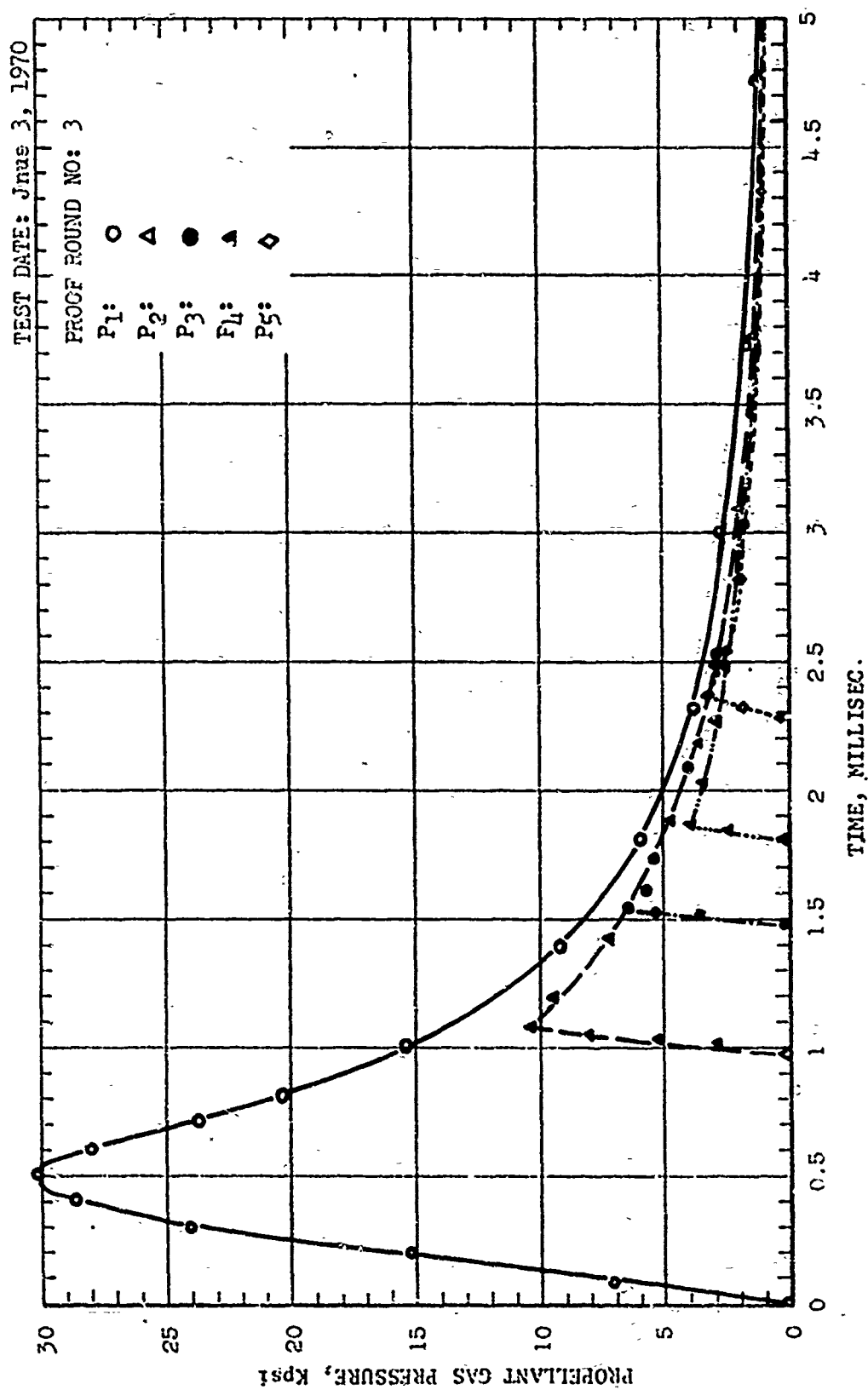




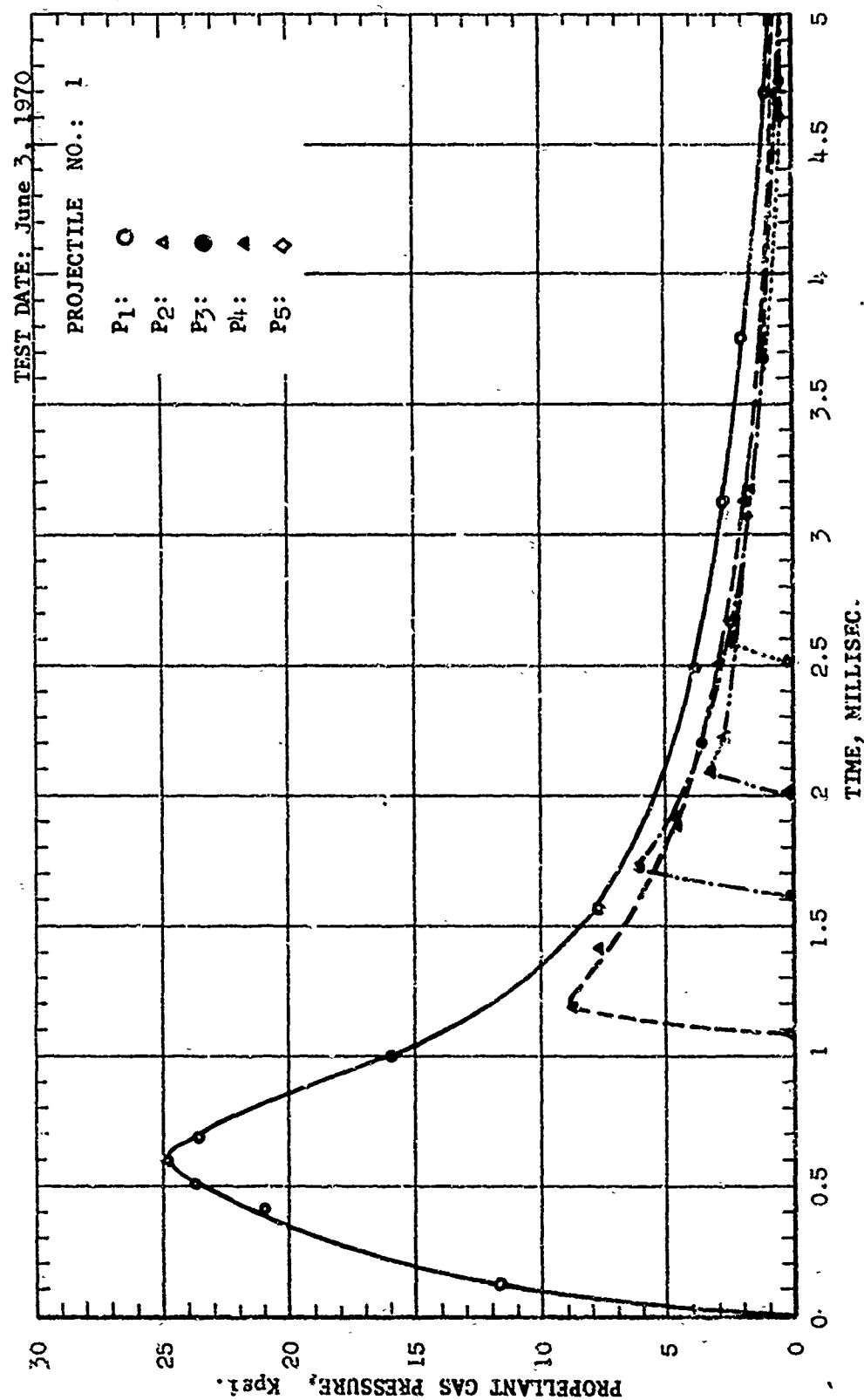


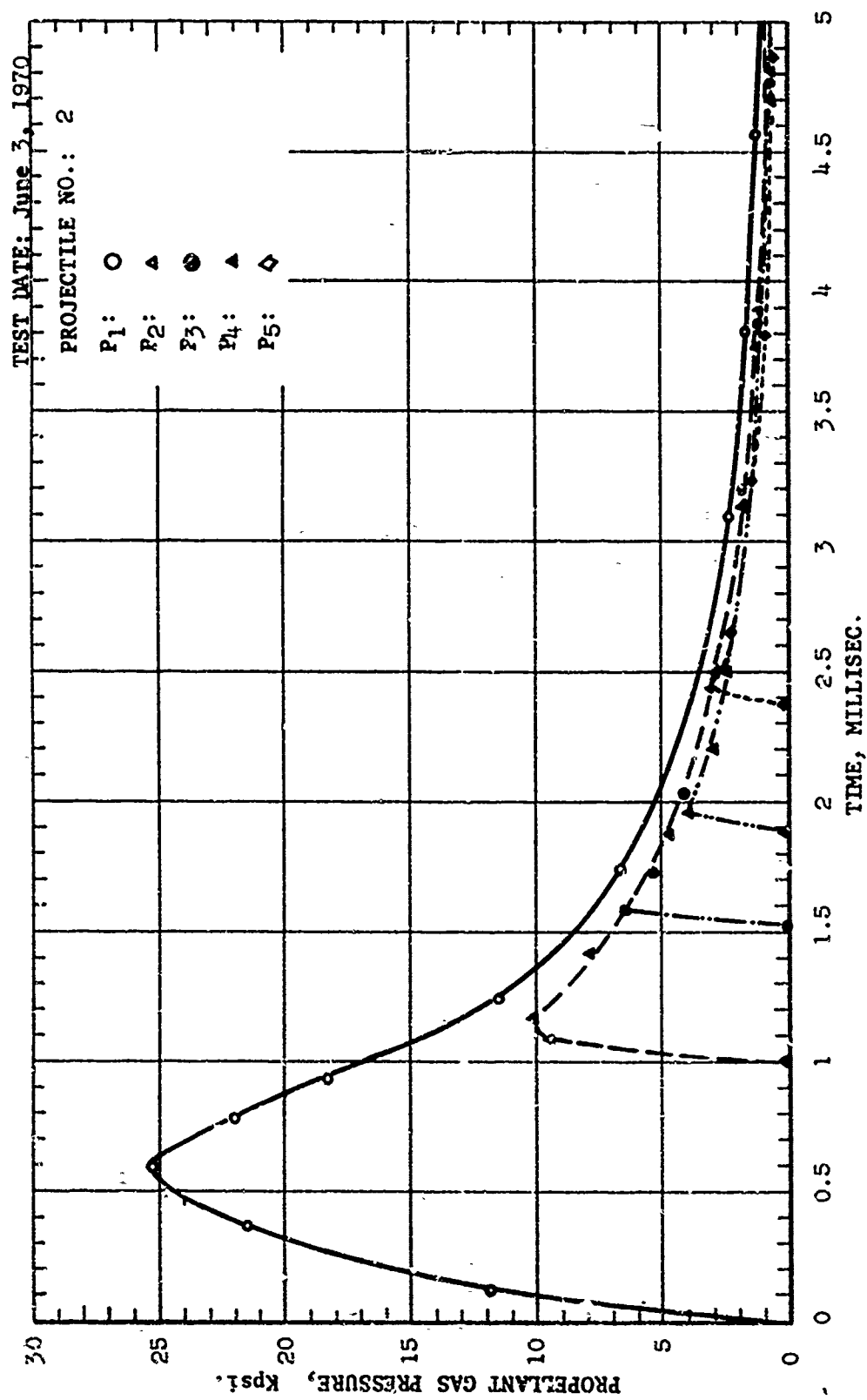


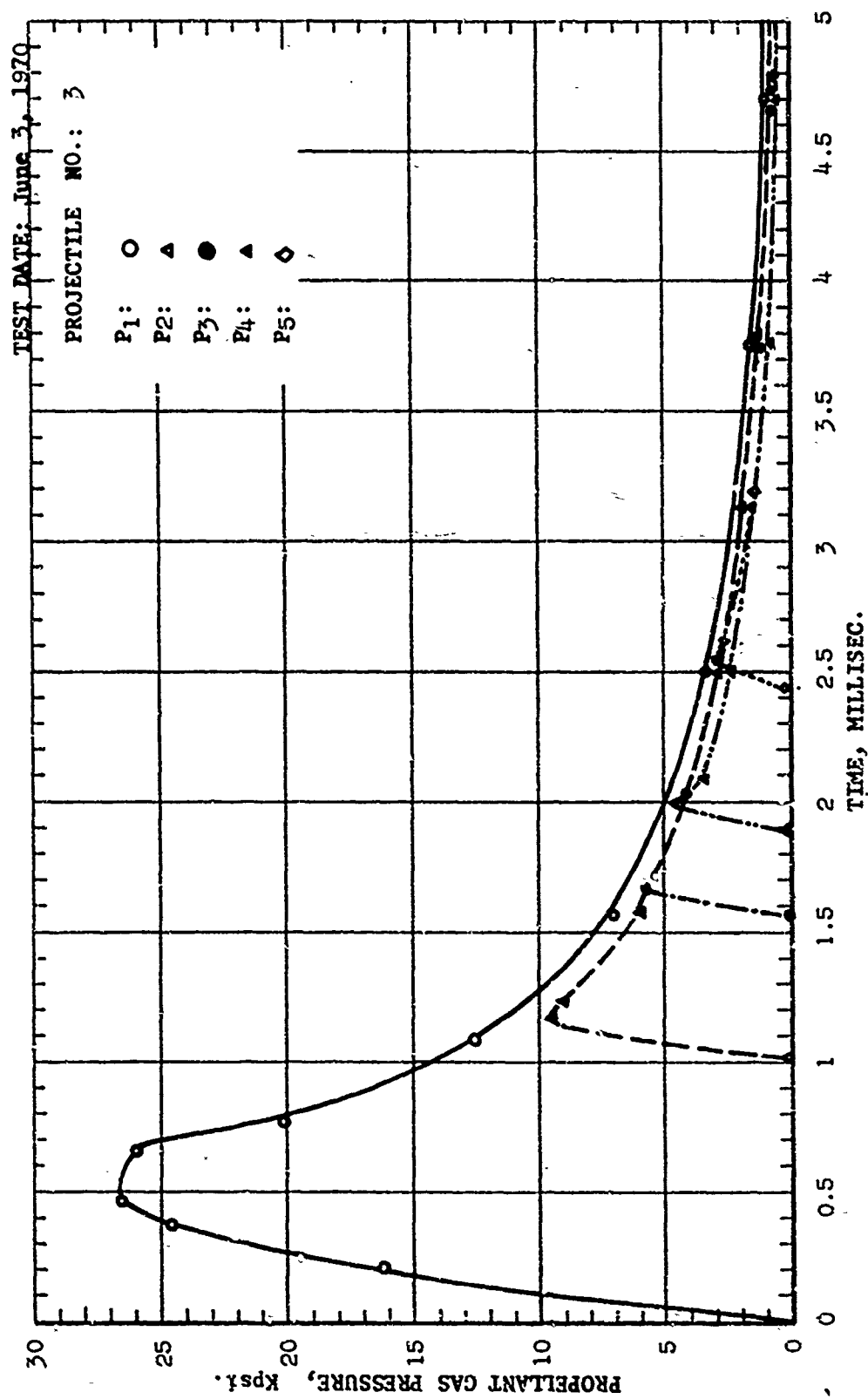


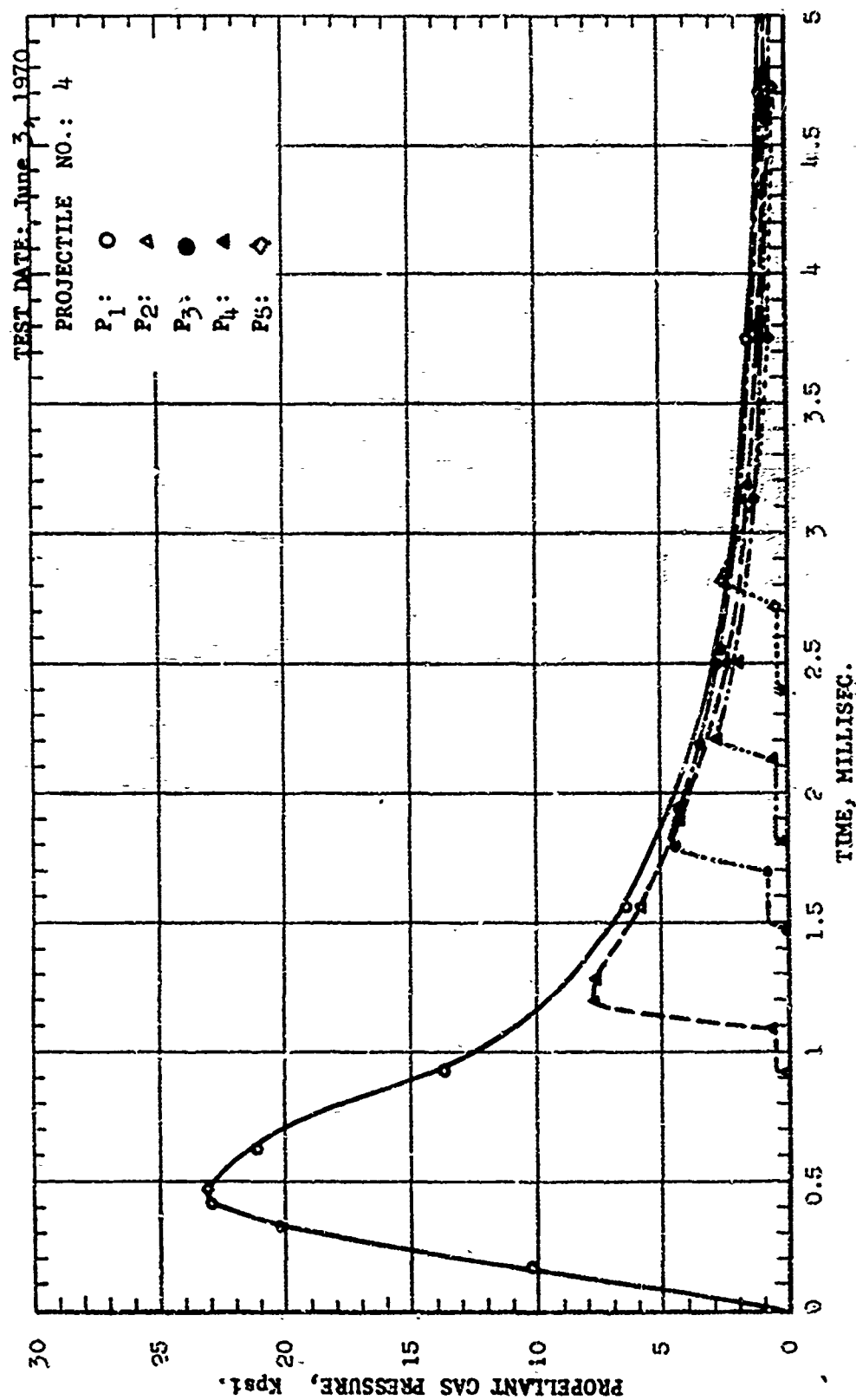


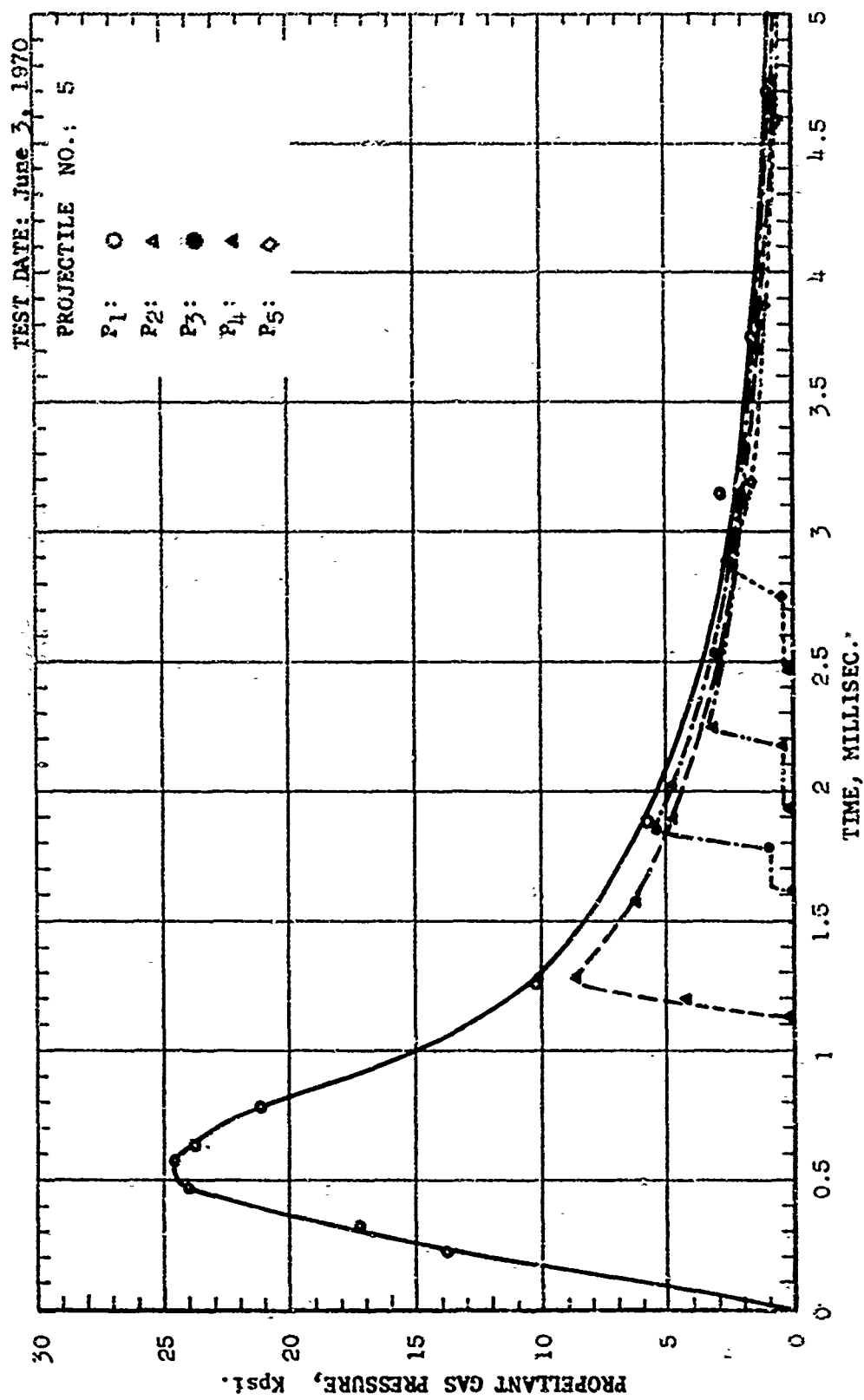


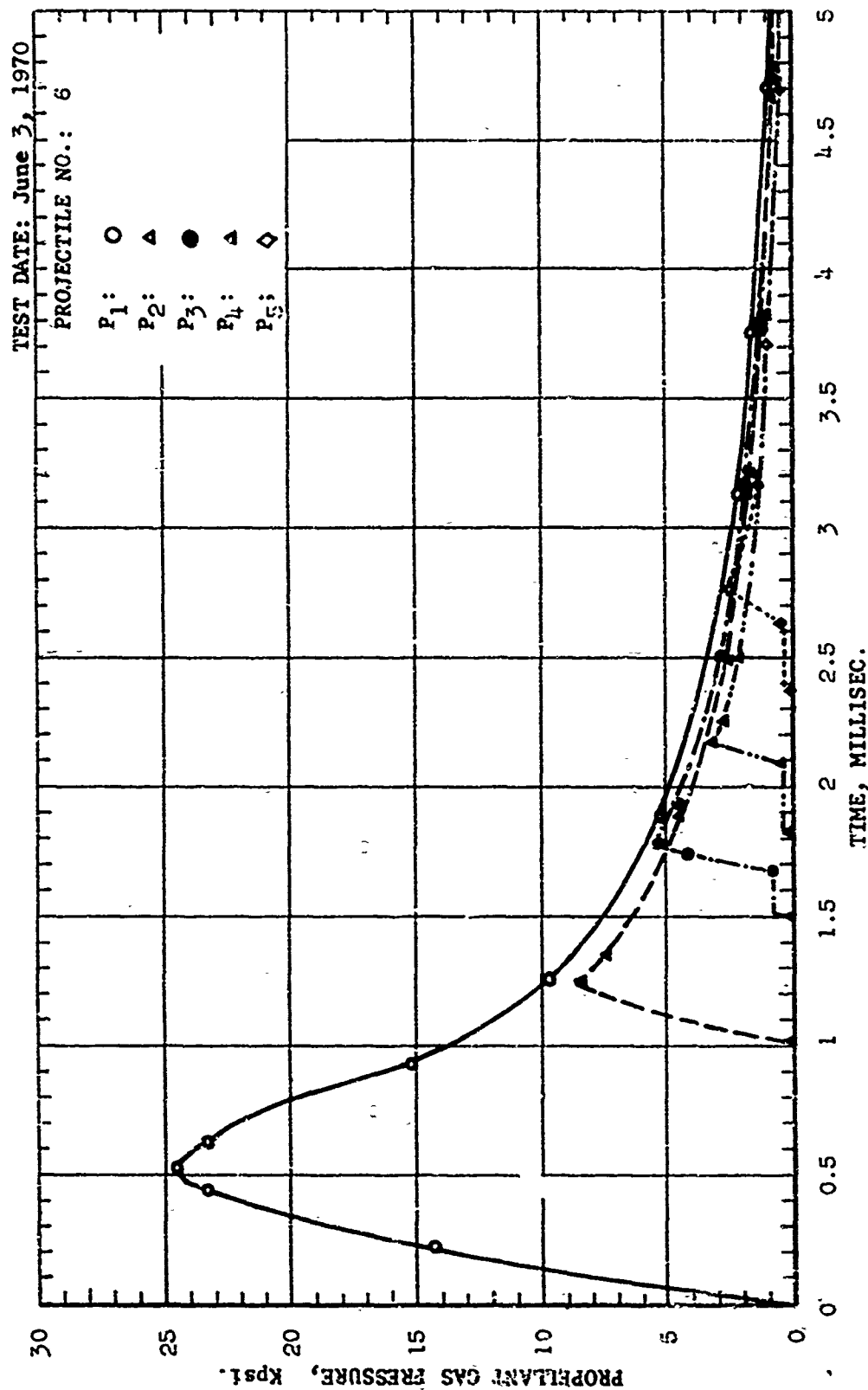


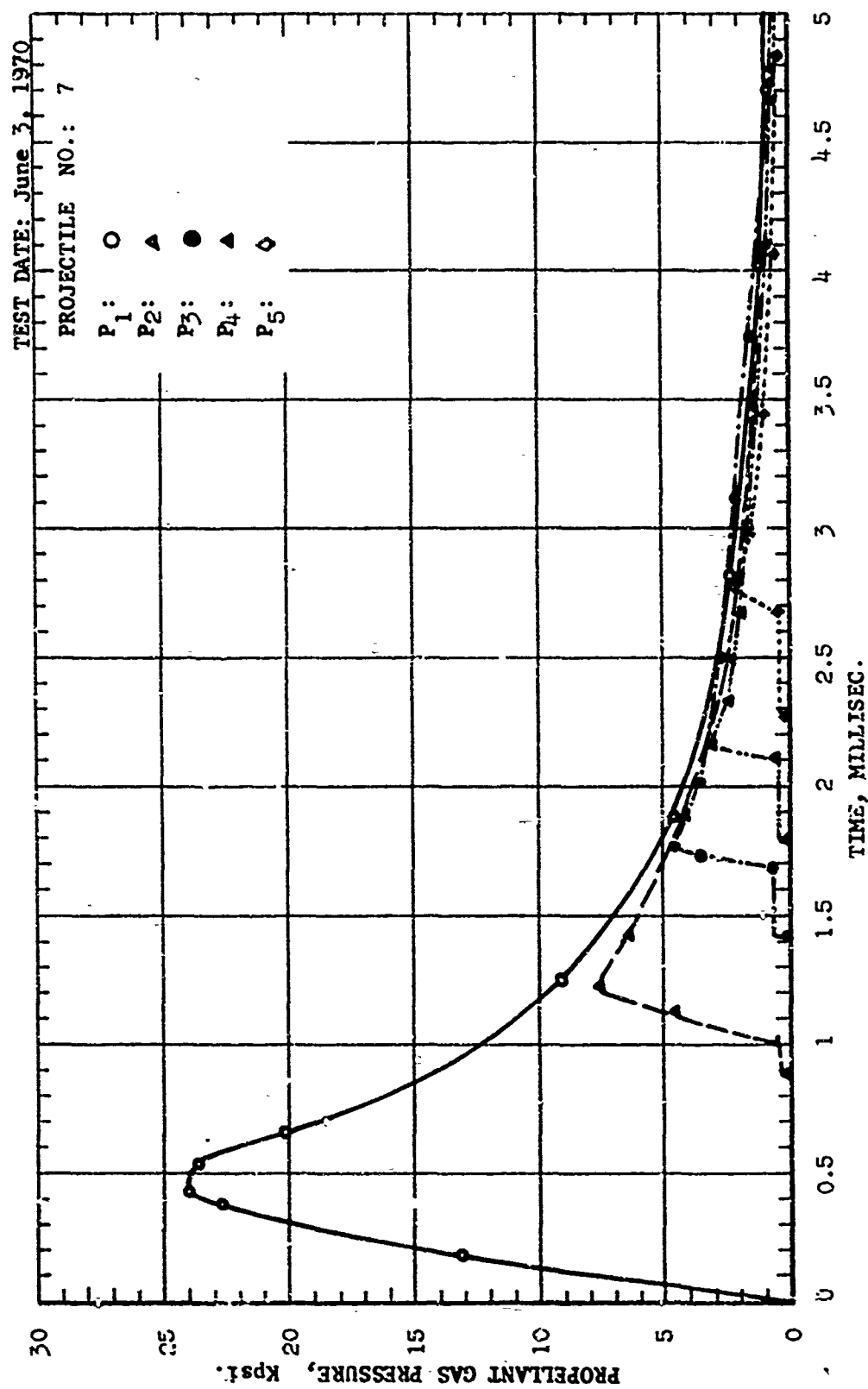


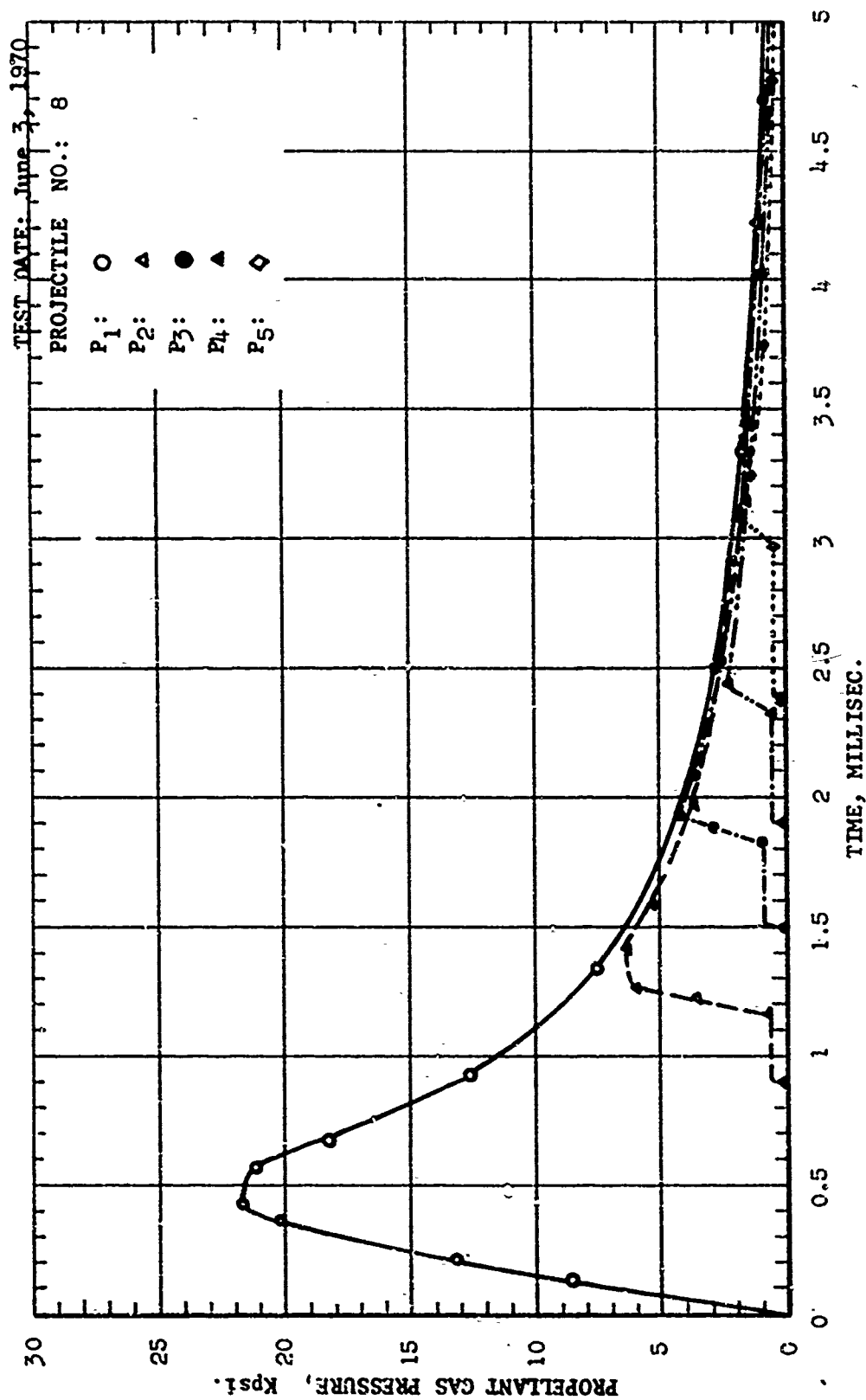




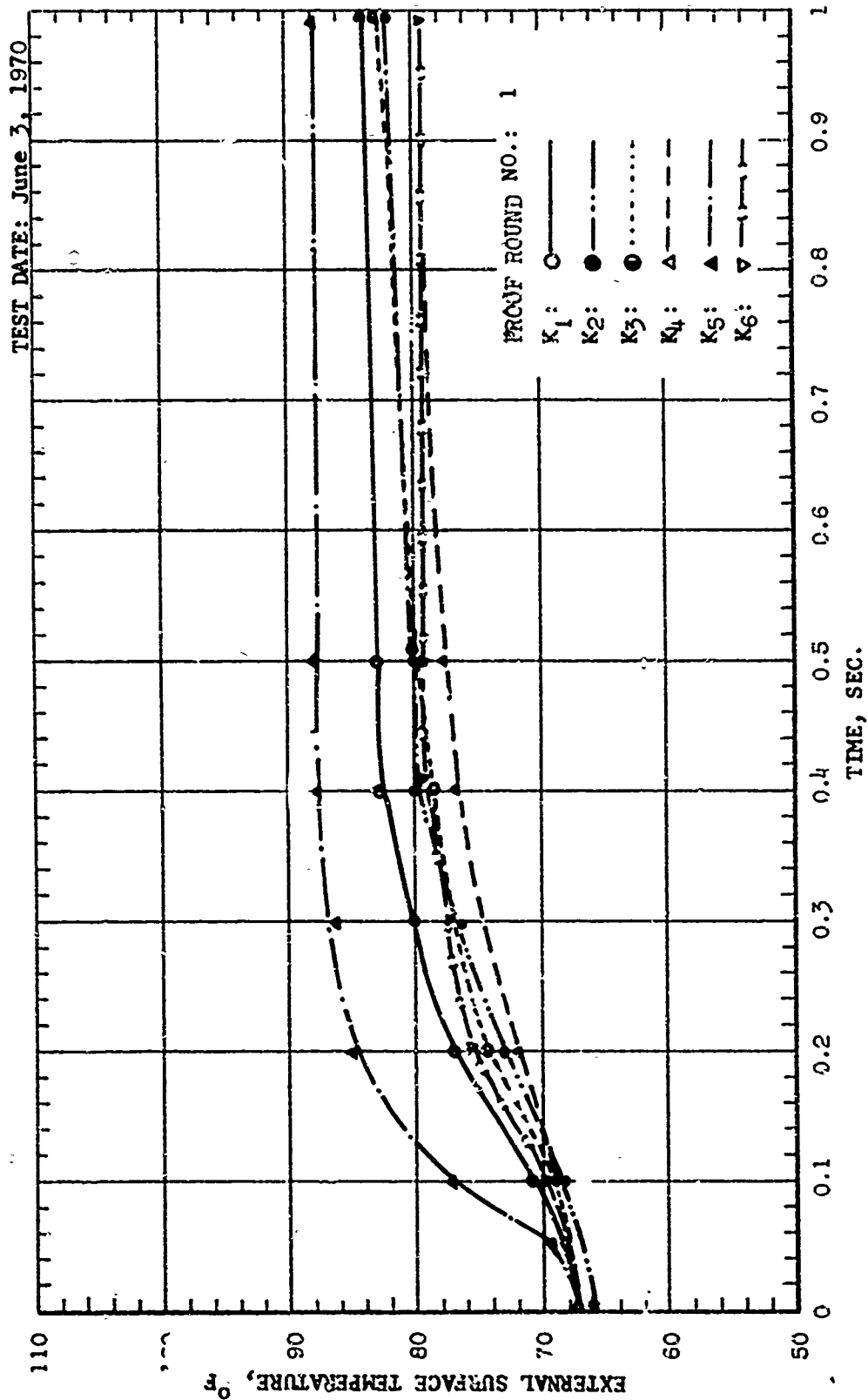


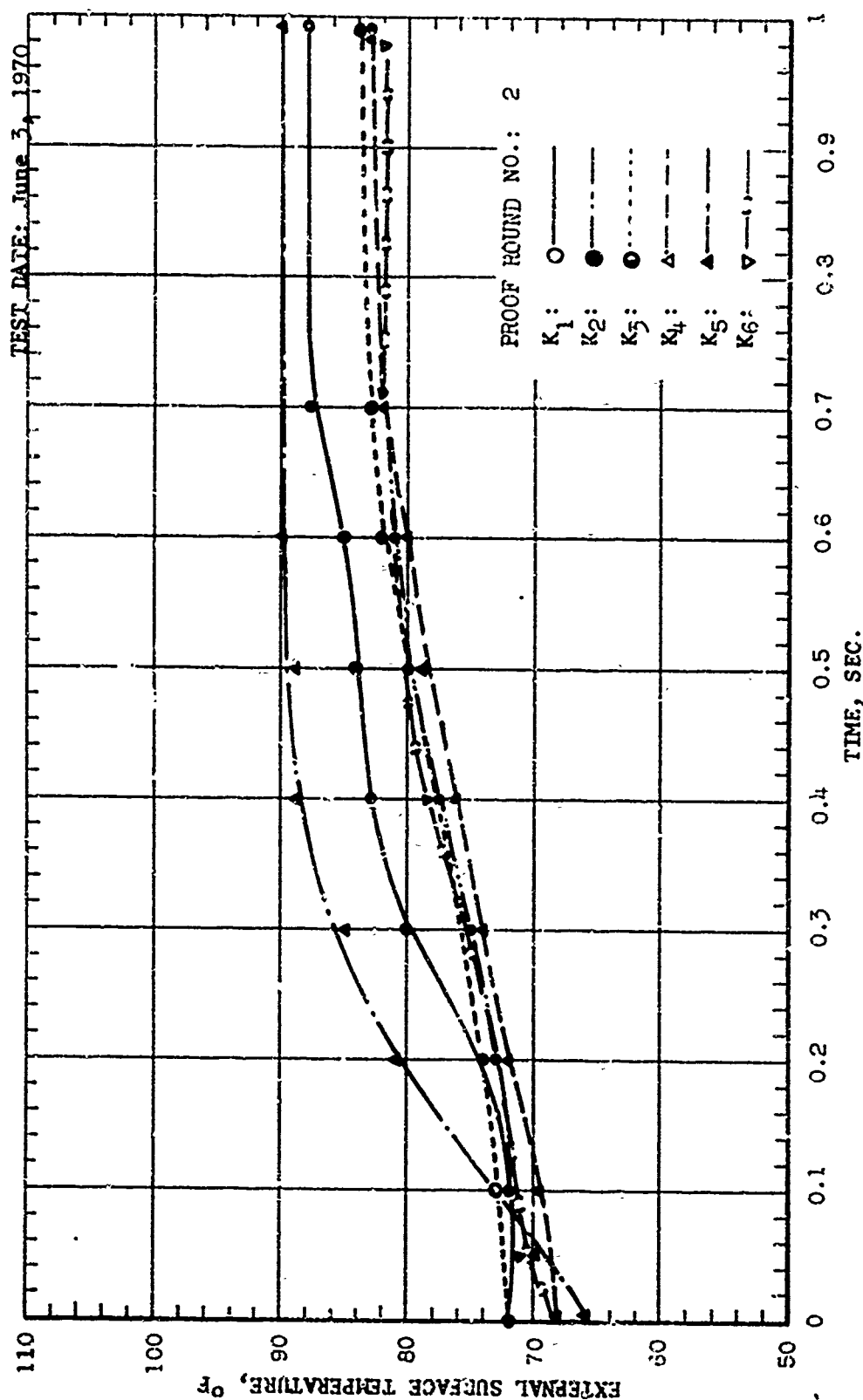


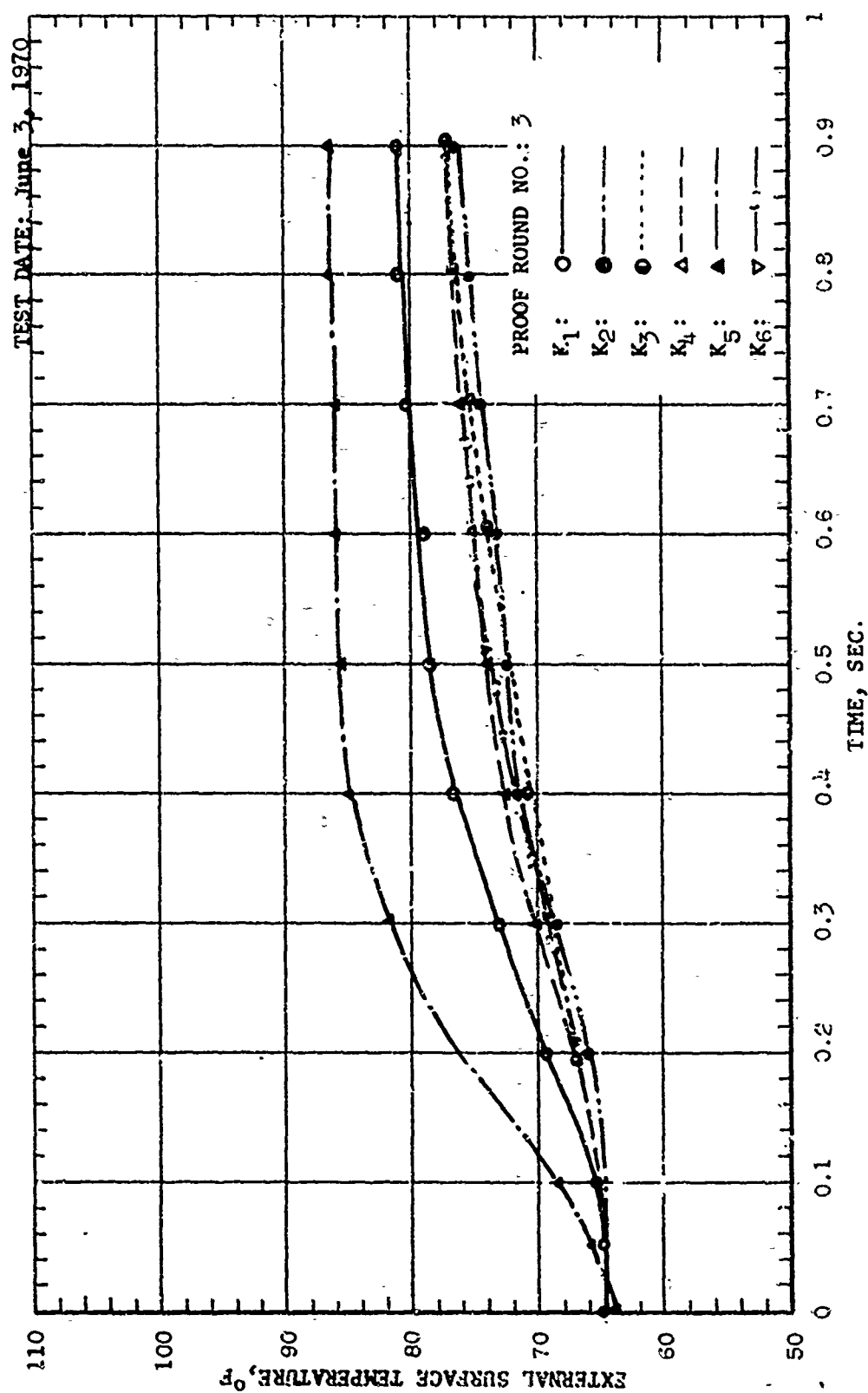


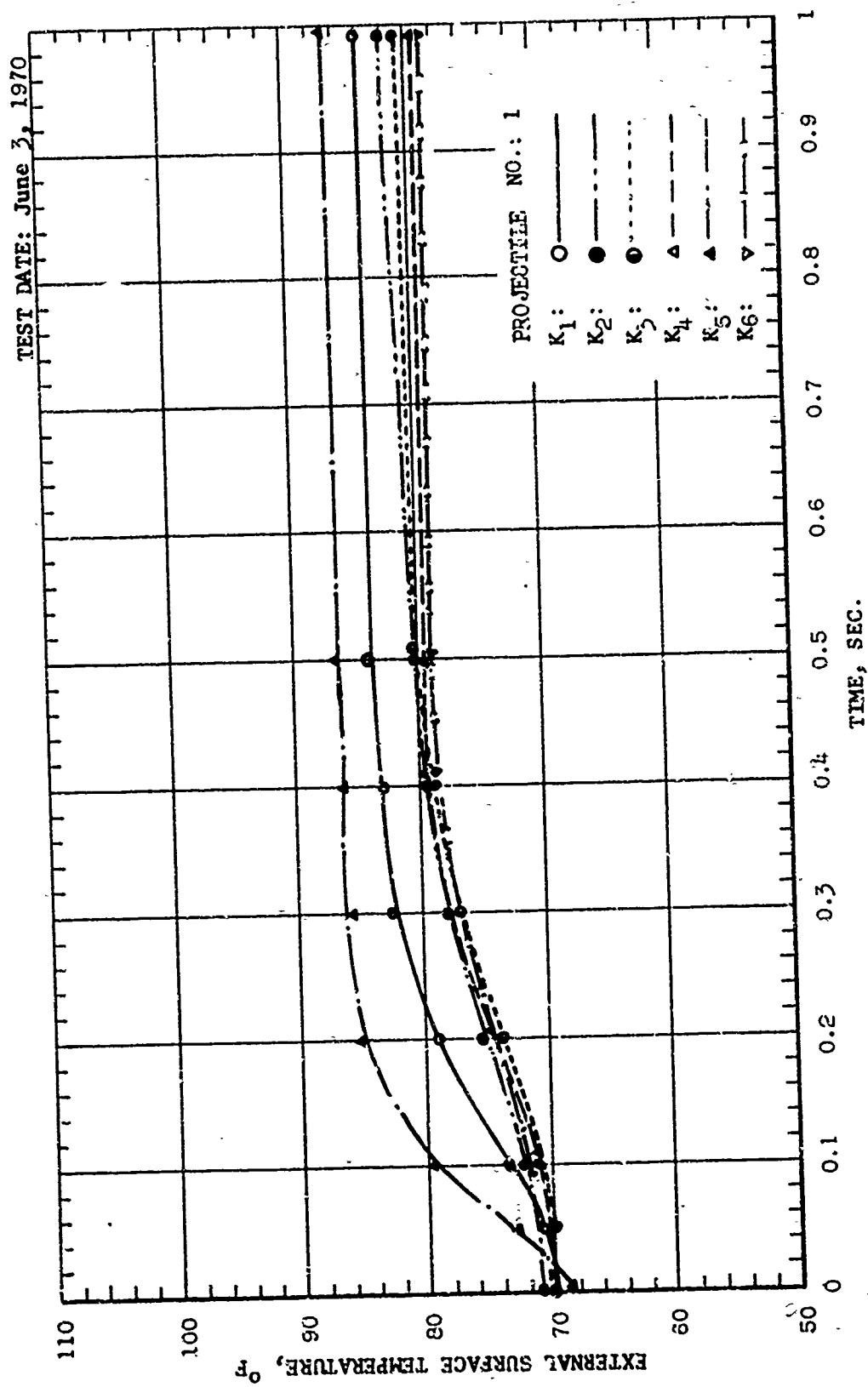


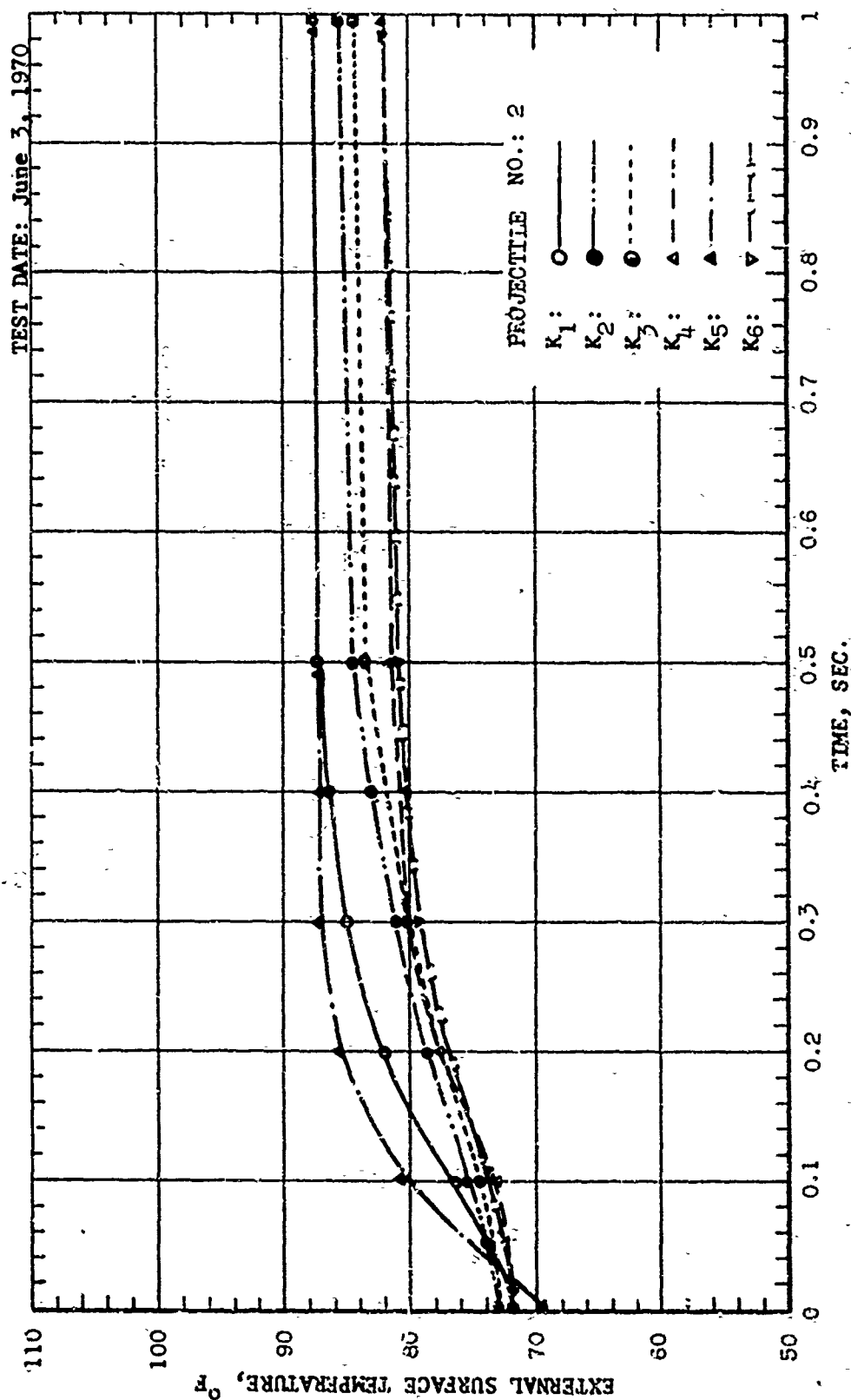


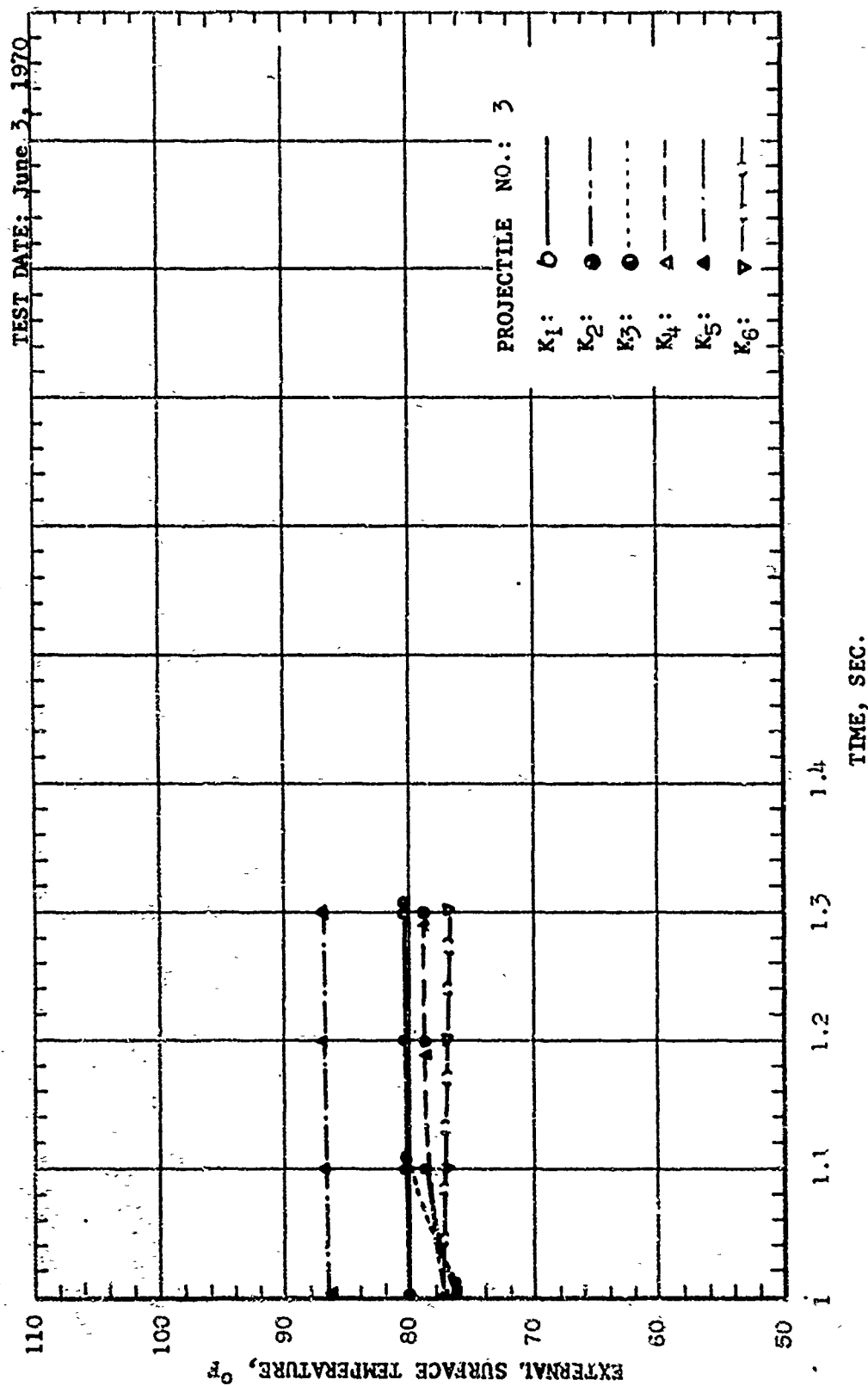


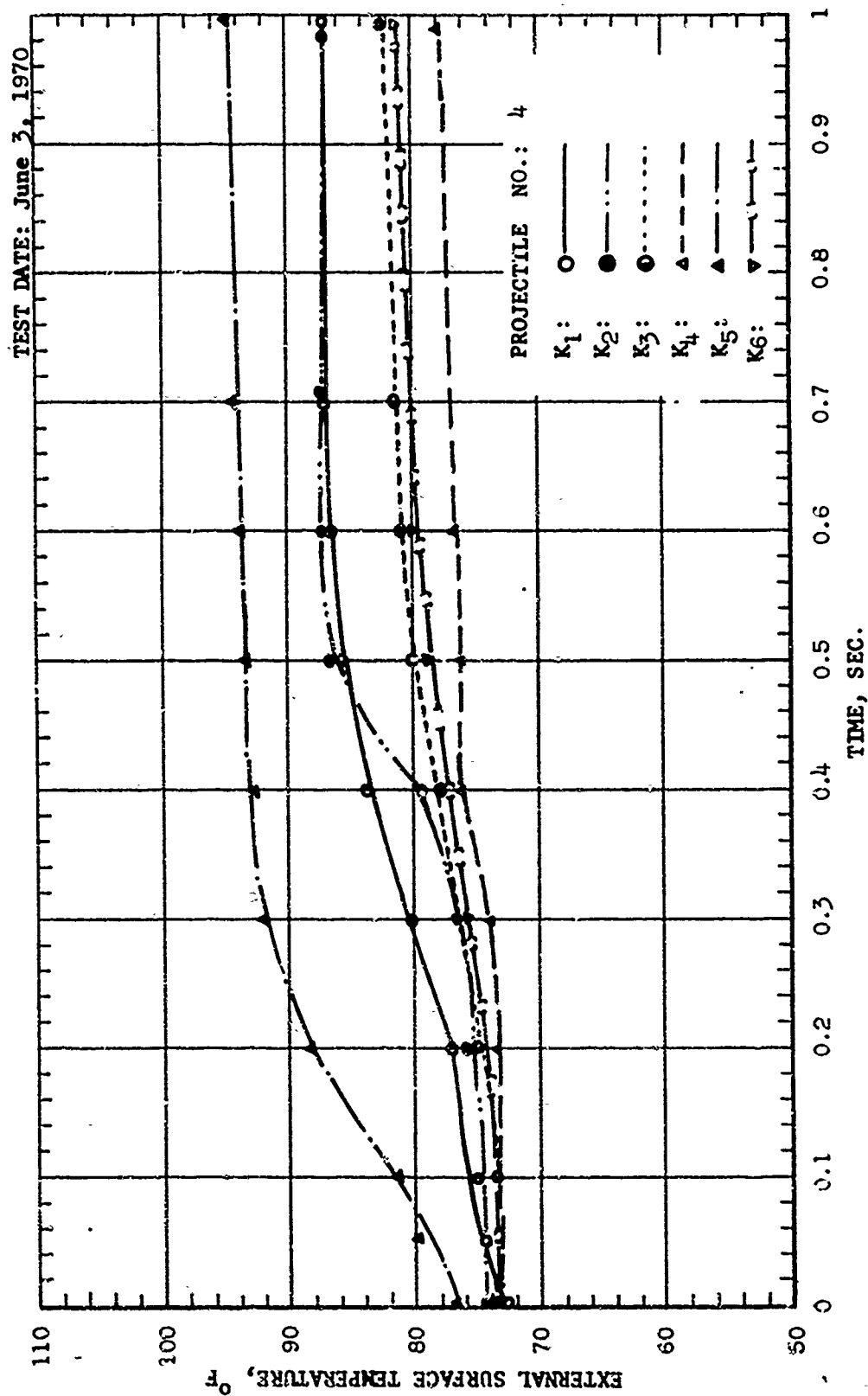


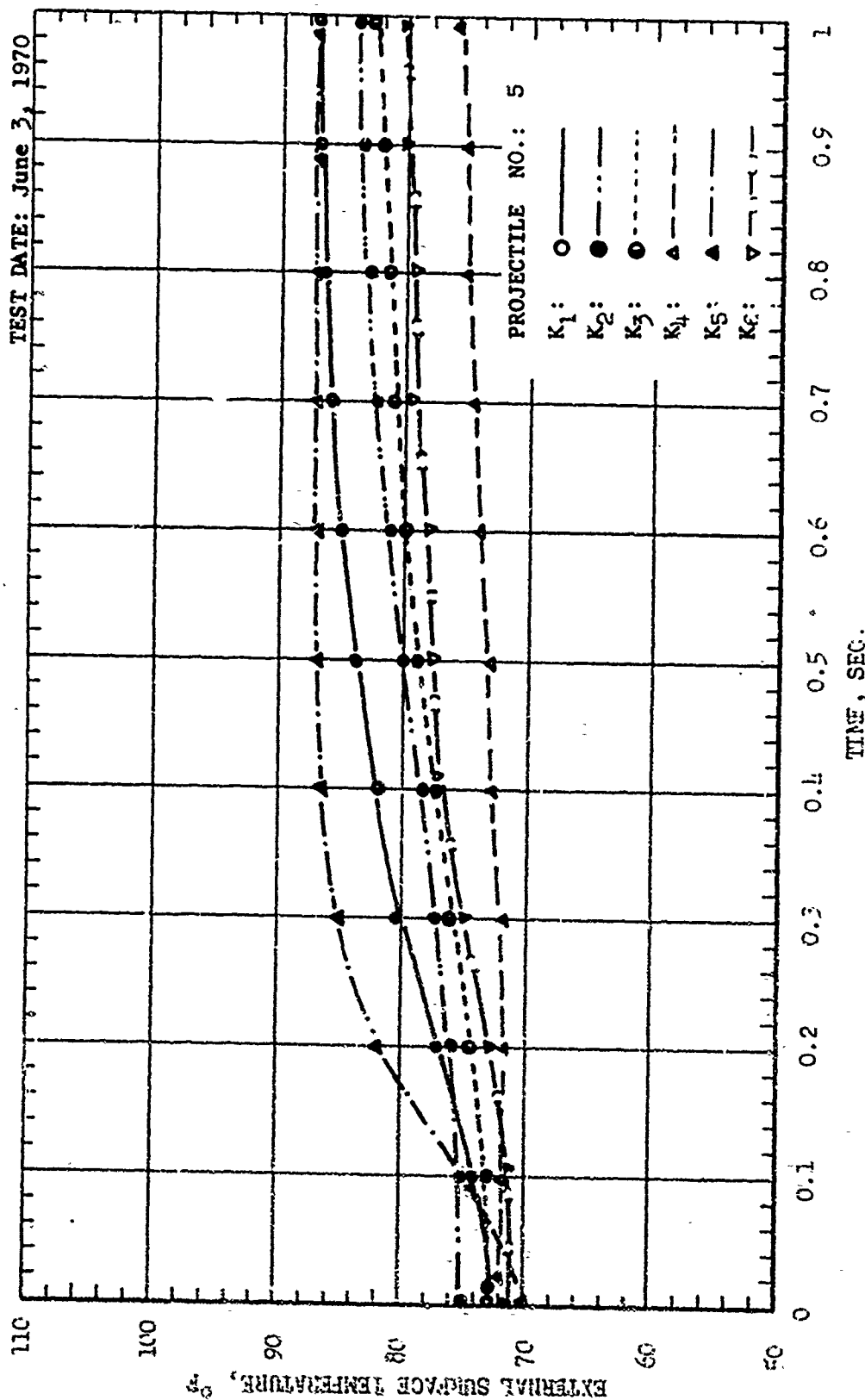




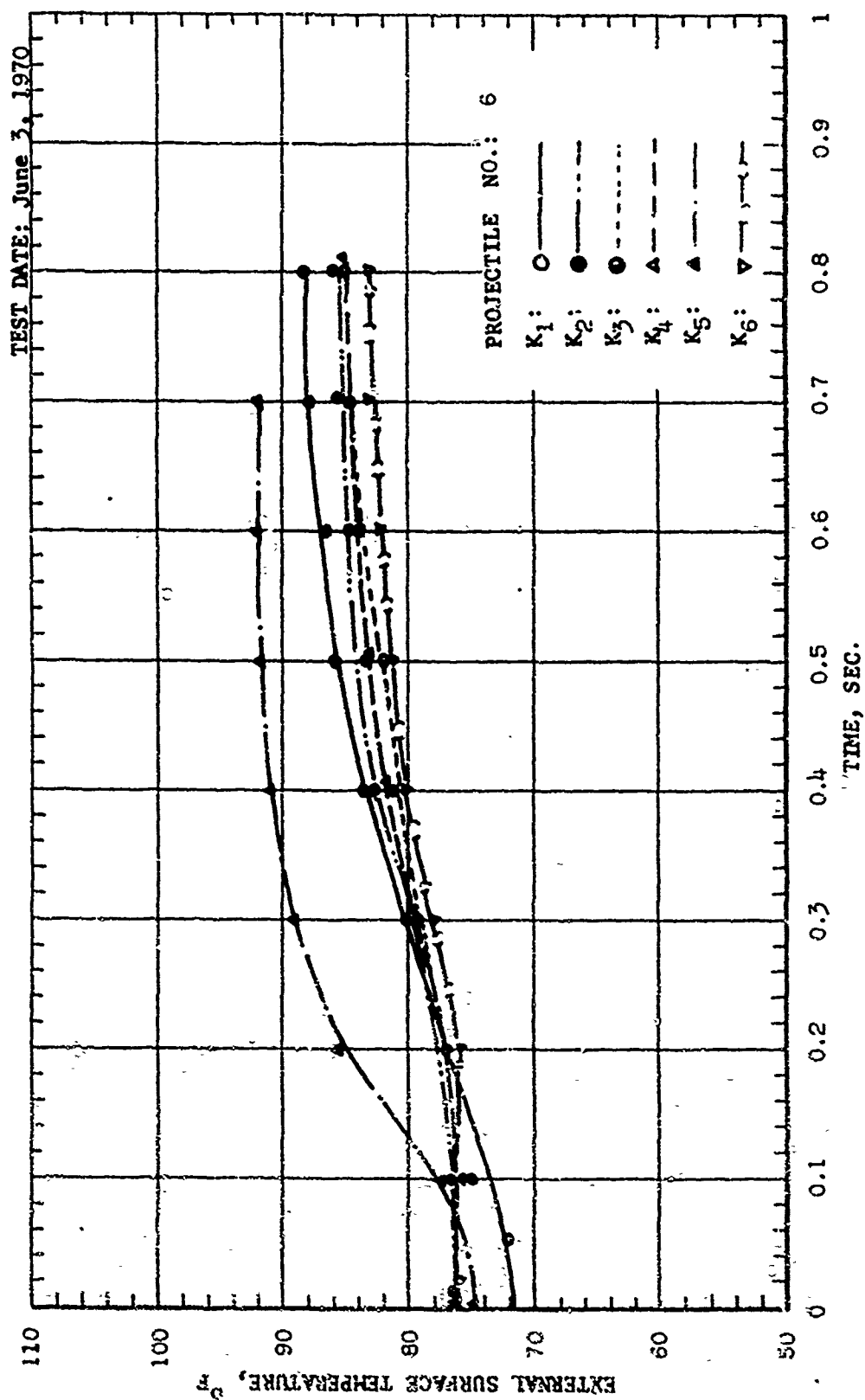


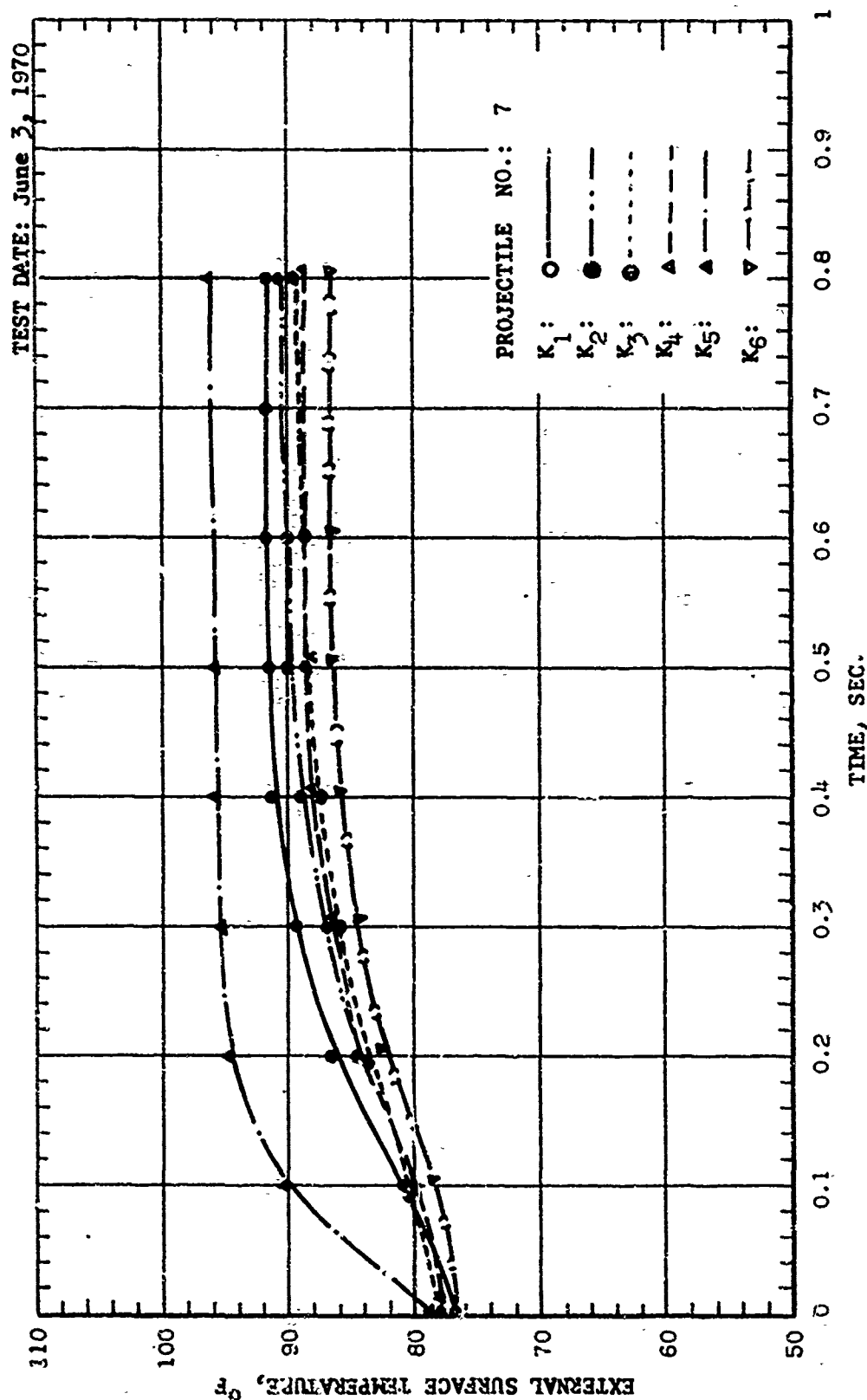


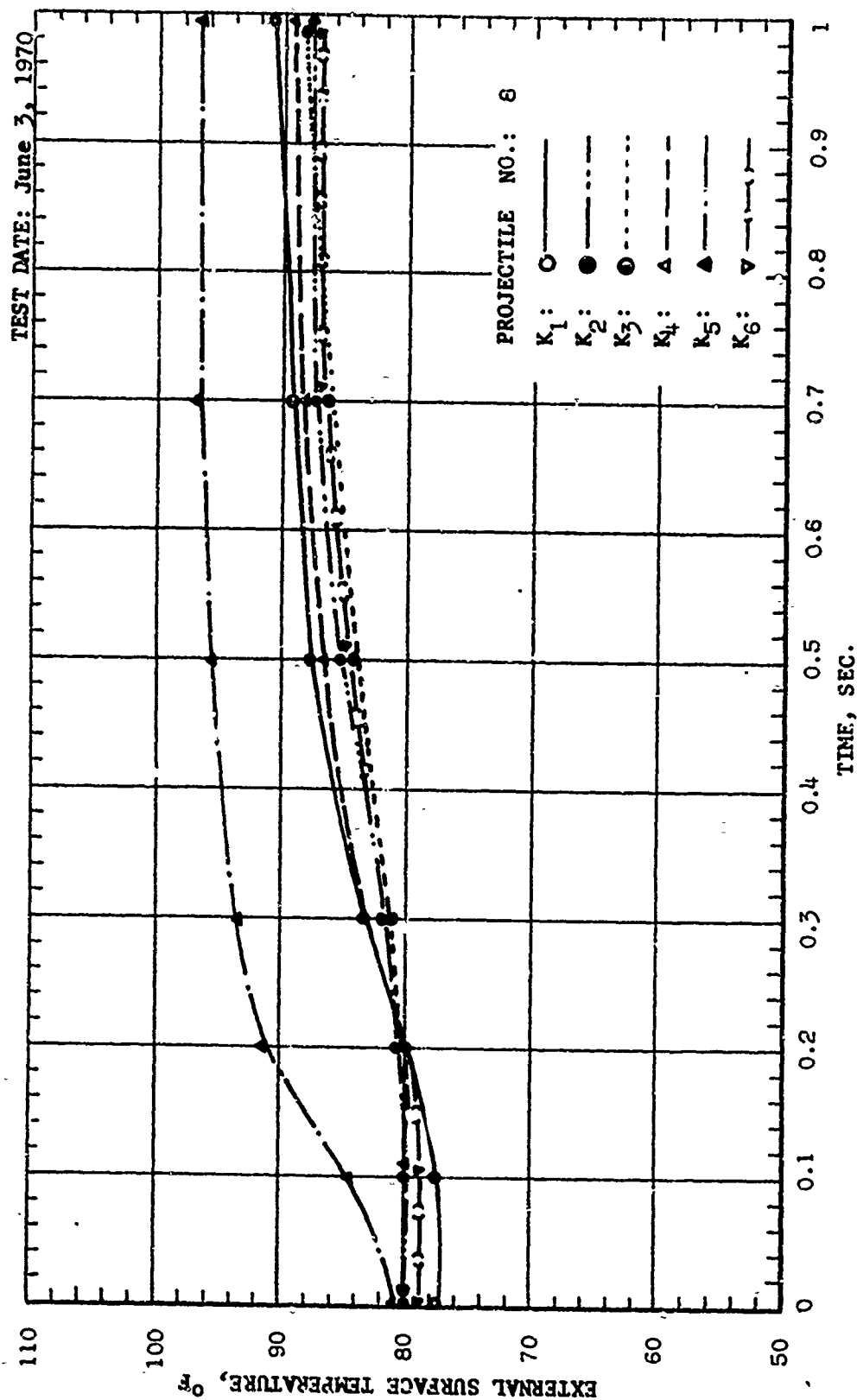








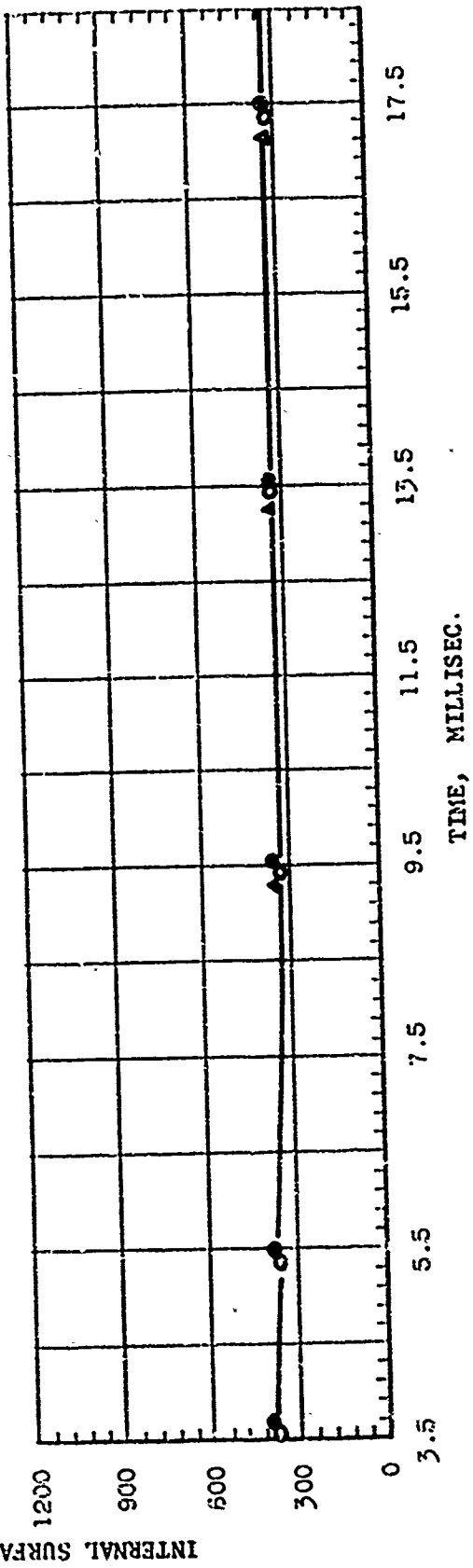
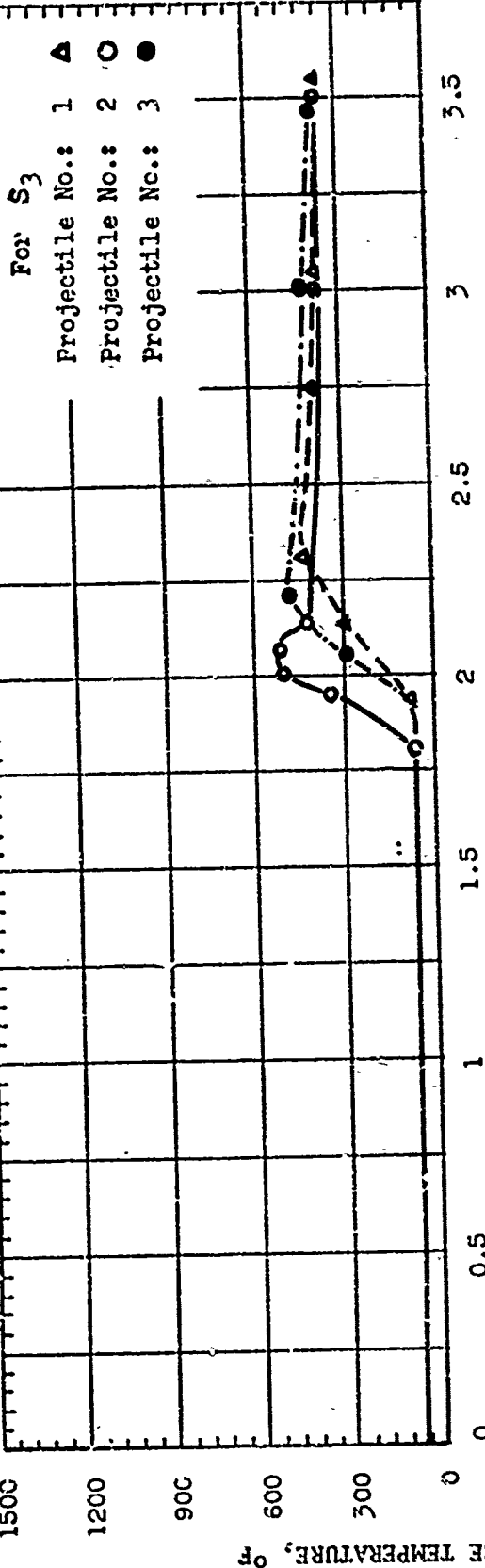


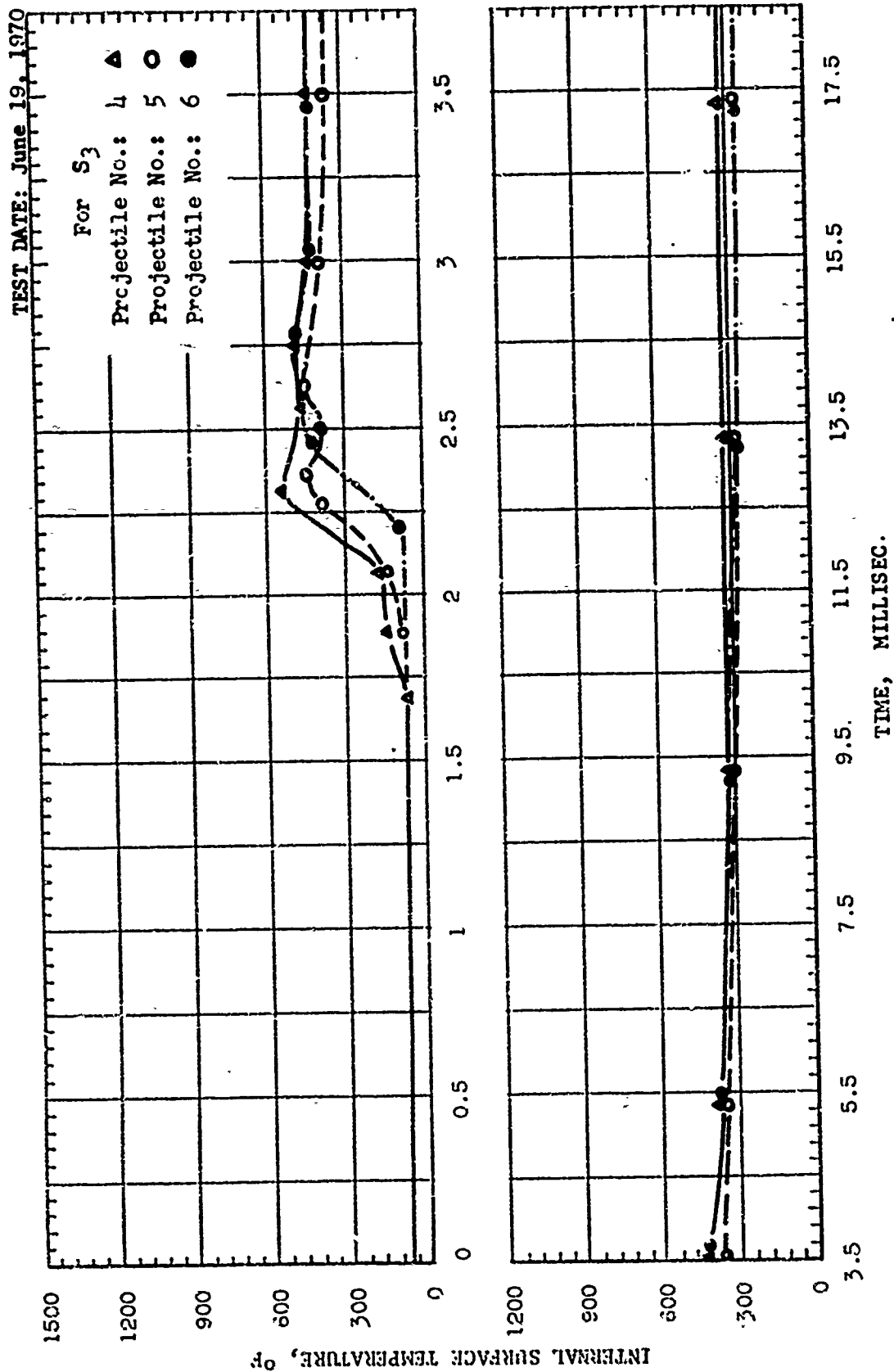


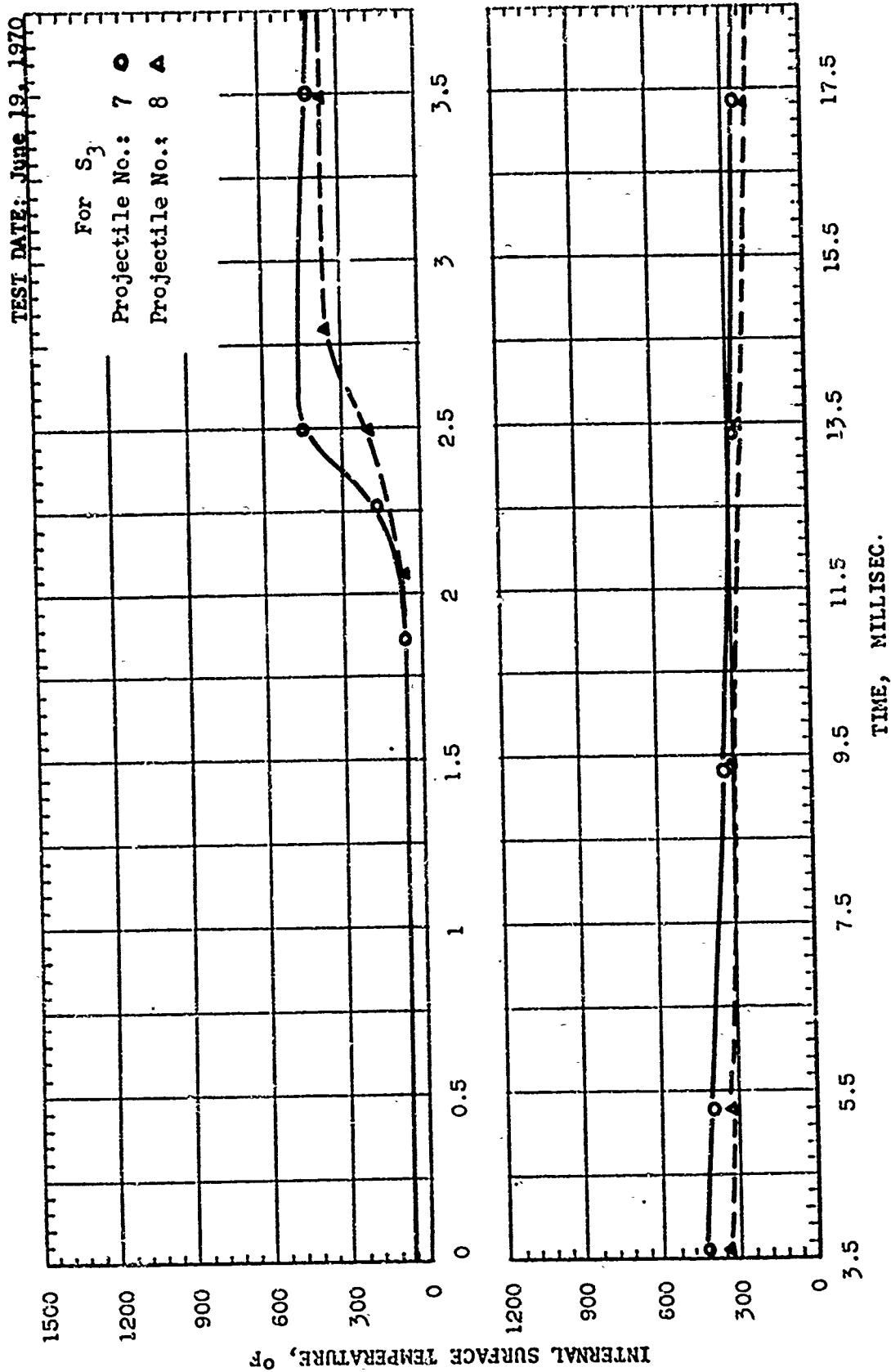
## APPENDIX IIIB EXPERIMENTAL DATA (June 19, 1970)

NOTE: See Fig. III-1 for Arrangement of Probes

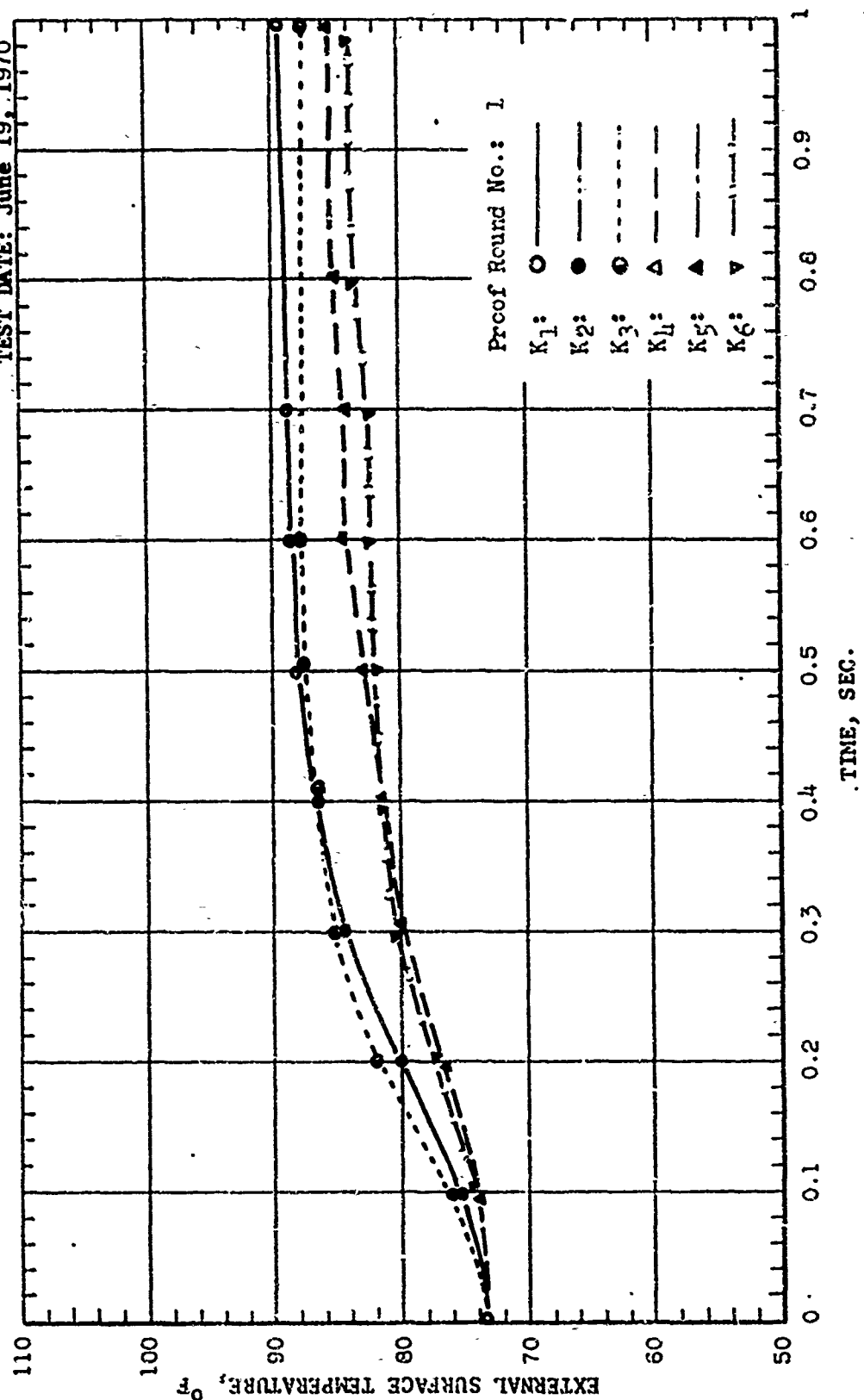
TEST DATE: June 13, 1970



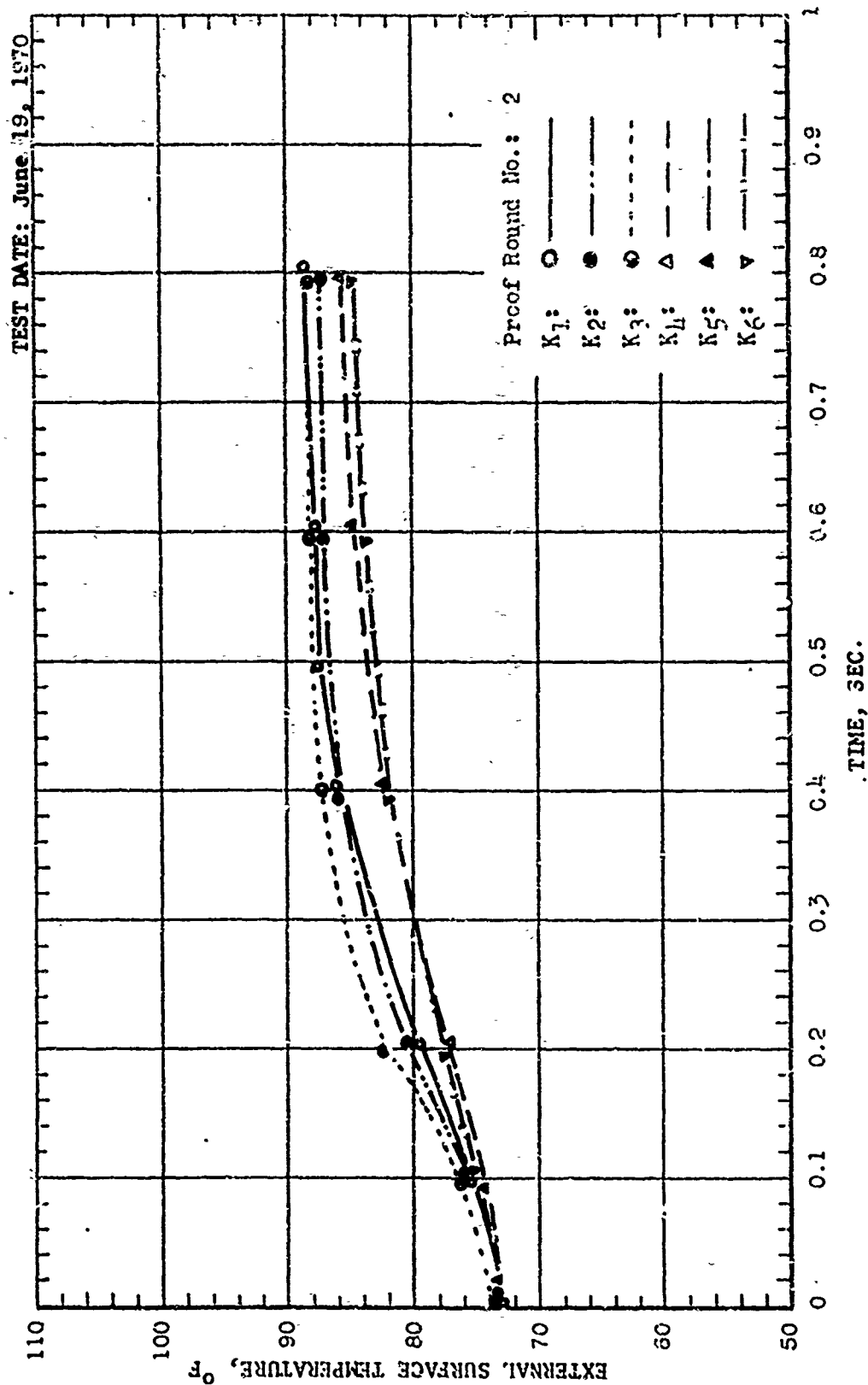


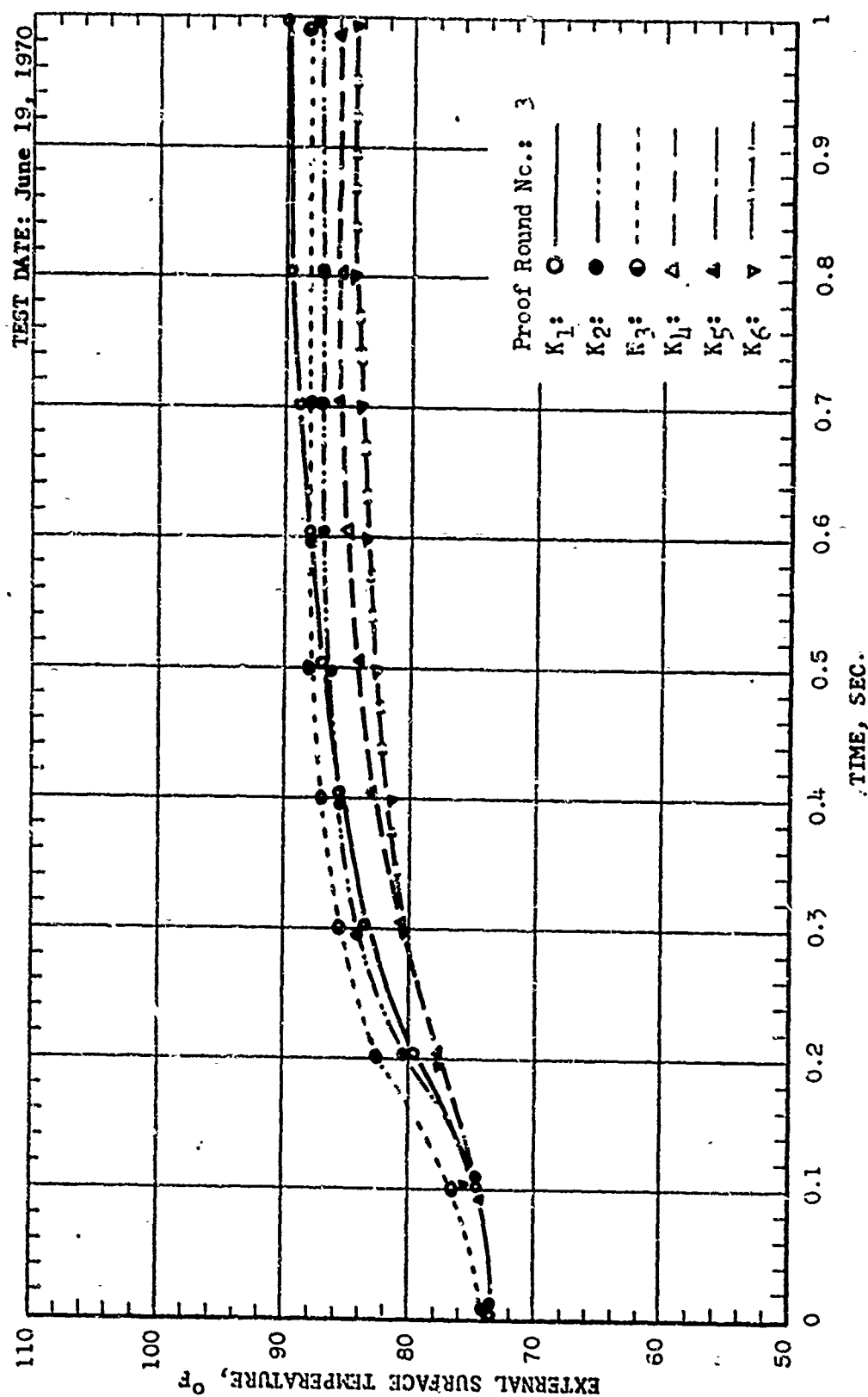


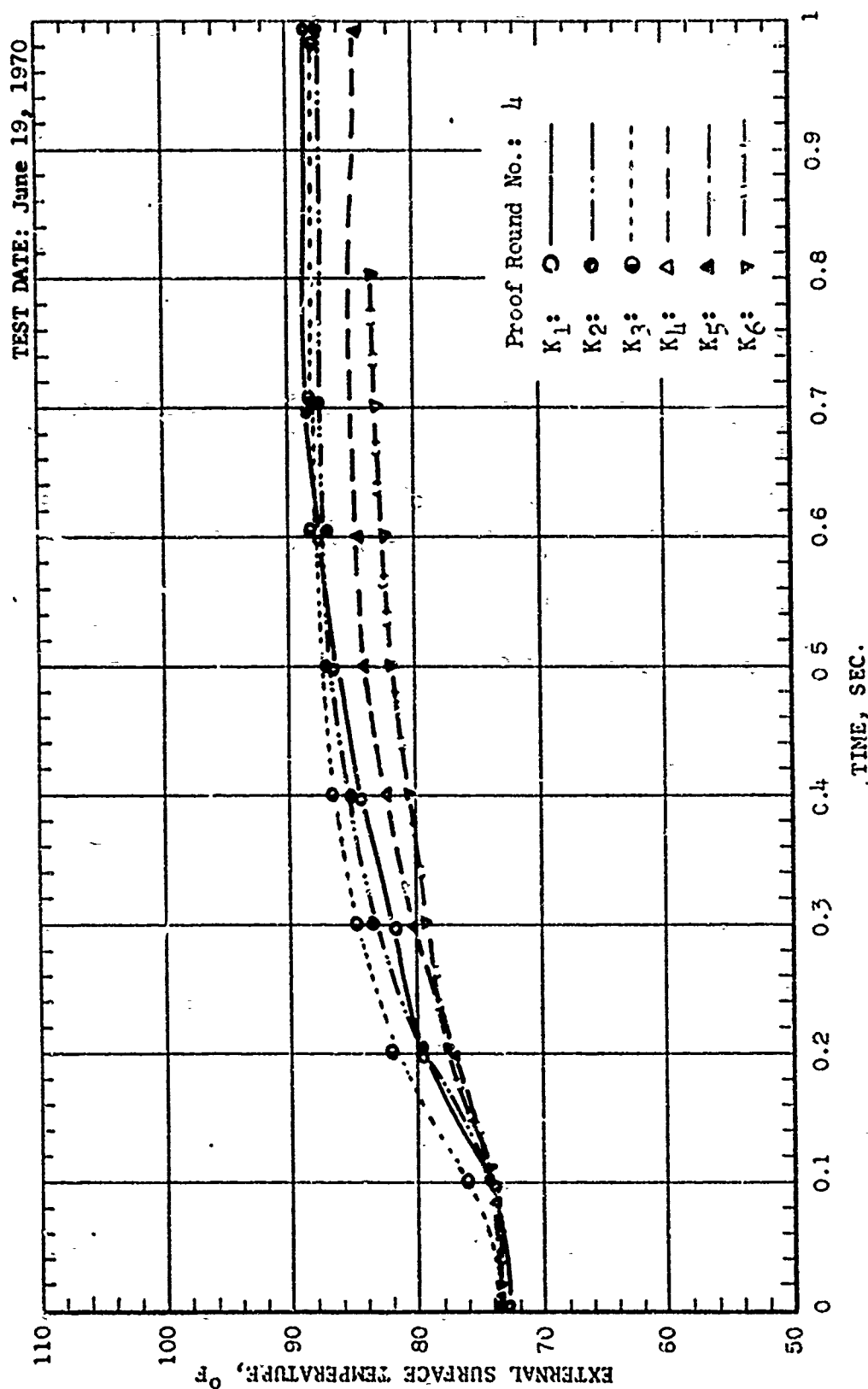
TEST DATE: June 19, 1970

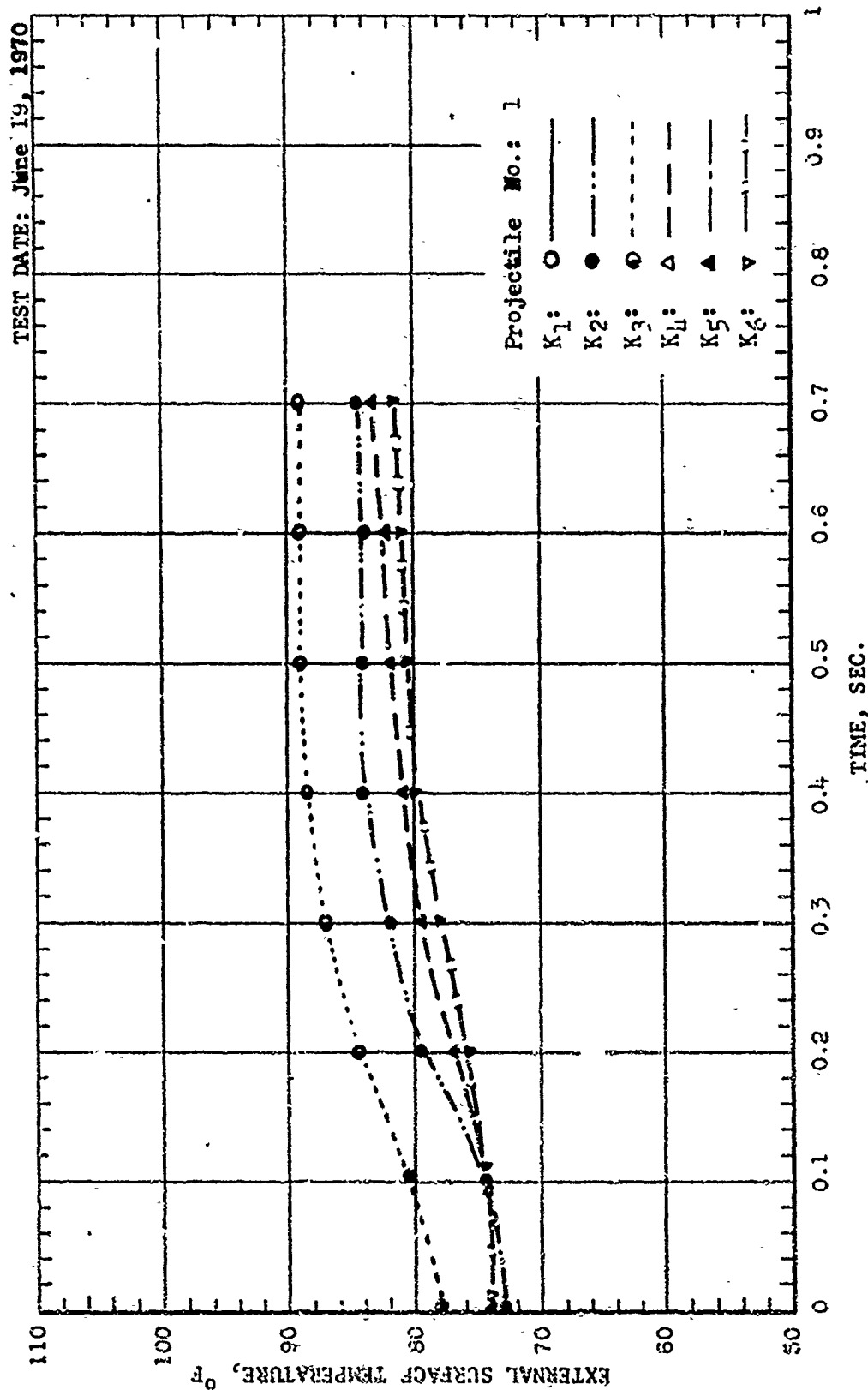


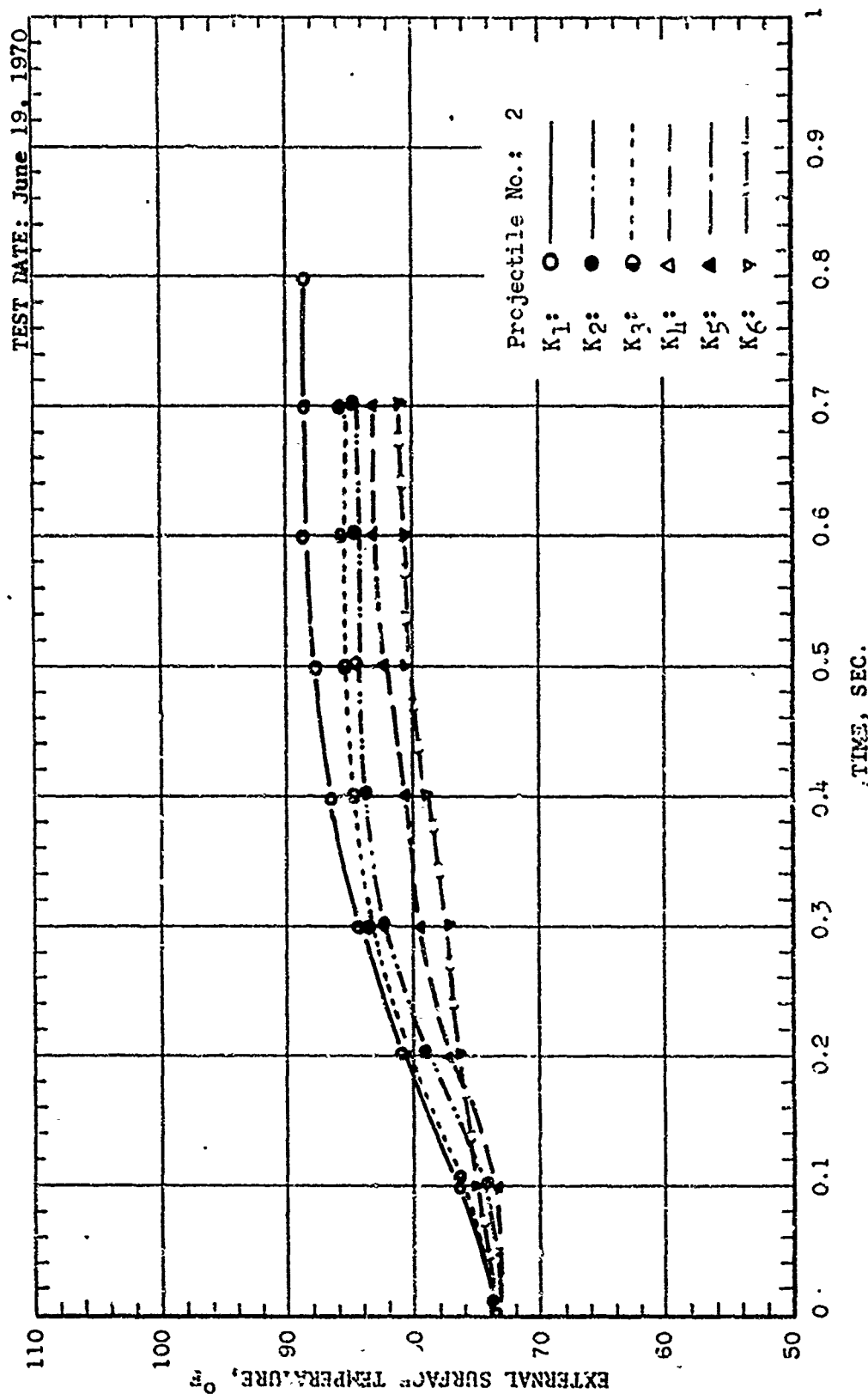


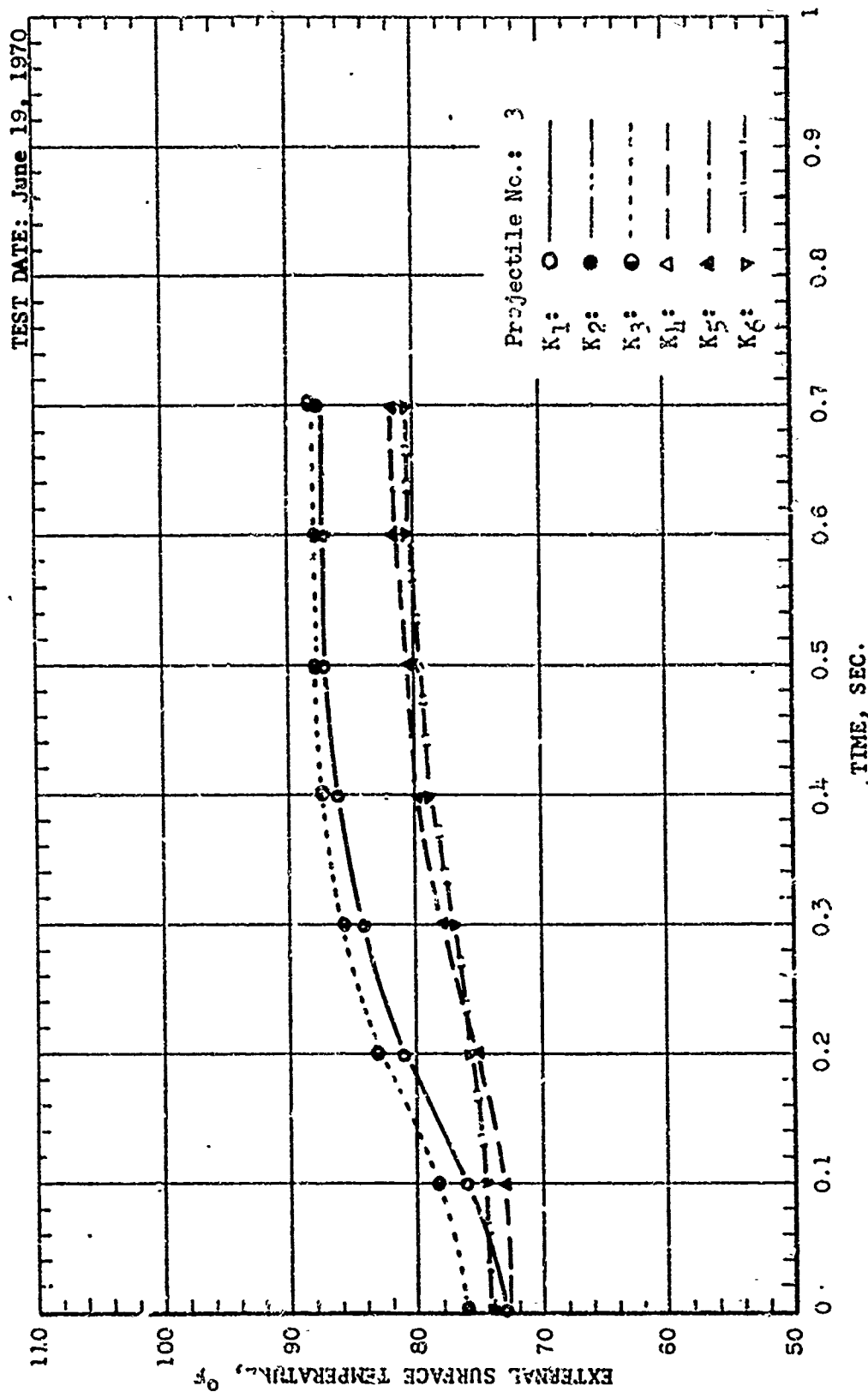


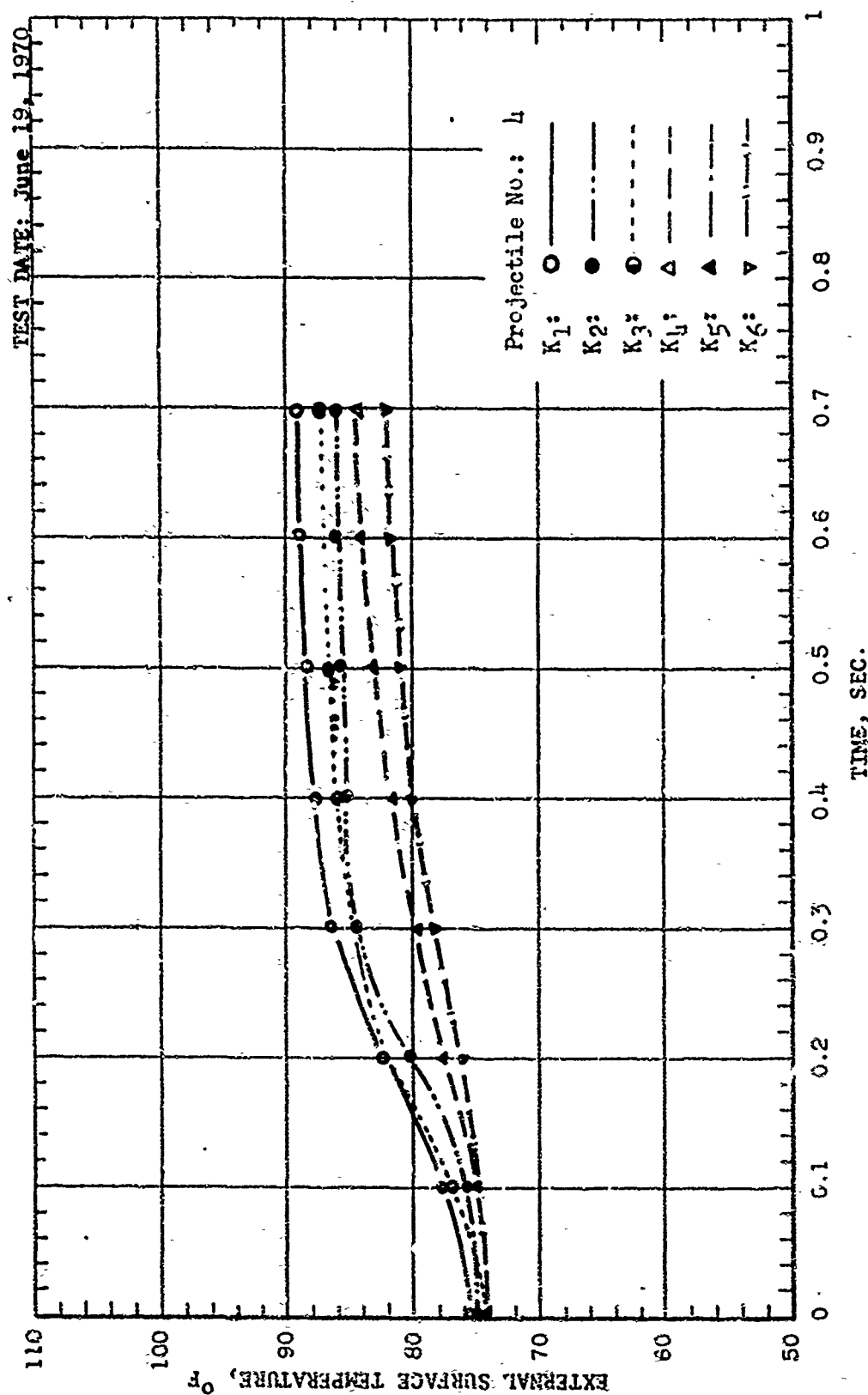


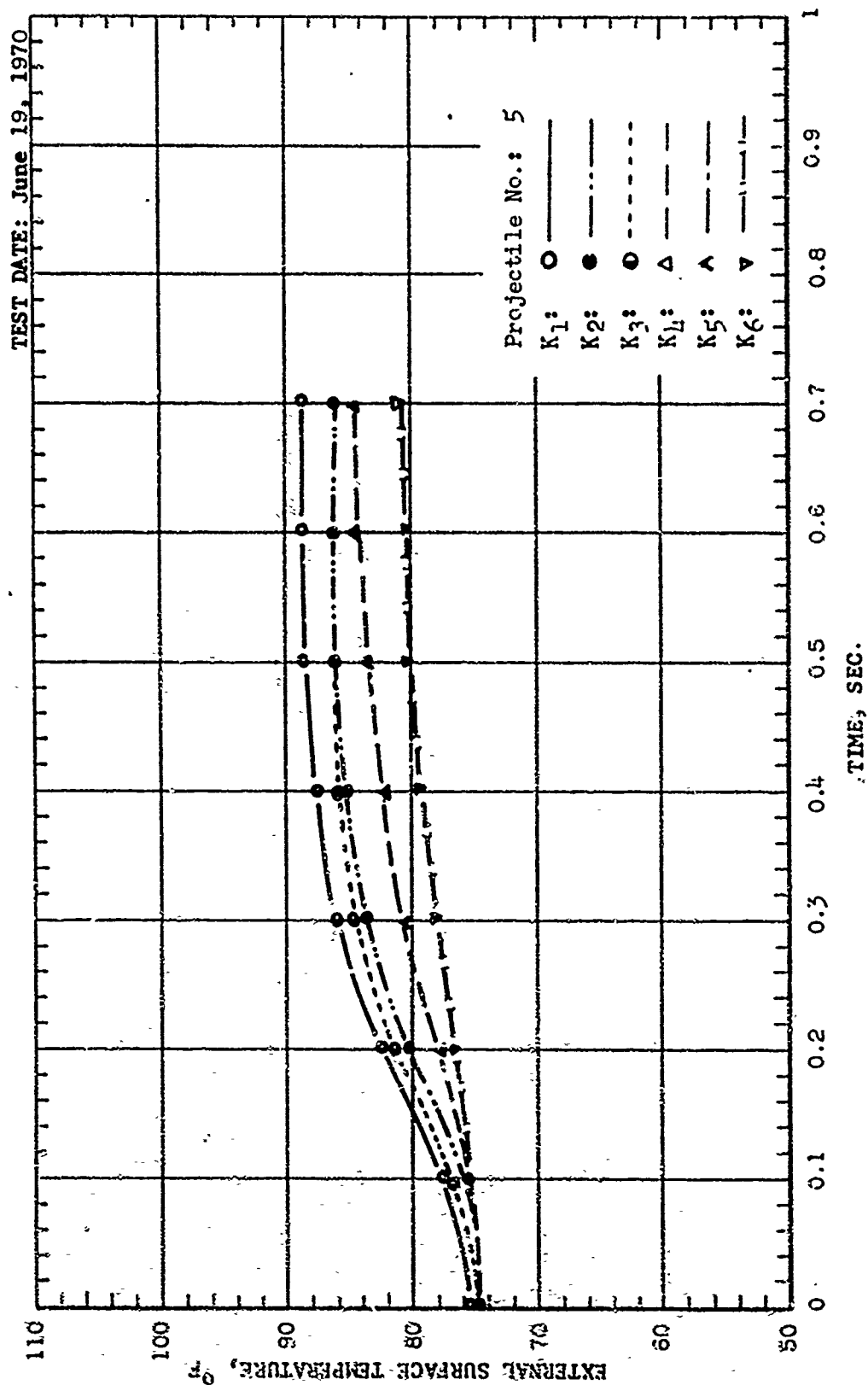




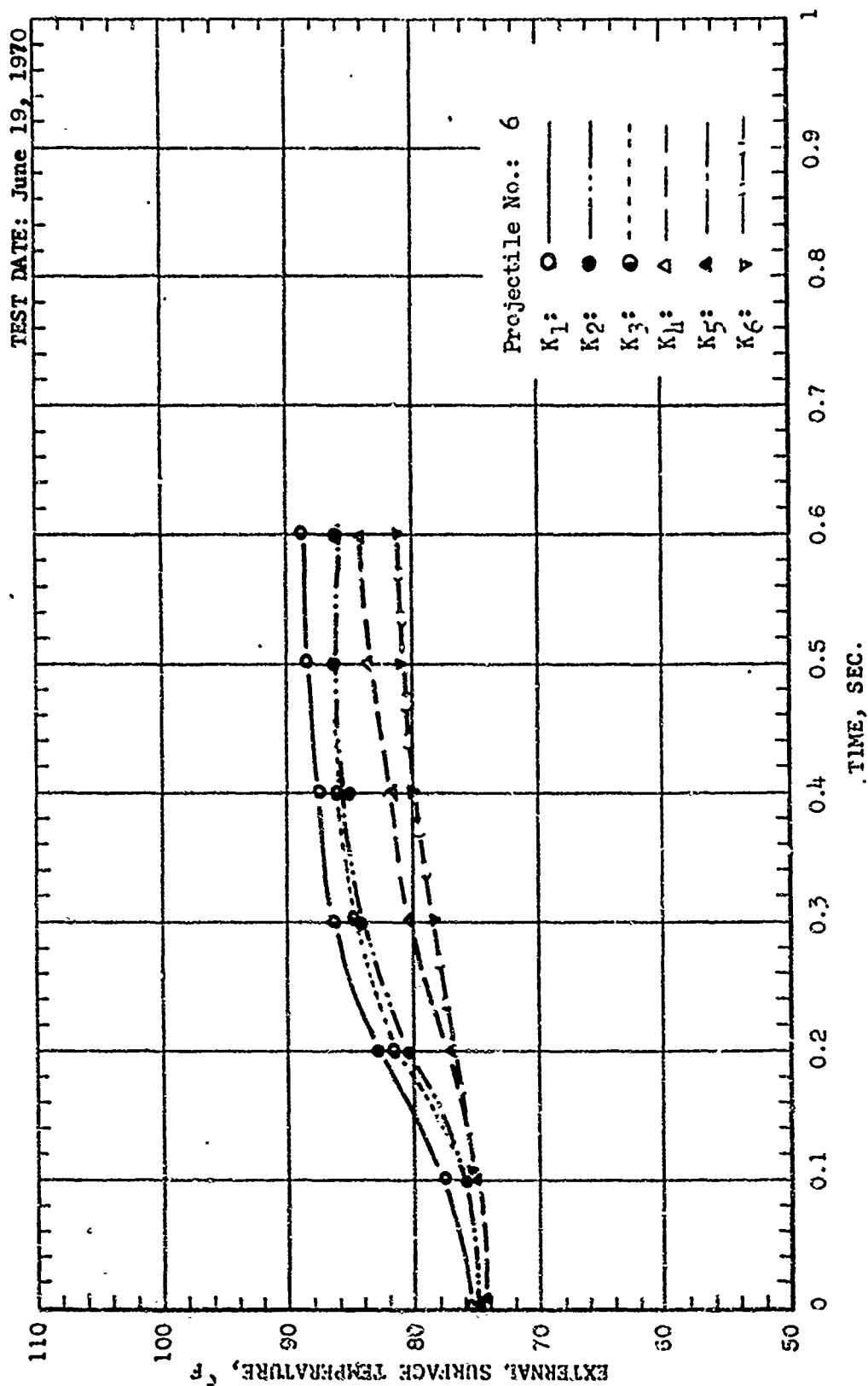


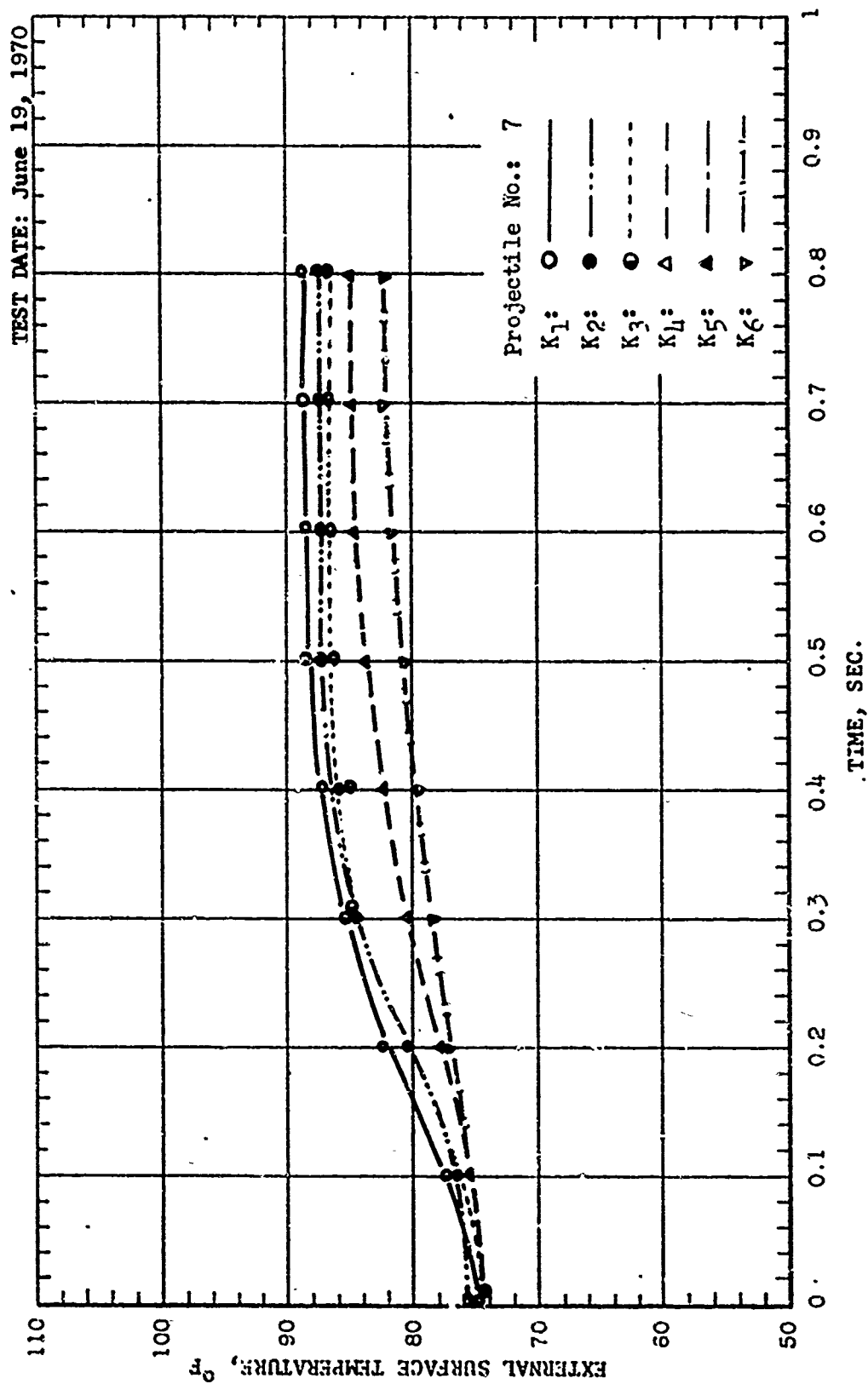


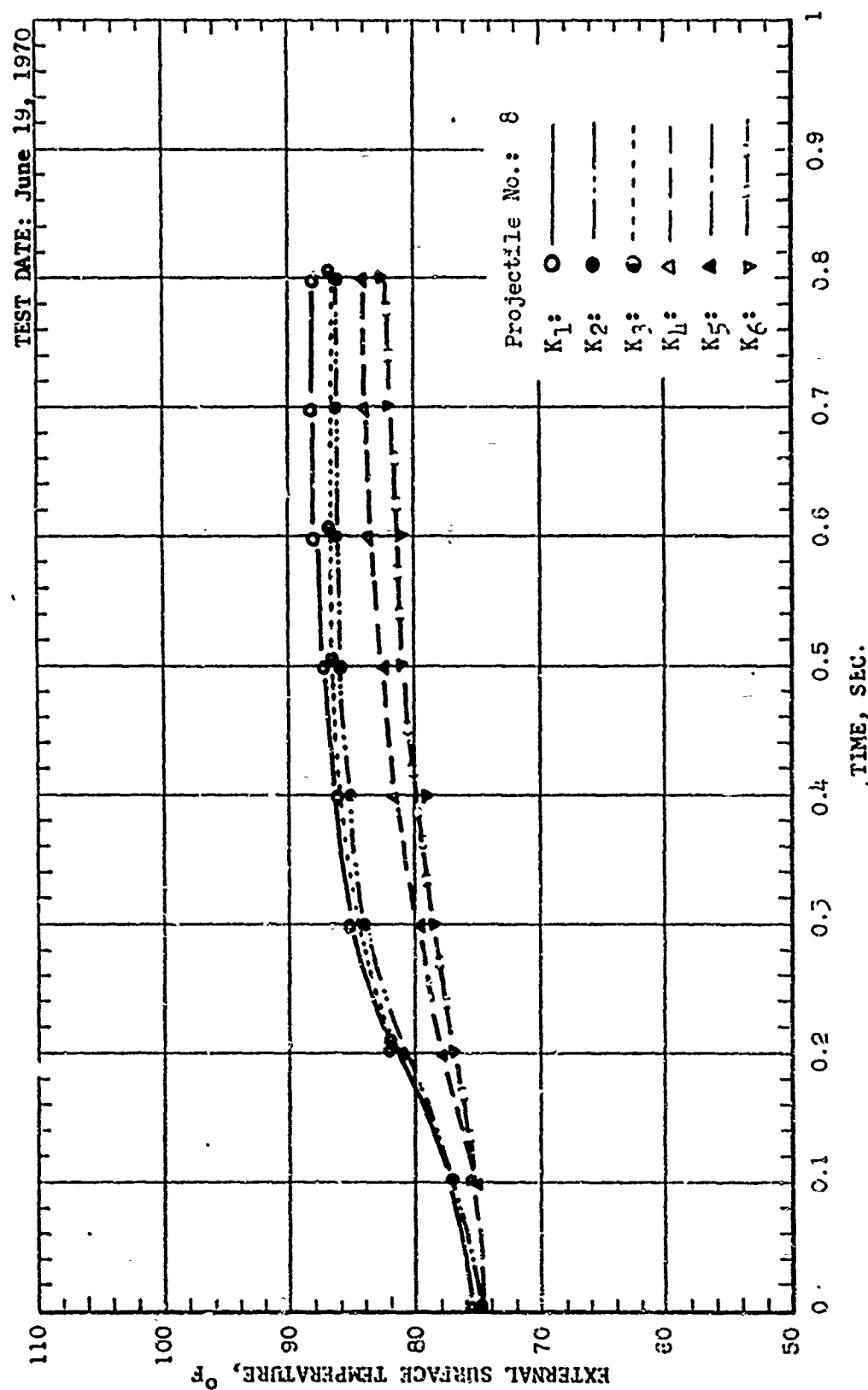


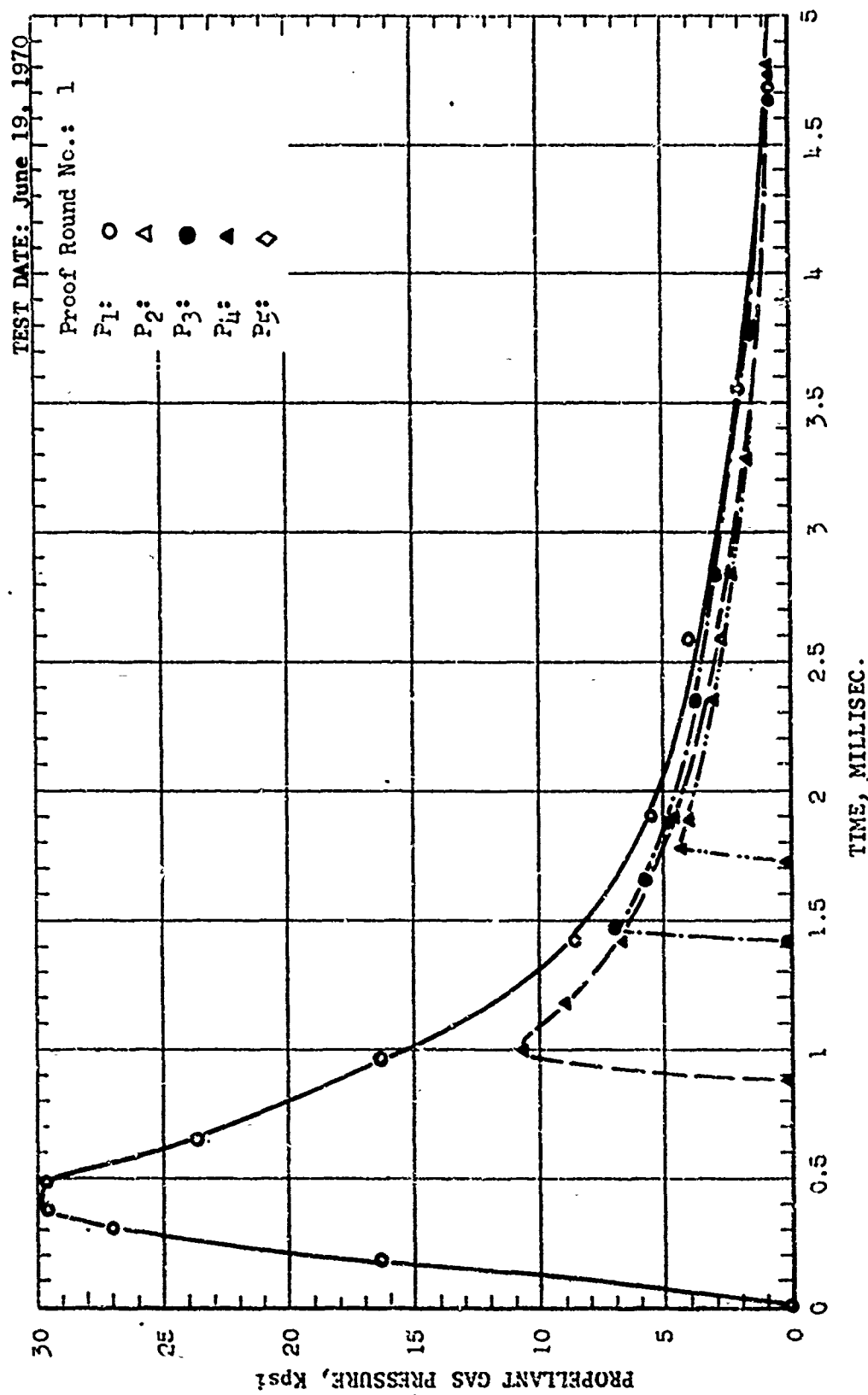


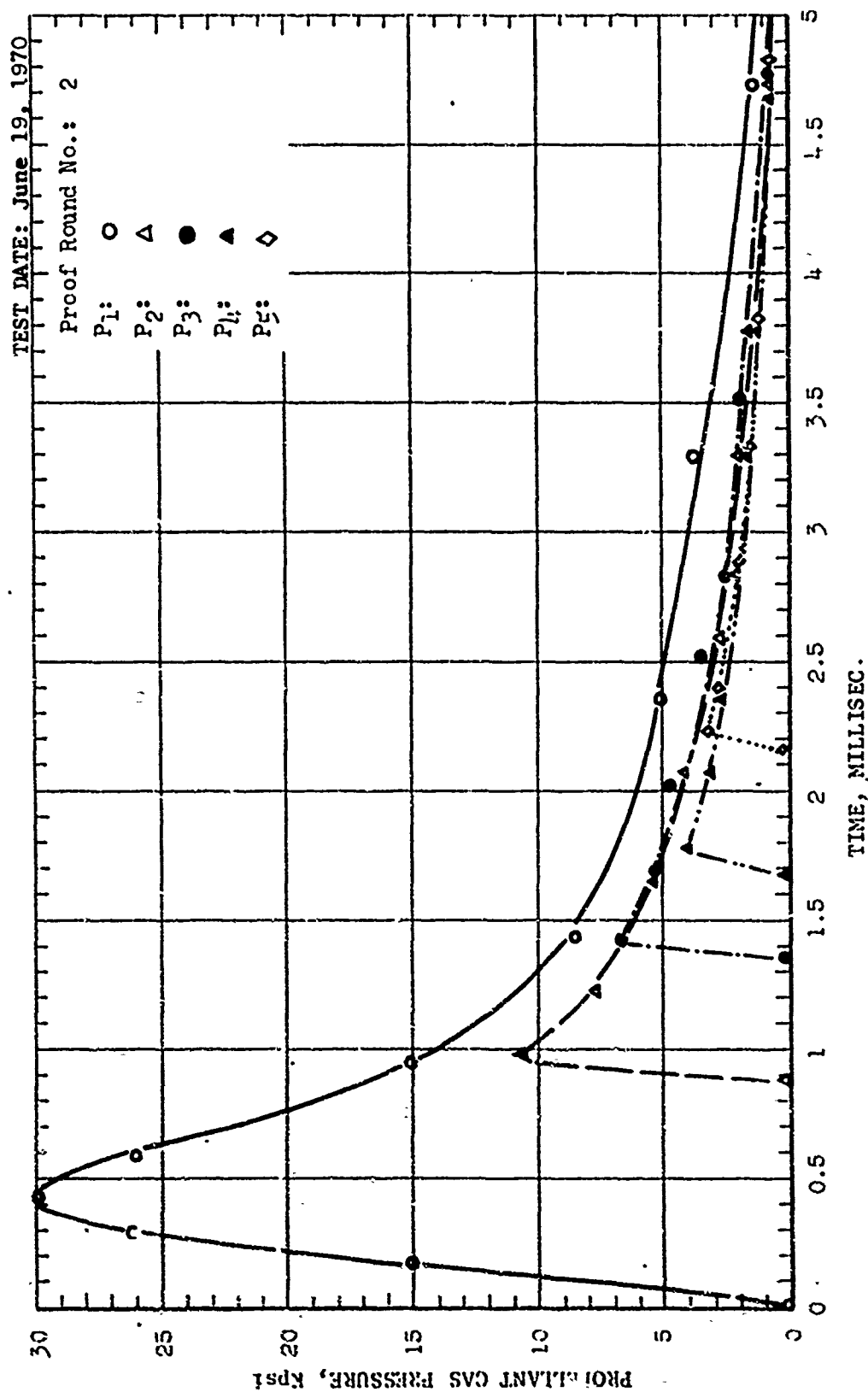


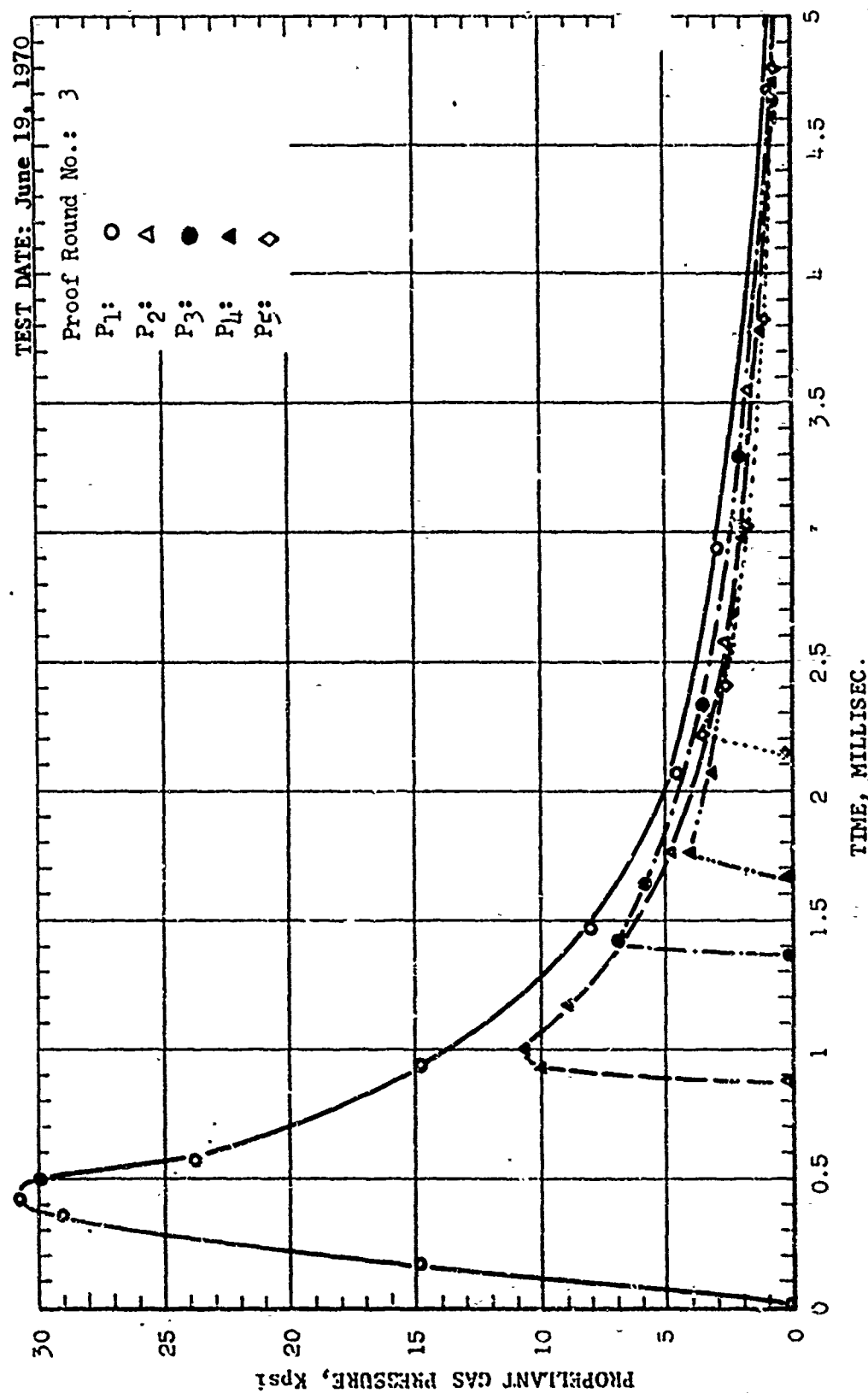


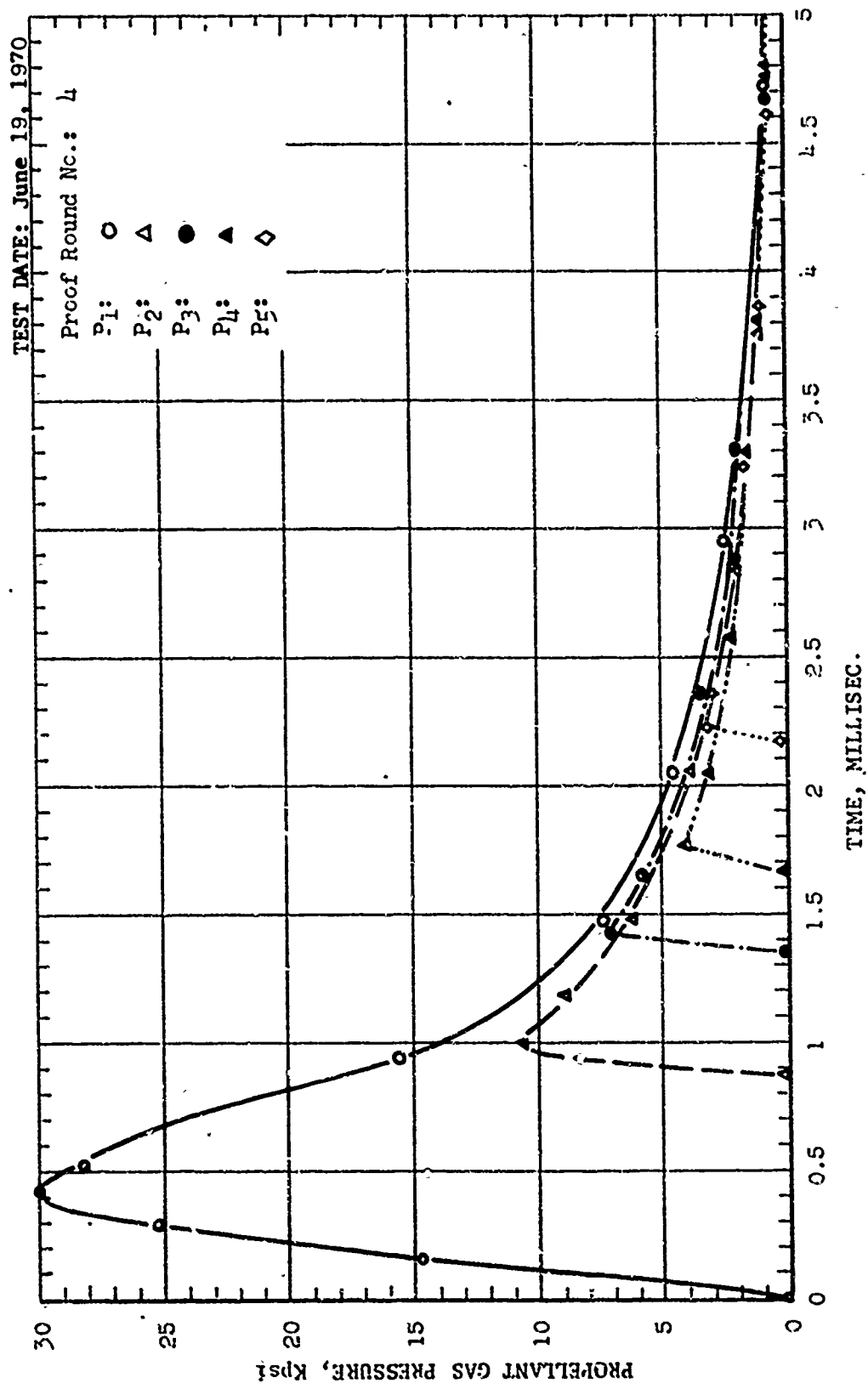


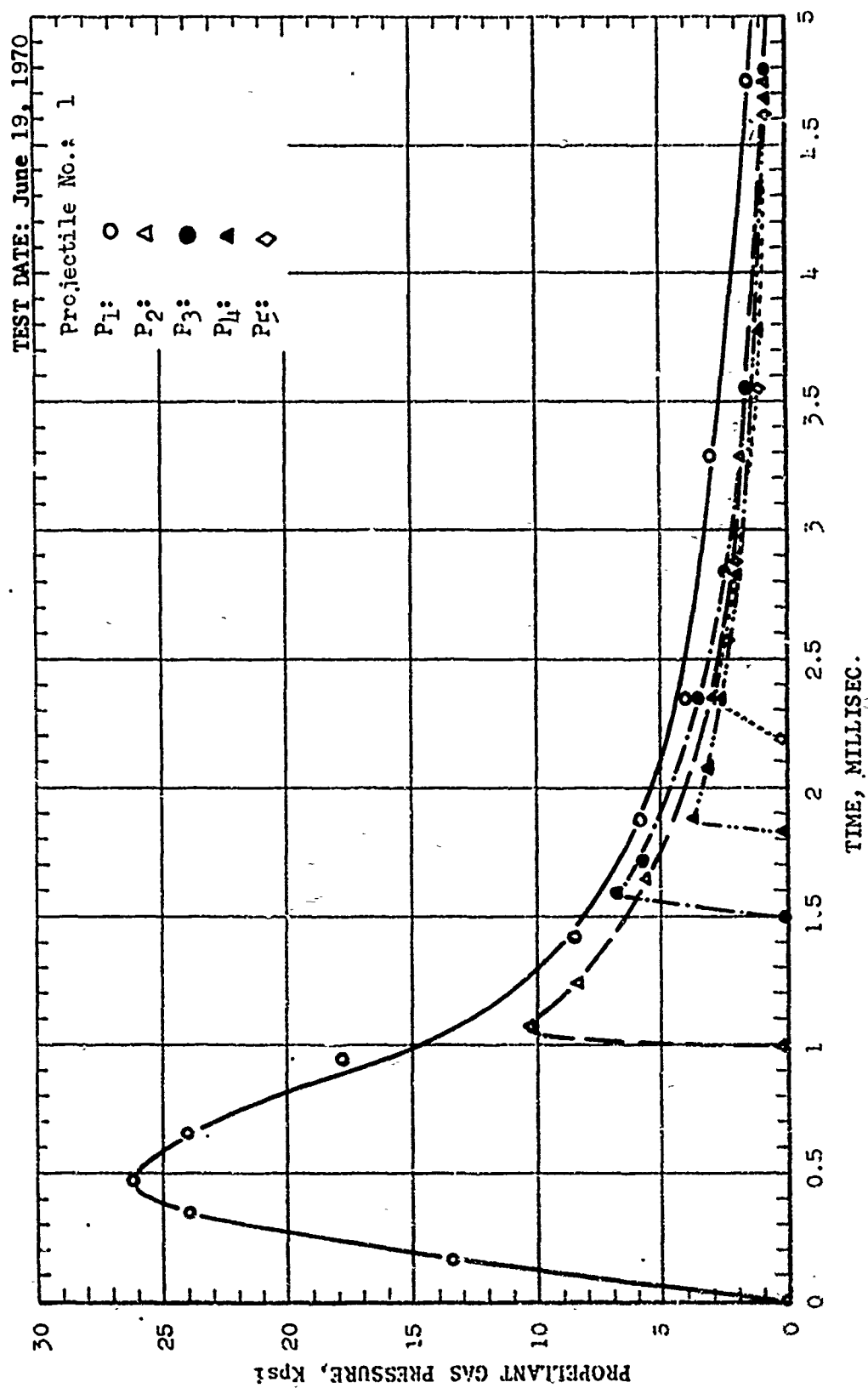




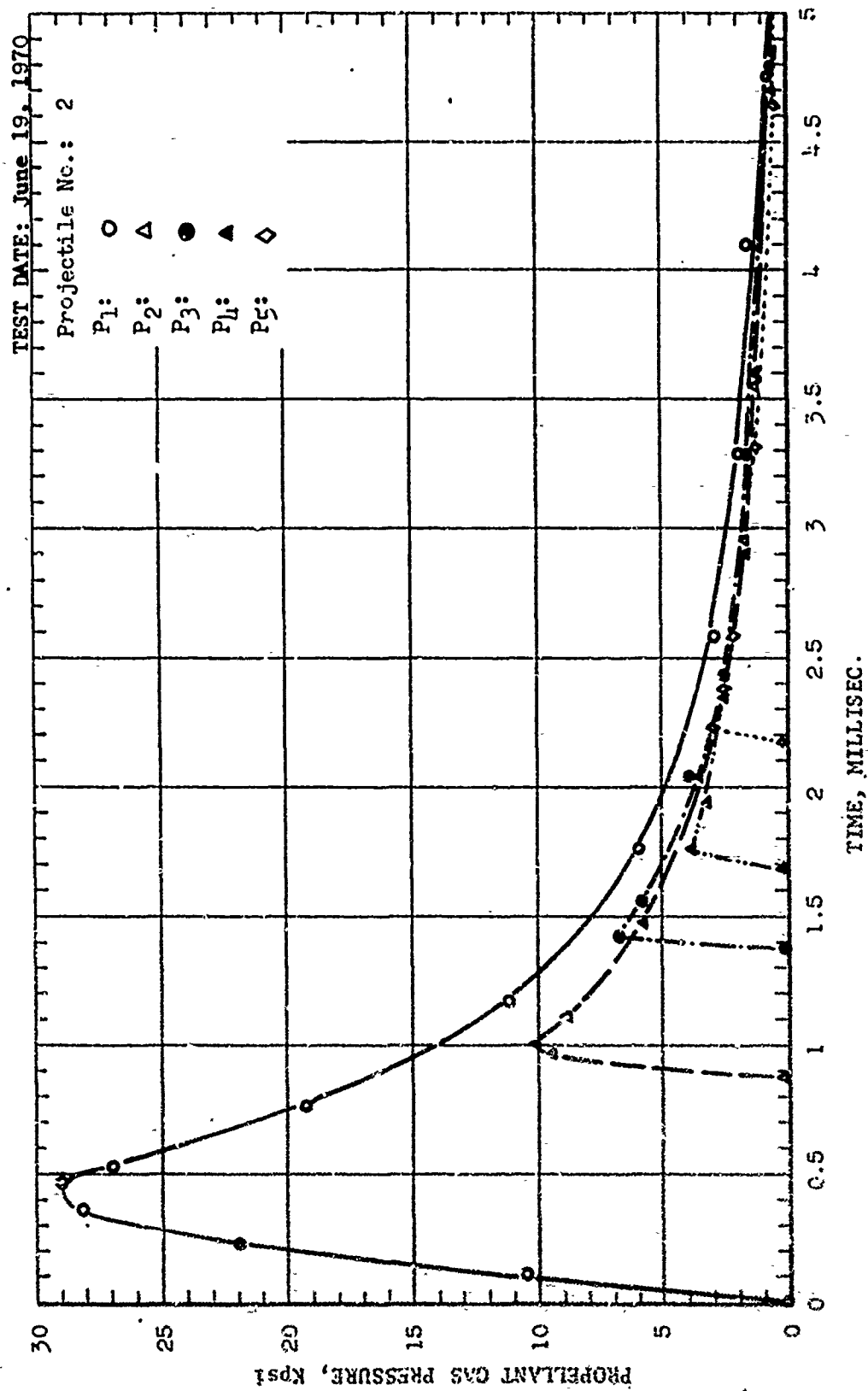


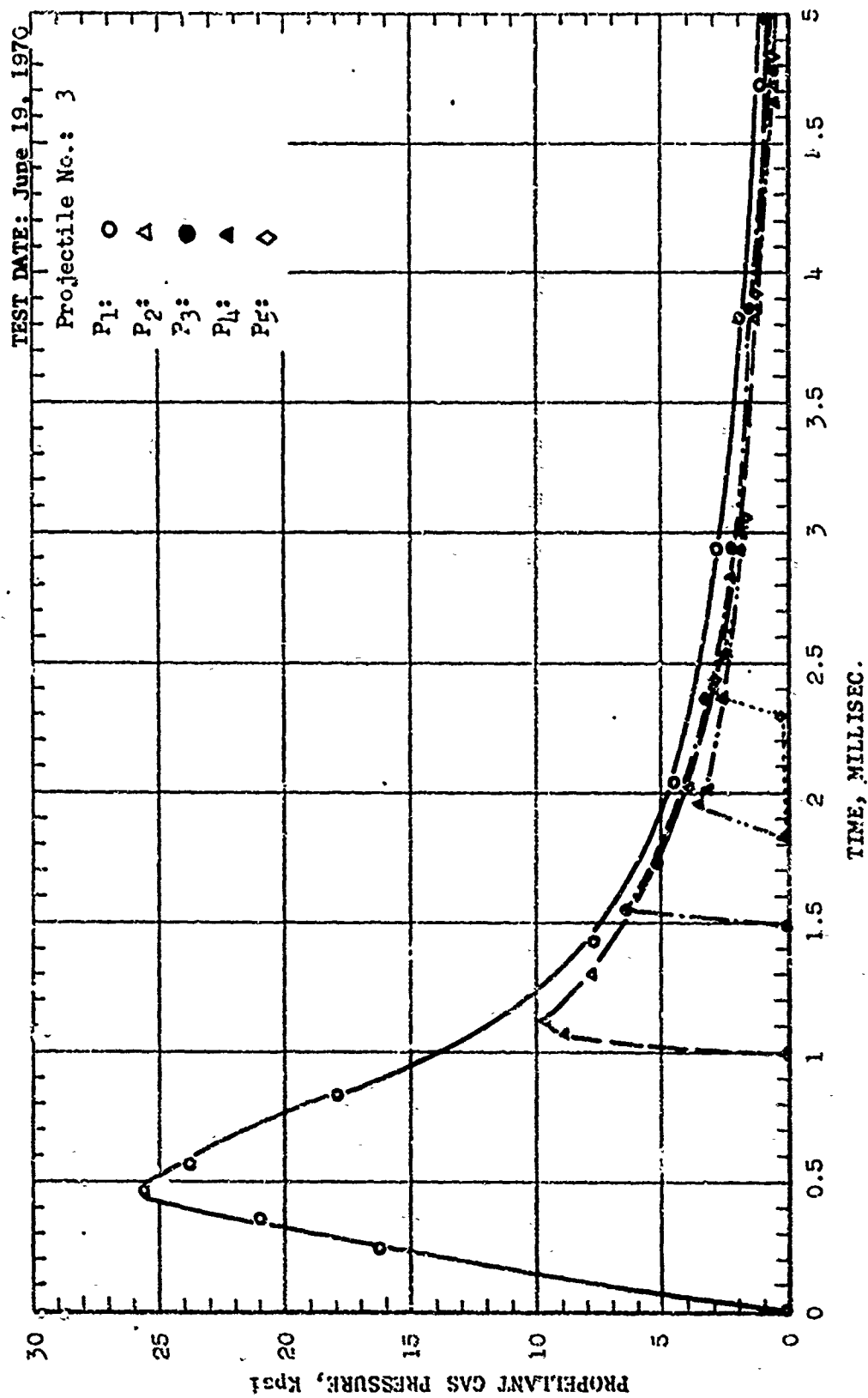


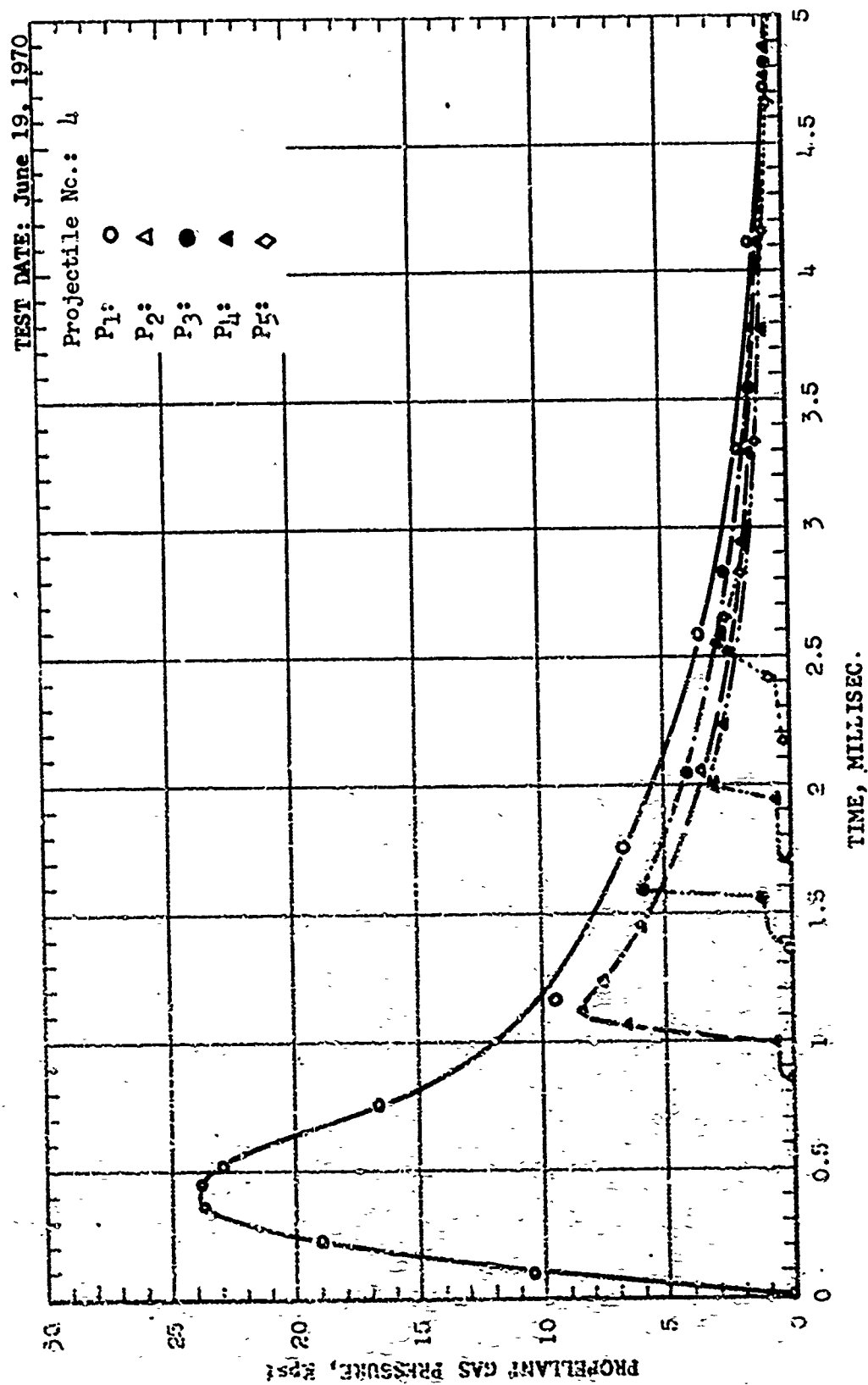


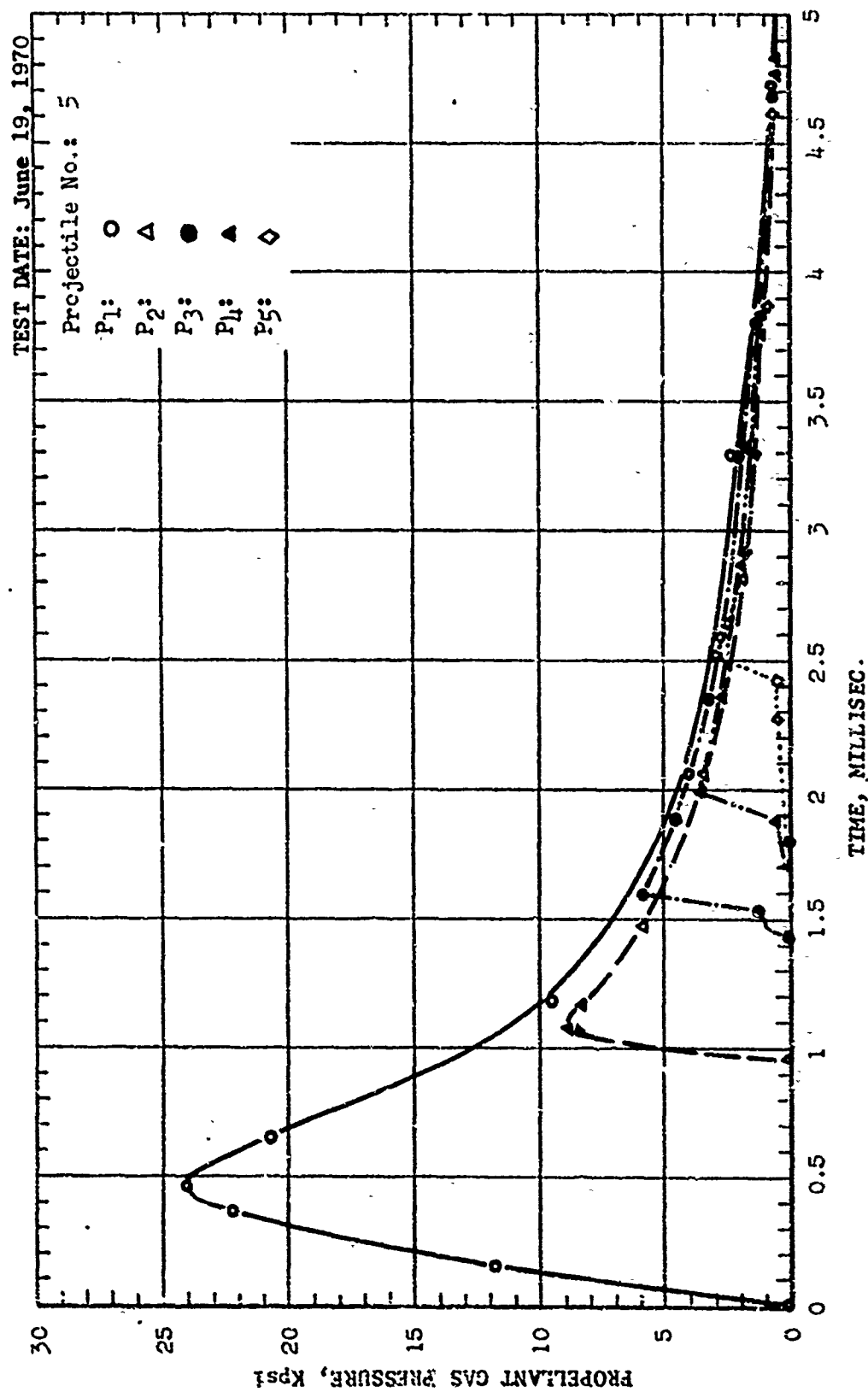


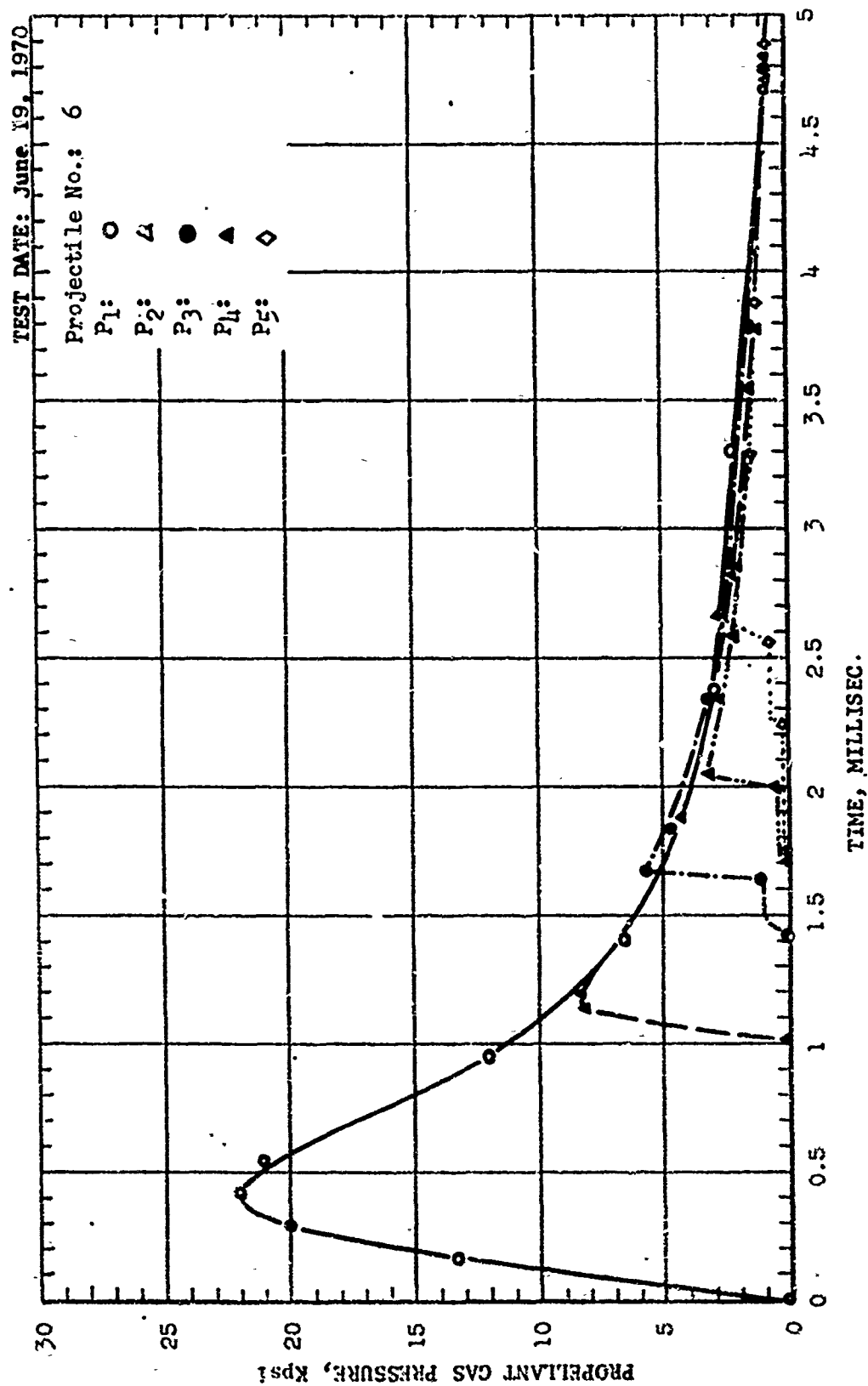


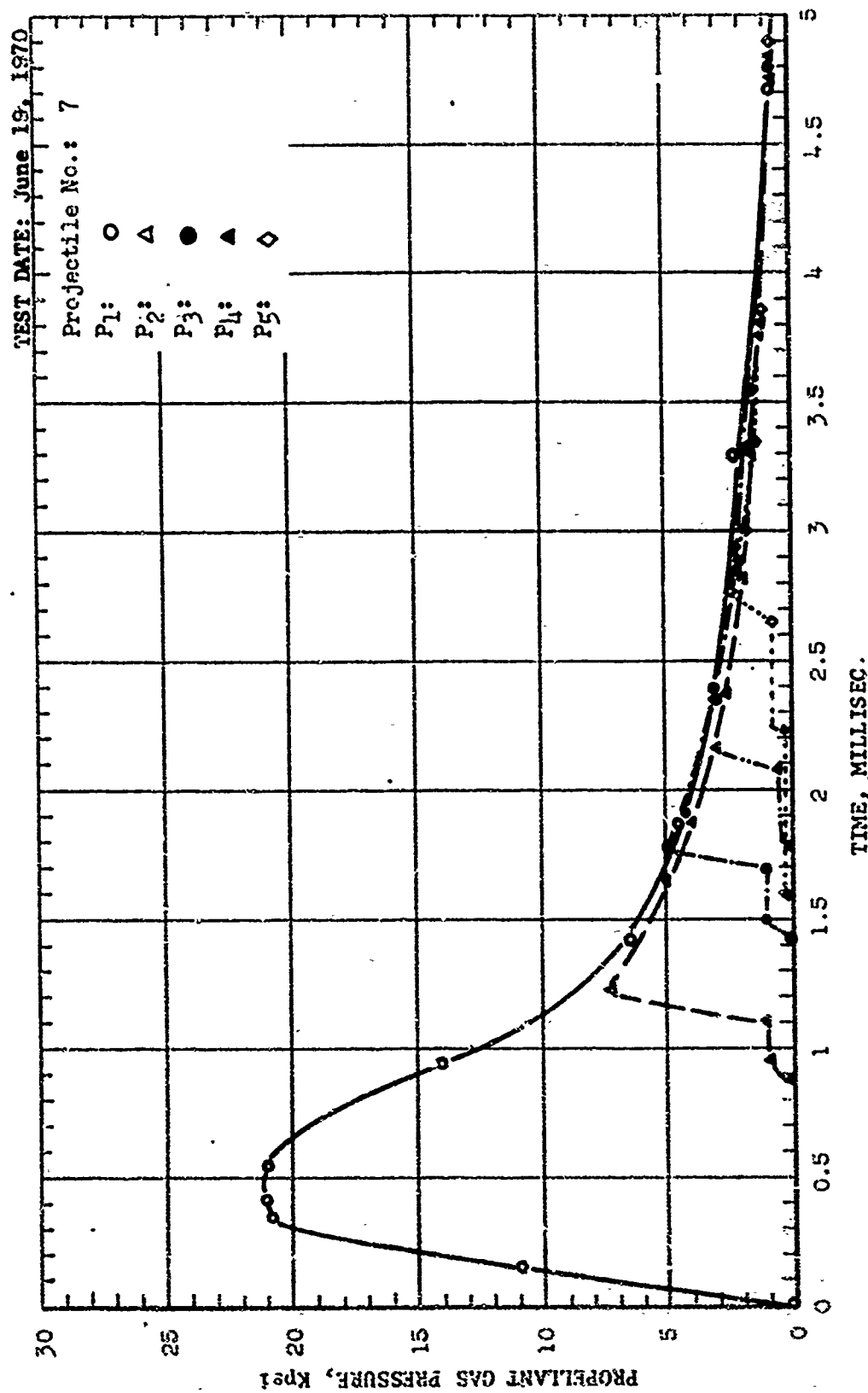


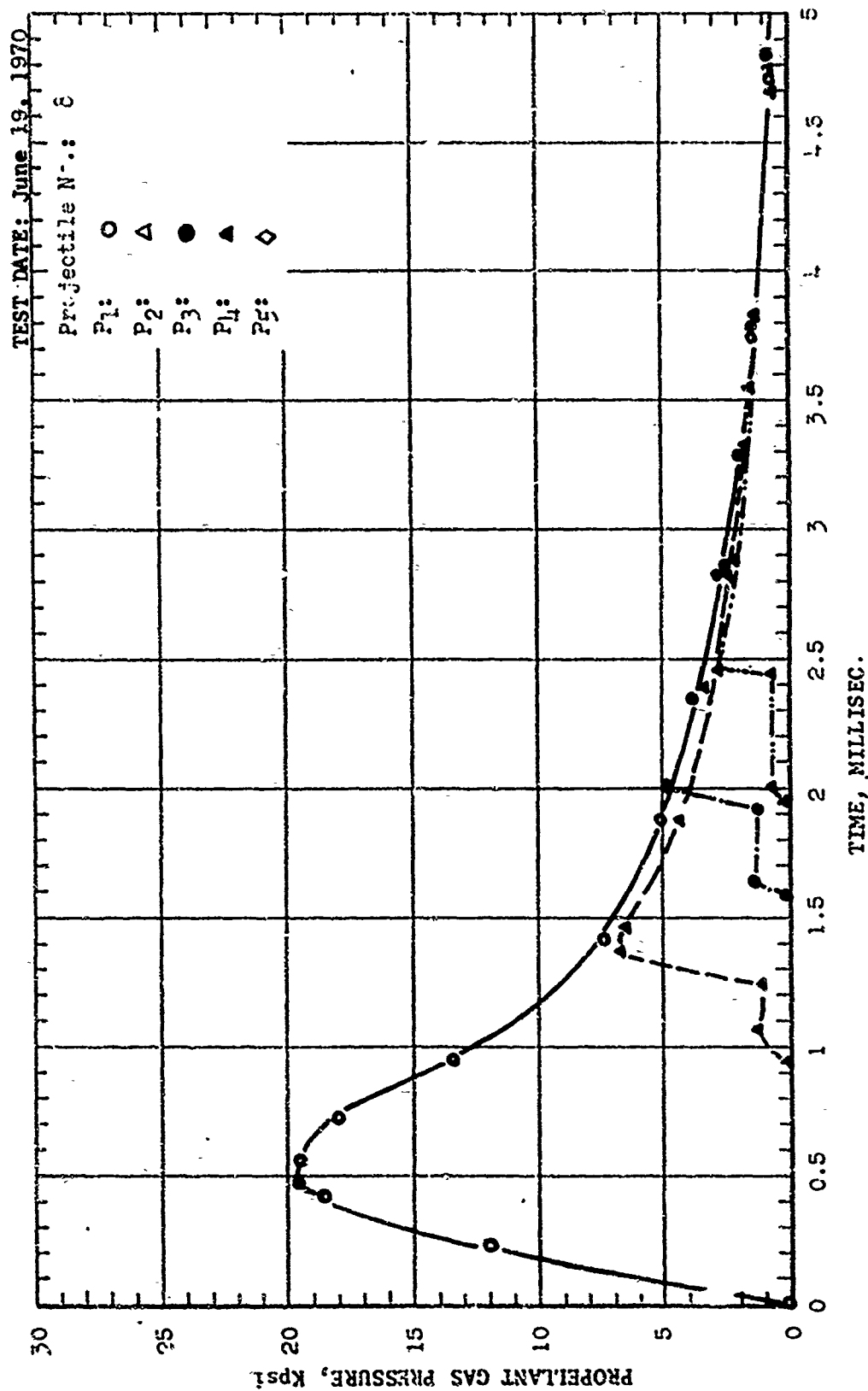








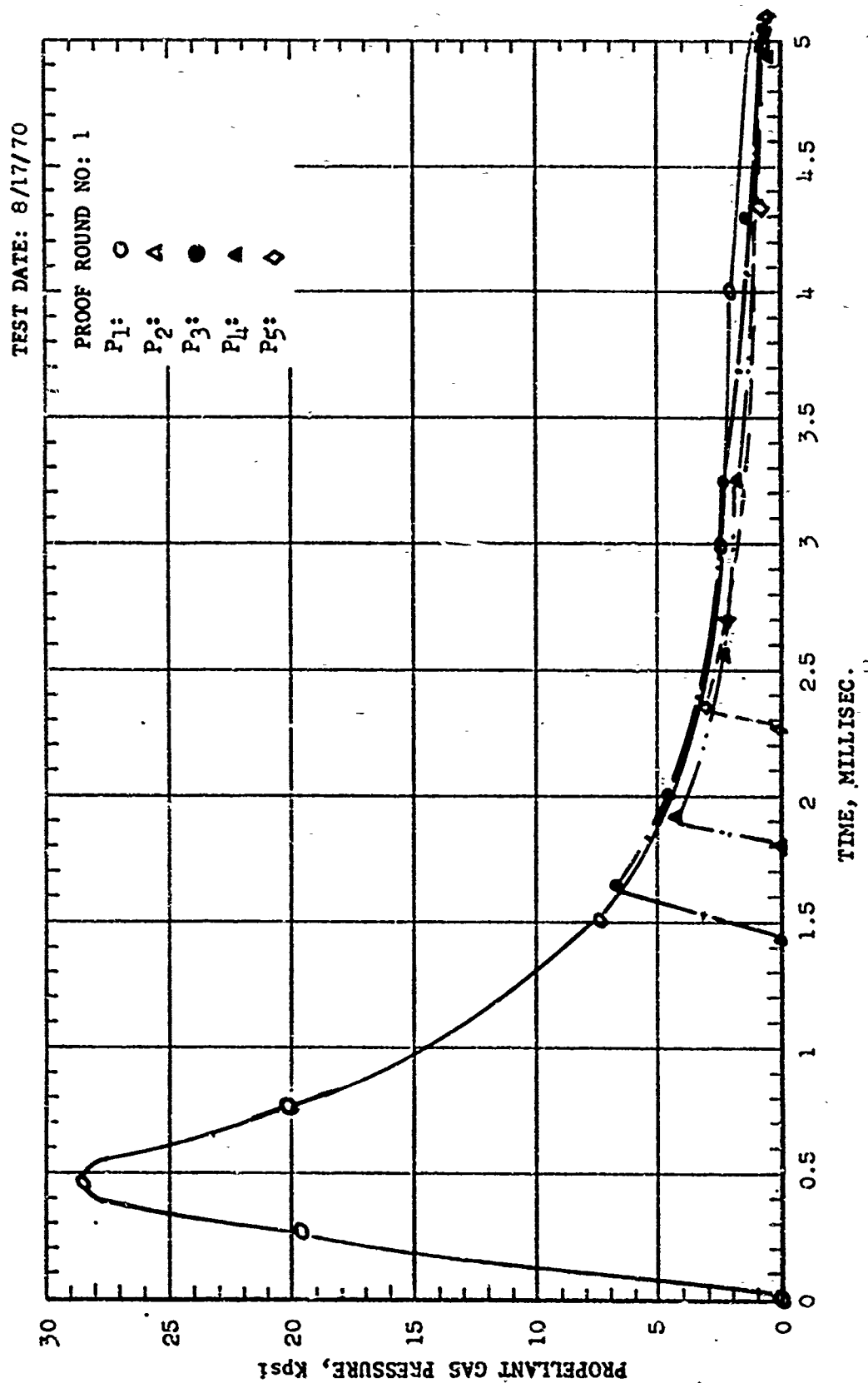


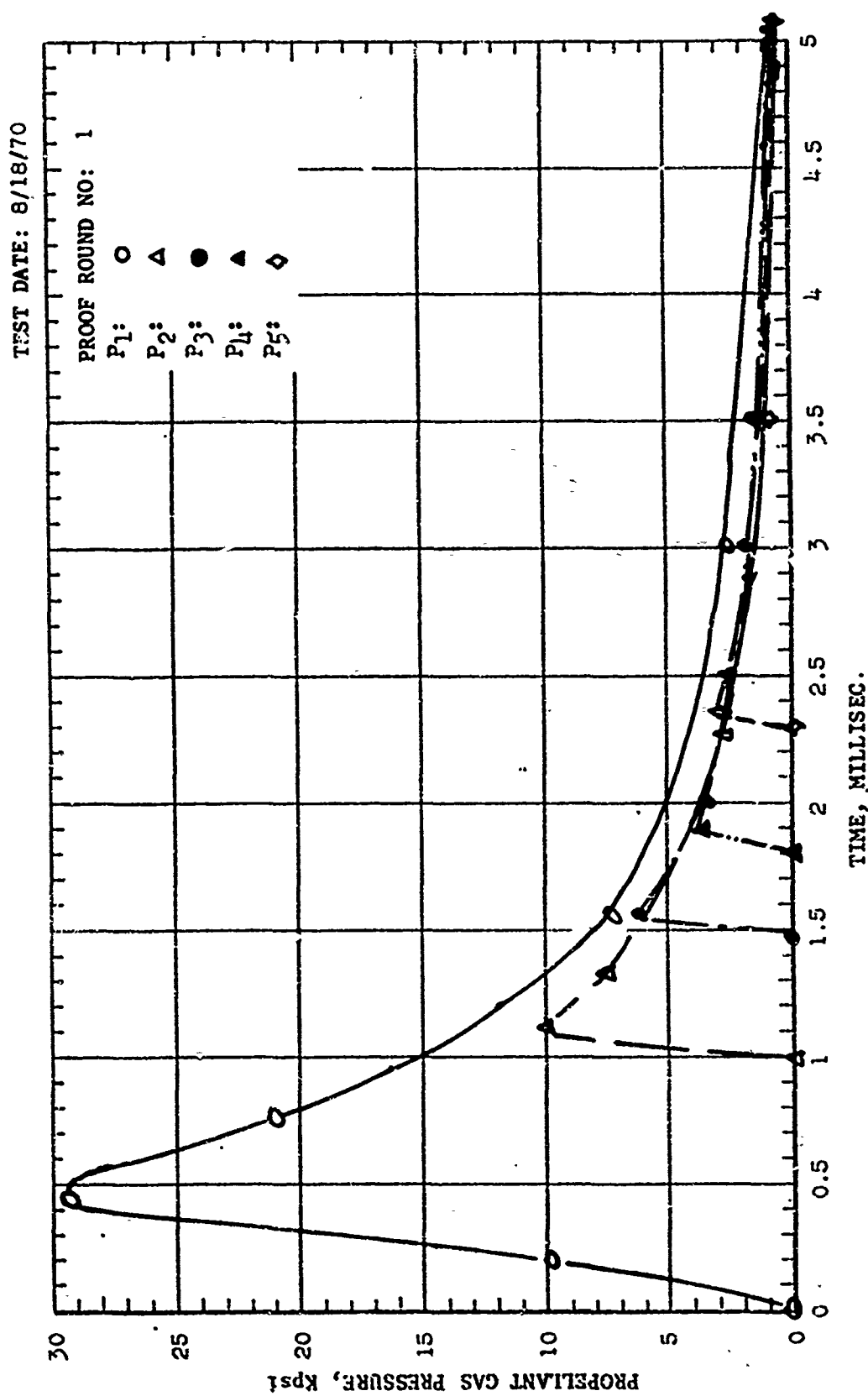


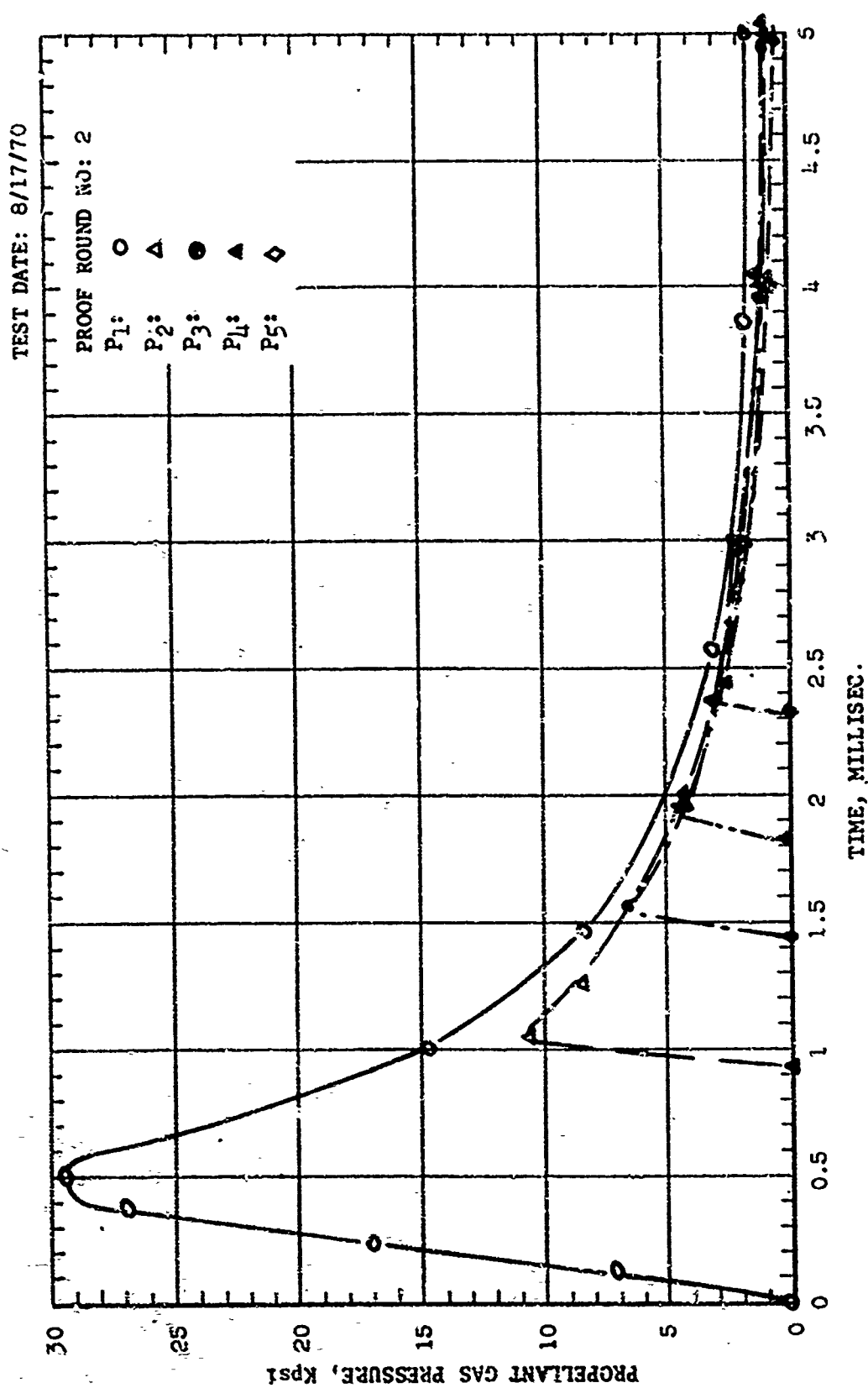
## APPENDIX IIJC EXPERIMENTAL DATA (August 17, 1970)

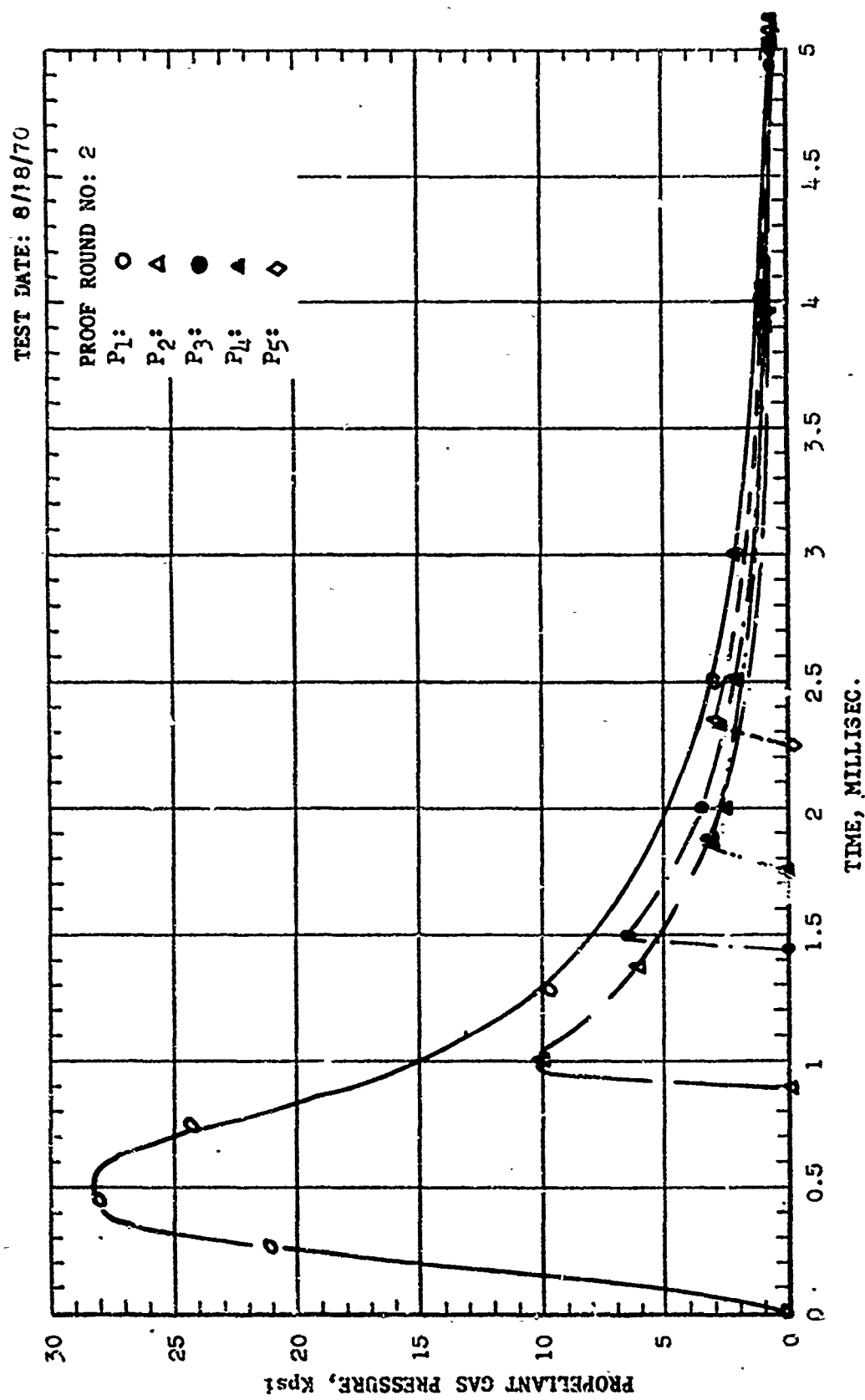
NOTE: See Fig. III-1 for Arrangement of Probes  
No temperature data were available

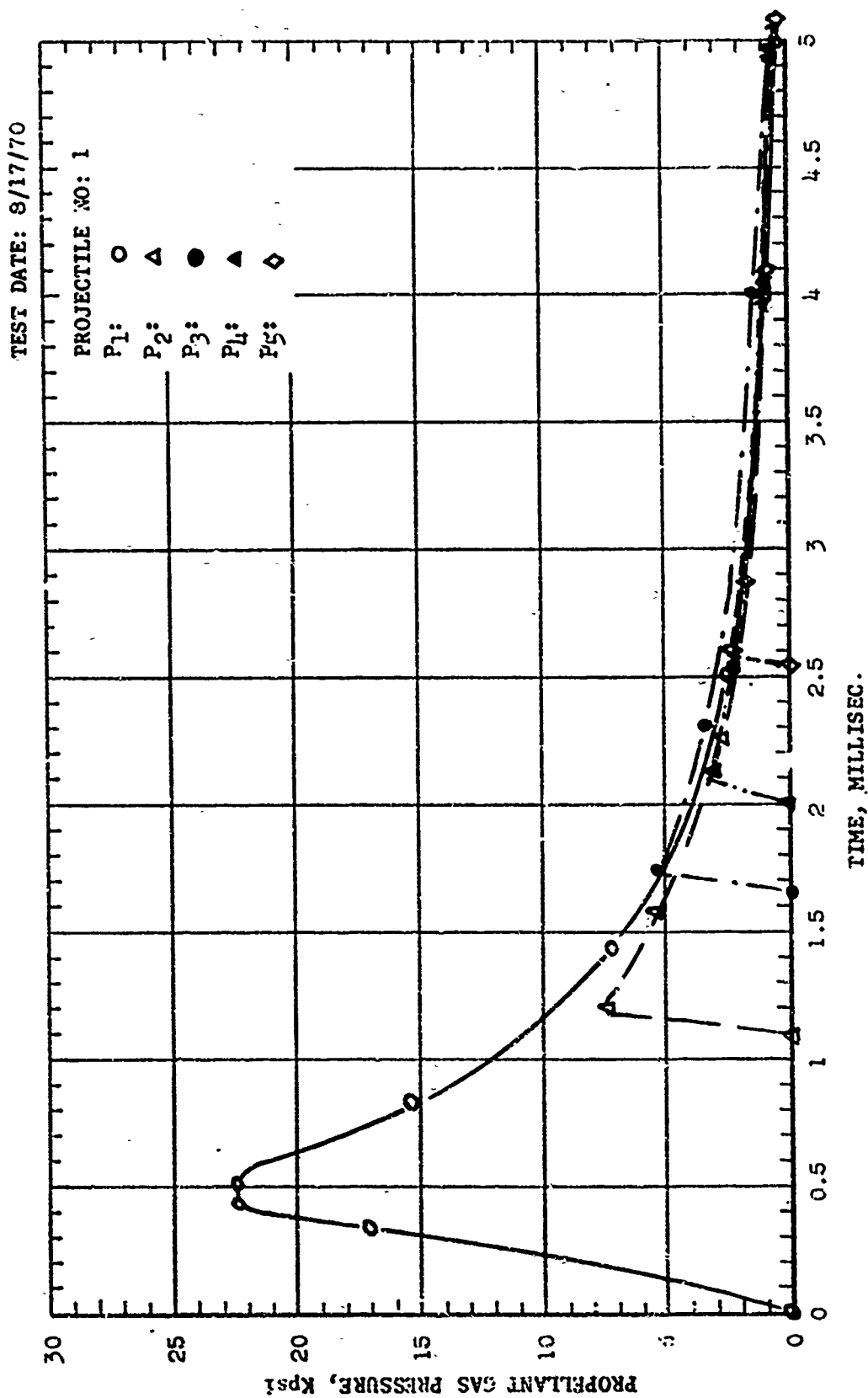












TEST DATE: 8/17/70

PROJECTILE NO: 2

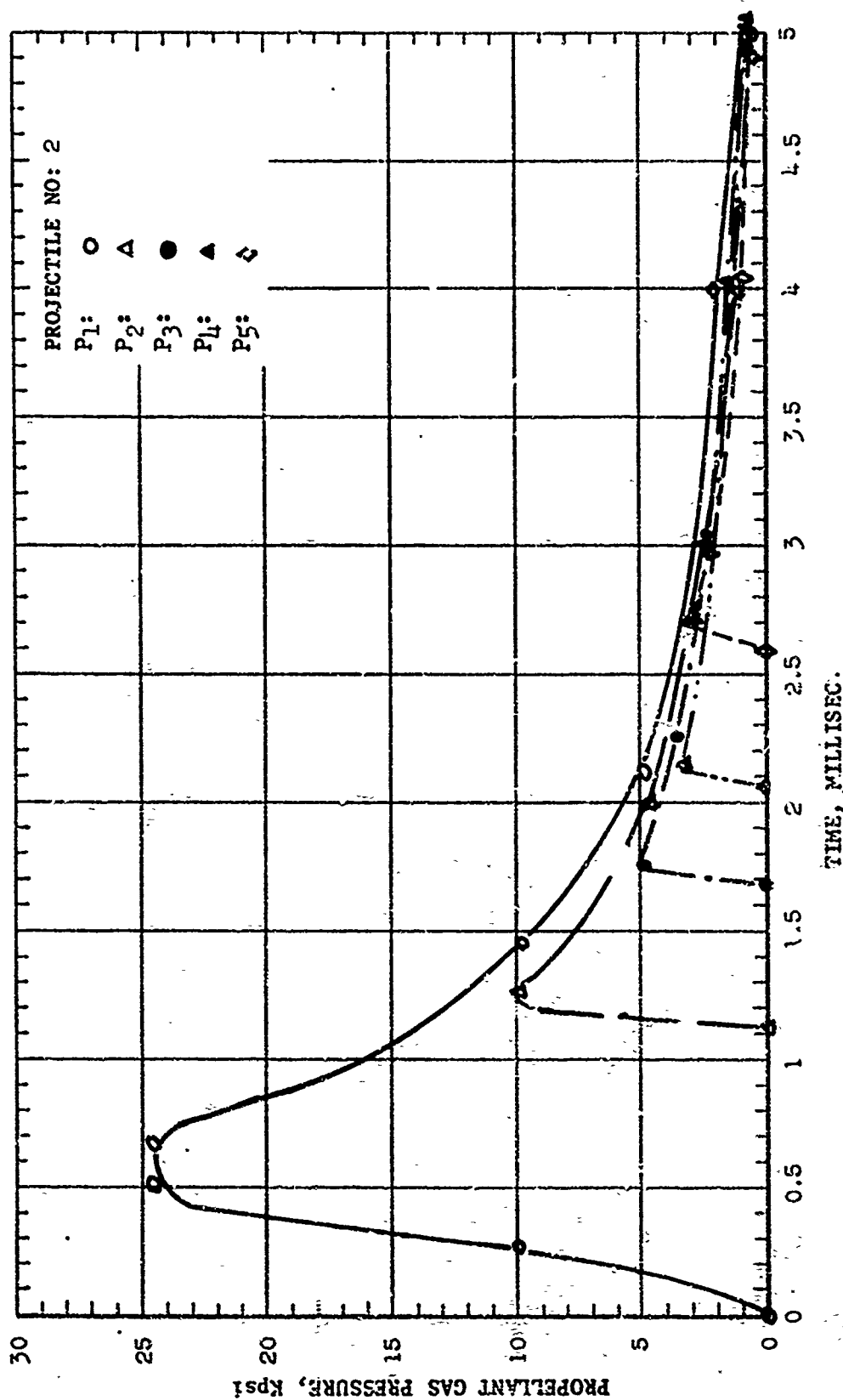
P<sub>1</sub>: ○

P<sub>2</sub>: △

P<sub>3</sub>: ●

P<sub>4</sub>: ▲

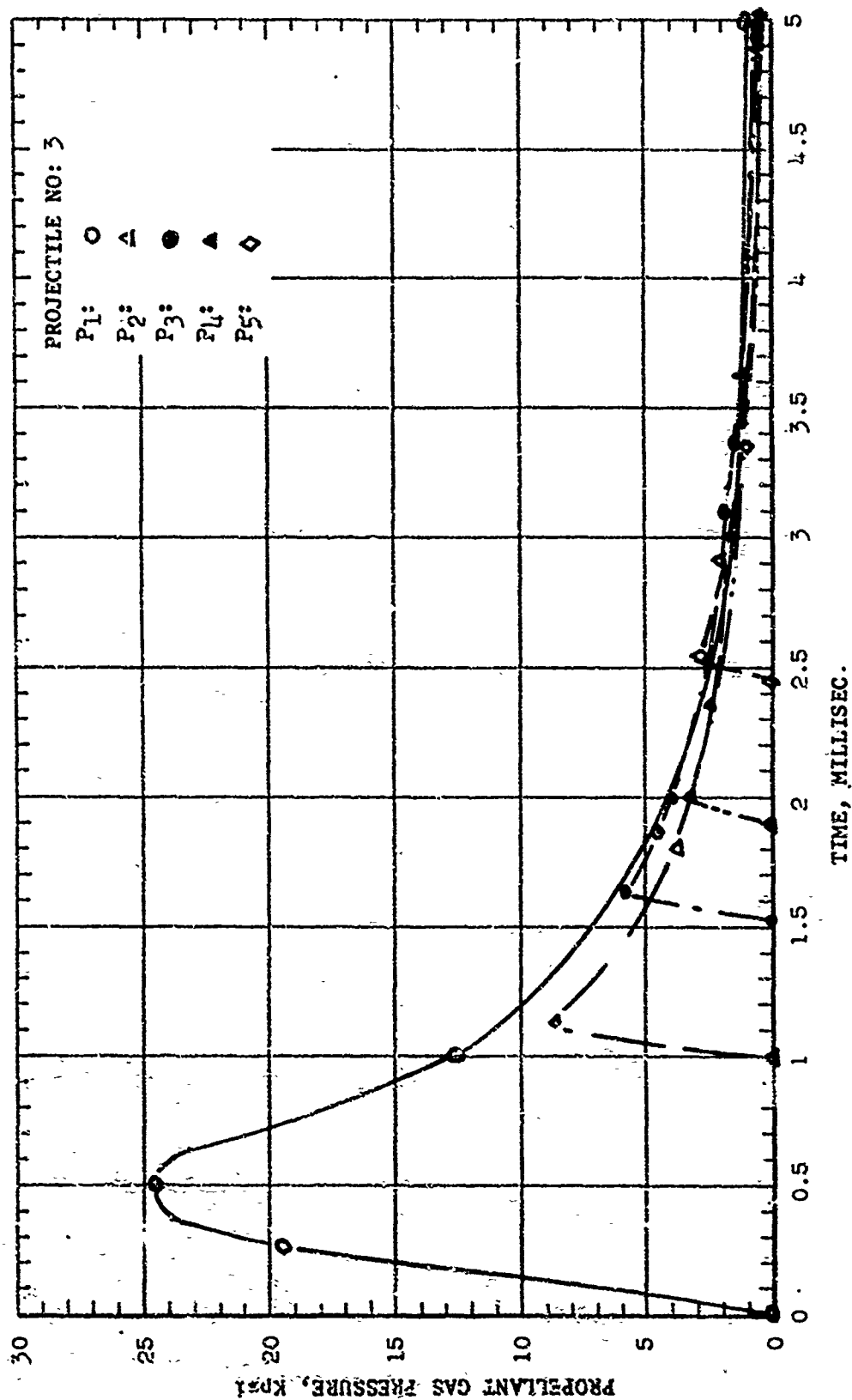
P<sub>5</sub>: ◆

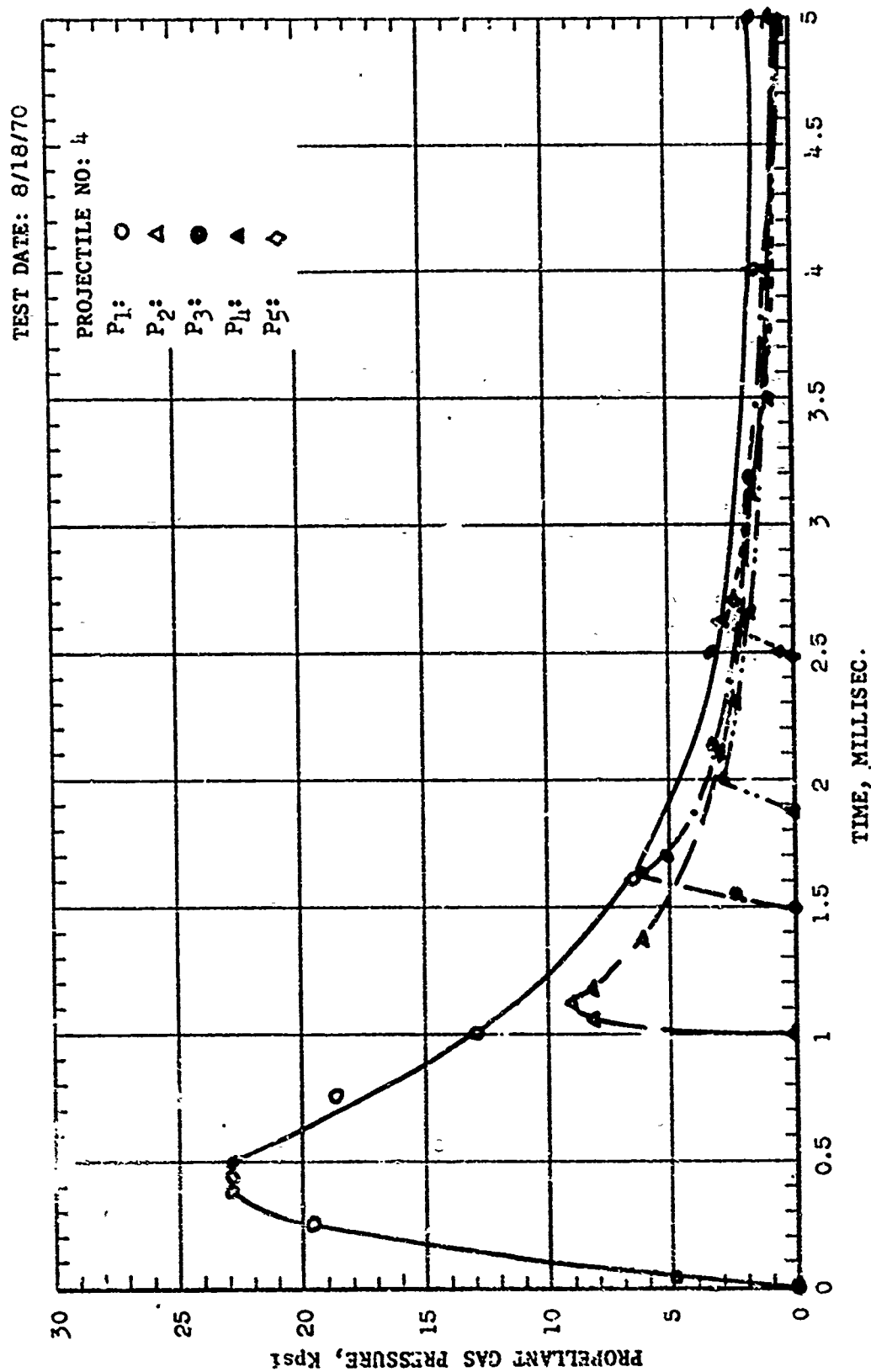


TEST DATE: 8/18/70

PROJECTILE NO: 3

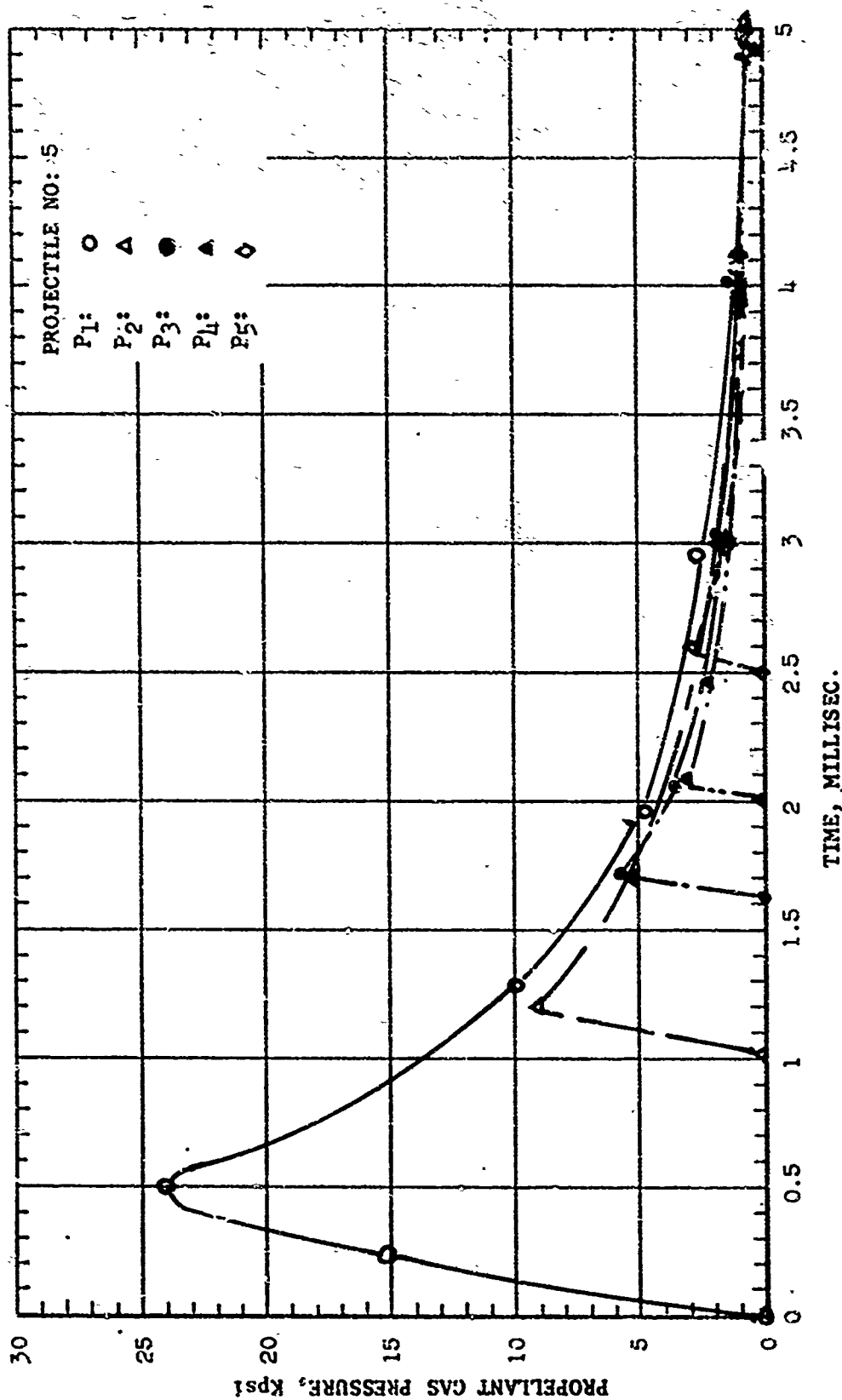
P<sub>1</sub>: ○  
P<sub>2</sub>: △  
P<sub>3</sub>: ●  
P<sub>4</sub>: ▲  
P<sub>5</sub>: ◇

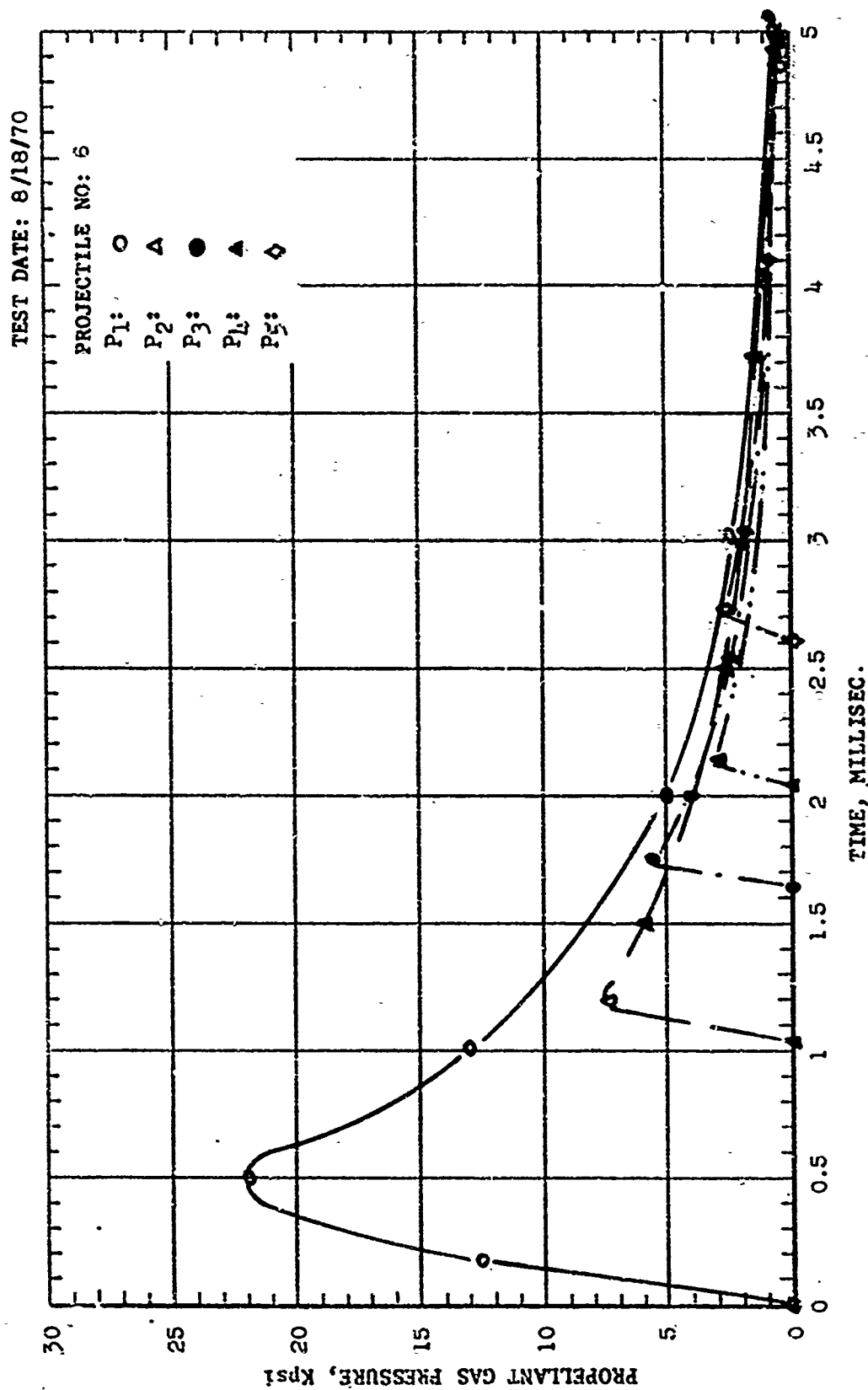






TEST DATE: 8/18/70





TEST DATE: 8/18/70

PROJECTILE NO: 7

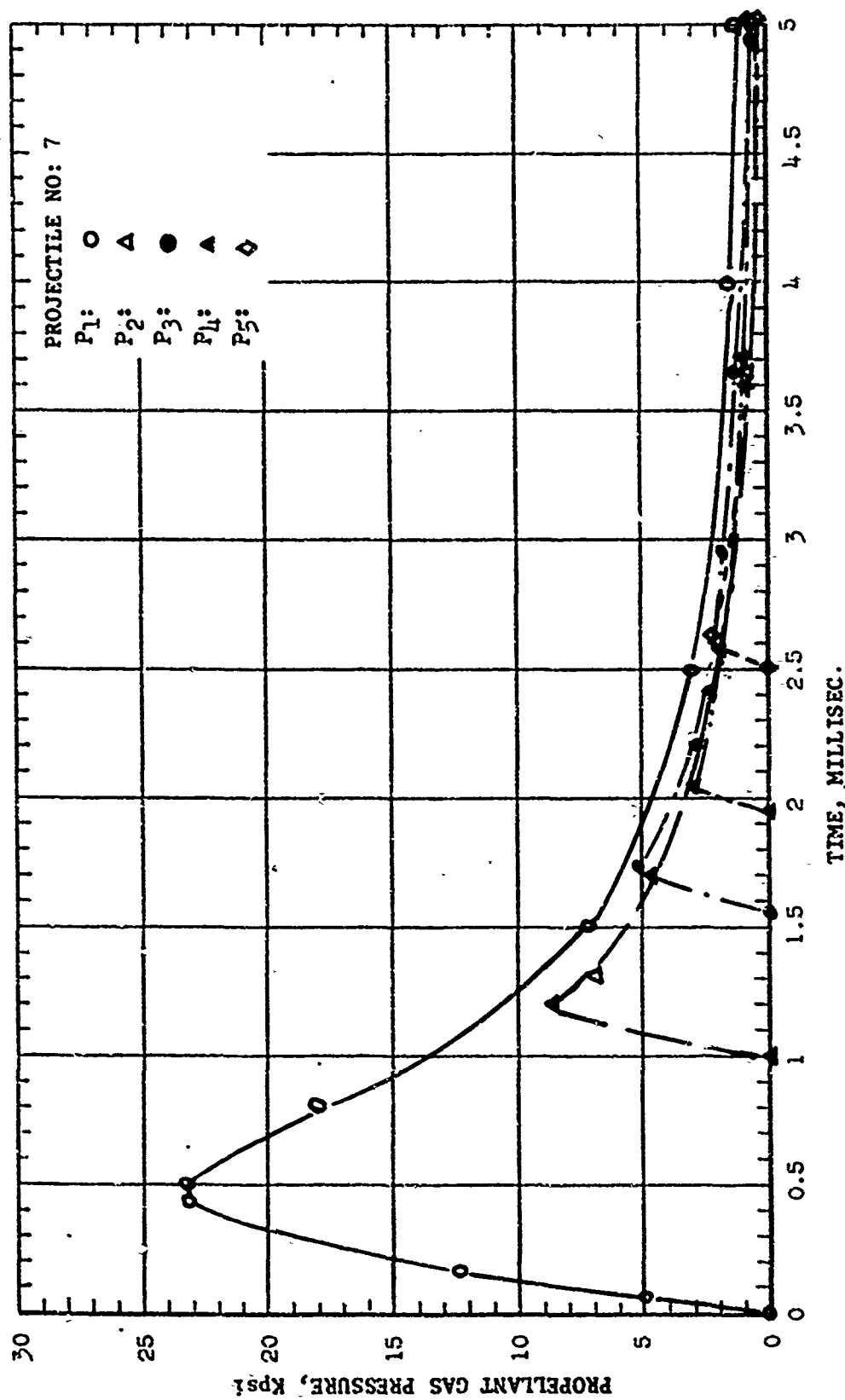
P<sub>1</sub>: ○

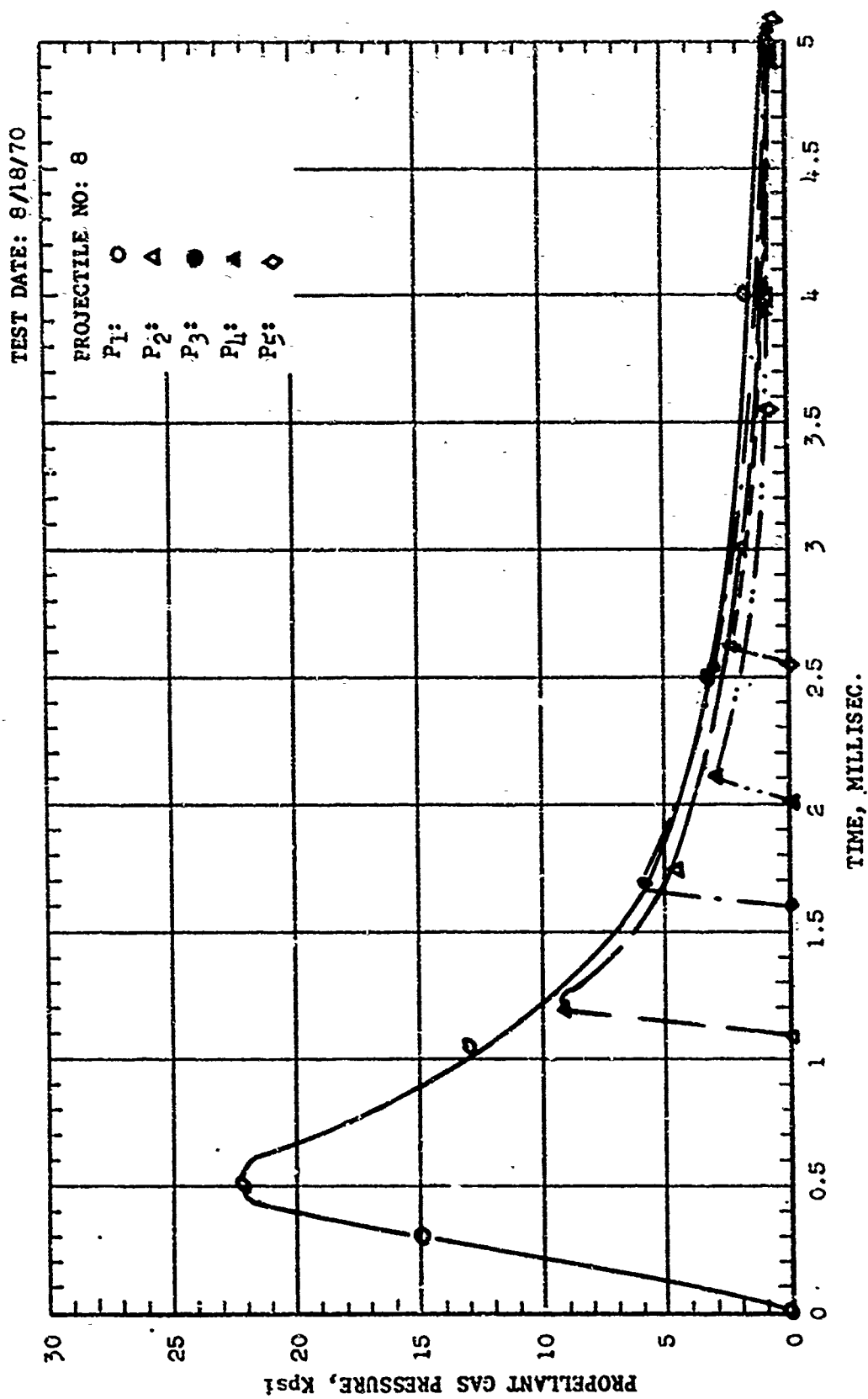
P<sub>2</sub>: △

P<sub>3</sub>: ●

P<sub>4</sub>: ▲

P<sub>5</sub>: ◇





## APPENDIX YA.

## DETERMINATION OF CONSTANTS FOR EQS. (5-6) AND (5-11)

Pressure, see Fig II-3 and Fig III-1

$$P_2 = 10.2 \text{ KPSi, at } z = 0.26804$$

$$P_e = 3 \text{ KPSi, at } z = 1, \text{ i.e., at exit}$$

Temperature, estimated from Fig. II-2 and Ref. [3] Fig. 9

$$T_{s1} = 2100^\circ\text{F, at } z = 0.26804$$

$$T_{se} = 1200^\circ\text{F, at } z = 1$$

Then dimensionless density

$$\rho = \frac{\bar{p}}{\bar{p}_r} = \frac{P_2 T_{se}}{P_e T_{s1}} = 2.21$$

From Eq. (5-11)  $C'$  is determined as

$$C' = \rho z_p = 2.21 \times 0.26804 = 0.5928$$

## APPENDIX VIA

## DERIVATION OF EQS. (6-13) THROUGH (6-15) BY SIMILARITY TRANSFORMATION

Let new variables (One Parameter Group Theory)

$$\begin{aligned}\tilde{t} &= a^{\alpha_1} t & \tilde{y} &= a^{\alpha_2} y & \tilde{H} &= a^{\alpha_3} H \\ \tilde{p} &= a^{\beta_1} p & \tilde{u} &= a^{\beta_2} u\end{aligned}\quad (6A-1)$$

where  $a$  is a parameter,  $\alpha_1, \alpha_2, \alpha_3, \beta_1, \beta_2$  are constants. In terms of the above new variables Eqs (6-9) through (6-11) are written as follows

$$a^{\alpha_1 - \beta_1} \frac{\partial \tilde{p}}{\partial \tilde{t}} + a^{\alpha_2 - \beta_1 - \beta_2} \frac{\partial}{\partial \tilde{y}} (\tilde{u} \tilde{p}) + a^{-\beta_1 - \beta_2} \tilde{p} \tilde{H} = 0 \quad (6A-2)$$

$$\begin{aligned}a^{\alpha_1 - \beta_1 - \beta_2} \tilde{p} \frac{\partial \tilde{H}}{\partial \tilde{t}} + a^{\alpha_2 - \beta_1 - \beta_2 - \beta_3} \tilde{p} \frac{\partial \tilde{H}}{\partial \tilde{y}} + a^{-\beta_1 - 2\beta_2} \tilde{p} \tilde{H}^2 \\ = a^{-n\alpha_1} \tilde{u} \tilde{c}^n \tilde{t}^n + a^{2\alpha_2 - \beta_2} \frac{\partial \tilde{H}}{\partial \tilde{y}^2}\end{aligned}\quad (6A-3)$$

$$-a^{\alpha_2 - \beta_2 - \beta_1} \tilde{p} \tilde{u} \frac{\partial \tilde{p}}{\partial \tilde{y}} = \frac{1}{\tilde{p}^2} \left( \frac{\partial \tilde{p}}{\partial \tilde{y}} \right)^2 - a^{2\alpha_2} \frac{1}{\tilde{p}} \frac{\partial^2 \tilde{p}}{\partial \tilde{y}^2} \quad (6A-4)$$

In order to have a conformal invariance the index of parameter  $a$  in each term of the equation must be equal. That is

$$\alpha_1 - \beta_1 = \alpha_2 - \beta_1 - \beta_2 = -\beta_1 - \beta_2 \quad (6A-5)$$

$$\alpha_1 - \beta_1 - \beta_2 = \alpha_2 - \beta_1 - \beta_2 - \beta_3 = -\beta_2 - 2\beta_3 = -n\alpha_1 = 2\alpha_2 - \beta_2 \quad (6A-6)$$

$$2\alpha_2 - \beta_1 - \beta_2 = 2\alpha_2 \quad (6A-7)$$

The constants in the above equations, can be determined as follows

$$\frac{\alpha_2}{\alpha_1} = A \quad (6A-8)$$

from Eq. (6A-5) we obtain

$$\frac{\gamma_2}{\alpha_1} = A - 1 \quad \frac{\gamma_3}{\alpha_1} = -1 \quad (6A-9)$$

from Eq. (6A-7)

$$\frac{\gamma_1}{\alpha_1} = 1 - 2A \quad (6A-10)$$

from Eq. (6A-6)

$$\frac{\gamma_3}{\alpha_1} = 2A - n \quad (6A-11)$$

from Eqs (6A-9) and (6A-11)

$$2A - n = -1 \quad A = \frac{n-1}{2} \quad (6A-12)$$

Now we can define two new invariant variables  $\xi$  and  $\eta$  as follows:

$$\xi = \tilde{t}, \quad \eta = \frac{\tilde{y}}{\tilde{t} c_2 / \alpha_1} = \frac{\tilde{y}}{\tilde{t} A}$$

and let the dependent variables be

$$\tilde{p} = \int^{\frac{1}{\tilde{t}}} f_1(\eta) = \tilde{t}^{1-2A} f_1(\eta) \quad (6A-13)$$

$$\tilde{u} = \int^{\frac{1}{\tilde{t}}} f_2(\eta) = \tilde{t}^{A-1} f_2(\eta) \quad (6A-14)$$

$$\tilde{H} = \int^{\frac{1}{\tilde{t}}} f_3(\eta) = \tilde{t}^{-1} f_3(\eta) \quad (6A-15)$$

where  $f_1$ ,  $f_2$ , and  $f_3$  are functions of  $\eta$ .

By the chain rule we have

$$\begin{aligned}\frac{\partial \tilde{t}}{\partial \tilde{x}} &= [(1-2A)f_1 - A\eta f_1'] \tilde{t}^{-2A} \\ \frac{\partial \tilde{p}}{\partial \tilde{y}} &= f_1' \tilde{t}^{-1-2A} \\ \frac{\partial \tilde{H}}{\partial \tilde{x}} &= (-f_3 - A\eta f_3') \tilde{t}^{-2} \\ \frac{\partial \tilde{H}}{\partial \tilde{y}} &= f_3' \tilde{t}^{-1-A} \\ \frac{\partial \tilde{H}}{\partial \tilde{y}^2} &= f_3'' \tilde{t}^{-1-2A} \\ \frac{\partial^2 \tilde{p}}{\partial \tilde{y}^2} &= f_1'' \tilde{t}^{-1-4A} \\ \frac{\partial}{\partial \tilde{y}} (\tilde{u} \tilde{p}) &= (f_1' f_2 + f_1 f_2') \tilde{t}^{-2A}\end{aligned}\tag{6A-16}$$

Substituting Eqs (6A-12) into Eqs (6A-2), (6A-3) and (6A-4) we obtain a set of transformed ordinary differential equation

$$(f_2 - \frac{n-1}{2}\eta) f_1' + f_1 f_2' + (f_3 + n + 2) f_1 = 0\tag{6-13}$$

$$(f_1 f_2 - \frac{n-1}{2}\eta f_1) f_3' + (f_3 - 1) f_1 f_3 - f_3'' = mc'\tag{6-14}$$

$$2f_1^{-2} f_1'^2 + Pr f_2 f_1' - f_1^{-1} f_1'' = 0\tag{6-15}$$

where the parameter  $a$ 's cancel one another.



DETERMINATION OF  $f_1(\eta)$  AT  $\eta=0$  FOR EQ. (6-16)

From the transformation Eq (6-12)

$$f_1(\eta) = \rho t^{1.65} \quad (6B-1)$$

At the wall,  $y = 0$ ,  $\eta = 0$ , by equation of state

$$f_1(0) = \frac{p}{\theta_w x^{0.726}} t^{1.65} \quad (6B-2)$$

The pressure,  $p$  obtained from core solution Eq. (5-12) can be readily fed in.

The wall temperature  $\theta_w$  in Eq. (6B-2) is measured from Fig II-2 at positions

$z = 0.26804$ ,  $0.50763$ , and  $0.69451$ , for various time,  $t$ . Then  $f_1(0)$  at

different time are determined by a computer program. The resulted output

for  $f_1(0)$  (we used  $c$  in the place of  $f_1(0)$  in the computer program) is

tabulated in the following computer program. Since,  $f_1(0)$  should be a

constant in equations (6-13) through (6-15), hence the approximated value

of  $f_1(0)$  which is taken as average of various  $f_1(0)$  is computed. This

resulted in  $f_1(0) = 3.2$ .

## APPENDIX VIB (Continued)

```

*****
C * THE PURPOSE OF THIS JOB IS TO FIND CONSTANT Ci=fi(θ), NOTATION USED IN**
C * SEC. 1 WHICH IS USED AS A BOUNDARY CONDITION OF THE BOUNDARY LAYER*
C * SOLUTION *****
C * ALL VALUES ARE DIMENSIONLESS *****
C * TR=REF.TIME=1.6322 M.S. *****
C * TR=REF. TEMPERATURE=2173.9 RANKINE DEGREES *****
C * TEMPERATURE PROBE S1 IS AT Z=0.268G4, S2 AT Z=0.50763, S3 AT Z=0.69451 *****
C * FOR S1, AT Z=0.268G4, C SHOULD BE READ FROM T=0.551 TO T=1.409 *****
C * FOR S2, AT Z=0.50763, C SHOULD BE READ FROM T=0.919 TO T=1.409 *****
C * FOR S3, AT Z=0.69451, C SHOULD BE READ FROM T=1.103 TO T=1.409 *****
C *****
C * DIMENSION T(30), PB(30), THETA(3,30), C(3,30), X(3) *****
C * READ (5,107) (T(I),I=1,30),(PB(I),I=1,30),(X(I),I=1,3),((THETA(I,J *****
C * 1),J=1,30),I=1,3) *****
C * 100 FORMAT (8F10.5) *****
C * DO 3000 K=1,3 *****
C * DO 200 J=1,30 *****
C * THETA=P/DENSITY*0.726 *****
C * DENSITY(FROM SIMILARITY SOL.)=T**(-1.65)*F1 *****
C * AT THE INTERNAL SURFACE OF THE GUN BARREL F1(γ)=C=P*T**1.65/(THETA* *****
C * 0.726) *****
C * C(K,J)=(PB(J)-1.0800*X(K)/T(J)**3.65)*T(J)**1.65/(THETA(K,J)* *****
C * 10.726) *****
C * HERE X=(Z**2-ZP(0)**2)/2 *****
C * 200 CONTINUE *****
C * WRITE (6,1000) *****
C * 1000 FORMAT ( *****
C * 1(T) C(T) T PB(T) THETA *****
C * DO 1002 I=1,30 *****
C * WRITE (6,1001) T(I), PB(I), THETA(K,I), C(K,I) *****
C * 1001 FORMAT (4F20.5/) *****
C * 1002 CONTINUE *****
C * 3000 CONTINUE *****
C * CALL EXIT *****
C * END *****

```

S<sub>1</sub> At z = 0.26804

T	PR(T)	THETA	C
0.55100	3.26650	0.24400	6.19730
0.61300	2.80250	0.45900	3.45015
0.67400	2.46800	0.84500	1.96315
0.73500	2.19000	0.69800	2.46287
0.79600	1.94870	0.61200	2.87632
0.85800	1.72600	0.54700	3.24705
0.91900	1.54040	0.49600	3.59750
0.98000	1.37340	0.45000	3.94611
1.04200	1.22490	0.42750	4.11220
1.10300	1.11300	0.39500	4.45473
1.16400	1.01150	0.37200	4.70898
1.22500	0.91310	0.34900	4.93814
1.28700	0.83510	0.33100	5.17507
1.34800	0.77020	0.31200	5.47403
1.40900	0.71455	0.30300	5.63332

S<sub>2</sub> At z = 0.50763

T	PH(T)	THETA	C
0.91900	1.54040	0.24400	6.64217
0.98000	1.37340	0.58400	2.79421
1.04200	1.22490	0.56500	2.88611
1.10300	1.11300	0.49800	3.30322
1.16400	1.01150	0.46800	3.52504
1.22500	0.91310	0.44800	3.64129
1.28700	0.83510	0.44600	3.65358
1.34800	0.77020	0.44300	3.68358
1.40900	0.71455	0.44150	3.70842

S<sub>3</sub> At z = 0.69451

T	PH(T)	THETA	C
1.10300	1.11300	0.24400	6.18299
1.16400	1.01150	0.34900	4.37360
1.22500	0.91310	0.52800	2.87868
1.28700	0.83510	0.61300	2.49366
1.34800	0.77020	0.57000	2.70152
1.40900	0.71455	0.55100	2.81869

## APPENDIX VIC

\*\*\*CONTINUOUS SYSTEM MODELING PROGRAM\*\*\*

\*\*\*PROBLEM INPUT STATEMENTS\*\*\*

```

TITLE      UNSTEADY COMPRESSIBLE FLOW IN A TUBE
*          *****
* DENSITY = ((TIME)**(-1.65))*F1
* VEL, U = ((TIME)**(0.325))*F2
* VEL, W = 2*H=12*(TIME)**(-1)*F3
* BC1,BC2, AND BC3 ARE INITIAL COND. OF
* F1,F2, AND F3 RESPECTIVELY
* DBC1 AND DBC3 ARE INITIAL COND. OF
* DF1 AND DF3 RESPECTIVELY
* DB1=-7, 12 AND DBC3=2.024 ARE GUESSED
* VALUES
*          *****
* CCNST DBC1=-0.12,BC1=3.2,BC2=0.,DBC3=2.024,BC3=0.
* CONST K=0.75,K1=1.325,K2=1.65,K3=1.09
* RENAME TIME=ETA
* DYNAMIC

```

```

DDF1=F1*(2.*DF1**2/F1**2+K*F2*DF1)
DF2=(-1./F1)*((F2-K1*ETA)*DF1+(F3-K2)*F1)
DDF3=(F1*F2-K1*ETA*F1)*DF3*(F3-1.)*F1*F3-K3
DF1=INTGRL(DBC1,DDF1)
F1=INTGRL(DBC1,DF1)
F2=INTGRL(DBC2,DF2)
DF3=INTGRL(DBC3,DDF3)
F3=INTGRL(DBC3,DF3)
F4=F1*F2

```

```

TERMINAL
TIMER DELT=0.1,JUTDEL=0.1,PRDEL=0.1,FINTIM=10.
PRINT DF1,F1,DF2,F2,DF3,F3,F4
PRTPLOT F1,F2,F3,F4
END
STOP

```

$$ETA = \gamma, DF1 = f_1'(\gamma), F1 = f_1(\gamma), DF2 = f_2'(\gamma), F2 = f_2(\gamma), DF3 = f_3'(\gamma), F3 = f_3(\gamma), F4 = f_4 = f_1 \cdot f_2.$$

$$p = t^{-1.65} f_1(\gamma), \quad u = t^{0.325} f_2(\gamma), \quad w = H \cdot z = t^{-1} f_3(\gamma) \cdot z$$

Reproduced from  
best available copy.

ETA	DF1	F1	DF2	F2	DF3	F3	F4
0.0	-1.02000E-01	3.2000E 00	1.6500E 00	0.0	2.0240E 00	0.0	0.0
1.0000E-01	-1.02039E-01	3.0180E 00	1.4545E 00	1.5513E-01	1.8965E 00	1.7633E-01	4.9453E-01
2.0000E-01	-1.02707E-01	3.01756E 00	1.2727E 00	2.9136E-01	1.7391E 00	3.7331E-01	9.2525E-01
3.0000E-01	-1.03702E-01	3.01624E 00	1.01770E 00	4.1021E-01	1.5641E 00	5.4357E-01	1.2572E 00
4.0000E-01	-1.05150E-01	3.01480E 00	9.5830E-01	5.1323E-01	1.3820E 00	6.7000E-01	1.6160E 00
5.0000E-01	-1.07105E-01	3.01319E 00	8.0266E-01	6.0244E-01	1.2138E 00	8.2004E-01	1.8868E 00
6.0000E-01	-1.09648E-01	3.01136E 00	7.1114E-01	6.7920E-01	1.0374E 00	9.3135E-01	2.1143E 00
7.0000E-01	-1.20287E-01	3.00924E 00	6.0991E-01	7.4514E-01	8.7223E-01	1.0226E 00	2.3043E 00
8.0000E-01	-1.36922E-01	3.00675E 00	5.0554E-01	8.0158E-01	7.3728E-01	1.0174E 00	2.4589E 00
9.0000E-01	-1.51910E-01	3.00383E 00	4.0399E-01	8.4955E-01	6.1379E-01	1.0174E 00	2.5811E 00
1.0000E 00	-1.7980E-01	3.00134E 00	3.6475E-01	8.8476E-01	5.1385E-01	1.0230E 00	2.6723E 00
1.1000E 00	-4.4251E-01	2.9619E 00	2.9083E-01	9.2254E-01	4.0331E-01	1.0277E 00	2.7325E 00
1.2000E 00	-5.3766E-01	2.9125E 00	2.1404E-01	9.4783E-01	3.6079E-01	1.0317E 00	2.7660E 00
1.3000E 00	-6.3502E-01	2.8540E 00	1.2962E-01	9.6510E-01	3.2147E-01	1.0351E 00	2.7543E 00
1.4000E 00	-7.4251E-01	2.7851E 00	3.2846E-02	9.7334E-01	2.9536E-01	1.0382E 00	2.7199E 00
1.5000E 00	-8.5509E-01	2.7052E 00	-8.0343E-02	9.7110E-01	2.6856E-01	1.0402E 00	2.6271E 00
1.6000E 00	-9.6809E-01	2.6140E 00	-2.1531E-01	9.5648E-01	2.3833E-01	1.0434E 00	2.5027E 00
1.7000E 00	-1.0725E 00	2.5118E 00	-3.7291E-01	9.2727E-01	2.0225E-01	1.0457E 00	2.3291E 00
1.8000E 00	-1.1571E 00	2.4001E 00	-5.5361E-01	8.8113E-01	1.6833E-01	1.0478E 00	2.1148E 00
1.9000E 00	-1.2138E 00	2.2813E 00	-7.5409E-01	8.1588E-01	1.3511E-01	1.0491E 00	1.8613E 00
2.0000E 00	-1.2363E 00	2.1585E 00	-9.6735E-01	7.2988E-01	1.0160E-01	1.0517E 00	1.5754E 00
2.1000E 00	-1.2229E 00	2.0352E 00	-1.1830E 00	6.2233E-01	1.6753E-01	1.0535E 00	1.2660E 00
2.2000E 00	-1.01764E 00	1.9150E 00	-1.1388E 00	4.9362E-01	1.5209E-01	1.0551E 00	9.4528E-01
2.3000E 00	-1.0132E 00	1.8008E 00	-1.1570E 00	3.6454E-01	1.3733E-01	1.0566E 00	6.2202E-01
2.4000E 00	-1.0119E 00	1.6950E 00	-1.1719E 00	1.8158E-01	1.2202E-01	1.0578E 00	3.0000E-01
2.5000E 00	-9.1075E-01	1.5988E 00	-1.1825E 00	2.9340E-03	1.0703E-01	1.0590E 00	4.077.9E-02
2.6000E 00	-8.0714E-01	1.5129E 00	-1.1895E 00	-1.18294E-01	9.2817E-02	1.0600E 00	-2.7677E-01
2.7000E 00	-7.0649E-01	1.4373E 00	-1.1900E 00	-3.7259E-01	7.9672E-02	1.0609E 00	-2.3551E-01
2.8000E 00	-6.1238E-01	1.3714E 00	-1.1873E 00	-5.6160E-01	6.7743E-02	1.0619E 00	-1.7016E-01
2.9000E 00	-5.2680E-01	1.3145E 00	-1.1811E 00	-7.0460E-01	5.7247E-02	1.0622E 00	-9.8072E-01
3.0000E 00	-4.5054E-01	1.2657E 00	-1.1720E 00	-9.2289E-01	4.8047E-02	1.06274E 00	-1.1681E 00

(cont'd)

# UNSTEADY COMPRESSIBLE FLOW IN A TUBE

RKS INTEGRATION

Reproduced from  
best available copy.

ETA	OF1	F1	DF2	F2	UF2	F3	F4
3.1000E 00	-3.8361E-01	1.2241E 00	-1.6105E 00	-1.0289E 00	4.0121E-02	1.6318E 00	-1.3237E 00
3.2000E 00	-3.2549E-01	1.1887E 00	-1.4873E 00	-1.0244E 00	3.3365E-02	1.6355E 00	-1.0470E 00
3.3000E 00	-2.7545E-01	1.1587E 00	-1.3576E 00	-1.0386E 00	2.7656E-02	1.6335E 00	-1.0669E 00
3.4000E 00	-2.3261E-01	1.1333E 00	-1.2265E 00	-1.0516E 00	2.2864E-02	1.6410E 00	-1.0718E 00
3.5000E 00	-1.9611E-01	1.1120E 00	-1.0989E 00	-1.0632E 00	1.8862E-02	1.6431E 00	-1.0815E 00
3.6000E 00	-1.6512E-01	1.0939E 00	-9.7685E-01	-1.0736E 00	1.5533E-02	1.6448E 00	-1.0891E 00
3.7000E 00	-1.3887E-01	1.0788E 00	-8.6263E-01	-1.0827E 00	1.2774E-02	1.6474E 00	-1.0971E 00
3.8000E 00	-1.1668E-01	1.0660E 00	-7.5743E-01	-1.0908E 00	1.0442E-02	1.6474E 00	-2.0334E 00
3.9000E 00	-9.7958E-02	1.0553E 00	-6.6178E-01	-1.0979E 00	8.675E-03	1.6474E 00	-2.0383E 00
4.0000E 00	-8.2183E-02	1.0463E 00	-5.7576E-01	-2.0415E 00	7.3541E-03	1.6474E 00	-2.0383E 00
4.1000E 00	-6.8905E-02	1.0388E 00	-4.9909E-01	-2.0495E 00	5.7745E-03	1.6474E 00	-2.0383E 00
4.2000E 00	-5.7741E-02	1.0325E 00	-4.3128E-01	-2.0416E 00	4.7215E-03	1.6503E 00	-2.0383E 00
4.3000E 00	-4.8361E-02	1.0272E 00	-3.7168E-01	-2.0417E 00	3.8554E-03	1.6503E 00	-2.0383E 00
4.4000E 00	-4.0487E-02	1.0228E 00	-3.1959E-01	-2.0416E 00	3.1432E-03	1.6511E 00	-2.0383E 00
4.5000E 00	-3.3982E-02	1.0193E 00	-2.7427E-01	-2.0416E 00	2.5578E-03	1.6514E 00	-2.0383E 00
4.6000E 00	-2.8344E-02	1.0159E 00	-2.3409E-01	-2.0416E 00	2.0767E-03	1.6516E 00	-2.0383E 00
4.7000E 00	-2.3703E-02	1.0133E 00	-2.0107E-01	-2.0416E 00	1.6813E-03	1.6518E 00	-2.0383E 00
4.8000E 00	-1.9816E-02	1.0112E 00	-1.7186E-01	-2.0416E 00	1.3562E-03	1.6519E 00	-2.0383E 00
4.9000E 00	-1.6583E-02	1.0094E 00	-1.4677E-01	-2.0416E 00	1.0692E-03	1.6521E 00	-2.0383E 00
5.0000E 00	-1.3840E-02	1.0078E 00	-1.2526E-01	-2.0416E 00	8.6953E-04	1.6521E 00	-2.0383E 00
5.1000E 00	-1.1562E-02	1.0065E 00	-1.0686E-01	-2.0416E 00	6.8505E-04	1.6522E 00	-2.0383E 00
5.2000E 00	-9.6576E-03	1.0055E 00	-9.1141E-02	-2.0416E 00	5.4753E-04	1.6523E 00	-2.0383E 00
5.3000E 00	-8.0653E-03	1.0046E 00	-7.7733E-02	-2.0416E 00	4.1827E-04	1.6523E 00	-2.0383E 00
5.4000E 00	-6.7345E-03	1.0039E 00	-6.6308E-02	-2.0416E 00	3.1744E-04	1.6524E 00	-2.0383E 00
5.5000E 00	-5.6225E-03	1.0033E 00	-5.6585E-02	-2.0416E 00	2.3433E-04	1.6524E 00	-2.0383E 00
5.6000E 00	-4.6935E-03	1.0028E 00	-4.8317E-02	-2.0416E 00	1.6542E-04	1.6524E 00	-2.0383E 00
5.7000E 00	-3.9176E-03	1.0023E 00	-4.1291E-02	-2.0416E 00	1.0915E-04	1.6524E 00	-2.0383E 00
5.8000E 00	-3.2697E-03	1.0020E 00	-3.5325E-02	-2.0416E 00	6.2361E-05	1.6524E 00	-2.0416E 00
5.9000E 00	-2.7286E-03	1.0017E 00	-3.0261E-02	-2.0416E 00	3.5466E-05	1.6524E 00	-2.0416E 00
6.0000E 00	-2.2769E-03	1.0014E 00	-2.5567E-02	-2.0416E 00	-8.6245E-06	1.6524E 00	-2.0416E 00
6.1000E 00	-1.8999E-03	1.0012E 00	-2.2326E-02	-2.0416E 00	-3.5344E-05	1.6524E 00	-2.0416E 00
6.2000E 00	-1.5852E-03	1.0010E 00	-1.9423E-02	-2.0416E 00	-5.7619E-05	1.6524E 00	-2.0416E 00
6.3000E 00	-1.3225E-03	1.0009E 00	-1.6623E-02	-2.0416E 00	-7.6200E-05	1.6524E 00	-2.0416E 00
6.4000E 00	-1.1033E-03	1.0008E 00	-1.4407E-02	-2.0416E 00	-9.1856E-05	1.6524E 00	-2.0416E 00
6.5000E 00	-9.2039E-04	1.0007E 00	-1.2553E-02	-2.0416E 00	-1.0494E-04	1.6524E 00	-2.0416E 00

(cont'd)

Reproduced from  
best available copy.

6.6000E 00	-7.6777E-04	1.0000E 00	-1.0940E-02	-2.4142E 00	-1.1544E-04	1.6524E 00	-2.4157E 00
6.7000E 00	-6.4043E-04	1.0000E 00	-9.5927E-03	-2.4153E 00	-1.2544E-04	1.6524E 00	-2.4165E 00
6.8000E 00	-5.3419E-04	1.0000E 00	-8.4518E-03	-2.4162E 00	-1.3356E-04	1.6524E 00	-2.4173E 00
6.9000E 00	-4.4556E-04	1.0000E 00	-7.4839E-03	-2.4171E 00	-1.4145E-04	1.6523E 00	-2.4179E 00
7.0000E 00	-3.7163E-04	1.0000E 00	-6.6640E-03	-2.4177E 00	-1.4644E-04	1.6523E 00	-2.4185E 00
7.1000E 00	-3.0995E-04	1.0000E 00	-5.9692E-03	-2.4183E 00	-1.5164E-04	1.6523E 00	-2.4191E 00
7.2000E 00	-2.5850E-04	1.0000E 00	-5.3793E-03	-2.4189E 00	-1.5612E-04	1.6523E 00	-2.4196E 00
7.3000E 00	-2.1559E-04	1.0000E 00	-4.8778E-03	-2.4194E 00	-1.6024E-04	1.6523E 00	-2.4201E 00
7.4000E 00	-1.7979E-04	1.0000E 00	-4.4519E-03	-2.4198E 00	-1.6386E-04	1.6523E 00	-2.4205E 00
7.5000E 00	-1.4994E-04	1.0000E 00	-4.0398E-03	-2.4203E 00	-1.6709E-04	1.6523E 00	-2.4208E 00
7.6000E 00	-1.2504E-04	1.0000E 00	-3.7816E-03	-2.4207E 00	-1.6999E-04	1.6522E 00	-2.4212E 00
7.7000E 00	-1.0427E-04	1.0000E 00	-3.5191E-03	-2.4210E 00	-1.7259E-04	1.6522E 00	-2.4215E 00
7.8000E 00	-8.6952E-05	1.0000E 00	-3.2929E-03	-2.4214E 00	-1.7537E-04	1.6522E 00	-2.4218E 00
7.9000E 00	-7.2508E-05	1.0000E 00	-3.0927E-03	-2.4217E 00	-1.7750E-04	1.6522E 00	-2.4221E 00
8.0000E 00	-6.0462E-05	1.0000E 00	-2.9330E-03	-2.4220E 00	-1.7976E-04	1.6521E 00	-2.4224E 00
8.1000E 00	-5.0416E-05	1.0000E 00	-2.7898E-03	-2.4223E 00	-1.8191E-04	1.6521E 00	-2.4227E 00
8.2000E 00	-4.2038E-05	1.0000E 00	-2.6661E-03	-2.4225E 00	-1.8393E-04	1.6521E 00	-2.4230E 00
8.3000E 00	-3.5153E-05	1.0000E 00	-2.5589E-03	-2.4228E 00	-1.8586E-04	1.6521E 00	-2.4232E 00
8.4000E 00	-2.9227E-05	1.0000E 00	-2.4655E-03	-2.4230E 00	-1.8763E-04	1.6521E 00	-2.4234E 00
8.5000E 00	-2.4369E-05	1.0000E 00	-2.3839E-03	-2.4233E 00	-1.8935E-04	1.6521E 00	-2.4237E 00
8.6000E 00	-2.0319E-05	1.0000E 00	-2.3121E-03	-2.4235E 00	-1.9105E-04	1.6520E 00	-2.4239E 00
8.7000E 00	-1.6941E-05	1.0000E 00	-2.2476E-03	-2.4238E 00	-1.9266E-04	1.6520E 00	-2.4241E 00
8.8000E 00	-1.4124E-05	1.0000E 00	-2.1892E-03	-2.4241E 00	-1.9445E-04	1.6520E 00	-2.4243E 00
8.9000E 00	-1.1776E-05	1.0000E 00	-2.1367E-03	-2.4242E 00	-1.9621E-04	1.6520E 00	-2.4246E 00
9.0000E 00	-9.8180E-06	1.0000E 00	-2.0892E-03	-2.4244E 00	-1.9793E-04	1.6519E 00	-2.4248E 00
9.1000E 00	-8.1854E-06	1.0000E 00	-2.0459E-03	-2.4246E 00	-1.9962E-04	1.6519E 00	-2.4250E 00
9.2000E 00	-6.8242E-06	1.0000E 00	-2.0061E-03	-2.4248E 00	-2.0128E-04	1.6519E 00	-2.4252E 00
9.3000E 00	-5.6892E-06	1.0000E 00	-1.9693E-03	-2.4250E 00	-2.0291E-04	1.6519E 00	-2.4253E 00
9.4000E 00	-4.7430E-06	1.0000E 00	-1.9350E-03	-2.4252E 00	-2.0451E-04	1.6519E 00	-2.4255E 00
9.5000E 00	-3.9541E-06	1.0000E 00	-1.9029E-03	-2.4254E 00	-2.0609E-04	1.6519E 00	-2.4257E 00
9.6000E 00	-3.2963E-06	1.0000E 00	-1.8724E-03	-2.4256E 00	-2.0767E-04	1.6518E 00	-2.4259E 00
9.7000E 00	-2.7480E-06	1.0000E 00	-1.8435E-03	-2.4259E 00	-2.0912E-04	1.6518E 00	-2.4261E 00
9.8000E 00	-2.2908E-06	1.0000E 00	-1.8159E-03	-2.4259E 00	-2.1061E-04	1.6518E 00	-2.4263E 00
9.9000E 00	-1.9096E-06	1.0000E 00	-1.7883E-03	-2.4261E 00	-2.1205E-04	1.6518E 00	-2.4264E 00
1.0000E 01	-1.5919E-06	1.0000E 00	-1.7606E-03	-2.4263E 00	-2.1366E-04	1.6517E 00	-2.4266E 00



PAGE 1

ETA	MINIMUM 1.000E 00	F1	VERSUS ETA	MAXIMUM 3.200E 00
C,0				
1.0000E-01	3.2000E 00			
2.0000E-01	3.1800E 00			
3.0000E-01	3.1756E 00			
4.0000E-01	3.1624E 00			
5.0000E-01	3.1430E 00			
6.0000E-01	3.1319E 00			
7.0000E-01	3.1136E 00			
8.0000E-01	3.0924E 00			
9.0000E-01	3.0676E 00			
1.0000E 00	3.0333E 00			
1.1000E 00	3.0034E 00			
1.2000E 00	2.9619E 00			
1.3000E 00	2.9125E 00			
1.4000E 00	2.8542E 00			
1.5000E 00	2.7851E 00			
1.6000E 00	2.7052E 00			
1.7000E 00	2.6140E 00			
1.8000E 00	2.5118E 00			
1.9000E 00	2.4001E 00			
2.0000E 00	2.2813E 00			
2.1000E 00	2.1585E 00			
2.2000E 00	2.0352E 00			
2.3000E 00	1.9150E 00			
2.4000E 00	1.8008E 00			
2.5000E 00	1.6950E 00			
2.6000E 00	1.5983E 00			
2.7000E 00	1.5129E 00			
2.8000E 00	1.4373E 00			
2.9000E 00	1.3714E 00			
3.0000E 00	1.3145E 00			
	1.2657E 00			

(cont'd)

PAGE 2

 MAXIMUM  
 3.29JCE 00  
 I

VERSUS ETA

F1

 MINIMUM  
 1.0001F 00  
 I

F1

ETA

3.100CE 00	1.2241E 00	1.0001F 00	+
3.200CE 00	1.1887E 00	1.0001F 00	+
3.300CE 00	1.1587E 00	1.0001F 00	+
3.400CE 00	1.1333E 00	1.0001F 00	+
3.500CE 00	1.1120E 00	1.0001F 00	+
3.600CE 00	1.0939E 00	1.0001F 00	+
3.700CE 00	1.0788E 00	1.0001F 00	+
3.800CE 00	1.0666E 00	1.0001F 00	+
3.900CE 00	1.0553E 00	1.0001F 00	+
4.000CE 00	1.0463E 00	1.0001F 00	+
4.100CE 00	1.0388E 00	1.0001F 00	+
4.200CE 00	1.0325E 00	1.0001F 00	+
4.300CE 00	1.0272E 00	1.0001F 00	+
4.400CE 00	1.0228E 00	1.0001F 00	+
4.500CE 00	1.0190E 00	1.0001F 00	+
4.600CE 00	1.0159E 00	1.0001F 00	+
4.700CE 00	1.0133E 00	1.0001F 00	+
4.800CE 00	1.0112E 00	1.0001F 00	+
4.900CE 00	1.0094E 00	1.0001F 00	+
5.000CE 00	1.0078E 00	1.0001F 00	+
5.100CE 00	1.0066E 00	1.0001F 00	+
5.200CE 00	1.0055E 00	1.0001F 00	+
5.300CE 00	1.0046E 00	1.0001F 00	+
5.400CE 00	1.0039E 00	1.0001F 00	+
5.500CE 00	1.0033E 00	1.0001F 00	+
5.600CE 00	1.0028E 00	1.0001F 00	+
5.700CE 00	1.0023E 00	1.0001F 00	+
5.800CE 00	1.0020E 00	1.0001F 00	+
5.900CE 00	1.0017E 00	1.0001F 00	+
6.000CE 00	1.0014E 00	1.0001F 00	+
6.100CE 00	1.0012E 00	1.0001F 00	+
6.200CE 00	1.0010E 00	1.0001F 00	+
6.300CE 00	1.0009E 00	1.0001F 00	+
6.400CE 00	1.0008E 00	1.0001F 00	+
6.500CE 00	1.0007E 00	1.0001F 00	+

PAGE 1

 MAXIMUM  
 907334E-C1  
 I

F2 VERSUS tTA

 MINIMUM  
 -204263E 00  
 I

ETA	F2	MINIMUM	F2	VERSUS tTA	MAXIMUM
C0C	C0C	I			I
1,0000E-01	1,5513E-01				
2,0000E-01	2,9136E-01				
3,0000E-01	4,1021E-01				
4,0000E-01	5,1333E-01				
5,0000E-01	6,0244E-01				
6,0000E-01	6,7920E-01				
7,0000E-01	7,4514E-01				
8,0000E-01	8,0158E-01				
9,0000E-01	8,4955E-01				
1,0000E 00	8,8976E-01				
1,1000E 00	9,2254E-01				
1,2000E 00	9,4783E-01				
1,3000E 00	9,6510E-01				
1,4000E 00	9,7334E-01				
1,5000E 00	9,7110E-01				
1,6000E 00	9,5649E-01				
1,7000E 00	9,2727E-01				
1,8000E 00	8,8113E-01				
1,9000E 00	8,1538E-01				
2,0000E 00	7,2938E-01				
2,1000E 00	6,2233E-01				
2,2000E 00	4,9362E-01				
2,3000E 00	3,4541E-01				
2,4000E 00	1,8058E-01				
2,5000E 00	2,9840E-03				
2,6000E 00	-1,8294E-01				
2,7000E 00	-3,7259E-01				
2,8000E 00	-5,6160E-01				
2,9000E 00	-7,4669E-01				
3,0000E 00	-9,2289E-01				

(cont'd)

PAGE 2

 MAXIMUM  
 9.7334E-01  
 1

VERSUS FTA

F2

 MINIMUM  
 -2.4263E 00  
 1

ETA	F2	MINIMUM	F2	VERSUS FTA	MAXIMUM
3.1000E 00	-1.0896E 00	-2.4263E 00	1		9.7334E-01
3.2000E 00	-1.2446E 00	-2.4263E 00	1		9.7334E-01
3.3000E 00	-1.3868E 00	-2.4263E 00	1		9.7334E-01
3.4000E 00	-1.5161E 00	-2.4263E 00	1		9.7334E-01
3.5000E 00	-1.6323E 00	-2.4263E 00	1		9.7334E-01
3.6000E 00	-1.7360E 00	-2.4263E 00	1		9.7334E-01
3.7000E 00	-1.8279E 00	-2.4263E 00	1		9.7334E-01
3.8000E 00	-1.9089E 00	-2.4263E 00	1		9.7334E-01
3.9000E 00	-1.9797E 00	-2.4263E 00	1		9.7334E-01
4.0000E 00	-2.0415E 00	-2.4263E 00	1		9.7334E-01
4.1000E 00	-2.0952E 00	-2.4263E 00	1		9.7334E-01
4.2000E 00	-2.1416E 00	-2.4263E 00	1		9.7334E-01
4.3000E 00	-2.1817E 00	-2.4263E 00	1		9.7334E-01
4.4000E 00	-2.2162E 00	-2.4263E 00	1		9.7334E-01
4.5000E 00	-2.2459E 00	-2.4263E 00	1		9.7334E-01
4.6000E 00	-2.2713E 00	-2.4263E 00	1		9.7334E-01
4.7000E 00	-2.2930E 00	-2.4263E 00	1		9.7334E-01
4.8000E 00	-2.3116E 00	-2.4263E 00	1		9.7334E-01
4.9000E 00	-2.3275E 00	-2.4263E 00	1		9.7334E-01
5.0000E 00	-2.3411E 00	-2.4263E 00	1		9.7334E-01
5.1000E 00	-2.3527E 00	-2.4263E 00	1		9.7334E-01
5.2000E 00	-2.3626E 00	-2.4263E 00	1		9.7334E-01
5.3000E 00	-2.3710E 00	-2.4263E 00	1		9.7334E-01
5.4000E 00	-2.3792E 00	-2.4263E 00	1		9.7334E-01
5.5000E 00	-2.3843E 00	-2.4263E 00	1		9.7334E-01
5.6000E 00	-2.3895E 00	-2.4263E 00	1		9.7334E-01
5.7000E 00	-2.3940E 00	-2.4263E 00	1		9.7334E-01
5.8000E 00	-2.3978E 00	-2.4263E 00	1		9.7334E-01
5.9000E 00	-2.4011E 00	-2.4263E 00	1		9.7334E-01
6.0000E 00	-2.4039E 00	-2.4263E 00	1		9.7334E-01
6.1000E 00	-2.4063E 00	-2.4263E 00	1		9.7334E-01
6.2000E 00	-2.4084E 00	-2.4263E 00	1		9.7334E-01
6.3000E 00	-2.4102E 00	-2.4263E 00	1		9.7334E-01
6.4000E 00	-2.4117E 00	-2.4263E 00	1		9.7334E-01
6.5000E 00	-2.4131E 00	-2.4263E 00	1		9.7334E-01



PAGE 2

ETA	F3	MINIMUM 0.C	F3	VERSUS ETA	MAXIMUM 1.6524E 03
3.1000E 00	1.6318E 00				
3.2000E 00	1.6355E 00				
3.3000E 00	1.6385E 00				
3.4000E 00	1.6410E 00				
3.5000E 00	1.6431E 00				
3.6000E 00	1.6448E 00				
3.7000E 00	1.6462E 00				
3.8000E 00	1.6474E 00				
3.9000E 00	1.6484E 00				
4.0000E 00	1.6491E 00				
4.1000E 00	1.6498E 00				
4.2000E 00	1.6503E 00				
4.3000E 00	1.6507E 00				
4.4000E 00	1.6511E 00				
4.5000E 00	1.6514E 00				
4.6000E 00	1.6517E 00				
4.7000E 00	1.6518E 00				
4.8000E 00	1.6519E 00				
4.9000E 00	1.6520E 00				
5.0000E 00	1.6521E 00				
5.1000E 00	1.6522E 00				
5.2000E 00	1.6523E 00				
5.3000E 00	1.6523E 00				
5.4000E 00	1.6524E 00				
5.5000E 00	1.6524E 00				
5.6000E 00	1.6524E 00				
5.7000E 00	1.6524E 00				
5.8000E 00	1.6524E 00				
5.9000E 00	1.6524E 00				
6.0000E 00	1.6524E 00				
6.1000E 00	1.6524E 00				
6.2000E 00	1.6524E 00				
6.3000E 00	1.6524E 00				
6.4000E 00	1.6524E 00				
6.5000E 00	1.6524E 00				

PAGE 1

 MAXIMUM  
2.7606E 00  
I

F4 VERSUS ETA

 MINIMUM  
-2.4266E 00  
I

ETA	F4	MINIMUM	F4	VERSUS ETA	MAXIMUM
C.0	0.0	-2.4266E 00			I
1.0000E-01	4.9453E-01				
2.0000E-01	9.2525E-01				
3.0000E-01	1.2972E 00				
4.0000E-01	1.6160E 00				
5.0000E-01	1.8868E 00				
6.0000E-01	2.1148E 00				
7.0000E-01	2.3043E 00				
8.0000E-01	2.4589E 00				
9.0000E-01	2.5811E 00				
1.0000E 00	2.6723E 00				
1.1000E 00	2.7325E 00				
1.2000E 00	2.7606E 00				
1.3000E 00	2.7543E 00				
1.4000E 00	2.7109E 00				
1.5000E 00	2.6271E 00				
1.6000E 00	2.5002E 00				
1.7000E 00	2.3291E 00				
1.8000E 00	2.1148E 00				
1.9000E 00	1.8613E 00				
2.0000E 00	1.5754E 00				
2.1000E 00	1.2666E 00				
2.2000E 00	9.4528E-01				
2.3000E 00	6.2202E-01				
2.4000E 00	3.0607E-01				
2.5000E 00	4.7708E-03				
2.6000E 00	-2.7677E-01				
2.7000E 00	-5.3551E-01				
2.8000E 00	-7.7016E-01				
2.9000E 00	-9.8072E-01				
3.0000E 00	-1.1681E 00				

PAGE 2

 MAXIMUM  
 2.7606E 00  
 I

F4 VERSUS ETA

 MINIMUM  
 -2.4266E 00  
 I

ETA	F4	MINIMUM	MAXIMUM
3.1000E 00	-1.3337E 00	-2.4266E 00	2.7606E 00
3.2000E 00	-1.4794E 00	-2.4266E 00	2.7606E 00
3.3000E 00	-1.6069E 00	-2.4266E 00	2.7606E 00
3.4000E 00	-1.7182E 00	-2.4266E 00	2.7606E 00
3.5000E 00	-1.8150E 00	-2.4266E 00	2.7606E 00
3.6000E 00	-1.8991E 00	-2.4266E 00	2.7606E 00
3.7000E 00	-1.9719E 00	-2.4266E 00	2.7606E 00
3.8000E 00	-2.0349E 00	-2.4266E 00	2.7606E 00
3.9000E 00	-2.0893E 00	-2.4266E 00	2.7606E 00
4.0000E 00	-2.1361E 00	-2.4266E 00	2.7606E 00
4.1000E 00	-2.1765E 00	-2.4266E 00	2.7606E 00
4.2000E 00	-2.2112E 00	-2.4266E 00	2.7606E 00
4.3000E 00	-2.2410E 00	-2.4266E 00	2.7606E 00
4.4000E 00	-2.2667E 00	-2.4266E 00	2.7606E 00
4.5000E 00	-2.2886E 00	-2.4266E 00	2.7606E 00
4.6000E 00	-2.3075E 00	-2.4266E 00	2.7606E 00
4.7000E 00	-2.3236E 00	-2.4266E 00	2.7606E 00
4.8000E 00	-2.3375E 00	-2.4266E 00	2.7606E 00
4.9000E 00	-2.3493E 00	-2.4266E 00	2.7606E 00
5.0000E 00	-2.3595E 00	-2.4266E 00	2.7606E 00
5.1000E 00	-2.3682E 00	-2.4266E 00	2.7606E 00
5.2000E 00	-2.3756E 00	-2.4266E 00	2.7606E 00
5.3000E 00	-2.3820E 00	-2.4266E 00	2.7606E 00
5.4000E 00	-2.3875E 00	-2.4266E 00	2.7606E 00
5.5000E 00	-2.3921E 00	-2.4266E 00	2.7606E 00
5.6000E 00	-2.3962E 00	-2.4266E 00	2.7606E 00
5.7000E 00	-2.3996E 00	-2.4266E 00	2.7606E 00
5.8000E 00	-2.4026E 00	-2.4266E 00	2.7606E 00
5.9000E 00	-2.4051E 00	-2.4266E 00	2.7606E 00
6.0000E 00	-2.4073E 00	-2.4266E 00	2.7606E 00
6.1000E 00	-2.4093E 00	-2.4266E 00	2.7606E 00
6.2000E 00	-2.4109E 00	-2.4266E 00	2.7606E 00
6.3000E 00	-2.4123E 00	-2.4266E 00	2.7606E 00
6.4000E 00	-2.4136E 00	-2.4266E 00	2.7606E 00
6.5000E 00	-2.4147E 00	-2.4266E 00	2.7606E 00

(cont'd)



## APPENDIX VIIA

DERIVATION OF  $m_2(t)$  FOR EQ. (7-2) AND  $h_1(t)$  FOR EQ. (7-6)

The liquid film thickness right behind the projectile is  $h_1$  and total liquid flow rate squeezed from the small holes on the projectile is

$$\dot{M}_2 = \bar{\rho}_2 \bar{A} \sqrt{\frac{2\Delta p}{\bar{\rho}_2}} \quad (7A-1)$$

where

 $\bar{\rho}_2$  = density $\bar{A}$  = total cross-section area of the small holes $\Delta p$  = pressure difference between two ends of the small holes

In dimensionless, Eq (7A-1) is written as

$$\dot{m}_2 = \rho_2 a \sqrt{\frac{2\Delta p}{\rho_2}} \quad (7A-2)$$

where (See also Nomenclature)

$$\dot{m}_2 = \frac{\dot{M}_2}{\rho_2 L^2 U_1} \quad a = \frac{\bar{A}}{L^2}$$

$$\rho_2 = \frac{\bar{\rho}_2}{\rho_1} \quad p = \frac{\rho_1 U_1^2}{g}$$

Therefore the total amount of the liquid from the breach to the base of

the projectile which is at  $z = z_p(t)$  is  $m_2(t) = \rho_2 a \int_0^t \sqrt{\frac{2\Delta p(\lambda)}{\rho_2}} d\lambda \quad t \leq 1.09$

If  $\Delta p = \frac{p}{2}$  is assumed the difference in the pressure between the base of the projectile and exit hole of the projectile. We have

$$m_L(t) = \rho_L a \int_0^t \sqrt{\frac{p(\lambda)}{\rho_L}} d\lambda \quad t \leq 1.409 \text{ (2.3 mill:sec)}$$

To estimate the rate of coating on the wall of the barrel we note that

$$\dot{m}_L = (\rho_L \pi d_o \dot{h}_L) \dot{z}_p \quad (7A-3)$$

where

$$d_o = \frac{D_o}{L} = \text{diameter of the barrel}$$

$\dot{z}_p$  = velocity of the projectile

For conservation, Eq (7A-2) and Eq (7A-3) must be equal. Then

$$\dot{h}_L = \frac{a}{\pi d_o \dot{z}_p} \sqrt{\frac{2\Delta p}{\rho_L}} \quad (7A-4)$$

If we assume  $\Delta p = \frac{p}{2}$ ,  $p$  is obtained from the core solution Eq (5-12), Eq. (D-4) is rewritten as

$$\dot{h}_L = \frac{a}{\pi d_o \dot{z}_p} \sqrt{\frac{p}{\rho_L}} \quad (7A-5)$$